Faculty of Health Sciences

Forensic DNA phenotyping

Towards reliable and accurate DNA tests for prediction of eye colour, hair colour and biogeographical ancestry

Nina Mjølsnes Salvo

A dissertation for the degree of Philosophiae Doctor (PhD)   March 2024

Generated with AI

Table of Contents

Acknowledgements

Abbreviations

α-MSH	α-melanocyte stimulating hormone
AIM	Ancestry informative marker
ASIP	Agouti signalling protein
aSNPs	Ancestry informative SNPs
AUC	Area under the receiver characteristic operating curve
BAM	Binary alignment map
BGA	Biogeographical ancestry
cAMP	Cyclic adenosine 3´,5´-monophosphate
CE	Capillary electrophoresis
CNV	Copy number variations
ddNTP	Dideoxynucleotide
ddPCR	Droplet digital PCR
DCT	Dopachrome tautomerase
DHI	5,6-dihydroxyindole
DHICA	5,6-dihydroxyindole-2-carboxylic acid
DNA	Deoxyribonucleic acid
EC11	EyeColour 11
EVC	External visible characteristics
FDP	Forensic DNA phenotyping
GWAS	Genome-wide association studies
HERC2	HECT domain and RCC1-like domain 2
HMW	High molecular weight
INDEL	Insertion-deletion
IRF4	Interferon Regulatory Factor 4
kbp	Kilo base pair
KITLG	KIT ligand
LD	Linkage disequilibrium
LR	Likelihood ratio
NCKX4	K+-dependent Na+/Ca2+-exchanger isoform 4
NCKX5	K+-dependent Na+/Ca2+-exchanger isoform 5
MATP	Membrane-associated transporter protein
MC1R	Melanocortin-1 receptor

MH	Microhaplotypes
MITF	Microphthalmia-associated transcription factor
MPS	Massively parallel sequencing
OCA1	Oculocutaneous albinism type 1
OCA2	Oculocutaneous albinism type 2
OCA3	Oculocutaneous albinism type 3
OCA4	Oculocutaneous albinism type 4
OCA5	Oculocutaneous albinism type 5
OCA6	Oculocutaneous albinism type 6
PCR	Polymerase chain reaction
PIE	Pixel index of the eye
PGA	Prediction guide approach
pSNPs	Phenotype informative SNPs
RHC	Red hair colour
SAD	Seasonal affective disorder
SBE	Single base extension
SLC24A4	Solute carrier family 24, member 4
SLC24A5	Solute carrier family 24, member 5
SLC45A2	Solute carrier family 45, member 2
SNP	Single nucleotide polymorphism
STR	Short tandem repeats
TPCN2	Two pore channel protein 2
TYR	Tyrosinase
TYRP1	Tyrosinase-related protein 1
UV	Ultraviolet

List of papers

Paper 1

Predicting eye and hair colour in a Norwegian population using Verogen's ForenSeq^{TM} DNA signature prep kit. *Forensic Science International: Genetics.* **2021**;56:102620. doi:10.1016/j.fsigen.2021.102620.

Salvo N.M., Janssen K., Kirsebom M.K., Meyer O.S., Berg T., Olsen G.-H.

Paper 2

Biogeographical ancestry analyses using the ForenSeq^{TM} DNA Signature Prep kit and multiple prediction tools.

Salvo N.M., Olsen G.-H., Berg T., Janssen K.

Manuscript submitted for publication.

Paper 3

Prediction of Eye Colour in Scandinavians Using the EyeColour 11 (EC11) SNP Set. *Genes.* **2021**;12:821. doi: 10.3390/genes12060821.

Meyer O., Salvo N.M., Kjærbye A., Kjersem M., Andersen M., Sørensen E., Ullum H., Janssen K., Morling N., Børsting C., Olsen G.-H., Andersen J.D.

Paper 4

Experimental long-distance haplotyping of *OCA2-HERC2* variants. *Forensic Sci. Int. Genet. Suppl. Ser.* **2022**;8:188-190. doi: 10.1016/j.fsigss.2022.10.030.

Salvo N.M., Mathisen M.G., Janssen K., Berg T., Olsen G.-H.

Paper 5

Association between Variants in the *OCA2-HERC2* Region and Blue Eye Colour in *HERC2* rs12913832 AA and AG Individuals. *Genes.* **2023**;14:698. Doi: 10.3390/genes14030698

Salvo N.M., Andersen J.D., Janssen K., Meyer O.L., Berg T., Børsting C., Olsen G.-H.

Paper 6

Association between copy number variations in the *OCA2-HERC2* locus and human eye colour. *Forensic Sci. Int. Genet. Suppl. Ser.* **2022**;8:82–84. doi: 10.1016/j.fsigss.2022.09.030.

Salvo N.M., Janssen K., Olsen G.-H., Berg T., Andersen J.D.

Summary

Forensic DNA phenotyping (FDP) is the prediction of appearance and biogeographical ancestry (BGA) from crime scene DNA. FDP can aid police investigations in cases where there is no match with the DNA profile obtained from crime scene evidence. This is an emerging investigative tool but is so far only used in a few numbers of countries for casework. Prior to implementation in the forensic laboratory, the methods have to be evaluated and validated in order to disclose limitations and inaccuracies. Importantly, our knowledge on the genetics of human external visible characteristics is still not complete, and continuous investigations of genotype-phenotype associations are important to improve current available DNA tests for FDP. The aim of this thesis was to evaluate genotyping performance and prediction accuracies using the ForenSeq^{TM} Signature Prep Kit (Verogen) on a MiSeq FGx and various tools for eye colour, hair colour and BGA inference. To improve eye colour predictions, nine models were developed using a novel SNP panel (EC11), the widely used IrisPlex SNPs and the *HERC2* rs12913832, as well as three different reporting systems (quantitative, two-and three-category). Furthermore, we aimed to increase the genetic knowledge of eye colour pigmentation by sequencing the *OCA2-HERC2* region in 94 individuals with blue or brown eye colour. We demonstrated that the ForenSeq kit is reliable and sensitive. However, there are concerns about potentially undiscovered false homozygous genotypes, thus we suggested adjustments for the analysis criteria. BGA was inferred on a continental scale with high accuracies using the tools: the Universal Analysis Software (UAS), FROG-kb and GenoGeographer. A multiple-tool approach increased prediction accuracies. When predicting hair colour in four categories using the HIrisPlex web tool, we observed high accuracies for red and black, but lower for blond and brown hair colours. The prediction accuracies were increased by including shade and utilising the Prediction Guide Approach (PGA) provided with the tool. Blue and brown eye colour can be predicted with high accuracies using the IrisPlex panel or rs12913832 alone, but intermediate eye colour is both challenging to phenotype and to predict. Using a two-category model increased the prediction accuracies regardless of SNP panel used. Thus, using rs12913832 in a two-category model might be sufficient for predicting eye colour in general. However, the EC11 panel increased the number of correct predictions for individuals with blue eye colour in the Norwegian study population. We further identified novel genetic variants and copy number variations in the *OCA2-HERC2* region associated with blue eye colour that could potentially increase the accuracy of eye colour predictions in Scandinavians.

1 Introduction

1.1 Forensic genetics

DNA has been used for human identification ever since the discovery of minisatellite DNA by Jeffreys *et al.* [1] in 1985. The gold standard in forensic genetic investigations is to obtain DNA profiles from crime scene evidence and to compare these with DNA profiles generated from reference persons, e.g. a suspect or persons in a database for identification [2]. In Norway, DNA was used for the first time in a trial in 1988. Ten years later, in 1998, the first Norwegian criminal offender DNA database was established, enabling comparative matching of DNA profiles obtained from evidence material with persons registered in the database [3]. DNA profile analyses are not limited to crime scene evidence, and can also be used in paternity, relationship, and identification cases.

Today, forensic DNA analyses for identification utilise microsatellite regions, short tandem repeats (STRs), in the non-coding parts of the DNA [2]. These STRs comprise tandemly repeated units of most commonly four nucleotides, found throughout the human genome [4]. STRs are length polymorphisms, meaning that the number of repeats and thereby the length of the alleles varies highly among individuals [4]. One DNA profile includes several STR loci for discrimination between individuals. Because only a fraction of the genome is examined, statistical estimates of the random match probability of the DNA profile must be calculated based on measured frequencies of the STR alleles in a relevant population [5]. The discrimination power will increase with the number of STRs used, e.g. a DNA profile of 20 STRs provides a discrimination power higher than 1 in thousand billion [6]. In other words, the DNA profile will be near unique for one person (except for identical twins). The standard method for DNA profiling is based on amplification of multiple STR markers using polymerase chain reaction (PCR) and capillary electrophoresis (CE) [7,8]. Most modern kits include primers for over 20 STRs [6,9].

In contrast to STRs that are usually non-coding and vary in sequence length, single nucleotide polymorphisms (SNPs) are single-base variants that are located in both non-coding and coding regions and are the most common variants in the human genome [10]. SNPs can be causal or statistically associated with human characteristics, thus utilising these in forensic genetics opens for other applications than DNA profiling, such as DNA phenotyping [10,11]. The SNPs have a lower mutation rate than STRs which makes them mostly bi-allelic, and thus less

discriminative between individuals [12]. However, the lower mutation rate is advantageous in kinship and ancestry analysis [10].

Genotyping of SNPs in forensics is commonly performed by single base extension PCR (SBE-PCR) using the SNaPshot^{TM} multiplex system (Thermo Fisher Scientific) [13]. PCR products are separated and detected by CE, like in standard DNA profiling. This is a sensitive and robust method for genotyping but has limited multiplexing capacity.

Genotyping by massively parallel sequencing (MPS) in forensic genetics

During the past two decades, massively parallel sequencing (MPS, also known as next generation sequencing, NGS) has developed quickly, enabling high-throughput sequencing of near unlimited numbers (millions) of DNA sequences (reviewed in [14]). Compared to the PCR-CE, MPS enables an increased multiplexing ability, bringing new possibilities to the analysis of forensic DNA samples. It is possible to type a large number of markers, both SNPs and STRs, from small amounts of DNA [15]. It is also possible to combine different markers in one analysis, and to type more complexed markers such as microhaplotypes (MHs). MHs are multi-allelic markers of two to four closely linked SNPs on one fragment of maximum 300 bp [16]. In contrast to the bi-allelic stand-alone SNP, these may be highly suitable for mixture deconvolution in individual identification and for identifying familial relationships. The high-throughput targeted sequencing also achieves read depth information of the sequenced regions, enabling detection of the less studied copy-number variations (CNVs) from the MPS data [17]. CNVs are structural variants represented by deletions and duplications larger than 50 bp [18]. Importantly, the technology is also advantageous for STR analysis. Compared to the traditional PCR-CE method where only the length of the alleles is detected, MPS reads the actual nucleotide sequence of the DNA, and can provide sequence information on all the amplified DNA in a sample. Providing the actual sequence can be advantageous for STR analysis in complex mixtures as it might be possible to differentiate a minor contributor from noise and stutters, that is difficult by PCR-CE. Stutters are PCR-artefacts that are most commonly one repeat unit shorter or longer than the "real" STR allele [8].

The MPS technology is now widely used in many fields, e.g., clinical diagnostics of humans and taxonomy in biology [19,20]. Yet, in forensic genetics, MPS is still in the implementation phase for STR analysis in routine casework due to the requirement of a different analytical workflow and bioinformatic resources compared to PCR-CE [21,22]. However, because of the

multiplexing ability, MPS is becoming the number one choice for SNP typing for the emerging investigative tool forensic DNA phenotyping (FDP) for appearance and ancestry analyses [23].

1.2 Forensic DNA Phenotyping of appearance and ancestry - extended DNA analysis for forensic investigations

In cases where a DNA profile is obtained from crime scene evidence, but there are no suspects or database hit, the DNA profile may be of little value for the police investigations, except for information about gender. In cases of serious manner, such as murder, population mass screening can be used to search for persons that can match the DNA profile. However, this can be time consuming and expensive. Extended DNA analyses such as forensic DNA phenotyping (FDP) can in these cases be valuable for the investigation. FDP is the prediction of externally visible characteristics (EVCs), biogeographical ancestry (BGA) and age from crime scene DNA [23] (**Figure 1**). In contrast to STR profiling that provides confirmatory evidence, FDP is an investigative intelligence tool that can aid crime investigations by narrowing down a pool of potential suspects [11]. Additionally, FDP is highly beneficial for identifications of missing persons or disaster victims.
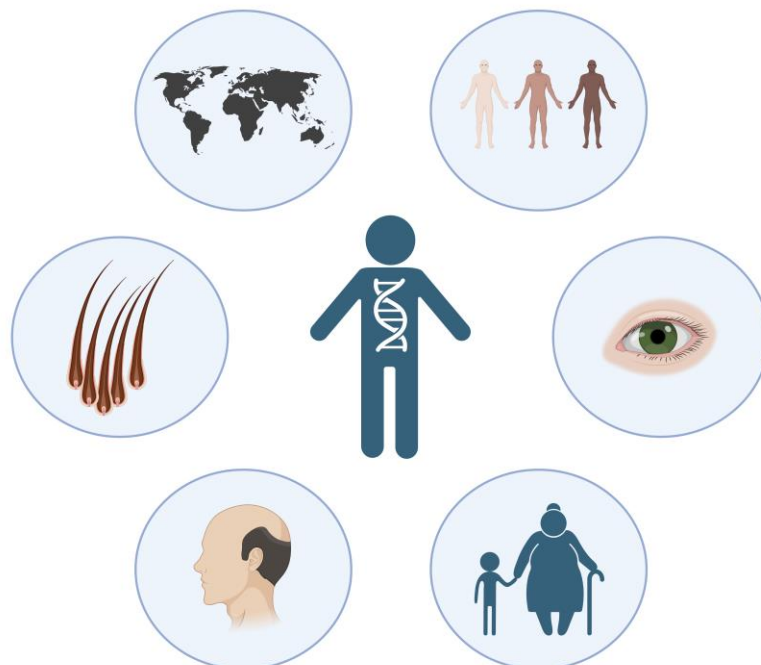

Figure 1: Forensic DNA Phenotyping (FDP) can portray a person´s potential age and appearance from DNA. Created with BioRender.com

In prediction of EVCs, variants (i.e., SNPs) in and around genes are used because they can be associated with human characteristics such as eye colour, hair colour, skin tone, hair morphology, baldness, body height or facial morphology [23]. In forensic genetics these SNPs are often referred to as phenotype informative SNPs (pSNPs). Most EVCs are inherited, but many are polygenetic and highly complex. Body height is an example of a trait with large genetic complexity. A recent Genome-Wide association study (GWAS) on body height revealed that over 12 000 significantly associated SNPs explained only 10-40% of height variations, depending on ancestry [24]. Pigmentation (i.e., eye, hair and skin colour) is recognised to be the least complex trait, and to date the best example of practical FDP [23]. Eye, hair and skin colour are prominent characteristics when describing a person's appearance. Similar to an eyewitness, FDP can provide leads to trace an unknown person and has therefore been referred to as a "biological witness" [11].

BGA analysis is used to infer a person's geographical region of origin, thereby indirectly portraying externally visible characteristics [25]. In contrast to FDP of appearance that utilises genetic knowledge on variants that are associated with specific phenotypes, BGA inference exploits genetic variation found between population by using ancestry informative markers (AIMs) that are differently distributed among various population groups [25]. By comparing a person's AIM profile to reference populations, we can infer which one is the most likely population of origin. The most used AIMs in FDP of ancestry are autosomal SNPs, often referred to as ancestry informative SNPs (aSNPs). Autosomal markers are biparental and thus reflect the geographic origins of both parents [26]. Markers located on the Y-chromosome or mitochondrial DNA can also be used. However they will only reflect the geographical origin of ancestors on the paternal or maternal lineage, respectively [27,28].

FDP is still not routinely used in police investigations in many countries, including Norway. However, continuous research is conducted to develop reliable DNA tests for FDP. This thesis focuses on the prediction of pigmentation traits, especially eye and hair colour, together with ancestry inference for forensic application. These topics will therefore be discussed in more detail.

4

1.3 Human pigmentation

Human pigmentary traits such as skin, hair and eye colour are determined by the pigment melanin. Melanin is produced and stored in subcellular organelles called melanosomes inside the melanocytes [29]. Melanocytes are located in the dermis and epidermis of the skin, in hair follicles and in the iris of the eyes. In skin and hair, the melanosomes are transferred from the melanocytes to surrounding keratinocytes, whereas they are retained inside the melanocytes in eyes [30]. Through melanogenesis, two types of pigment are produced: eumelanin (brown/black) and pheomelanin (red/yellow) [31]. It is the density and type of pigment inside the melanosomes as well as the density and distribution of the melanosomes in the cells that determine the phenotype [32]. Eyes that are perceived as blue have minimal pigmentation [33]. When there is little amount of pigment in the iris, light can traverse to the collagen fibrils, where only blue light is reflected. This reflection of light, and thus eye colour, is also dependent on stromal structure and patterns [34]. Moreover, brown and green-hazel eye colours are correlated with the ratio between eumelanin and pheomelanin, with more eumelanin observed in darker eyes [35].

Melanin is known to absorb ultraviolet (UV) light, thereby protecting cells against UV-radiation [36]. Global variation in human skin colour shows a strong correlation with incident UV light intensity, with a cline from dark skin colour near the equator to light skin colour near the poles [37,38]. Additionally, previtamin D_3 is synthesised in skin by exposure to UV radiation, and more melanin rich skin needs longer exposure to light to maximise vitamin D_3 production [39]. Therefore, it has also been hypothesised that lighter skin colour in the north, with lower UV light intensity, is advantageous for vitamin D_3 production [38]. In contrast to skin pigmentation, there is little global variation in eye colour, with brown being the dominating colour. Eye colour variation from brown to green-hazel to blue is almost exclusively found in Europeans, with blue eye colour dominating in Northern Europe [40]. It is not clear why the significant loss of pigmentation in the eyes has evolved in Europe, but there is strong evidence of selection pressure on the *HERC2-OCA2* region associated with blue eye colour in Europeans [41]. One theory points towards sexual selection as a possible explanation [42]. Another theory suggests that blue eye colour is advantageous in overcoming seasonal affective disorder (SAD) caused by limited daylight during long winters [37]. A link between blue eye colour and SAD has been observed, where blue eyed individuals responded positively to treatment using therapeutic morning light [43,44].

5

In the biosynthesis of melanin, tyrosinase (TYR) is one of the key enzymes that catalyses the first step in the melanogenesis by oxidating tyrosine to dopaquinone (Ito & Wakamatsu, 2008; reviewed in Pavan & Sturm, 2019) (**Figure 2**). The pathway to eumelanin from dopaquinone is catalysed by three enzymes in the tyrosinase-related protein family; TYR, tyrosinase-related protein 1 (TYRP1) and dopachrome tautomerase (DCT, previously known as TYRP2). The pathway to pheomelanin starts spontaneously with presence of cysteine. Therefore, melanogenesis and the pheomelanin/eumelanin ratio is dependent on TYR activity and tyrosine- and cysteine availability. Furthermore, TYR activity is pH dependent, thus ion transport into the melanosomes is crucial [46,47]. The melanocortin 1 receptor (MC1R), a melanocytic G-protein located in the membrane of melanocytes, is important in the regulation of TYR transcription [48]. MC1R acts as a switch from pheomelanin to eumelanin synthesis (**Figure 2**).
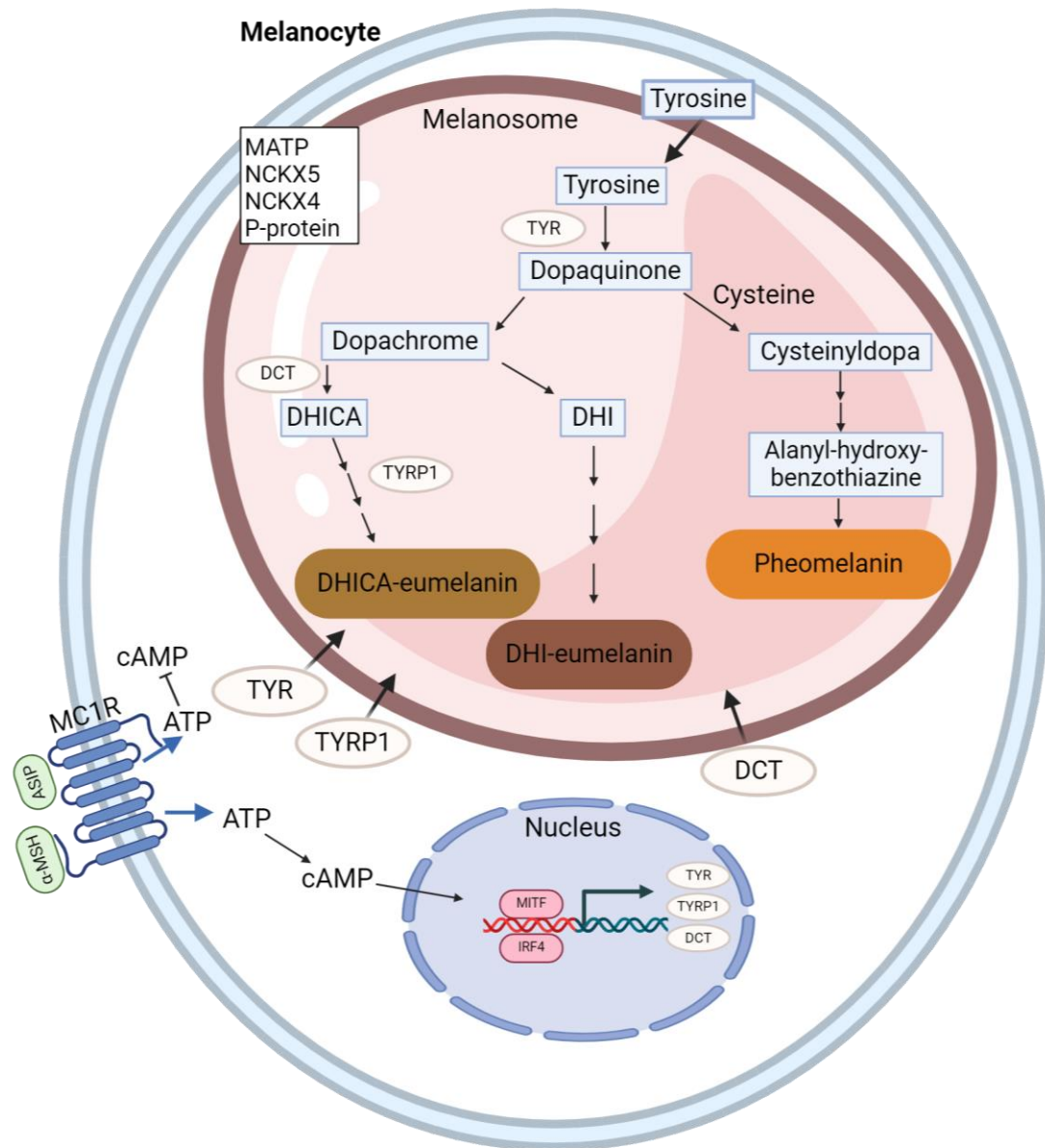
Figure 2: Melanogenesis with key proteins involved. Tyrosinase (TYR) catalyses the first step in the melanogenesis by oxidating tyrosine to dopaquinone. Dopaquinone is an intermediate for both eumelanin and pheomelanin. If cysteine is available in the melanosome, cysteinyldopa will spontaneously be produced, which will then result in the production of the red/yellow pheomelanin. In the absence of cysteine, dopachrome will be formed and will either spontaneously decompose to 5,6-dihydroxyindole (DHI) or produce 5,6-dihydroxyindole-2-carboxylic acid (DHICA) catalysed by DCT. DHI will form the dark brown or black DHI-eumelanin, whereas tyrosinase-related protein 1 (TYRP1) catalyse the production of the lighter colour DHICA-eumelanin. The solute carrier transmembrane family proteins, MATP, NCKX5, NCKX4 and the melanosomal transport P-protein are all suggested to be important for ion transport and TYR trafficking. Transcription of TYR, TYRP1 and DCT is activated by the microphthalmia-associated transcription factor (MITF), which is regulated by the melanocortin

1 receptor (MC1R). The transmembrane G-protein, MC1R acts as a switch from pheomelanin to eumelanin synthesis. When the agonist α-MSH binds MC1R, the adenylate cyclase is activated, which furthermore leads to an elevation of intracellular cAMP, and thereby upregulating transcription of MIFT through the cAMP signalling pathway. Contrary, the antagonist agouti signalling protein (ASIP) compete with α-MSH, leading to downregulation of MITF and thereby TYR. The low TYR activity favours pheomelanin production as opposed to eumelanin production. (Reviewed in [31]). Created with BioRender.com, redrawn from [49].

1.3.1 Human pigmentation genes

Pigmentation is highly inherited, with only minimal influence from environmental factors. Eye colour is least influenced by environmental factors because melanin is retained in the melanocytes within the iris throughout life [30]. Melanin in dermis and epidermis of the skin and in hair follicles is continuously produced and secreted [30,50]. Thus, skin and hair colour are subjected to change with exposure to light (UV-radiation) and ageing. When skin is exposed to UV radiation, melanocytes start to produce more melanin for protection, resulting in a darker colour (tanning) [51]. However, this change is relatively small and will not change the phenotype. Hair colour can darken with age from blond to brown due to a phenomenon called age-dependent darkening, which will change the phenotype to some degree [52]. Furthermore, aging can lead to loss of pigment (hair greying) or even loss of hair (baldness), which will completely change the phenotype [53,54]. Many genes are involved in the synthesis of melanin [31]. Although the precise function of many of these genes is unclear, genetic variants found in these genes may be involved in normal pigmentation variation or cause pigmentation disorders.

Melanocortin 1 receptor (*MC1R*) and Agouti signalling protein (*ASIP*)
MC1R is often referred to as the red hair colour gene, as variants are strongly associated with the red hair colour (RHC) phenotype (that is defined by red hair and freckled fair skin with decreased tanning response to UV-radiation) [55]. This is a highly polymorphic gene with over 200 identified variants. In addition to the RHC phenotype, some are also associated with increased melanoma and nonmelanoma skin cancer risk [56,57]. Variants are classified as high penetrance (*R*) (such as rs1805007, rs1805008, rs1805009, rs1805006, rs11547464 and rs1110440) and low penetrance variants (*r*) (such as rs1805005, rs2228479 and rs885479) [58]. In red haired individuals, two *R* variants are often observed, either in a homozygous or a compound heterozygous state [59]. However, *R/r* genotypes have also been observed in some

red haired individuals [58]. ASIP is an antagonist to MC1R. By blocking α-MSH from binding, ASIP is possibly downregulating eumelanogenesis and thereby stimulating pheomelanogenesis [60,61]. One haplotype (rs1015362:G – rs4911414:T) upstream of the *ASIP* gene was also found to be associated with the RHC phenotype [62].

TYR and *TYRP1*

Mutations in *TYR* are related to oculocutaneous albinism type 1 (OCA1), which is one of the most frequent form of albinism with complete lack of pigmentation [63,64]. However, some polymorphisms are associated with normal variation of human pigmentation. The SNPs rs1042602, rs1126809 and rs1393350 (the latter two are in strong linkage disequilibrium, LD) have been shown to be associated with eye, hair and skin colour, although with varying effects [65–68]. Complete loss-of-function mutations in *TYRP1* cause OCA3 albinism, a moderate hypopigmentation condition that is most often observed as red hair and reddish-brown skin in Africans [64,69]. Although the precise function of TYRP1 in the melanocytes is still unknown, it is suggested that mutations can affect maturation and stability of TYR [70]. Some *TYRP1* SNPs are also identified to be associated with normal variation of human pigmentation, e.g., rs683, rs1408799 and rs387907171 [66,71,72].

Oculocutaneous albinism 2 (OCA2)

OCA2 encodes the OCA2 melanosomal transmembrane P protein, suggested to be important for trafficking of TYR and TYRP1 [73]. Additionally, OCA2 may play a crucial role in pH-regulation of the melanosomes [74]. Mutations in *OCA2* can cause OCA2 albinism [75], which is observed as various degrees of hypopigmentation [64]. Moreover, *OCA2* is known as the most important gene for normal eye colour variation. Notably, The SNP rs12913832, which is located in the in HECT domain and RCC1-like domain 2 (*HERC2*) 21k bp upstream the *OCA2* promoter, is nearly the perfect predictor for brown and blue eye colour [76,77]. This SNP is known to work as a distal enhancer and regulates the transcription of *OCA2* [78]. *OCA2* expression is upregulated in heavily pigmented melanocytes, carrying the wild type rs12913832:A allele. In contrast, *OCA2* expression is downregulated in poorly pigmented melanocytes carrying the derived rs12913832:G allele. Hence, the rs12913832:GG genotype is strongly associated with blue eye colour [76,77,79]. It is also almost exclusively restricted to Europeans. Other variants in *OCA2* are also associated with normal eye colour variation, such as the missense mutations rs1800407, rs74653330 and rs121918166. These mutations have been associated with blue and green eye colours on a rs12913832:A background, suggesting

9

them to act as penetrance modifiers of the locus [77,80]. Variants in the *OCA2-HERC2* locus have also been associated with skin and hair pigmentation [81–83].

SLC45A2, SLC24A4 and SLC24A5

Solute carrier family 45, member 2 (*SLC45A2*) encodes the membrane-associated transporter protein (MATP). Mutations can cause OCA4 albinism in humans [64]. The precise function of the protein in the melanosomes is still unclear [46]. However, it is suggested to be important for melanosomal pH-regulation and TYR trafficking, similar to OCA2 [84,85]. The missense mutation rs16891982, is associated with normal pigmentation variation in eye, hair and skin colour [71,86,87]. The rs16891982:G allele is nearly fixed in European populations and close to absent in African and South-East Asian populations (1000 Genomes Project Consortium, 2015). Therefore, the SNP is also an important marker in BGA inference [88,89]. The solute carrier family 24, member 5 (*SLC24A5*) encodes the K+-dependent Na+/Ca2+ exchanger 5 (NCKX5) protein, which is also suggested to play an important role in ion trafficking in the melanosomes [90,91]. Mutations have been associated with OCA6 albinism [92]. The SNP rs1426654 is strongly associated with skin pigmentation, and is also used as a marker for ancestry inference because the A allele is almost fixed in Europeans [89,90,93]. Variants in a third solute carrier member, solute carrier family 24, member 4 (*SLC24A4),* encoding NCKX4, has also been associated with normal pigmentation [68,94].

Above I presented some key genes involved in human pigmentation, and some of the well-known SNPs associated with pigmentary traits. The continuously growing availability of data from GWAS [95] has furthermore identified numerous of variants that are also associated with human pigmentation, also in other pigmentation genes such as *IRF4*, *KITLG* and *TPCN2* [62,68,94].

1.3.2 Prediction of eye, hair and skin colour

In inference of EVCs, a posterior probability of a trait is usually calculated given the genetic knowledge about variants (i.e., SNPs) that are either causal or statistically associated with the trait of interest. In the field of forensic genetics, inference of EVCs is often referred to as "prediction" of EVCs, and I will use this terminology in this thesis.

The first model used for forensic application was prediction of red-non red hair colour using variants in *MC1R* [96]. Then, prediction models for eye colour were developed, followed by models for hair colour in several categories, and lastly skin colour [71,79,81,97–102]. Today, all these traits can be predicted with various degrees of accuracies [23].

One of the first eye colour prediction studies focused on the *OCA2* gene [103]. *OCA2* was considered to be "the" eye colour gene because several studies had pointed towards *OCA2* as the gene that explained most of the variation in eye colour [104–106]. The most important break-through for eye colour prediction was the identification of rs12913832 in *HERC2,* an enhancer of *OCA2,* as an almost perfect predictor for blue and brown eye colour [76,77]. Sturm *et al.* [77] found a high correlation between eye colour variation and rs12913832 alone. In 2009, a comprehensive study on the predictive value of 24 eye colour SNPs from eight genes, found that six SNPs from six genes (*HERC2* rs12913832, *OCA2* rs1800407, *SLC24A4* rs12896399, *SLC45A2* rs16891982, *TYR* rs1393350 and *IRF4* rs12203592) was sufficient to accurately predict eye colours in three categories (brown, blue and intermediate) [71]. When predicting eye colour in a sample set of 2364 Dutch individuals, they achieved overall high prediction accuracies, expressed as area under the receiver characteristic operating curve (AUC)s, of 0.93 for brown and 0.91 for blue eye colour. However, the accuracy for intermediate eye colour was considerably lower, with an AUC value of 0.72. AUC-values range from 0 to 1, where 1 represents 100% accuracy and 0.5 represent random guessing [107].

Based on the study from Liu *et al.* [71] in 2009, the first eye colour prediction system validated for forensic application, the IrisPlex, was developed in 2011 using the same six SNP [79,108]. The IrisPlex system consisted of an SBE-CE multiplex genotyping assay and a statistical prediction model calculating probabilities for each of the three eye colour categories blue, brown and intermediate eye colour. Today, the underlying database includes 9466 individuals, and the model is reported to accurately predict brown and blue eye colour with AUCs of 0.95 and 0.94, respectively [100,109,110]. The prediction accuracy for intermediate eye colour is still considerably lower, with an AUC of 0.74. The IrisPlex has become one of the most popular models for prediction of eye colour and has been evaluated in several populations (e.g. [111–113]).

Subsequent to the development of the IrisPlex, various studies presented eye colour prediction models with partially overlapping SNPs to the IrisPlex [82,97,114,115]. These models used

different mathematical- and phenotyping strategies. However, they all included rs12913832 and were able to predict blue and brown eye colour with high accuracies. Allwood & Harbison [102] used a classification tree model approach based on four SNPs that were overlapping with the IrisPlex SNPs. Instead of including the *HERC2* rs12913832, they applied another *HERC2* SNP, rs1129038, which is in almost complete LD with rs12913832 and were able to predict blue and brown eye colour with accuracies of 89% and 94%, respectively. Ruiz *et al.* [97] developed a model, named *Snipper* by using the IrisPlex SNPs together with *HERC2* and *OCA2* SNPs that were partly or in strong LD. They were able to slightly increase the prediction accuracy for intermediate (green-hazel) eye colour. Using *Snipper* they were also able to predict eye colour based on incomplete SNP profiles using a naïve Bayesian likelihood-based classification approach.

The first DNA tests for hair colour were restricted to red vs. non red predictions, using variants in *MC1R* [96,116]. In 2011, Branicki *et al.* [81] presented a model that was able to predict all four hair colour categories (red, black, brown and blond) with high prediction accuracies using 22 SNPs from 11 genes (*MC1R*, *HERC2*, *IRF4*, *TYR*, *EXOC2*, *SLC45A2*, *TYRP1*, *OCA2*, *SLC24A4*, *ASIP* and *KITLG*) in a Polish population of 385 individuals. Based on this study and the IrisPlex model, the first assay for simultaneous prediction of both eye and hair colour, the HIrisPlex, was developed and validated for forensic application [98,110]. By using these 22 SNPs, and a model-underlying database of 1878 individuals, they report prediction probabilities for blond (AUC=0.84), brown (AUC=0.74), red (AUC=0.93) and black (AUC=0.86) hair colour categories as well as light or dark shade [98,100]. The strongest association was observed between variants in *MC1R* and red hair colour. Hence, red hair colour had the highest prediction accuracy. The models for both eye and hair colour are now also included in a forensically validated commercial MPS assay, the ForenSeq™ DNA Signature Prep Kit [117].

The first comprehensive study on skin colour prediction for forensic application was by Maronas *el al.* [99] in 2014. From a discovery panel of 59 markers typed in 285 samples from Europeans and non-Europeans, they selected 10 SNPs from eight genes (*SLC45A2, SLC24A5, KITLG, ASIP, TYRP1, OCA2, SLC24A4* and *TPCN2*) for a skin colour predictive test. Skin colour was categorised as white, intermediate or black based on mean value of reflectance measured with a reflectance spectrophotometer. Using a naïve Bayes classification system, the model was able to predict white (AUC=0.999) and black (AUC=0.966) skin colour with high accuracies. However, the AUC for intermediate skin colour was lower, 0.803. Predicting skin

colour can be challenging due to the intercontinental distribution of skin colour variants. In a heterogenous global population, it can be difficult to differentiate if a SNP is associated with a trait or population stratification [118]. Due to a small sample size and few populations represented in the study by Maronas *et al.* [99], it was suggested to re-examine the 10 SNPs in a more extensive study [100].

In 2017, Walsh *et al.* [100] presented a skin colour study on 2025 individuals from 31 global populations. By carefully selecting 36 SNPs from 16 genes, they developed a model capable of predicting skin colour on a global scale. Phenotypes were categorised following the Fitzpatrick scale [119], using the final categories: "very pale", "pale", "intermediate", "dark" and "black". Using multinomial logistic regression modelling, the AUC values for very pale (0.83), dark (0.98) and dark-black (0.99) skin colour were considerably higher than pale (0.76) and intermediate (0.78) skin colour. They also compared the prediction ability of the 10 SNPs from Maronas *et al.* [99] with the 36 SNPs in a three category model on the global population data. The prediction accuracies using the 36 SNPs were considerably higher than with the 10 SNPs.

The skin colour prediction model by Walsh *et al.* [100] was later published as an extension of the HirisPlex system, enabling simultaneous eye, hair and skin colour predictions [101]. The HIrisPlex-S model including a total of 41 SNPs for eye, hair and skin colour prediction has now also been included in several MPS assays for both the MiSeq and Ion Torrent sequencing platforms [120–123].

1.4 Human population structure

Genetic difference between human population groups arises partly because humans are not fully interbreeding [25,26]. Geographical distance and geophysical barriers have led to genetic isolation and local selection of mutations [25]. Furthermore, selection pressure is influenced by environmental factors such as climate, diet, or exposure to diseases. Thus, early human groups from different geographic regions have different genetic features.

1.4.1 Biogeographical ancestry inference

BGA inference in forensic genetics utilises the knowledge of the worldwide population genetic structure from human population studies [124–127]. Rosenberg *et al.* [124] estimated that in

five to seven world groups, approximately 4% of the genetic variation was between groups. This variation can be exploited for BGA inference in for instance clinical and anthropological research studies by using AIM panels consisting of thousands of genetic markers. However, due to limited amounts of available DNA in forensic samples, smaller panels of AIMs have been preferred. These panels consist of generally less than 200 AIMs [25,89,128]. When using few AIMs, it is important to have a well-balanced panel with carefully selected markers based on their ability to differentiate between global groups [25,129]. Ideally, the AIM has a fixed allele in one population and not in others. It is also important to use a substantial number of reference populations [130,131]. During the past two decades many panels have been designed to distinguish between continental population groups [130,132,133]. Most of the panels consists of autosomal markers such as SNPs, MHs and/or insertion-deletions (INDELs) [133–135].

The first AIM-SNP assay for forensic application was commercially developed, by the DNAprint Company in 2003 [136]. Using 176 autosomal AIMs typed with the SNPstream system it was possible to distinguish four continental populations. Subsequently, DNA tests presented multiplexes using SBE-PCR, e.g., a 34-plex by the SNP for ID Consortium [137,138]. The marker selection process for the 34-plex panel was criticised for using limited population data, leading to ascertainment bias [25]. In the following years, several studies presented AIM-SNPs with the focus on designing a balanced panel to differentiate global groups [88,89,128].

In 2009, Kosoy *et al.* [128] presented a panel of 128 SNPs (the Seldin panel) with the focus on African, European and Native American ancestry. When analysing the panel with additional populational samples, Kidd *et al.* [139] showed that the Seldin panel had potential for a broad global application of ancestry inference but was not optimal for European and Asian populations. In 2013-2014, Kidd *et al.* [89,140] presented an efficient and globally useful panel of 55 non-overlapping SNPs (namely the Kidd panel) together with an online prediction tool, FROG-kb (https://frog.med.yale.edu/FrogKB/, accessed 09. February 2024) [89,140]. Inclusion of further reference populations in FROG-kb using the 55 Kidd panel have demonstrated the possibility of higher resolution of ancestry, especially for North African and South-Sentral Asian populations [131,141]. Another panel of 74 SNPs was designed to improve inference within Eastern Asia [142]. Simultaneously, Phillips *et al.* [88] developed a panel with 128 AIMs, the Global AIM-SNP panel, overlapping with the 55 Kidd panel, to further differentiate Native American and Oceanian populations and to provide a near perfectly

balanced differentiation of the five continental population groups. During this time period, MPS was emerging in forensic genetic research laboratories, and the already designed AIM panels were included in MPS assays for BGA analysis [143]. The Seldin panel and the Kidd panel were included in commercially available MPS assays validated for forensic analysis, the 165 AIM-SNP Precision ID Ancestry Panel by Thermo Fisher Scientific (including primer pairs for both Kidd and Seldin panels) [144] and the ForenSeq[TM] DNA Signature Prep Kit by Verogen (including primer pairs for the Kidd panel together with the HIrisPlex SNPs and other forensically relevant markers) [117].

The growing availability of fully open resources of whole genome sequencing data [145–147] and the application of MPS are now allowing larger panels to continuously being developed together with prediction models using large reference datasets for differentiation of up to seven global population groups [132,133,148–150].

1.5 Using forensic DNA phenotyping in casework

After many years of research, analytical techniques for FDP analysis have been developed and validated for case work [23]. However, FDP analysis is practiced in a few EU member states only [26]. Schneider *et al.* [26] presented an overview of the legal situation concerning forensic DNA phenotyping in 24 EU member states, for which information was available (updated from a report by Samuel & Prainsack on behalf of the VISAGE project (Samuel & Prainsack, 2018)). Only two countries, the Netherlands and Slovakia, had permission by law to use FDP analysis. Germany had recently changed the law to permit FDP of appearance and age, but FDP of ancestry analysis is still forbidden. In seven countries, FDP was not explicitly legally regulated, and was considered allowed for practical purposes. The legal and regulatory framework for eight of the European countries can be viewed in details in the report by Samuel & Prainsack [151]. In a European-wide online survey from 2019, 105 laboratories from 32 countries answered questions regarding implementation of MPS in forensic genetics, including DNA phenotyping in casework [22]. Between 11 and 20% of the participants reported that they had used phenotype SNPs in casework, and 24% had used ancestry SNPs. However, 15-21% reported that they were not legally permitted to perform this type of analysis [22].

The main concerns in the debate about the legalisation of DNA phenotyping in casework focus on the discrimination against minority groups, privacy, and over-interpretation of the findings

[152,153]. This is also an ongoing public debate in Norway where FDP is so far used in some selected cases only. Norway has no laws explicitly regulating the use of such intelligence tool. In 2018, a report by the Norwegian Biotechnology Advisory Board was published discussing the ethical challenges using FDP in police investigations [154]. The main conclusions were that the use of FDP analysis could enhance public general safety in Norway. Therefore, the police should be allowed to use quality assured DNA tests in cases of serious manner. However, the usage should be investigated in more detail prior to implementation.

The Centre for Forensic Genetics in Tromsø is in the process of implementing FDP applications using MPS. Prior to implementation of FDP analysis in a forensic laboratory, both the analysis methods and the prediction tools need to be validated. These validation studies provide information on errors and limitations that should be included in the reports to the police, so they can make an informed decision about the application of the FDP outcome in the specific investigation. Moreover, continuous research is needed in order to further improve these DNA tests.

1.6 Objectives

- Evaluate MPS analysis and prediction tools for eye and hair colour prediction (Paper 1).
- Evaluate MPS analysis and prediction tools for ancestry analyses (Paper 2).
- Develop an improved model and strategy for eye colour prediction in Scandinavian populations (Paper 3).
- Increase the understanding of the genetics for eye colour variation (Paper 4, 5 and 6).

2 Material and Methods

This chapter provides an overview of the main methods used in the papers included in this thesis. A more detailed description of all methods and material can be found in the papers.

2.1 Study population

Samples have been collected in Tromsø and Bodø, in Northern Norway, from 2015 to 2018. In total 756 individuals volunteered to participate by donating blood and answering a questionnaire about family ancestry, description of eye colour, hair colour and skin colour. Additionally, for the first 540 individuals, high resolution photographs of the eyes and hair were taken, and skin lightness was measured with a Natural Colour System Colour Scan 2.0 under the upper arm. Among the remaining ~200 individuals eye photographs were only taken of some of them. To avoid related individuals, participants were also asked not to participate if they knew that a close relative had participated.

In total 396 women and 360 men at the age 18 to 70 (average 32.8 years) participated. They were all residing in Norway but had various family ancestry (Paper 2). The vast majority (~80%) of the participants had Norwegian ancestry. Depending on the information available and the quality of the photographs, they were included in the different studies as follows:

Paper 1

540 participants with hair colour information and 519 participants with eye colour information were selected for evaluation of the genotyping performance of the 24 HIrisPlex SNPs using the ForenSeq™ DNA Signature Prep Kit and the prediction performance of the SNPs using the HIrisPlex web tool.

Paper 2

730 participants with ancestry information were selected for evaluation of the genotyping performance of 56 aSNPs using the ForenSeq™ DNA Signature Prep Kit and the prediction performance of the SNPs using the prediction tools: UAS, FROG-kb and GenoGeographer.

Paper 3

Discovery data set: 757 individuals from Denmark, Sweden or Italy collected in different studies by our colleagues in Denmark [155,156], were used to genotype 44 pigmentary variants for selection of the 12 variants that were used in the eye colour prediction models.

Model data set: 523 individuals of the Norwegian study population with eye colour information were selected for genotyping of 14 variants to evaluate the performance of nine eye colour prediction models.

Paper 4

40 participants were selected based on eye colour and genotype information found in Paper 1 and 3 to experimentally haplotype three variants associated with eye colour: rs12913832, rs1800407 and rs74653330.

Paper 5

The *OCA2-HERC2* region was genotyped by MPS in 94 individuals (43 with blue eye colour and 51 with brown eye colour) with the *HERC2* rs12913832:AA and AG genotype. These individuals were selected based on eye colour and genotype information found in Paper 1 and 3. Based on the genetic findings in the *OCA2-HERC2* region, eight candidate variants were selected and genotyped in 446 individuals with eye colour information.

Paper 6

The MPS data of the 94 individuals from Paper 5 was used to search for CNVs associated with blue eye colour.

2.2 Ethical considerations and approvals

All participants gave informed and signed consent and were subsequently anonymised. They voluntarily contributed and were given adequate information about storage and usage of the material. No identifiable information has been published in any of the papers.

The use of the samples collected in Norway (Paper 1-6) was approved by the Faculty of Health Sciences, UiT The Arctic University of Norway (reference number 2021/2034). The material used in the discovery dataset in Paper 3 was approved by the Danish Ethical Committee (M-

20090237, H-4-2009-125, and H-3-2012-023), the Ethical Committee of Azienda Ospedaliera Ospedal Sant'Anna di Como (U.0026484.23-11-2012), and the Ethical Committee of the University of Milan-Bicocca (P.U. 0033373/12).

2.3 DNA genotyping

2.3.1 Massively parallel sequencing on the Illumina platform

Currently there are three main NGS bench-top sequencers used in forensic genetics: the Illumina's MiSeq FGx and the ThermoFisher's Ion Torrent PGM and Ion S5 [15]. In the studies of this thesis, the MiSeq FGx Illumina platform was used. Hence only this platform is discussed in detail.

Prior to genotyping by MPS, libraries are prepared by attaching 5´ and 3´adapter oligos to fragmented or amplified DNA (**Figure 3**). For multiplexing and pooling of samples, indexes/barcodes can also be ligated to the DNA fragments [14]. On the Illumina instrument, the sample is loaded onto a flow cell which is coated with adapter-complimentary oligos, enabling binding of single-strand sequencing libraries [157] (**Figure 3**). Illumina uses sequencing by synthesis technology [157]. This technology utilises fluorescently labelled nucleotides that are incorporated into DNA template strands during the sequencing cycle where they are detected and imaged, followed by enzymatically cleavage allowing the next cycle of incorporation. In this way, millions of clusters can be sequenced in parallel. Post sequencing, the output data is analysed and aligned with a reference genome by a bioinformatic software.
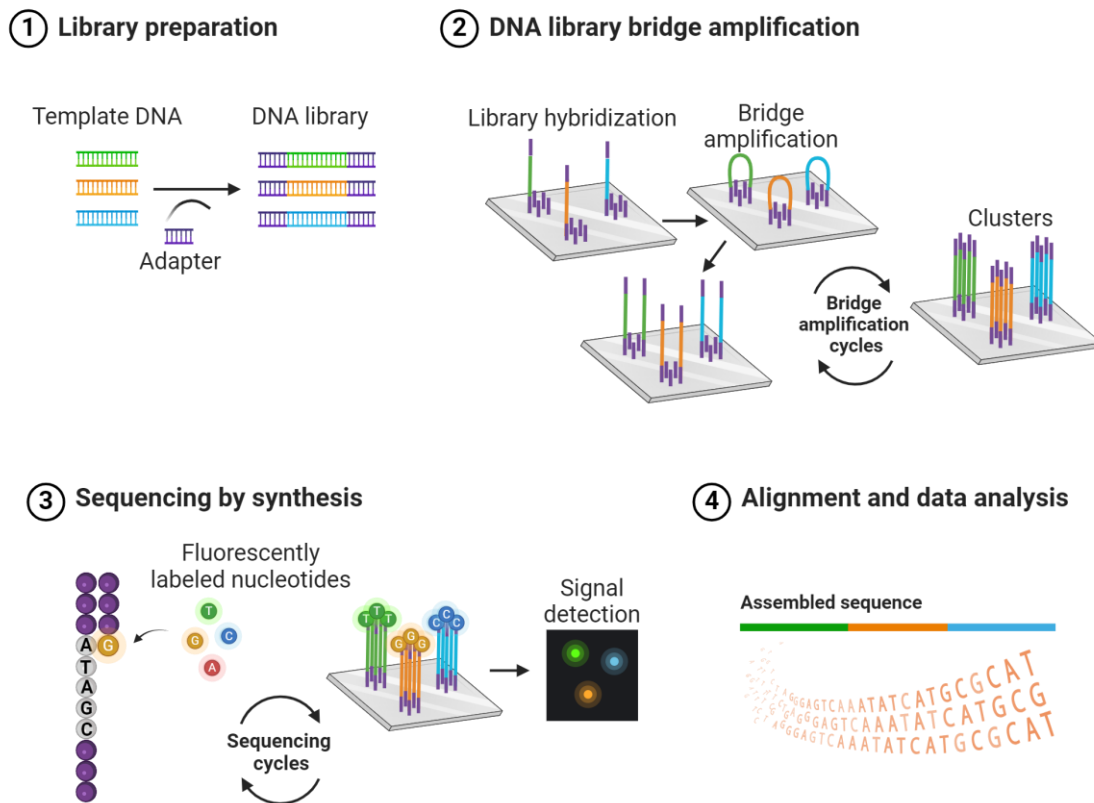
Figure 3: Principle of sequencing on the Illumina platform. (1) Fragmented template DNA is ligated with adaptors in the library preparation stage. (2) Libraries with pooled single strand DNA templates hybridise to the flow cell where cycles of bridge amplification start, resulting in clusters of amplified DNA. (3) One fluorescent labelled nucleotide is incorporated to each amplified template strand per sequencing cycle, followed by signal detection. (4) Sequences are assembled and aligned with reference genome for further data analysis [157]. Created with BioRender.com

The purpose of genotyping a forensic sample is to screen for variants in markers of established forensic significance. This requires targeted enrichment for the sequences of interests in order to separate them from the whole genomic background. Compared with whole-genome sequencing, targeted sequencing ensures cost effective, accurate and efficient typing of the selected regions in order to identify sequence variants with high specificity. Currently, there are to major approaches, the PCR amplicon-based target enrichment and hybrid capture based enrichment [158].

20

Targeted sequencing using the ForenSeq^{TM} DNA Signature Prep kit

The ForenSeq^{TM} DNA Signature Prep kit from Verogen (evaluated in Paper 1 and 2) utilises the PCR amplicon-based target enrichment approach (**Figure 4**). With this approach, multiple primers are designed to work simultaneously in a multiplex reaction to amplify the sequences of interest, prior to library preparation [158]. This is in particular successful for samples with limited amount of DNA, such as forensic samples. The ForenSeq kit is designed and validated for forensic analyses using the MiSeq FGx (Illumina) sequencing platform. It is part of an integrated workflow for library preparation. sequencing and data analyses in the Universal Analysis Software (UAS). The kit provides two primer mixes, Primer mix A and B, where the Primer mix B includes primers for 27 autosomal STRs, 24 Y-STRs, 7 X-STRs, 94 identity SNPs, 56 BGA SNPs and 22 phenotype SNPs enabling identification, BGA and phenotype analyses simultaneously. The kit was considered highly relevant for routine casework at the Centre for Forensic Genetics and was therefore evaluated in Paper 1 for phenotype analyses and in Paper 2 for BGA analyses.
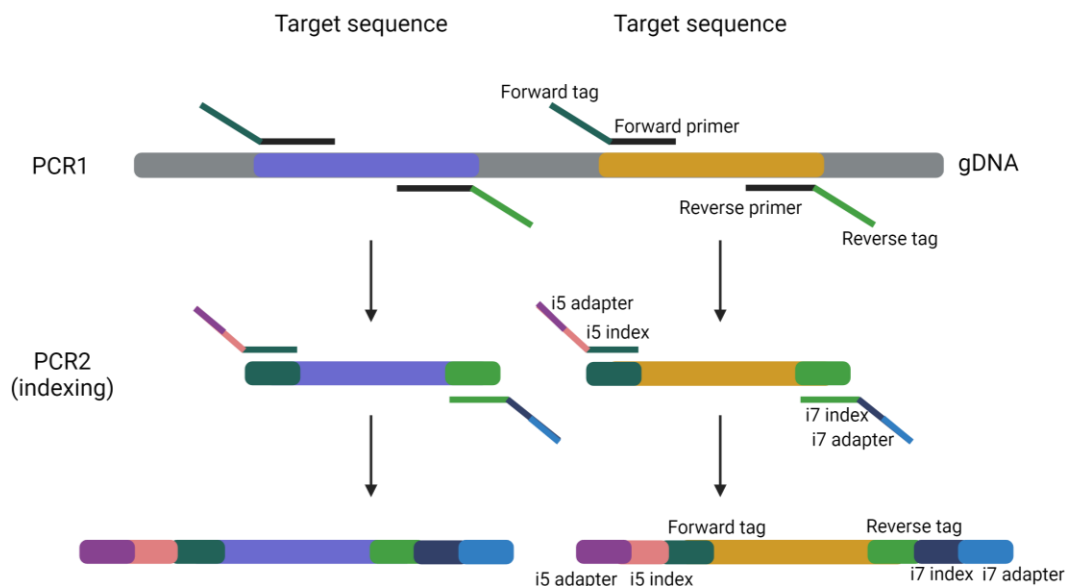
Figure 4: Principle of PCR amplicon-based target enrichment with the ForenSeq^{TM} DNA Signature Prep assay. In PCR1, tagged target specific primers are multiplexed to amplify sequences

of interest. In PCR2, tagged target fragments are indexed with adapters that are complementary to the oligos on the flow cell for sequencing. Created with BioRender.com

Targeted sequencing using the SureSelectXT HS2 target enrichment system

The SureSelectXT HS2 target enrichment system by Agilent Technologies, utilises the hybrid capture approach (**Figure 5**). The principle for this approach is to enrich regions of interest by employing probes/baits [158]. The probes are designed to hybridise to the sequence of interest and to isolate and capture the fragments using magnetic beads. Prior to target enrichment, the input DNA is fragmented by either acoustic shearing or enzymatic cleavage. The SureSelectXT HS2 system provides a one-day workflow of the target enrichment and library prep for the Illumina sequencing platform. Agilent also provides a freely available software, SureDesign, to easily create custom panels. This was highly suitable for the study in Paper 5, as the aim was to search for undiscovered variants for eye colour prediction in the *OCA2-HERC2* locus of ~500kbp. A custom probe library was designed to capture 427 954bp in the locus using 15 627 probes (Paper 5). Using the SureSelectXT HS2 system with paired-end sequencing on the Illumina platform also resulted in sufficient coverage throughout the region to perform CNV analysis in Paper 6.
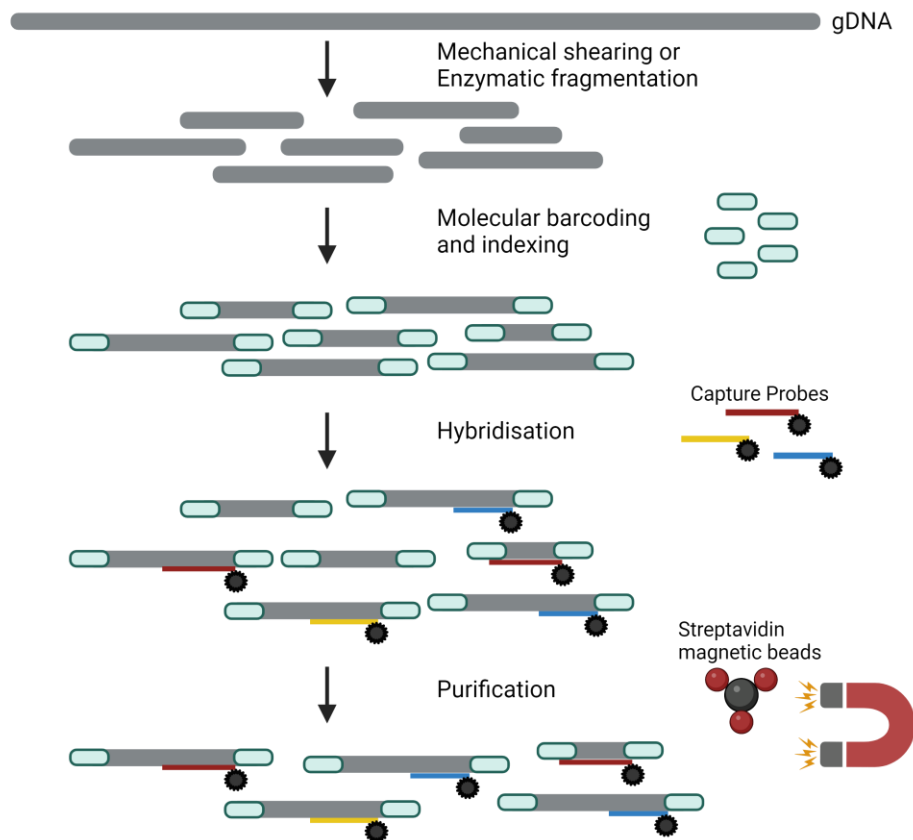
Figure 5: Principle of Target enrichment by hybrid capture using SureSelect. Genomic DNA is first fragmented. Then, molecular barcodes, dual indexes and adapters for the Illumina platform are ligated to the fragments. Fragments are hybridised with the probe capture library and captured by streptavidin magnetic beads prior to PCR amplification and sequencing. Created with BioRender.com.

2.3.2 Single base extension PCR (SBE-PCR)

Single base extension PCR (SBE-PCR) with the commercial kit SNaPshot (Life Technologies), also called minisequencing, is a commonly used typing method for SNPs in forensics [13] (**Figure 6**). Because only a single base needs to be typed, primers are designed to anneal immediately adjacent to the target SNP. The primer is extended with a fluorescent labelled dideoxynucleotide (ddNTP) that is complementary to the target SNP position. Post PCR, the fragments can be separated and detected by CE. Multiplexing is possible by designing primers that differ in length, in addition to utilising different fluorescent colour labels on each of the four ddNTPs.
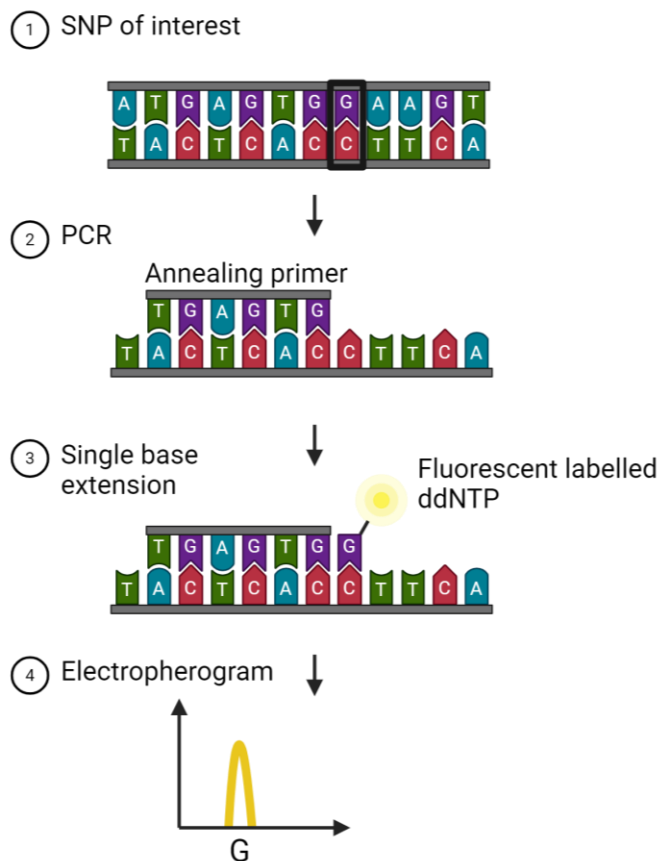
Figure 6: Principle of SNP typing using single base extension PCR (SBE-PCR). Template DNA with the target SNP (1) is amplified with the primer annealing immediately upstream to the SNP (2). The polymerase incorporates a fluorescent labelled ddNTP in the SNP position, complementary to the template (3). A peak representing the SNP allele, G, is presented in an electropherogram (4). Created with BioRender.com

The SNaPshot multiplex system is highly suitable when only few SNPs are analysed. In the studies of Paper 3 and 5, panels of 8-12 candidate SNPs were screened in ~500 individuals for eye colour association and prediction analysis. Compared to high-throughput sequencing, SBE-PCR by SNaPshot is both cost effective and time saving when genotyping few SNPs.

2.3.3 Experimental haplotyping using droplet digital PCR (ddPCR)

Droplet digital PCR using Bio-Rad's QX200 Droplet Digital™ PCR (ddPCR™) system, enables genetic analysis, of maximum two SNP variants, in a single DNA molecule [159]. Prior to PCR, ~1nl droplets are emulsified using oil, containing DNA and PCR mixture (including

fluorescent labelled probes) (**Figure 7**). Up to 20 000 droplets are generated per sample, ideally containing maximum one DNA molecule each. PCR amplification occurs independently inside the droplets. A droplet reader detects fluorescence through a two-colour detector (hence only two variants can be detected per analysis). Droplets are classified as positive or negative based on their fluorescent amplitude. Absolute quantification is calculated based on droplet volume and the proportion of positive droplets relative to the total number of droplets.

The purpose of the study in Paper 4 was to determine which alleles in heterozygous SNPs were on the same chromosome. Heterozygous *HERC2* rs12913832:AG individuals (genotyped in Paper 1) that were also heterozygous at either *OCA2* rs1800407 or *OCA2* rs74653330 (genotyped in Paper 1 and 3) were selected. The genomic distance between the *HERC2* rs12913832 and the two *OCA2* variants was ~135kb and could thus not be experimentally haplotyped using the MPS platform. Illumina platforms with the sequencing by synthesis technology are only able to read lengths of maximum 300bps [14]. Using ddPCR, the theoretical upper limit of DNA fragment length is ~500kb in droplets of ~1nl. It has been experimentally demonstrated that it is possible to analyse fragments up to 200kb [160,161]. Hence, ddPCR was a promising method to haplotype *OCA2-HERC2* variants. Moreover, with new high molecular weight (HMW) DNA extraction methods longer fragments can be isolated than what was possible with traditional methods [162].
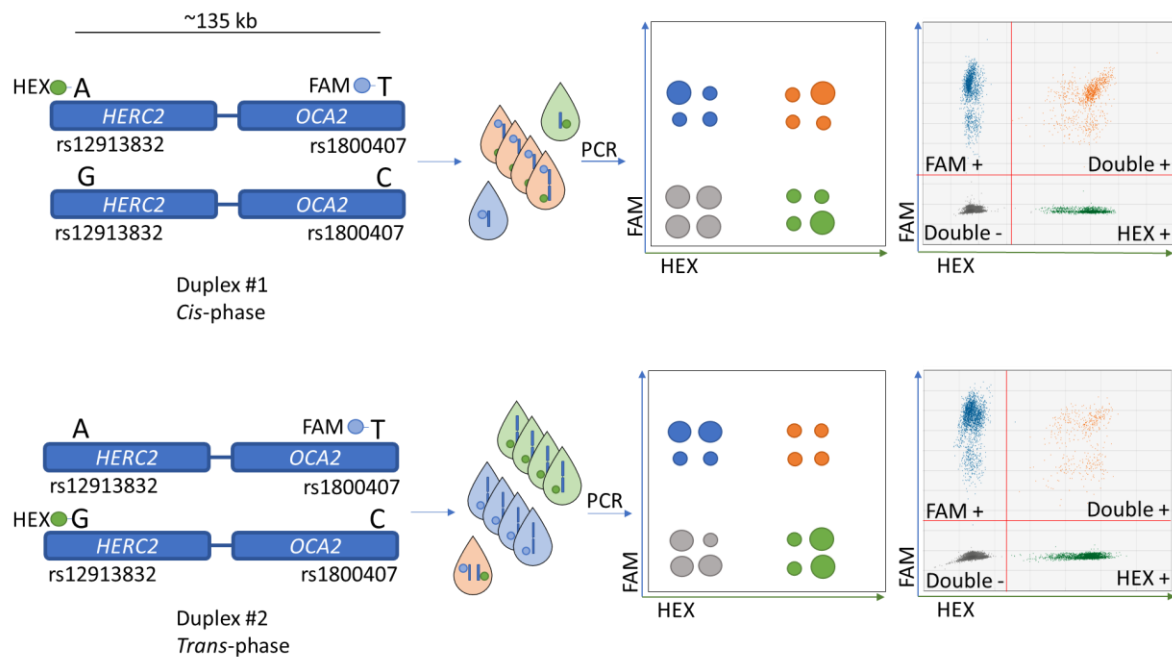
Figure 7: Experimental haplotyping by droplet digital PCR (ddPCR). A genomic DNA sample together with HEX/FAM-labelled *HERC2-OCA2* duplex assays is emulsified into droplets prior to PCR and droplet fluorescence readings. The 2-D plots show expected fluorescence clusters for linked (top) and unlinked (bottom) alleles. The following droplet clusters are shown: double negative (grey), FAM positive (blue), HEX positive (green) and FAM and HEX positive (orange). Thresholds (red lines) are drawn between clusters to ensure correct designation of droplets.

2.4 Analysis of sequencing data

MPS produces large amounts of data when sequencing millions of DNA fragments. Thus, bioinformatic pipelines need to be designed in order to analyse the output data.

In Paper 1 and 2, the UAS, that is integrated in the ForenSeq workflow, was used to analyse the genetic data. The software provided a user-friendly output of the data, presenting genotype data for the different markers in addition to BGA and phenotype predictions (pSNPs and aSNPs evaluated in paper 1 and 2, respectively).

In Paper 5, we adopted and modified a bioinformatic pipeline already established by the research group at the Section of Forensic Genetics at the University of Copenhagen for targeted MPS data obtained using an Illumina platform (**Figure 8**). The sequencing output are automatically converted to FASTQ files by a software on the platform. Furthermore, a

bioinformatic pipeline is designed to process the data in order to perform genetic analyses of interest. FASTQ-files containing all the output data are trimmed using different bioinformatic tools to remove low quality data, as well as molecular barcodes and adapters that were ligated to the DNA fragments in the library preparation step prior to sequencing. Furthermore, the trimmed files are aligned to human reference genome and converted into readable binary alignment map (BAM) files. These files can then be used to analyse the DNA, e.g., different tools can be used to detect single base variants or CNVs. In Paper 6 we used the BAM files from Paper 5 to search for CNVs (**Figure 8**).
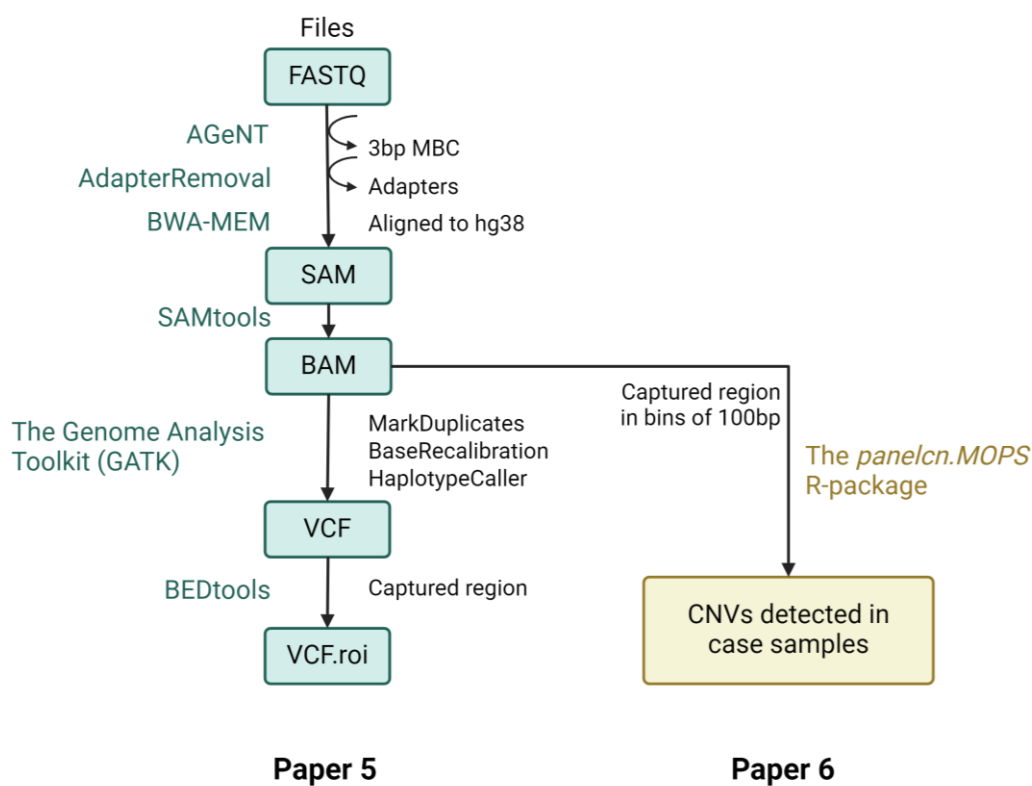
Figure 8: Bioinformatic pipeline used to process and analyse the targeted MPS data in Paper 5 and 6. SAM=sequence alignment map, BAM=binary alignment map, VCF=variant call format, roi=region of interest, CNV=copy-number variation. Created with BioRender.com

In contrast to a commercial software, an in-house bioinformatic pipeline provides analysis flexibility and transparency for quality assurance through every step. Because we were screening for (possibly rare) genetic variations between blue and brown eyed individuals in the whole *OCA2-HERC2* region, a self-designed pipeline was the most appropriate choice.

2.5 Prediction models and tools

Prediction models and tools vary in how they are trained, which statistical approach is used and how they report the predictions.

In Paper 1, we utilised the HIrisPlex prediction tool freely available online (https://hirisplex.erasmusmc.nl/, accessed 24 February 2024), for eye and hair colour predictions using the 24 pSNPs typed by the ForenSeq kit. The eye and hair colour prediction tool within the UAS (provided with the kit), did not predict hair colour shade, and was therefore not used in this study.

In Paper 2, the UAS was used to infer BGA and the results were compared to the predictions produced by two other freely available tools, the FROG-kb and GenoGeographer. These were chosen based on the aSNP panel that was genotyped utilising the kit. Additionally, the three tools infer BGA using different statistical models with different underlying reference data, which can influence the prediction outcome. Hence, a comparison study of these tools was valuable when evaluating BGA for forensic usage.

In Paper 3, we developed and compared prediction models using a discovery data set to select candidate variants, and a model data set to both train and test the various models using leave-one-out cross-validation. Models were designed to both compare with and improve existing models. Thus, they included different numbers of variants (both commonly used SNPs for FDP and new variants) and different reporting systems (quantitative and categorial).

3 Results (summary of papers)

This chapter includes summaries of Paper 1 to 6 (**Figure 9**).
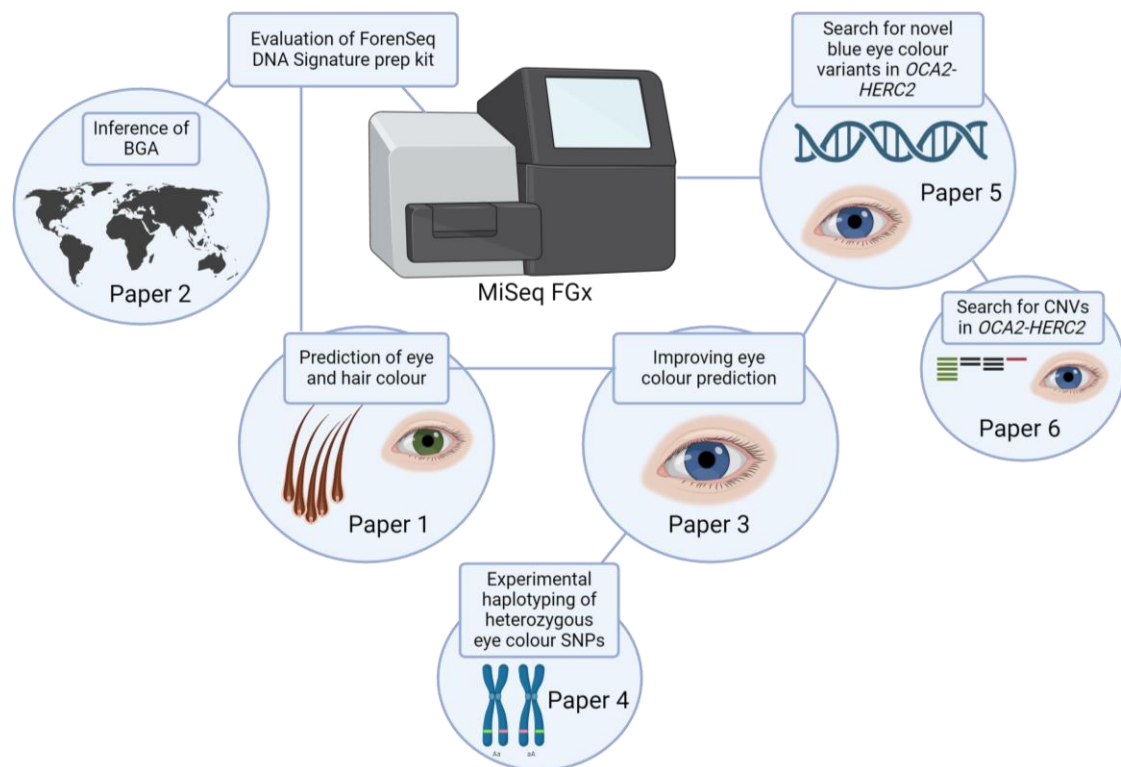
Figure 9: In paper 1 and 2 we evaluated the technical performance of Verogen`s ForenSeq[TM] DNA Signature Prep kit and the predictive performance of HIrisPlex for eye and hair colour predictions, as well as various prediction tools for BGA inference. Based on limitations found in already developed systems for eye colour prediction (as demonstrated in Paper 1), new SNPs and prediction models were presented in Paper 3. Furthermore, in Paper 4 we explore the genetics in heterozygous *HERC2* rs12913832 individuals with varying eye colour (from blue to brown). In Paper 5 and 6 we further explore the genetics in individuals with blue eye colour that were predicted to have brown eye colour with rs12913832 in Paper 1 and 3. Created with BioRender.com

3.1 Paper 1

Predicting eye and hair colour in a Norwegian population using Verogen's ForenSeq™ DNA signature prep kit.

Forensic DNA phenotyping (FDP) is emerging as an investigative tool in forensic casework. The tool is still not used in routine casework in Norway but is being implemented in the forensic laboratories. Prior to implementation it is highly important to evaluate both the genotyping method and the prediction tools used. The purpose of this study was to evaluate the technical and predictive performance of the HIrisPlex SNPs when genotyped using Verogen's ForenSeq™ DNA Signature Prep kit on the MiSeq FGx system and the HIrisplex web tool (https://hirisplex.erasmusmc.nl/, accessed 27. February 2024). The study population comprised 540 individuals residing in Norway, where blue or intermediate eye colour, and light hair colour such as blond or light brown is common. We demonstrated that the system was highly reliable typing complete HIrisPlex SNP profiles with DNA input down to 125 pg. False homozygous genotypes were observed in low input samples. These can have an impact on the prediction outcome, especially when observed in the most important predictor for eye colour, rs12913832. We therefore suggested to increase the interpretation threshold from 30 to 100 reads for low input samples, or to avoid analysing such samples at all. When predicting eye colour with the HIrisPlex web tool, blue and brown eye colour were predicted with high accuracies (AUCs of 0.85 and 0.94, respectively). No individuals were predicted to have intermediate eye colour. Based on the most important eye colour predictor, rs12913832, only 70.9% of individuals with the GG genotype had the expected blue eye colour, and only 79% and 39% of individuals with the AA and AG genotype, respectively, had the expected brown eye colour. Furthermore, by using quantitative eye colour measurements (PIE-scores), we detected population specific genotype-phenotype associations. Interestingly, individuals with the rs12913832 AA genotype and Norwegian ancestry had significantly higher PIE-scores (perceived as intermediate towards blue eye colour) than rs12913832 AA individuals of non-northern European ancestry. Prediction of hair colour showed somewhat lower accuracies than eye colour predictions. Red and black hair colour had the highest AUC values (0.97 and 0.93 respectively), whereas blond and brown hair had the lowest (0.72 and 0.70, respectively). The low accuracies for blond and brown hair colours may be, at least partly, the result of age-depending hair colour darkening, for which there is no data in our study.

3.2 Paper 2

Biogeographical ancestry analyses using the ForenSeq™ DNA Signature Prep Kit and multiple prediction tools.

The purpose of this study was to evaluate the technical and predictive performance of the 56 aiSNPs using Verogen's ForenSeq™ DNA Signature Prep kit on the MiSeq FGx system and the UAS. The prediction outcome from the UAS was further compared to other prediction tools, FROG-kb and GenoGeographer. The aiSNP panel was typed in 730 individuals with various biogeographical ancestries. A reference set of 200 Norwegians was included in the underlying reference data in FROG-kb and GenoGeographer prior to prediction analysis. A test set of 530 individuals was used to evaluate the prediction outcomes. Of the 530 test individuals, 503 were of European ancestry (of which 395 were Norwegian), 22 were non-European (North African, Sub-Saharan African, Asian, East Asian, Middle Eastern and Siberian) and five had family co-ancestry from either Europe and Asia or Europe and Africa. The kit performed well with complete aiSNP profiles with DNA input down to 250pg. We observed some SNPs with average low read depth, making them disposed for drop out. Hence, we suggested being careful when typing the 56 aiSNPs in samples with lower than the recommended DNA input of 1ng. Both Europeans and non-Europeans were predicted with high accuracy using the FROG-kb and GenoGeographer. The Europeans were also predicted with high accuracy using the UAS, but due to limited underlying reference populations, less than half of the non-Europeans could be predicted. As expected, none of the tools was able to correctly predict the individuals with co-ancestry. The reason for discrepancies in prediction outcome between the tools may be due to different underlying reference data and statistical models used. Hence, it is important to evaluate these tools prior to implementation for forensic casework. The UAS is highly suitable for initial BGA inference, but it should be supplemented with FROG.kb and/or GenoGeographer.

3.3 Paper 3

Prediction of Eye Colour in Scandinavians Using the EyeColour 11 (EC11) SNP Set.

The purpose of this study was to develop an eye colour prediction model with improved prediction accuracies, compared to the results from Paper 1. We selected genetic variants for eye colour prediction from 44 SNPs discovered in two previous in-depth sequencing studies of individuals with incorrectly predicted eye colour using the IrisPlex SNPs. The 44 SNPs, including the IrisPlex SNPs, were typed in a European population (n=757) using the iPLEX™

Assay (Agena Bioscience, Hamburg, Germany) and analysed with matrix-assisted laser desorption-ionization time of flight mass spectrometry (MALDI-TOF MS) using the MassARRAY Analyzer 4 System (Agena Bioscience, Hamburg, Germany). Based on seven different mathematical models the SNPs were ranked according to the mean variable importance. In total, 11 variants (EC11) from 6 different genes (*HERC2, OCA2*, *SLC45A2*, *TYRP1*, *SLC24A4* and *TYR*) were selected for eye colour prediction and were further genotyped using the SNaPshot^{TM} multiplex system in an independent Norwegian study population (n=523). Four of the six IrisPlex SNPs were included (rs12913832, rs16891982, rs1800407 and rs12896399), of which rs12913832 was ranked as the best performing SNP. The variants rs121918166 and rs74653330 had independently very low frequencies in the European population (<0.01). When combined, they were ranked as the second-best performing variants. Nine eye colour prediction models were developed using leave-one-out cross-validation on the Norwegian data set. The nine models included three different reporting systems (quantitative, two-category and three-category) and three different SNP sets (EC11, IrisPlex Norway and rs12913832). The prediction accuracies were further compared with the IrisPlex Web tool using the three-category system. EC11 had the smallest error across all reporting systems, whereas the IrisPlex Web had the highest. By thoroughly analysing these models based on error, sensitivity and specificity, we demonstrate tree main considerations. The first consideration was the reference population. The IrisPlex Norway and IrisPlex Web were based on the same SNPs (the IrisPlex SNPs) but were modelled on different reference populations. IrisPlex Norway was modelled on the target population and showed overall a lower prediction error than IrisPlex Web. The second consideration was the SNP set. EC11 showed a slightly lower prediction error than the other three models. Inclusion of the *OCA2* variants rs121918166 and rs74653330 in EC11 increased the prediction accuracy in blue-eyed Norwegians that were incorrectly predicted using rs12913832 and IrisPlex Norway. However, the differences between models using 11 SNPs (EC11), 6 SNPs (IrisPlex Norway and IrisPlex Web) and 1 SNP (rs12913832), were so small that our findings support previous studies suggesting that it might be sufficient to use only rs12913832 for eye colour prediction in two categories (blue and brown). The third consideration was the reporting strategy. The overall correct predictions across the different SNP sets were higher using the two-category system as opposed to the three-category system.

3.4 Paper 4

Experimental long-distance haplotyping of *OCA2-HERC2* variants.

Based on the knowledge from Paper 1 and 3 we hypothesised that rs12913832 AG individuals with a missense *OCA2* mutation (in rs74653330 or rs1800407) on the opposite chromosome (*trans*-phase) than the derived G allele in rs12913832, would have lighter eye colour than the individuals with the same variants on the same chromosome (*cis*-phase). To test this, we performed experimental haplotyping by droplet digital PCR of *HERC2* and *OCA2* variants in 40 individuals with heterozygous *HERC2* rs12913832 that were observed to have blue, intermediate and brown eye colour in Paper 1. Because the genomic distance between rs12913832 in *HERC2* and the *OCA2* variants was ~135kbp, we first demonstrated that it was possible to isolate long DNA fragments (up to 210 kb) using the Monarch® HMW DNA Extraction Kit. These were long enough to experimentally haplotype *OCA2-HERC2* variants. Then, using droplet digital PCR, we were able to identify three haplotypes in this study population; rs12913832:A-rs1800407:T (n=22), rs12913832:A-rs1800407:C (n=1) and rs12913832:A-rs74653330:T (n=16). The one individual with rs12913832:A-rs1800407:C had the expected brown eye colour, and rs12913832:A-rs74653330:T individuals (n=16) had lighter eye colour (higher PIE-scores) than rs12913832:A-rs1800407:T individuals. However rs12913832:A-rs1800407:T individuals had varying eye colours, questioning the effect of rs1800407 on eye colour. These findings demonstrate that we still do not fully understand the genetics of eye colour.

3.5 Paper 5

Association between Variants in the *OCA2-HERC2* Region and Blue Eye Colour in *HERC2* rs12913832 AA and AG Individuals.

Based on Paper 1, 3 and 4 we hypothesised that undiscovered variants in *OCA2-HERC2* are associated with blue eye colour in rs12913832:AA and AG individuals that have previously been predicted to have brown eye colour. In this study, we performed an in-depth sequencing analysis of the *OCA2-HERC2* region in rs12913832:AA and AG individuals from the study in Paper 1. The ~500kbp *OCA2-HERC2* region was sequenced in 96 individuals using the SureSelectXT HS2 target enrichment system on a MiSeq FGx. The individuals were grouped into a control group of 51 individuals (with brown eye colour) and a study group of 43 individuals (with blue eye colour). Furthermore, selected candidate variants were genotyped using the SNaPshot™ multiplex system in 446 individuals from the Norwegian study population. Based on statistical association testing (Fisher´s exact test and Kruskal-Wallis test)

five novel *OCA2-HERC2* variants were selected based on their association with blue eye colour (rs74409036:A, rs78544415:T, rs72714116:T, rs191109490:C and rs551217952:C). The novel variants were assessed together with the *OCA2* variants rs74653330 and rs121918166 that were found to be associated with blue eye colour in these individuals in Paper 3. In total 86% of the blue-eyed rs12913832:AA and AG individuals carried at least one of these seven variants. Interestingly, blue eye colour in all the three rs12913832:AA individuals could be explained. When analysed in the Norwegian study population, 11 haplotypes were identified by estimation using PHASE based on these seven variants in combination with the rs12913832:AA, AG and GG genotypes. These haplotypes were highly correlated to eye colour (linear regression, adjusted R^2 =0.80). Thus, these novel variants were suggested to be included in future prediction models. Because some variants in the *OCA2-HERC2* region are also associated with skin pigmentation, association of these variants with skin colour was also assessed in the Norwegian study population. However, lighter pigmentation was only observed in rs12913832:AA and AG individuals with the rs74653330:T allele.

3.6 Paper 6

Association between copy number variations in the *OCA2-HERC2* locus and human eye colour.

In this study, we analysed the MPS data from Paper 5 for CNVs using the R-package *panelcn.MOPS* – CNV detection tool for NGS panel data. Based on read depth, we assessed if small duplications or deletions could be associated with blue eye colour in rs12913832 AA and AG individuals. With the preliminary results on this small dataset, we identified candidate regions in *OCA2* or near the *OCA2* enhancer, with duplications and deletions that could potentially explain blue eye colour in these individuals (25 regions in rs12913832 AG individuals and two regions in rs12913832 AA individuals). To our knowledge, this study is the first to present CNVs to be associated with eye colour variation in rs12913832:AA or AG individuals. However, more research is needed to confirm these results.

4 Discussion and future perspectives

Prior to implementation of new analyses methods in the forensic laboratory it is important to thoroughly evaluate and validate the methods in order to reveal performance accuracy and limitations that might be important to take into consideration when conducting the analysis. The focus of the studies in this thesis was the performance of both genotyping and prediction accuracy of DNA tests for FDP analyses. Limitations revealed in the prediction of eye colour were investigated further to improve the prediction precision. These studies can be used as a foundation for implementation of FDP analysis, with the aim to provide these analyses as an investigative tool for the police.

The ForenSeq^{TM} DNA Signature Prep Kit (Verogen) on the MiSeq FGx platform provides a streamlined workflow for genotyping, data analysis and prediction of eye colour, hair colour and BGA. In Paper 1 and 2 we evaluated the genotyping of the 22 pSNPs (HIrisPlex SNPs) and the 56 aSNPs (55 Kidd panel plus rs1919550) for phenotyping and ancestry analysis using this kit. The main results were in agreement with others and showed that it is a sensitive and robust typing system [117,163–165]. Our biggest concern was undiscovered allele drop out, leading to false homozygous genotypes and thereby possibly misleading predictions. This can in general have implications when it occurs in SNPs for appearance and ancestry prediction, but it can have a major impact if it occurs in the main predictor for eye colour, *HERC2* rs12913832, as an incorrect genotype might result in completely wrong prediction. Importantly, allele drop out was observed in apparently high-quality samples following the default criteria for interpretation set by the Universal Analysis Software (UAS). We therefore suggested to use a more stringent interpretation threshold and not analysing samples with less than the recommended input DNA of 1ng. These findings highlight the necessity of a thorough evaluation prior to implementation.

With adjusted analyses criteria, we consider the ForenSeq kit suitable for casework in our laboratory. The advantage utilising this kit for FDP analysis is that DNA profiling with STRs can be analysed simultaneously. In addition to the Primer mix B that includes primers for both FDP analysis and DNA profiling, the kit also includes a Primer mix A for DNA profiling analyses only. In this way, the forensic laboratory can choose between the two targeted primer mixes depending on which analyses the police requests. Evaluation of the genotyping performance of the STRs and Primer mix A was out of the scope for this thesis, but other studies

35

have evaluated the genotyping of these markers in both primer mixes and also found them to be reliable [117,163]. Currently, the ForenSeq[TM] DNA Signature Prep kit is the only commercial kit for simultaneous FDP and DNA profiling analyses on the MiSeq FGx system, which is advantageous in routine forensic casework.

Another important step in implementation of the analysis is an in-house validation of the genotyping system. Because DNA from a crime scene is sampled from different environments, the sample often contain little DNA, are partly degraded, contain PCR inhibitors or are a mixture of DNA from several contributors. Hence, analysing crime scene DNA can often be challenging. A validation of the method should therefore include systematic studies of inhibition, mixture, degradation and sensitivity, as well as repeatability and reproducibility. As part of the evaluation in Paper 1 and 2, we performed a sensitivity study only. The other systematic studies of the quality parameters will be the next step towards implementation in our laboratory. Mixture detection and deconvolution is challenging with binary markers such as bi-allelic SNPs. In a forensic routine workflow, mixture detection will usually be done following the STR analysis. Using the ForenSeq kit, the analyst will get an immediate indication if the sample is single source based on the STR results, which is preferable for FDP analysis. However, albeit challenging, several studies have demonstrated the possibility of detecting mixtures in SNP panels using MPS by analysing allele read counts and heterozygosity, which could also be assessed in our in-house validation [120,121,143,166]. Testing the inhibitor-tolerance of the kit´s chemistry might be especially beneficial for PCR-based methods for MPS that rely on DNA polymerisation. Studies have shown that the initial PCR step in library preparation might be the bottleneck for sequencing quality on the Illumina platform, and that the choice of DNA polymerase in high-throughput sequencing is important [167–169]. Sidstedt *et al.* [169] tested the impact of two inhibitors, humic acid and hematin, on the ForenSeq chemistry when analysing STRs. Both the inhibitors negatively affected the initial PCR resulting in lower read counts and fewer successfully typed loci. We demonstrated in Paper 1 and 2 that unsuccessfully typed loci might cause misleading FDP predictions, highlighting the importance of a robust chemistry when analysing forensic samples.

Parallel to our studies, the VISAGE consortium has developed the VISAGE Basic Tool (BT) and the VISAGE Enhanced Tool (ET) for appearance and ancestry inference [121,170]. Compared to the ForenSeq kit, the VISAGE BT includes the HIrisPlex-S SNPs, adding analysis for skin colour, as well as an increased number of autosomal aSNPs for BGA inference. This

tool was developed using the Ampliseq chemistry for the Ion S5 platform, but it has also been evaluated to be a reliable and robust tool for the PowerSeq and ForenSeq chemistry on the MiSeq FGx System [122,123]. Although, the tool is yet not commercially available it could be considered for evaluation in our laboratory as it provides some more prediction information. The VISAGE ET for Appearance and Ancestry inference, provides an enhanced panel for BGA including autosomal SNPs (bi- and tri-allelic SNPs), X-SNPs, Y-SNPs and autosomal Microhaplotypes, which may be highly valuable to increase accuracy in BGA inference. Interestingly, the tool also includes markers for prediction of eyebrow colour, freckling, hair shape and male pattern baldness (in addition to the HIrisPlex-S markers), all showing medium accuracies (AUCs varying from 0.60-0.80) [23].

4.1 Biogeographical ancestry inference

The ForenSeq system uses the 56 aSNP panel to infer BGA with the UAS. In Paper 2, we compared prediction accuracies using the UAS and two freely available tools FROG-kb and GenoGeographer. All three tools demonstrated accurate predictions for individuals with European ancestry. However, due to the tools´ different underlying reference populations and statistical methods, discrepancies were observed when inferring BGA for individuals with non-European ancestry. The UAS could only differentiate three global groups: Europeans, Africans and East Asians. Hence, more than half of the non-Europeans could not be inferred. Notably, our study population for the non-Europeans comprised 22 individuals only. No individuals of Native American and Oceanian ancestry were included; thus, prediction accuracies of these population groups could not be assessed. However, our findings support using a multiple prediction tool approach to increase the prediction accuracy for BGA inference in forensic casework, which is also advocated by others [171,172]. In order to use a multiple-tool approach in, we will have to decide on a reporting strategy, especially in cases where the tools provide different prediction outcomes. One strategy could be to use the UAS for initial analysis because it is included in the ForenSeq workflow, and it accurately predicts Europeans. Furthermore, if an inconclusive prediction is obtained, the FROG-kb and GenoGeographer should be used. In cases of ambiguous results by all three tools, the results might be reported as inconclusive.

The inference resolution of BGA highly depends on both the number of AIMs and the reference populations used. The 56 aSNP panel used in the ForenSeq system includes the 55 Kidd panel, which was designed to differentiate the main global population groups based on a small

balanced panel [89]. STRUCTURE analyses using this SNP panel have shown the ability to differentiate up to nine global regions, highly dependent on the reference populations used [89,131,141]. The underlying reference data in the model for BGA predictions is especially important because the prediction outcome directly depends on the reference populations available. The correct ancestry can only be inferred if the actual population is represented among the reference populations. It is therefore recommended to provide the reference population dataset used in the report to the police [23,26]. Furthermore, when reporting ancestry inferences of an unknown DNA donor, it is important not to overinterpret the results. Subcontinental ancestry can be difficult to predict due to migration and less distinctiveness between populations. It is therefore more challenging to find AIMs with high enough informativeness for subpopulations. If the AIM panel is designed to differentiate global groups, it is thus important to report only at this level and not subpopulations.

The recent progress in MPS is enabling improved panels to be developed using a larger number of AIMs than the Kidd panel, being able to differentiate some subcontinental populations. Recently, several non-commercial MPS assays have been developed and validated for forensic application being able to differentiate up to seven continental groups, e.g., the MAPlex, the MPSplex, the VISAGE BT and the VISAGE ET [121,122,149,170,173]. However, a challenge using such assays in the forensic laboratory is the current lack of a streamline workflow, including data processing and statistical analysis tools for predictions. The BGA analysis is somewhat more complicated because a bioinformatic pipeline must be implemented and validated. Two statistical analysis tools that are recognised as reliable methods for BGA analysis with these assays are STRUCTURE and PCA plots [25,174,175]. To perform the BGA estimation with these tools, the forensic laboratory has to obtain their own global reference dataset. This can be done by collecting SNP data from publicly available whole-genome databases such as the 1000 Genomes Project (1KGP) [176], the Human Genome Diversity Project – Centre d′ Etude du Polymorphisme Humain (HGDP-CEPH) [177], the Simons Genome Diversity Project (SGDP) [146] and Estonian Biocentre Human Genome Diversity Panel (EGDP) [147], but the compilation requires some bioinformatic knowledge. For some AIM panels, the SNIPPER app suit (http://mathgene.usc.es/snipper/, accessed 04. March 2024) provides reference population sets that can be downloaded by the user, e.g. for the VISAGE BT ancestry panel and for the ForenSeq DNA Signature 56 aSNP panel, enabling BGA analysis. Additionally, SNIPPER provides both LR and PCA analysis where users can upload their own SNP data. LR analysis is recommended when reporting the inference [25].

Another important consideration when inferring BGA, is the tools' ability to detect co-ancestry in individuals with admixed backgrounds. Detection of co-ancestry can be difficult using relatively few autosomal markers for continental differentiation, especially if co-ancestry is not represented in the reference data [25]. For instance, it can be difficult to differentiate co-ancestry of individuals with recent familial admixed backgrounds and individuals from regions with historical population admixture, generally found in continental margin regions. As an example, Middle Eastern populations often have a mixed genetic structure from Europe and Asia; thus, it can be difficult to know if an individual has familial co-ancestry from Europe and Asia or if the individual is Middle Eastern. This might explain why two of the individuals with co-ancestry from Europe and Asia in our study (Paper 2) were predicted to be Middle Eastern using GenoGeographer. It is therefore advocated that inference of biogeographic ancestry should also include uniparental DNA analysis (Y-chromosomal and mitochondrial DNA) [26]. Recent advancements have enabled the development of MPS tools for Y-analysis and whole mitochondrial genome sequencing for forensic DNA samples [178,179]. Additionally, some MPS assays for BGA analyses, e.g., the VISAGE ET and PhenoTrivium, have also included Y and/or X SNPs in addition to the autosomal markers enhancing the possibility of detecting ancestral admixture [148,150].

4.2 Prediction of eye and hair colour

In paper 1, we evaluated the performance of the HIrisPlex web tool when predicting eye and hair colour in a Norwegian study population. The population had high frequencies of blue and intermediate eye colour, and blond and brown hair colour. Supporting the results from other studies, we demonstrated high prediction accuracies for blue and brown eye colour, as well as red and black hair colour [98,111–113,180]. However, in this study we also revealed some possibly population-specific genotype-phenotype associations highlighting the importance of population-specific testing prior to implementation. Notably, the UAS included in the ForenSeq system also provides predictions of eye and hair colour using the same statistical model as the HIrisPlex web tool. However, the UAS was not utilised because it does not provide predictions for hair shade.

Prediction of hair colour is in general challenging because the phenotype can change by age. A person can have blond hair in early childhood and brown hair as an adult, a phenomenon called age-dependent darkening. Additionally, hair can lose its pigmentation and turn grey or white in late adulthood [53], and some people might experience hair loss (baldness) [54]. In Paper 1 we observed most inaccuracies in individuals with brown hair who were predicted to have blond hair. Despite not having information about childhood hair colour, we pointed towards age-dependent hair colour darkening as a possible explanation for these inaccuracies. Kukla-Bartoszek *et al.* [52] demonstrated this by studying individuals who had reported blond hair colour in early childhood and had later undergone hair colour darkening. The darkening negatively affected the prediction accuracy using the HIrisPlex system. Due to the lack of biomarkers for hair colour darkening, the HIrisPlex model cannot differentiate individuals that are affected by age-dependent change from the individuals that have remained blond [98]. Itou *et al.* [181,182] have studied hair colour darkening in Japanese individuals and found that the total amount of melanin and the mol% of pheomelanin and DHI-eumelanin correlated with age-dependent hair colour darkening. They also found that the darkening of hair in females might be due to enlargement of the melanosomes with age [183]. However more research needs to be conducted to understand the molecular mechanisms causing this change, and to understand why this happens to some people and not others. In our study the participants reported hair colour in their twenties to avoid occurrence of hair greying and hair loss. However, it had been highly interesting to have information about childhood hair colour in our study population because age-dependent hair darkening is recognised as a common phenomenon.

The prediction guide approach (PGA) provided with the HIrisPlex web tool is highly useful for interpretation of the prediction outcome because it takes shade into account in addition to the basic hair colour categories (blond, brown, red and black). Except for red hair, the colour categories overlap, especially for dark blond and light brown hair. In our study (Paper 1), 331 individuals had dark blond or light brown hair colour. Using the PGA model, we considered this group as one because the hair colours are difficult to differentiate. This might also eliminate some of the inaccuracies that are possibly caused by age-dependent darkening. We demonstrated an increase in prediction accuracy from 61% to 76% for this group, suggesting to always apply the PGA for interpretation of the hair colour predictions.

For eye colour predictions using the IrisPlex web tool, the greatest challenge is the intermediate category. In Paper 1, 34% of the individuals in the Norwegian study population had

intermediate eye colour and none of these were predicted correctly. Many studies have highlighted this shortcoming of the model [79,111–113]. However, despite many attempts on improving prediction accuracy for intermediate eye colour, we yet lack good markers for this category [71,97,109,184]. The main issue might be that "intermediate" is not one colour. The category comprises of many perceived eye colours e.g. green and hazel, which also makes it challenging to categorise. In Paper 1 we discussed the challenges with subjective categorisation, and the difficulty of comparing studies. We categorised the Norwegian population based on observation from photographs of the eyes. Nine untrained observers categorised the eyes into four groups: blue, intermediate-blue, intermediate-brown and brown. We observed some disagreement between observers, especially between blue and intermediate-blue, and brown and intermediate-brown. Maybe some of the individuals in the intermediate-blue and intermediate-brown categories would have been categorised as blue or brown if we only used three categories. However, disagreements in how different people will perceive eye colour are expected to occur [185].

The alternative to predict eye colour in categories is to use an objective quantitative approach [156,186,187]. Although using quantitative measurements might be suitable for genotype-phenotype association studies when searching for new variants, it may not be practical when reporting to the police, as the report should be easy to interpret. Atwood *et al.* [188] assessed the reporting of available service providers of FDP analyses in Australia and highlighted the need for standardisation. The IrisPlex system uses a three-category reporting system, but based on the recognised challenges to predict intermediate eye colour, Pietroni *et al.* [155] suggested to only use two categories (blue and brown). In paper 1 and 3 we demonstrated that the intermediate category is both difficult to identify and to predict. By developing nine different models based on three different marker panels (EC11, IrisPlex or rs12913832), and three different reporting systems (quantitative, two-category or three-category), we showed that the two-category system increased prediction accuracy compared to the three-category system, regardless of the marker panel used (Paper 3). Furthermore, the overall difference in error rate between EC11, IrisPlex and rs12913832 was so small that it may be sufficient to predict eye colours solely based on rs12913832. The Section of Forensic Genetics in Denmark is offering FDP of eye colour to the police based on rs12913832 and the two-category system. They report the prediction as likelihood ratios (LR). When using only two categories they use two hypotheses, H_1: The person has brown eyes and H_2: The person has blue eyes. In Paper 3 we argue that using only rs12913832 will ensure that no genetic markers linked to disease will be

used, which is an ethical concern raised in the debate about legalisation of FDP [11]. Moreover, we argued that rs12913832 is already included in SNP panels for BGA inference, making it convenient when performing FDP analyses for both BGA and eye colour.

Variations in population specific associations between eye colours and the IrisPlex SNPs has been shown to affect the prediction outcome in several studies, suggesting that the model should both be trained and tested on the intendent target population [97,102,155,184,189,190]. This was demonstrated in Paper 3 by comparing the IrisPlex web tool with a IrisPlex model trained on the Norwegian study population from Paper 1. With the IrisPlex Norway model we were able to obtain some intermediate eye colour predictions, which was not possible with the IrisPlex web tool. Hence, the IrisPlex Norway had an overall lower error rate than the IrisPlex web tool. Additionally, in our evaluation of the eye colour predictions using the IrisPlex web tool in the Norwegian population in Paper 1, we observed that the prediction accuracy for blue eye colour was lower than reported by other European populations [98,112,113]. When using the quantitative measurement Pixel Index of the Eye (PIE)-score [156] to assess genotype-phenotype associations we disclosed some rare associations. Despite a small sample size, we showed for the first time that Norwegians carrying the rs12913832:AA genotype had significantly higher PIE-score ("more blue" eye colour) than non-northern Europeans with the same genotype. This finding was highly surprising because the A allele in rs12913832 act as an *OCA2* enhancer, which should lead to normal pigment production. It has been suggested that the non-synonymous *OCA2* SNP rs1800407 act as a penetrance modifier of rs12913832 and could therefor explain the lighter eye colour in these individuals [77,156]. However, we did not observe this association in our study. Instead, we observed an association between the PIE-score and *SLC45A2* rs16891982 in the rs12913832:AA individuals, a SNP commonly used for BGA inference. Because the *SLC45A2* encodes the MATP protein, with possibly similar functions as OCA2 [84,85], we hypothesised that the lighter eye colour in Norwegians could be due to an instable MATP protein in rs16891982:G individuals, which was demonstrated in a mouse model by Le *et al*. [191]. The gene *SLC45A2* may therefore also be a suitable target searching for new genetic variants for blue eye colour. However, this was not pursued further in the studies of this thesis but could be investigated in future projects.

Similar inaccuracies for eye colour predictions as observed in the Norwegian study population in Paper 1 have also been reported in other Scandinavian populations [80,155]. A majority, but not all individuals with blue or brown eye colour are predicted correctly with IrisPlex (or

rs12913832). A research group in Denmark searched for new genetic variants associated with brown eye colour in rs12913832:GG individuals, and blue eye colour in rs12913832:AG individuals [80,192]. They identified variants in *OCA2* associated with blue eye colour and variants in *TYRP1*, *TYR* and *SLC24A4* associated with brown eye colour. These studies were used as a foundation for the EC11 panel, that was developed attempting to improve eye colour predictions in Scandinavian populations. In Paper 3 we demonstrated that the EC11 SNP panel was slightly better than the IrisPlex panel and rs12913832 when predicting eye colour in the Norwegian study population. Due to the inclusion of the non-synonymous *OCA2* variants rs121918166 and rs74653330, the EC11 two-category model increased the prediction accuracy of blue-eyed rs12913832:AG and AA individuals. These two variants were found at very low frequencies in the Scandinavian populations (<0.01), and none were detected in the Italian population used in the study. Globally, the variant allele rs74653330:T is also found in East Asian populations associated with skin colour variation [83], whereas the variant allele rs121918166:T is mainly found in Scandinavians [80]. These variants have previously been suggested to act as penetrance modifiers of rs12913832, similar to rs1800407, explaining blue eye colour in rs12913832:AG individuals [80]. Our findings in Paper 3 support this suggestion. Thus, the EC11 panel should be considered for eye colour predictions in Scandinavia.

Despite the increased correct predictions using the EC11 panel, we still observed inaccuracies, demonstrating that we do not fully understand the genetics of eye colour, especially in individuals with the genotype rs12913832:AG. In Paper 1 we observed that rs12913832:AG individuals in the Norwegian population had varying eye colour from blue to brown, with PIE-scores ranging from -1 (perceived brown) to 1 (perceived blue). This is not unique to our study [156]. We also observed in Paper 1 and 3 that individuals with heterozygous rs1800407 or rs74653330 on a rs12913832:AG background had varying PIE-scores. It has been hypothesised that the chromosomal phase of these alleles in compound heterozygous individuals might be associated with eye colour variation [80,156]. In detail, in blue eyed individuals, the *OCA2* variants are expected to be on the opposite chromosome (*trans*-phase) to the derived rs12913832:G allele [80,156]. In this way, one chromosome would harbour rs12913832:G, reducing transcription of *OCA2,* while the other chromosome would harbour the non-synonymous variant leading to a variant OCA2 protein with possibly reduced function. Contrary, in brown-eyed individuals, the derived rs12913832:G allele is expected to be on the same chromosome (*cis*-phase) as the *OCA2* variant, leaving one chromosome with enhanced *OCA2* transcription of a normal functioning OCA2 protein. Haplotyping of these variants has

previously been estimated computationally using the software PHASE [80], but so far not experimentally. The challenge with experimental haplotyping of the *HERC2* rs12913832 SNP with the *OCA2* variants is the long genomic distance between them (~135kb). Due to the rapid advancement in long-read sequencing, new HMW DNA extraction methods have been developed, enabling the isolation of much longer DNA fragments than with traditional extraction methods [162]. In Paper 4 we demonstrated that it was possible to isolate long enough DNA fragments with a commercial HMW extraction kit to haplotype *HERC2* and *OCA2* SNPs. The experimental haplotyping revealed that all compound heterozygous rs12913832 and rs74653330 individuals had the derived rs12913832:G allele in *trans* phase with the rs74653330:T variant. These individuals had intermediate and blue eye colours, supporting the theory about rs74653330 acting as a penetrance modifier of rs12913832. However, we did not observe a correlation between chromosomal phasing of rs12913832-rs1800407 and eye colour, questioning the importance of rs1800407 in eye colour formation. Notably, the sample size in this study was small, and more individuals should be haplotyped.

Because of the evidential strong selection pressure on *OCA2-HERC2* in blue eyed Europeans [41], we furthermore investigated this region in the attempt to increase our knowledge about the genetics of eye colour formation (Paper 5 and 6). By sequencing the ~500kbp region encompassing *OCA2* and *HERC2* rs12913832, we identified both new single nucleotide variants and CNVs, i.e. small deletions or duplications, to be associated with blue eye colours in rs12913832 AA and AG individuals in the Norwegian study population. We recognise that the sample size was small and thus all statistical association calculations in Paper 5 were based on raw *p*-values. More samples are therefore needed for better statistical power.

All five single nucleotide variants identified in the *OCA2-HERC2* locus to be associated with blue eye colour were located within introns (Paper 5). In contrast to exon variants that sometimes alter the amino acid sequence, the functional consequences of intronic variants may be difficult to predict. Some intronic variants are functional, e.g. by affecting mRNA splicing or expression of a gene, and can thus modulate the phenotype [78,193,194]. However, intronic variants can also be associated with a phenotype by being in LD with another functional variant. Only one of the five identified variants in our study was predicted to be in a regulatory region by the SCREEN: Search Candidate cis-Regulatory Elements by ENCODE platform [195]. The remaining four variants might therefore be in strong LD with other unidentified functional variants. Notably, not all regulatory regions in the genome have been defined, which means

that the lack of predictions for being in a regulatory region does not necessarily mean that the variants are not in such a region.

The detection of CNVs in *OCA2-HERC2* was especially interesting because there has been little information about associations between CNVs from MPS data and eye colour variation so far. Currently, most GWAS focus on SNPs when studying associations between traits and genetic variation, whereas copy-number-based GWAS from MPS data has been scarce [196]. This might be partly due to methodological difficulties and limited availability of large datasets [196,197]. However, genomic structural variation is well known to impact human traits [198]. The rs12913832 in *HERC2* is known to act as a distal enhancer of *OCA2* by forming a chromatin loop to the *OCA2* promoter [78]. Structural variation in the gene could therefore potentially disrupt this chromatin-loop formation, and thereby downregulate pigment production. In Paper 6 we identified 32 regions in *OCA2* or close to rs12913832 with CNVs that were significantly associated with blue eye colour in rs12913832:AG individuals. Additionally, 14 regions in rs12913832:AA individuals were identified to be associated with blue eye colour using raw *p*-values. These findings were preliminary and should be verified in a larger study population. However, based on the results from this study, we suggest more focus on CNVs in the future when studying normal pigmentation variation.

In the studies that are included in this thesis, we have pointed out limitations with existing tools for eye and hair colour predictions. Furthermore, we have identified new variants and CNVs that can improve eye colour predictions in Scandinavia. The focus was on rs12913832:AA and AG individuals that were incorrectly predicted by the IrisPlex model (and rs12913832). However, we also observed incorrect predictions in individuals carrying the rs12913832:GG genotype, also using the EC11 prediction models, demonstrating that we do not fully understand the genetic determinants of eye colour. Furthermore, none of the newly identified variants in our studies could be associated with intermediate eye colour. A recent large eye colour GWAS including almost 195 000 individuals identified 124 independent associations explaining only about 50% of human eye colour variation, demonstrating that eye colour might be more complex than previously thought [199]. They also identified genes involved in iris morphology and structure to be associated with eye colour. Hence, investigating genes for stromal structure might increase our understanding about eye colour variations. Furthermore, functional and epigenetic studies might be required to better understand the genetics of eye colour variation and pigmentation in general.

The purpose of FDP analyses is to provide investigative leads to the police where no other leads are available, similar to an eyewitness. Our intention is to provide a DNA test for the police with detailed, accurate and reliable information. Although the genetic understanding of human pigmentation variation is not complete, we demonstrate that the current DNA tests for FDP provide high prediction accuracies for blue and brown eye colour, red and black hair colour and ancestry on a continental scale. Combined, these can give an indication to what a person might look like, which can be highly valuable for the police in order to find potential suspects in criminal investigations.

5 Main conclusions

- The ForenSeq^{TM} DNA Signature Prep kit is highly reliable and sensitive for genotyping the pSNPs (HIrisPlex SNPs) and aSNPs on the MiSeq FGx platform. Detection of unexpected false homozygous loci in seemingly high-quality samples, demonstrated the necessity of this evaluation in order to adjust the interpretation criteria.

- Biogeographical ancestry on a continental scale can be inferred with high accuracies using the 56 aSNP panel. Due to discrepancies in prediction outcome observed between the tools using different underlying reference data and statistical approaches, a multiple-prediction-tool approach is recommended.

- With current available prediction tools, blue and brown eye colour and red and black hair colour have the highest prediction accuracies, whereas intermediate eye colour and blond and brown eye colour are more difficult to predict accurately.

- It might be sufficient to predict eye colour in two categories (blue and brown) using rs12913832 only. However, inclusion of the non-synonymous *OCA2* variants rs121918166 and rs74653330 increase prediction accuracy for blue eye colour in Scandinavians.

- The *OCA2-HERC2* locus harbours more variants (single nucleotide variants and CNVs) associated with eye colour variations that might increase prediction accuracy. However, more research is needed to increase the genetic understanding of human eye colour formation.

References

1   Jeffreys AJ, Wilson V, Thein SL. Hypervariable 'minisatellite' regions in human DNA. *Nature* **1985**;314:67–73. https://doi.org/10.1038/314067a0.

2   Butler JM. Short Tandem Repeat Markers. Fundam. Forensic DNA Typing, Elsevier Inc.; **2010**, p. 147–73. https://doi.org/10.1016/B978-0-12-374999-4.00008-4.

3   Sundar T. DNA-register til bruk i straffesaker. *Tidsskr Den Nor Legeforening* **2000**;120.

4   Butler JM. Short Tandem Repeat (STR) Loci and Kits. Adv. Top. Forensic DNA Typing Methodol., Elsevier Inc.; **2012**, p. 99–139. https://doi.org/10.1016/B978-0-12-374513-2.00005-1.

5   Butler JM. Statistical Interpretation Overview. Adv. Top. Forensic DNA Typing Interpret., Elsevier Inc.; **2015**, p. 213–37. https://doi.org/10.1016/B978-0-12-405213-0.00009-9.

6   Ludeman MJ, Zhong C, Mulero JJ, Lagacé RE, Hennessy LK, Short ML, et al. Developmental validation of GlobalFiler^{TM} PCR amplification kit: a 6-dye multiplex assay designed for amplification of casework samples. *Int J Legal Med* **2018**;132:1555–73. https://doi.org/10.1007/s00414-018-1817-5.

7   Butler JM. Capillary Electrophoresis: Principles and Instrumentation. Adv. Top. Forensic DNA Typing, Elsevier Inc.; **2012**, p. 141–65. https://doi.org/10.1016/B978-0-12-374513-2.00006-3.

8   Butler JM. STR Genotyping and Data Interpretation. Fundam. Forensic DNA Typing, Elsevier Inc.; **2010**, p. 205–27. https://doi.org/10.1016/B978-0-12-374999-4.00010-2.

9   Ensenberger MG, Lenz KA, Matthies LK, Hadinoto GM, Schienman JE, Przech AJ, et al. Developmental validation of the PowerPlex® Fusion 6C System. *Forensic Sci Int Genet* **2016**;21:134–44. https://doi.org/10.1016/j.fsigen.2015.12.011.

10   Butler JM. Single Nucleotide Polymorphisms and Applications. Adv. Top. Forensic DNA Typing Methodol., Elsevier Inc.; **2012**, p. 347–69. https://doi.org/10.1016/B978-0-12-374513-2.00012-9.

11   Kayser M. Forensic DNA Phenotyping: Predicting human appearance from crime scene material for investigative purposes. *Forensic Sci Int Genet* **2015**;18:33–48. https://doi.org/10.1016/J.FSIGEN.2015.02.003.

12   Gill P. An assessment of the utility of single nucleotide polymorphisms (SNPs) for forensic purposes. *Int J Legal Med* **2001**;114:204–10.

13   Fondevila M, Børsting C, Phillips C, de la Puente M, Santos C, EUROFORGEN-NoE Consortium, et al. Forensic SNP Genotyping with SNaPshot: Technical Considerations for the Development and Optimization of Multiplexed SNP Assays. *Forensic Sci Rev* **2017**;29:57–76.

14   Børsting C, Morling N. Next generation sequencing and its applications in forensic genetics. *Forensic Sci Int Genet* **2015**;18:78–89. https://doi.org/10.1016/J.FSIGEN.2015.02.002.

15   Ballard D, Winkler-Galicki J, Wesoły J. Massive parallel sequencing in forensics: advantages, issues, technicalities, and prospects. *Int J Legal Med* **2020**;134:1291–303. https://doi.org/10.1007/s00414-020-02294-0.

16   Oldoni F, Kidd KK, Podini D. Microhaplotypes in forensic genetics. *Forensic Sci Int Genet* **2019**;38:54–69. https://doi.org/10.1016/J.FSIGEN.2018.09.009.

17   Quenez O, Cassinari K, Coutant S, Lecoquierre F, Le Guennec K, Rousseau S, et al. Detection of copy-number variations from NGS data using read depth information: a diagnostic performance evaluation. *Eur J Hum Genet* **2021**;29:99–109. https://doi.org/10.1038/s41431-020-0672-2.

18   Alkan C, Coe BP, Eichler EE. Genome structural variation discovery and genotyping. *Nat Rev Genet* **2011**;12:363–76. https://doi.org/10.1038/nrg2958.

19   Di Resta C, Galbiati S, Carrera P, Ferrari M. Next-generation sequencing approach for the diagnosis of human diseases: open challenges and new opportunities. *EJIFCC* **2018**;29:4–14.

20   Deiner K, Bik HM, Mächler E, Seymour M, Lacoursière-Roussel A, Altermatt F, et al. Environmental DNA metabarcoding: Transforming how we survey animal and plant communities. *Mol Ecol* **2017**;26:5872–95. https://doi.org/10.1111/mec.14350.

21   de Knijff P. From next generation sequencing to now generation sequencing in forensics. *Forensic Sci Int Genet* **2019**;38:175–80. https://doi.org/10.1016/j.fsigen.2018.10.017.

22   Gross TE, Fleckhaus J, Schneider PM. Progress in the implementation of massively parallel sequencing for forensic genetics: results of a European-wide survey among professional users. *Int J Legal Med* **2021**;135:1425–32. https://doi.org/10.1007/s00414-021-02569-0.

23   Kayser M, Branicki W, Parson W, Phillips C. Recent advances in Forensic DNA Phenotyping of appearance, ancestry and age. *Forensic Sci Int Genet* **2023**;65:102870. https://doi.org/10.1016/j.fsigen.2023.102870.

24   Yengo L, Vedantam S, Marouli E, Sidorenko J, Bartell E, Sakaue S, et al. A saturated map of common genetic variants associated with human height. *Nature* **2022**;610:704–12. https://doi.org/10.1038/s41586-022-05275-y.

25   Phillips C. Forensic genetic analysis of bio-geographical ancestry. *Forensic Sci Int Genet* **2015**;18:49–65. https://doi.org/10.1016/J.FSIGEN.2015.05.012.

26   Schneider PM, Prainsack B, Kayser M. The use of forensic DNA phenotyping in predicting appearance and biogeographic ancestry. *Dtsch Arztebl Int* **2019**;116:873–80. https://doi.org/10.3238/arztebl.2019.0873.

27   Syndercombe Court D. The Y chromosome and its use in forensic DNA analysis. *Emerg Top Life Sci* **2021**;5:427–41. https://doi.org/10.1042/ETLS20200339.

28   Kivisild T. Maternal ancestry and population history from whole mitochondrial genomes. *Investig Genet* **2015**;6:3. https://doi.org/10.1186/s13323-015-0022-2.

29   Marks MS, Seabra MC. The melanosome: membrane dynamics in black and white. *Nat Rev Mol Cell Biol* **2001**;2:738–48. https://doi.org/10.1038/35096009.

30   Sturm RA. Molecular genetics of human pigmentation diversity. *Hum Mol Genet* **2009**;18:R9–17. https://doi.org/10.1093/hmg/ddp003.

31   Pavan WJ, Sturm RA. The Genetics of Human Skin and Hair Pigmentation. *Annu Rev Genomics Hum Genet* **2019**;20:41–72. https://doi.org/10.1146/annurev-genom-083118-015230.

32   Yamaguchi Y, Brenner M, Hearing VJ. The Regulation of Skin Pigmentation. *J Biol Chem* **2007**;282:27557–61. https://doi.org/10.1074/jbc.R700026200.

33   Prota G, Hu D-N, Vincensi MR, McCormick SA, Napolitano A. Characterization of Melanins in Human Irides and Cultured Uveal Melanocytes From Eyes of Different Colors. *Exp Eye Res* **1998**;67:293–9. https://doi.org/10.1006/exer.1998.0518.

34   Sturm RA, Larsson M. Genetics of human iris colour and patterns. *Pigment Cell Melanoma Res* **2009**;22:544–62. https://doi.org/10.1111/j.1755-148X.2009.00606.x.

35   Wakamatsu K, Hu D, McCormick SA, Ito S. Characterization of melanin in human iridal and choroidal melanocytes from eyes with various colored irides. *Pigment Cell Melanoma Res* **2008**;21:97–105. https://doi.org/10.1111/j.1755-148X.2007.00415.x.

36   Anderson RR, Parrish JA. The Optics of Human Skin. *J Invest Dermatol* **1981**;77:13–9. https://doi.org/10.1111/1523-1747.ep12479191.

37   Sturm RA, Duffy DL. Human pigmentation genes under environmental selection. *Genome Biol* **2012**;13:248–248. https://doi.org/10.1186/gb-2012-13-9-248.

38   Jablonski NG, Chaplin G. The evolution of human skin coloration. *J Hum Evol*

2000;39:57–106. https://doi.org/10.1006/jhev.2000.0403.

39   Holick MF, MacLaughlin JA, Doppelt SH. Regulation of Cutaneous Previtamin D3 Photosynthesis in Man: Skin Pigment Is Not an Essential Regulator. *Science (80-)* **1981**;211:590–3. https://doi.org/10.1126/science.6256855.

40   Katsara M-A, Nothnagel M. True colors: A literature review on the spatial distribution of eye and hair pigmentation. *Forensic Sci Int Genet* **2019**;39:109–18. https://doi.org/10.1016/j.fsigen.2019.01.001.

41   Donnelly MP, Paschou P, Grigorenko E, Gurwitz D, Barta C, Lu R-B, et al. A global view of the OCA2-HERC2 region and pigmentation. *Hum Genet* **2012**;131:683–96. https://doi.org/10.1007/s00439-011-1110-x.

42   Frost P. European hair and eye color: A case of frequency-dependent sexual selection? *Evol Hum Behav* **2006**;27:85–103. https://doi.org/10.1016/J.EVOLHUMBEHAV.2005.07.002.

43   Goel N, Terman M, Terman JS. Depressive symptomatology differentiates subgroups of patients with seasonal affective disorder. *Depress Anxiety* **2002**;15:34–41. https://doi.org/10.1002/da.1083.

44   Terman JS, Terman M. Photopic and scotopic light detection in patients with seasonal affective disorder and control subjects. *Biol Psychiatry* **1999**;46:1642–8. https://doi.org/10.1016/S0006-3223(99)00221-8.

45   Ito S, Wakamatsu K. Chemistry of Mixed Melanogenesis—Pivotal Roles of Dopaquinone. *Photochem Photobiol* **2008**;84:582–92.

46   Bellono NW, Oancea E V. Ion transport in pigmentation. *Arch Biochem Biophys* **2014**;563:35–41. https://doi.org/10.1016/j.abb.2014.06.020.

47   Ancans J, Tobin DJ, Hoogduijn MJ, Smit NP, Wakamatsu K, Thody AJ. Melanosomal pH Controls Rate of Melanogenesis, Eumelanin/Phaeomelanin Ratio and Melanosome Maturation in Melanocytes and Melanoma Cells. *Exp Cell Res* **2001**;268:26–35. https://doi.org/10.1006/excr.2001.5251.

48   Ito S, Wakamatsu K. Diversity of human hair pigmentation as studied by chemical analysis of eumelanin and pheomelanin. *J Eur Acad Dermatology Venereol* **2011**;25:1369–80. https://doi.org/10.1111/j.1468-3083.2011.04278.x.

49   Andersen JD. Genetic investigation of eye and skin colours [dissertation]. Copenhagen: University of Copenhagen, **2015**.

50   Lin JY, Fisher DE. Melanocyte biology and skin pigmentation. *Nature* **2007**;445:843–50. https://doi.org/10.1038/nature05660.

51   Brenner M, Hearing VJ. The Protective Role of Melanin Against UV Damage in Human Skin. *Photochem Photobiol* **2008**;84:539–49. https://doi.org/10.1111/j.1751-1097.2007.00226.x.

52   Kukla-Bartoszek M, Pośpiech E, Spólnicka M, Karłowska-Pik J, Strapagiel D, Żądzińska E, et al. Investigating the impact of age-depended hair colour darkening during childhood on DNA-based hair colour prediction with the HIrisPlex system. *Forensic Sci Int Genet* **2018**;36:26–33. https://doi.org/10.1016/j.fsigen.2018.06.007.

53   Commo S, Gaillard O, Bernard BA. Human hair greying is linked to a specific depletion of hair follicle melanocytes affecting both the bulb and the outer root sheath. *Br J Dermatol* **2004**;150:435–43. https://doi.org/10.1046/j.1365-2133.2004.05787.x.

54   Heath AC, Nyholt DR, Gillespie NA, Martin NG. Genetic Basis of Male Pattern Baldness. *J Invest Dermatol* **2003**;121:1561–4. https://doi.org/10.1111/j.1523-1747.2003.12615.x.

55   Valverde P, Healy E, Jackson I, Rees JL, Thody AJ. Variants of the melanocyte–stimulating hormone receptor gene are associated with red hair and fair skin in humans. *Nat Genet* **1995**;11:328–30. https://doi.org/10.1038/ng1195-328.

56   Tagliabue E, Gandini S, García-Borrón JC, Maisonneuve P, Newton-Bishop J, Polsky D, et al. Association of Melanocortin-1 Receptor Variants with Pigmentary Traits in Humans: A Pooled Analysis from the M-Skip Project. *J Invest Dermatol* **2016**;136:1914–7. https://doi.org/10.1016/j.jid.2016.05.099.

57   García-Borrón JC, Abdel-Malek Z, Jiménez-Cervantes C. MC1R, the cAMP pathway, and the response to solar UV: extending the horizon beyond pigmentation. *Pigment Cell Melanoma Res* **2014**;27:699–720. https://doi.org/10.1111/pcmr.12257.

58   Duffy DL, Box NF, Chen W, Palmer JS, Montgomery GW, James MR, et al. Interactive effects of MC1R and OCA2 on melanoma risk phenotypes. *Hum Mol Genet* **2004**;13:447–61. https://doi.org/https://doi.org/10.1093/hmg/ddh043.

59   Mengel-From J, Børsting C, Sanchez JJ, Eiberg H, Morling N. Determination of cis/trans phase of variations in the MC1R gene with allele-specific PCR and single base extension. *Electrophoresis* **2008**;29:4780–7. https://doi.org/10.1002/elps.200800107.

60   Le Pape E, Passeron T, Giubellino A, Valencia JC, Wolber R, Hearing VJ. Microarray analysis sheds light on the dedifferentiating role of agouti signal protein in murine melanocytes via the Mc1r. *Proc Natl Acad Sci* **2009**;106:1802–7. https://doi.org/10.1073/pnas.0806753106.

61   Videira IF dos S, Moura DFL, Magina S. Mechanisms regulating melanogenesis*. *An Bras Dermatol* **2013**;88:76–83. https://doi.org/10.1590/S0365-05962013000100009.

62   Sulem P, Gudbjartsson DF, Stacey SN, Helgason A, Rafnar T, Jakobsdottir M, et al. Two newly identified genetic determinants of pigmentation in Europeans. *Nat Genet* **2008**;40:835–7. https://doi.org/10.1038/ng.160.

63   Tomita Y, Takeda A, Okinaga S, Tagami H, Shibahara S. Human oculocutaneous albinism caused by single base insertion in the tyrosinase gene. *Biochem Biophys Res Commun* **1989**;164:990–6. https://doi.org/10.1016/0006-291X(89)91767-1.

64   Grønskov K, Ek J, Brondum-Nielsen K. Oculocutaneous albinism. *Orphanet J Rare Dis* **2007**;2:43. https://doi.org/10.1186/1750-1172-2-43.

65   Shriver MD, Parra EJ, Dios S, Bonilla C, Norton H, Jovel C, et al. Skin pigmentation, biogeographical ancestry and admixture mapping. *Hum Genet* **2003**;112:387–99. https://doi.org/10.1007/s00439-002-0896-y.

66   Frudakis T, Thomas M, Gaskin Z, Venkateswarlu K, Chandra KS, Ginjupalli S, et al. Sequences associated with human iris pigmentation. *Genetics* **2003**;165:2071. https://doi.org/10.1093/GENETICS/165.4.2071.

67   Duffy DL, Zhao ZZ, Sturm RA, Hayward NK, Martin NG, Montgomery GW. Multiple Pigmentation Gene Polymorphisms Account for a Substantial Proportion of Risk of Cutaneous Malignant Melanoma. *J Invest Dermatol* **2010**;130:520–8. https://doi.org/10.1038/jid.2009.258.

68   Sulem P, Gudbjartsson DF, Stacey SN, Helgason A, Rafnar T, Magnusson KP, et al. Genetic determinants of hair, eye and skin pigmentation in Europeans. *Nat Genet* **2007**;39:1443–52. https://doi.org/10.1038/ng.2007.13.

69   Boissy RE, Zhao H, Oetting WS, Austin LM, Wildenberg SC, Boissy YL, et al. Mutation in and lack of expression of tyrosinase-related protein-1 (TRP-1) in melanocytes from an individual with brown oculocutaneous albinism: a new subtype of albinism classified as "OCA3." *Am J Hum Genet* **1996**;58:1145–56.

70   Toyofuku K, Wada I, Valencia JC, Kushimoto T, Ferrans VJ, Hearing VJ. Oculocutaneous albinism types 1 and 3 are ER retention diseases: mutation of tyrosinase or Tyrp1 can affect the processing of both mutant and wild-type proteins. *FASEB J* **2001**;15:2149–61. https://doi.org/10.1096/fj.01-0216com.

71   Liu F, van Duijn K, Vingerling JR, Hofman A, Uitterlinden AG, Janssens ACJW, et al. Eye color and the prediction of complex phenotypes from genotypes. *Curr Biol* **2009**;19:R192–3. https://doi.org/10.1016/J.CUB.2009.01.027.

72   Eimear K, Timpson NJ, Sikora M, Yee M-C, Moreno-Estrada A, Eng C, et al. Melanesian Blond Hair Is Caused by an Amino Acid Change in TYRP1. *Science (80-)* **2012**;336:554–554.

73   Toyofuku K, Valencia JC, Kushimoto T, Costin G, Virador VM, Vieira WD, et al. The Etiology of Oculocutaneous Albinism (OCA) Type II: The Pink Protein Modulates the Processing and Transport of Tyrosinase. *Pigment Cell Res* **2002**;15:217–24. https://doi.org/10.1034/j.1600-0749.2002.02007.x.

74   Puri N, Gardner JM, Brilliant MH. Aberrant pH of Melanosomes in Pink-Eyed Dilution (p) Mutant Melanocytes. *J Invest Dermatol* **2000**;115:607–13. https://doi.org/10.1046/j.1523-1747.2000.00108.x.

75   Rinchik EM, Bultman SJ, Horsthemke B, Lee ST, Strunk KM, Spritz RA, et al. A gene for the mouse pink-eyed dilution locus and for human type II oculocutaneous albinism. *Nature* **1993**;361:72–6.

76   Eiberg H, Troelsen J, Nielsen M, Mikkelsen A, Mengel-From J, Kjaer KW, et al. Blue eye color in humans may be caused by a perfectly associated founder mutation in a regulatory element located within the HERC2 gene inhibiting OCA2 expression. *Hum Genet* **2008**;123:177–87. https://doi.org/10.1007/s00439-007-0460-x.

77   Sturm RA, Duffy DL, Zhao ZZ, Leite FPN, Stark MS, Hayward NK, et al. A Single SNP in an Evolutionary Conserved Region within Intron 86 of the HERC2 Gene Determines Human Blue-Brown Eye Color. *Am J Hum Genet* **2008**;82:424. https://doi.org/10.1016/J.AJHG.2007.11.005.

78   Visser M, Kayser M, Palstra R-J. HERC2 rs12913832 modulates human pigmentation by attenuating chromatin-loop formation between a long-range enhancer and the OCA2 promoter. *Genome Res* **2012**;22:446–55. https://doi.org/10.1101/gr.128652.111.

79   Walsh S, Liu F, Ballantyne KN, van Oven M, Lao O, Kayser M. IrisPlex: A sensitive DNA tool for accurate prediction of blue and brown eye colour in the absence of ancestry information. *Forensic Sci Int Genet* **2011**;5:170–80. https://doi.org/10.1016/J.FSIGEN.2010.02.004.

80   Andersen JD, Pietroni C, Johansen P, Andersen MM, Pereira V, Børsting C, et al. Importance of nonsynonymous OCA2 variants in human eye color prediction. *Mol Genet Genomic Med* **2016**;4:420–30. https://doi.org/10.1002/mgg3.213.

81   Branicki W, Liu F, van Duijn K, Draus-Barini J, Pośpiech E, Walsh S, et al. Model-based prediction of human hair color using DNA variants. *Hum Genet* **2011**;129:443–54. https://doi.org/10.1007/s00439-010-0939-8.

82   Spichenok O, Budimlija ZM, Mitchell AA, Jenny A, Kovacevic L, Marjanovic D, et al. Prediction of eye and skin color in diverse populations using seven SNPs. *Forensic Sci Int Genet* **2011**;5:472–8. https://doi.org/10.1016/j.fsigen.2010.10.005.

83   Eaton K, Edwards M, Krithika S, Cook G, Norton H, Parra EJ. Association Study Confirms the Role of Two OCA2 Polymorphisms in Normal Skin Pigmentation Variation in East Asian Populations. *Am J Hum Biol* **2015**;27:520–5. https://doi.org/10.1002/ajhb.22678.

84   Dooley CM, Schwarz H, Mueller KP, Mongera A, Konantz M, Neuhauss SCF, et al. Slc45a2 and V-ATPase are regulators of melanosomal pH homeostasis in zebrafish, providing a mechanism for human pigment evolution and disease. *Pigment Cell Melanoma Res* **2013**;26:205–17. https://doi.org/10.1111/pcmr.12053.

85   Costin G-E, Valencia JC, Vieira WD, Lamoreux ML, Hearing VJ. Tyrosinase processing and intracellular trafficking is disrupted in mouse primary melanocytes carrying the underwhite (uw) mutation. A model for oculocutaneous albinism (OCA) type 4. *J Cell Sci* **2003**;116:3203–12. https://doi.org/10.1242/jcs.00598.

86   Branicki W, Brudnik U, Draus-Barini J, Kupiec T, Wojas-Pelc A. Association of the SLC45A2 gene with physiological human hair colour variation. *J Hum Genet* **2008**;53:966–71. https://doi.org/10.1007/s10038-008-0338-3.

87   Stokowski RP, Pant PVK, Dadd T, Fereday A, Hinds DA, Jarman C, et al. A Genomewide Association Study of Skin Pigmentation in a South Asian Population. *Am J Hum Genet* **2007**;81:1119–32. https://doi.org/10.1086/522235.

88   Phillips C, Parson W, Lundsberg B, Santos C, Freire-Aradas A, Torres M, et al. Building a forensic ancestry panel from the ground up: The EUROFORGEN Global AIM-SNP set. *Forensic Sci Int Genet* **2014**;11:13–25. https://doi.org/10.1016/J.FSIGEN.2014.02.012.

89   Kidd KK, Speed WC, Pakstis AJ, Furtado MR, Fang R, Madbouly A, et al. Progress toward an efficient panel of SNPs for ancestry inference. *Forensic Sci Int Genet* **2014**;10:23–32. https://doi.org/10.1016/J.FSIGEN.2014.01.002.

90   Lamason RL, Mohideen M-APK, Mest JR, Wong AC, Norton HL, Aros MC, et al. SLC24A5, a Putative Cation Exchanger, Affects Pigmentation in Zebrafish and Humans. *Science (80-)* **2005**;310:1782–6. https://doi.org/10.1126/science.1116238.

91   Ginger RS, Askew SE, Ogborne RM, Wilson S, Ferdinando D, Dadd T, et al. SLC24A5 Encodes a trans-Golgi Network Protein with Potassium-dependent Sodium-Calcium Exchange Activity That Regulates Human Epidermal Melanogenesis. *J Biol*

Chem **2008**;283:5486–95. https://doi.org/10.1074/jbc.M707521200.

92   Wei A-H, Zang D-J, Zhang Z, Liu X-Z, He X, Yang L, et al. Exome Sequencing
      Identifies SLC24A5 as a Candidate Gene for Nonsyndromic Oculocutaneous Albinism.
      J Invest Dermatol **2013**;133:1834–40. https://doi.org/10.1038/jid.2013.49.

93   Norton HL, Kittles RA, Parra E, McKeigue P, Mao X, Cheng K, et al. Genetic
      Evidence for the Convergent Evolution of Light Skin in Europeans and East Asians.
      Mol Biol Evol **2006**;24:710–22. https://doi.org/10.1093/molbev/msl203.

94   Han J, Kraft P, Nan H, Guo Q, Chen C, Qureshi A, et al. A Genome-Wide Association
      Study Identifies Novel Alleles Associated with Hair Color and Skin Pigmentation.
      PLOS Genet **2008**;4:e1000074. https://doi.org/10.1371/JOURNAL.PGEN.1000074.

95   Uffelmann E, Huang QQ, Munung NS, de Vries J, Okada Y, Martin AR, et al.
      Genome-wide association studies. *Nat Rev Methods Prim* **2021**;1:59.
      https://doi.org/10.1038/s43586-021-00056-9.

96   Grimes EA, Noake PJ, Dixon L, Urquhart A. Sequence polymorphism in the human
      melanocortin 1 receptor gene as an indicator of the red hair phenotype. *Forensic Sci Int*
      2001;122:124–9. https://doi.org/10.1016/S0379-0738(01)00480-7.

97   Ruiz Y, Phillips C, Gomez-Tato A, Alvarez-Dios J, Casares de Cal M, Cruz R, et al.
      Further development of forensic eye color predictive tests. *Forensic Sci Int Genet*
      2013;7:28–40. https://doi.org/10.1016/J.FSIGEN.2012.05.009.

98   Walsh S, Liu F, Wollstein A, Kovatsi L, Ralf A, Kosiniak-Kamysz A, et al. The
      HIrisPlex system for simultaneous prediction of hair and eye colour from DNA.
      Forensic Sci Int Genet **2013**;7:98–115. https://doi.org/10.1016/J.FSIGEN.2012.07.005.

99   Maroñas O, Phillips C, Söchtig J, Gomez-Tato A, Cruz R, Alvarez-Dios J, et al.
      Development of a forensic skin colour predictive test. *Forensic Sci Int Genet*
      2014;13:34–44. https://doi.org/10.1016/j.fsigen.2014.06.017.

100   Walsh S, Chaitanya L, Breslin K, Muralidharan C, Bronikowska A, Pospiech E, et al.
      Global skin colour prediction from DNA. *Hum Genet* **2017**;136:847–63.
      https://doi.org/10.1007/s00439-017-1808-5.

101   Chaitanya L, Breslin K, Zuñiga S, Wirken L, Pośpiech E, Kukla-Bartoszek M, et al.
      The HIrisPlex-S system for eye, hair and skin colour prediction from DNA:
      Introduction and forensic developmental validation. *Forensic Sci Int Genet*
      2018;35:123–35. https://doi.org/10.1016/j.fsigen.2018.04.004.

102   Allwood JS, Harbison S. SNP model development for the prediction of eye colour in
      New Zealand. *Forensic Sci Int Genet* **2013**;7:444–52.

https://doi.org/10.1016/J.FSIGEN.2013.03.005.

103   Frudakis T, Terravainen T, Thomas M. Multilocus OCA2 genotypes specify human iris colors. *Hum Genet* **2007**;122:311–26. https://doi.org/10.1007/s00439-007-0401-8.

104   Rebbeck TR, Kanetsky PA, Walker AH, Holmes R, Halpern AC, Schuchter LM, et al. P Gene as an Inherited Biomarker of Human Eye Color. *Cancer Epidemiol Biomarkers Prev* **2002**;11:782–4.

105   Sturm RA, Frudakis TN. Eye colour: portals into pigmentation genes and ancestry. *Trends Genet* **2004**;20:327–32. https://doi.org/10.1016/j.tig.2004.06.010.

106   Eiberg H, Mohr J. Assignment of Genes Coding for Brown Eye Colour (BEY2) and Brown Hair Colour (HCL3) on Chromosome 15q. *Eur J Hum Genet* **1996**;4:237–41. https://doi.org/10.1159/000472205.

107   Fawcett T. An introduction to ROC analysis. *Pattern Recognit Lett* **2006**;27:861–74. https://doi.org/10.1016/j.patrec.2005.10.010.

108   Walsh S, Lindenbergh A, Zuniga SB, Sijen T, de Knijff P, Kayser M, et al. Developmental validation of the IrisPlex system: Determination of blue and brown iris colour for forensic intelligence. *Forensic Sci Int Genet* **2011**;5:464–71. https://doi.org/10.1016/j.fsigen.2010.09.008.

109   Walsh S, Wollstein A, Liu F, Chakravarthy U, Rahu M, Seland JH, et al. DNA-based eye colour prediction across Europe with the IrisPlex system. *Forensic Sci Int Genet* **2012**;6:330–40. https://doi.org/10.1016/J.FSIGEN.2011.07.009.

110   Walsh S, Chaitanya L, Clarisse L, Wirken L, Draus-Barini J, Kovatsi L, et al. Developmental validation of the HIrisPlex system: DNA-based eye and hair colour prediction for forensic and anthropological usage. *Forensic Sci Int Genet* **2014**;9:150–61. https://doi.org/10.1016/J.FSIGEN.2013.12.006.

111   Dembinski GM, Picard CJ. Evaluation of the IrisPlex DNA-based eye color prediction assay in a United States population. *Forensic Sci Int Genet* **2014**;9:111–7. https://doi.org/10.1016/J.FSIGEN.2013.12.003.

112   Kastelic V, Pośpiech E, Draus-Barini J, Branicki W, Drobnič K. Prediction of eye color in the Slovenian population using the IrisPlex SNPs. *Croat Med J* **2013**;54:381–6. https://doi.org/10.3325/cmj.2013.54.381.

113   Salvoro C, Faccinetto C, Zucchelli L, Porto M, Marino A, Occhi G, et al. Performance of four models for eye color prediction in an Italian population sample. *Forensic Sci Int Genet* **2019**;40:192–200. https://doi.org/10.1016/J.FSIGEN.2019.03.008.

114   Mengel-From J, Børsting C, Sanchez JJ, Eiberg H, Morling N. Human eye colour and

HERC2, OCA2 and MATP. *Forensic Sci Int Genet* **2010**;4:323–8.
https://doi.org/10.1016/J.FSIGEN.2009.12.004.

115 Valenzuela RK, Henderson MS, Walsh MH, Garrison NA, Kelch JT, Cohen-Barak O,
et al. Predicting phenotype from genotype: Normal pigmentation. *J Forensic Sci*
2010;55:315–22. https://doi.org/10.1111/j.1556-4029.2009.01317.x.

116 Branicki W, Brudnik U, Kupiec T, Wolañska-Nowak P, Wojas-Pelc A. Determination
of Phenotype Associated SNPs in the MC1R Gene. *J Forensic Sci* **2007**;52:349–54.
https://doi.org/10.1111/j.1556-4029.2006.00361.x.

117 Jäger AC, Alvarez ML, Davis CP, Guzmán E, Han Y, Way L, et al. Developmental
validation of the MiSeq FGx Forensic Genomics System for Targeted Next Generation
Sequencing in Forensic DNA Casework and Database Laboratories. *Forensic Sci Int
Genet* **2017**;28:52–70. https://doi.org/10.1016/J.FSIGEN.2017.01.011.

118 Tam V, Patel N, Turcotte M, Bossé Y, Paré G, Meyre D. Benefits and limitations of
genome-wide association studies. *Nat Rev Genet* **2019**;20:467–84.
https://doi.org/10.1038/s41576-019-0127-1.

119 Fitzpatrick TB. The Validity and Practicality of Sun-Reactive Skin Types I Through
VI. *Arch Dermatol* **1988**;124:869–71.
https://doi.org/10.1001/archderm.1988.01670060015008.

120 Breslin K, Wills B, Ralf A, Ventayol Garcia M, Kukla-Bartoszek M, Pospiech E, et al.
HIrisPlex-S system for eye, hair, and skin color prediction from DNA: Massively
parallel sequencing solutions for two common forensically used platforms. *Forensic
Sci Int Genet* **2019**;43:102152. https://doi.org/10.1016/j.fsigen.2019.102152.

121 Xavier C, De La Puente M, Mosquera-Miguel A, Freire-Aradas A, Kalamara V, Vidaki
A, et al. Development and validation of the VISAGE AmpliSeq basic tool to predict
appearance and ancestry from DNA. *Forensic Sci Int Genet* **2020**;48.
https://doi.org/10.1016/j.fsigen.2020.102336.

122 Palencia-Madrid L, Xavier C, De La Puente M, Hohoff C, Phillips C, Kayser M, et al.
Evaluation of the VISAGE Basic Tool for Appearance and Ancestry Prediction Using
PowerSeq Chemistry on the MiSeq FGx System. *Genes (Basel)* **2020**;11:708.
https://doi.org/10.3390/genes11060708.

123 Xavier C, de la Puente M, Sidstedt M, Junker K, Minawi A, Unterländer M, et al.
Evaluation of the VISAGE basic tool for appearance and ancestry inference using
ForenSeq® chemistry on the MiSeq FGx® system. *Forensic Sci Int Genet*
2022;58:102675. https://doi.org/10.1016/j.fsigen.2022.102675.

124   Rosenberg NA, Pritchard JK, Weber JL, Cann HM, Kidd KK, Zhivotovsky LA, et al. Genetic structure of human populations. *Science (80-)* **2002**;298:2381–5. https://doi.org/10.1126/science.1078311.

125   Wang S, Lewis CM, Jakobsson M, Ramachandran S, Ray N, Bedoya G, et al. Genetic Variation and Population Structure in Native Americans. *PLoS Genet* **2007**;3:e185. https://doi.org/10.1371/journal.pgen.0030185.

126   Friedlaender JS, Friedlaender FR, Reed FA, Kidd KK, Kidd JR, Chambers GK, et al. The Genetic Structure of Pacific Islanders. *PLoS Genet* **2008**;4:e19. https://doi.org/10.1371/journal.pgen.0040019.

127   Li JZ, Absher DM, Tang H, Southwick AM, Casto AM, Ramachandran S, et al. Worldwide Human Relationships Inferred from Genome-Wide Patterns of Variation. *Science (80-)* **2008**;319:1100–4. https://doi.org/10.1126/science.1153717.

128   Kosoy R, Nassir R, Tian C, White PA, Butler LM, Silva G, et al. Ancestry informative marker sets for determining continental origin and admixture proportions in common populations in America. *Hum Mutat* **2009**;30:69–78. https://doi.org/10.1002/humu.20822.

129   Cheung EYY, Phillips C, Eduardoff M, Lareu MV, McNevin D. Performance of ancestry-informative SNP and microhaplotype markers. *Forensic Sci Int Genet* **2019**;43:102141. https://doi.org/10.1016/J.FSIGEN.2019.102141.

130   Soundararajan U, Yun L, Shi M, Kidd KK. Minimal SNP overlap among multiple panels of ancestry informative markers argues for more international collaboration. *Forensic Sci Int Genet* **2016**;23:25–32. https://doi.org/10.1016/J.FSIGEN.2016.01.013.

131   Pakstis AJ, Kang L, Liu L, Zhang Z, Jin T, Grigorenko EL, et al. Increasing the reference populations for the 55 AISNP panel: the need and benefits. *Int J Legal Med* **2017**;131:913–7. https://doi.org/10.1007/s00414-016-1524-z.

132   de la Puente M, Ruiz-Ramírez J, Ambroa-Conde A, Xavier C, Pardo-Seco J, Álvarez-Dios J, et al. Development and Evaluation of the Ancestry Informative Marker Panel of the VISAGE Basic Tool. *Genes (Basel)* **2021**;12:1284. https://doi.org/10.3390/genes12081284.

133   Phillips C, McNevin D, Kidd KK, Lagacé R, Wootton S, de la Puente M, et al. MAPlex - A massively parallel sequencing ancestry analysis multiplex for Asia-Pacific populations. *Forensic Sci Int Genet* **2019**;42:213–26. https://doi.org/10.1016/J.FSIGEN.2019.06.022.

134   Kidd KK, Speed WC, Pakstis AJ, Podini DS, Lagacé R, Chang J, et al. Evaluating 130

microhaplotypes across a global set of 83 populations. *Forensic Sci Int Genet* **2017**;29:29–37. https://doi.org/10.1016/J.FSIGEN.2017.03.014.

135 Pereira R, Phillips C, Pinto N, Santos C, Sebd S. Straightforward Inference of Ancestry and Admixture Proportions through Ancestry-Informative Insertion Deletion Multiplexing. *PLoS One* **2012**;7:29684. https://doi.org/10.1371/journal.pone.0029684.

136 Halder I, Shriver M, Thomas M, Fernandez JR, Frudakis T. A panel of ancestry informative markers for estimating individual biogeographical ancestry and admixture from four continents: utility and applications. *Hum Mutat* **2008**;29:648–58. https://doi.org/10.1002/humu.20695.

137 Phillips C, Salas A, Sánchez JJ, Fondevila M, Gómez-Tato A, Álvarez-Dios J, et al. Inferring ancestral origin using a single multiplex assay of ancestry-informative marker SNPs. *Forensic Sci Int Genet* **2007**;1:273–80. https://doi.org/10.1016/J.FSIGEN.2007.06.008.

138 Fondevila M, Phillips C, Santos C, Freire Aradas A, Vallone PM, Butler JM, et al. Revision of the SNPforID 34-plex forensic ancestry test: Assay enhancements, standard reference sample genotypes and extended population studies. *Forensic Sci Int Genet* **2013**;7:63–74. https://doi.org/10.1016/j.fsigen.2012.06.007.

139 Kidd JR, Friedlaender FR, Speed WC, Pakstis AJ, De La Vega FM, Kidd KK. Analyses of a set of 128 ancestry informative single-nucleotide polymorphisms in a global set of 119 population samples. *Investig Genet* **2011**;2:1. https://doi.org/10.1186/2041-2223-2-1.

140 Nievergelt CM, Maihofer AX, Shekhtman T, Libiger O, Wang X, Kidd KK, et al. Inference of human continental origin and admixture proportions using a highly discriminative ancestry informative 41-SNP panel. *Investig Genet* **2013**;4:13. https://doi.org/10.1186/2041-2223-4-13.

141 Pakstis AJ, Gurkan C, Dogan M, Balkaya HE, Dogan S, Neophytou PI, et al. Genetic relationships of European, Mediterranean, and SW Asian populations using a panel of 55 AISNPs. *Eur J Hum Genet* **2019**:1–9. https://doi.org/10.1038/s41431-019-0466-6.

142 Li C-X, Pakstis AJ, Jiang L, Wei Y-L, Sun Q-F, Wu H, et al. A panel of 74 AISNPs: Improved ancestry inference within Eastern Asia. *Forensic Sci Int Genet* **2016**;23:101–10. https://doi.org/10.1016/J.FSIGEN.2016.04.002.

143 Eduardoff M, Gross TE, Santos C, de la Puente M, Ballard D, Strobl C, et al. Inter-laboratory evaluation of the EUROFORGEN Global ancestry-informative SNP panel by massively parallel sequencing using the Ion PGM^TM. *Forensic Sci Int Genet*

2016;23:178–89. https://doi.org/10.1016/j.fsigen.2016.04.008.

144   Al-Asfi M, McNevin D, Mehta B, Power D, Gahan ME, Daniel R. Assessment of the Precision ID Ancestry panel. *Int J Legal Med* **2018**;132:1581–94. https://doi.org/10.1007/s00414-018-1785-9.

145   Auton A, Abecasis GR, Altshuler DM, Durbin RM, Abecasis GR, Bentley DR, et al. A global reference for human genetic variation. *Nature* **2015**;526:68–74. https://doi.org/10.1038/nature15393.

146   Mallick S, Li H, Lipson M, Mathieson I, Gymrek M, Racimo F, et al. The Simons Genome Diversity Project: 300 genomes from 142 diverse populations. *Nature* **2016**;538:201–6. https://doi.org/10.1038/nature18964.

147   Pagani L, Lawson DJ, Jagoda E, Mörseburg A, Eriksson A, Mitt M, et al. Genomic analyses inform on migration events during the peopling of Eurasia. *Nature* **2016**;538:238–42. https://doi.org/10.1038/nature19792.

148   Ruiz-Ramírez J, de la Puente M, Xavier C, Ambroa-Conde A, Álvarez-Dios J, Freire-Aradas A, et al. Development and evaluations of the ancestry informative markers of the VISAGE Enhanced Tool for Appearance and Ancestry. *Forensic Sci Int Genet* **2023**;64:102853. https://doi.org/10.1016/j.fsigen.2023.102853.

149   Phillips C, Amigo J, Tillmar AO, Peck MA, de la Puente M, Ruiz-Ramírez J, et al. A compilation of tri-allelic SNPs from 1000 Genomes and use of the most polymorphic loci for a large-scale human identification panel. *Forensic Sci Int Genet* **2020**;46:102232. https://doi.org/10.1016/j.fsigen.2020.102232.

150   Diepenbroek M, Bayer B, Schwender K, Schiller R, Lim J, Lagacé R, et al. Evaluation of the Ion AmpliSeq^TM PhenoTrivium Panel: MPS-Based Assay for Ancestry and Phenotype Predictions Challenged by Casework Samples. *Genes (Basel)* **2020**;11:1398. https://doi.org/10.3390/genes11121398.

151   Samuel G, Prainsack B. Regulatory landscape of forensic DNA phenotyping in Europe VISAGE. **2018**.

152   Samuel G, Prainsack B. Shifting Ethical Boundaries in Forensic Use of DNA. *Jahrb Für Wiss Und Ethik* **2019**;24:155–72. https://doi.org/10.1515/jwiet-2019-0007.

153   Samuel G, Prainsack B. Civil society stakeholder views on forensic DNA phenotyping: Balancing risks and benefits. *Forensic Sci Int Genet* **2019**;43:102157. https://doi.org/10.1016/j.fsigen.2019.102157.

154   Petersen T, Halvorsen K, Borge OJ. DNA i politiarbeid: Nye metoder, nye problemstillinger. The Norwegian Biotechnology Advisory Board. **2018**.

155   Pietroni C, Andersen JD, Johansen P, Andersen MM, Harder S, Paulsen R, et al. The effect of gender on eye colour variation in European populations and an evaluation of the IrisPlex prediction model. *Forensic Sci Int Genet* **2014**;11:1–6. https://doi.org/10.1016/J.FSIGEN.2014.02.002.

156   Andersen JD, Johansen P, Harder S, Christoffersen SR, Delgado MC, Henriksen ST, et al. Genetic analyses of the human eye colours using a novel objective method for eye colour classification. *Forensic Sci Int Genet* **2013**;7:508–15. https://doi.org/10.1016/j.fsigen.2013.05.003.

157   Illumina. An introduction to Next-Generation Sequencing Technology **2017**:1–16 [accessed 27. March 2024]. Available from: https://www.illumina.com/content/dam/illumina-marketing/documents/products/illumina_sequencing_introduction.pdf.

158   Singh RR. Target Enrichment Approaches for Next-Generation Sequencing Applications in Oncology. *Diagnostics* **2022**;12:1539. https://doi.org/10.3390/diagnostics12071539.

159   Olmedillas-López S, García-Arranz M, García-Olmo D. Current and Emerging Applications of Droplet Digital PCR in Oncology. *Mol Diagn Ther* **2017**;21:493–510. https://doi.org/10.1007/s40291-017-0278-8.

160   Regan JF, Kamitaki N, Legler T, Cooper S, Klitgord N, Karlin-Neumann G, et al. A Rapid Molecular Approach for Chromosomal Phasing. *PLoS One* **2015**;10:e0118270. https://doi.org/10.1371/JOURNAL.PONE.0118270.

161   Regan J, Karlin-Neumann G. Phasing DNA markers using digital PCR. *Methods Mol Biol* **2018**;1768:489–512. https://doi.org/10.1007/978-1-4939-7778-9_28/FIGURES/10.

162   Trigodet F, Lolans K, Fogarty E, Shaiber A, Morrison HG, Barreiro L, et al. High molecular weight DNA extraction strategies for long-read sequencing of complex metagenomes. *Mol Ecol Resour* **2022**;22:1786–802. https://doi.org/10.1111/1755-0998.13588.

163   Guo F, Yu J, Zhang L, Li J. Massively parallel sequencing of forensic STRs and SNPs using the Illumina® ForenSeq™ DNA Signature Prep Kit on the MiSeq FGx™ Forensic Genomics System. *Forensic Sci Int Genet* **2017**;31:135–48. https://doi.org/10.1016/J.FSIGEN.2017.09.003.

164   Churchill JD, Novroski NMM, King JL, Seah LH, Budowle B. Population and performance analyses of four major populations with Illumina's FGx Forensic

Genomics System. *Forensic Sci Int Genet* **2017**;30:81–92.
https://doi.org/10.1016/j.fsigen.2017.06.004.

165   Sharma V, Jani K, Khosla P, Butler E, Siegel D, Wurmbach E. Evaluation of
ForenSeq^TM Signature Prep Kit B on predicting eye and hair coloration as well as
biogeographical ancestry by using Universal Analysis Software (UAS) and available
web-tools. *Electrophoresis* **2019**;40:1353–64. https://doi.org/10.1002/elps.201800344.

166   Bleka Ø, Eduardoff M, Santos C, Phillips C, Parson W, Gill P. Open source software
EuroForMix can be used to analyse complex SNP mixtures. *Forensic Sci Int Genet*
2017;31:105–10. https://doi.org/10.1016/j.fsigen.2017.08.001.

167   Aird D, Ross MG, Chen W-S, Danielsson M, Fennell T, Russ C, et al. Analyzing and
minimizing PCR amplification bias in Illumina sequencing libraries. *Genome Biol*
2011;12:R18. https://doi.org/10.1186/gb-2011-12-2-r18.

168   Brandariz-Fontes C, Camacho-Sanchez M, Vilà C, Vega-Pla JL, Rico C, Leonard JA.
Effect of the enzyme and PCR conditions on the quality of high-throughput DNA
sequencing results. *Sci Rep* **2015**;5:8056. https://doi.org/10.1038/srep08056.

169   Sidstedt M, Steffen CR, Kiesler KM, Vallone PM, Rådström P, Hedman J. The impact
of common PCR inhibitors on forensic MPS analysis. *Forensic Sci Int Genet*
2019;40:182–91. https://doi.org/10.1016/j.fsigen.2019.03.001.

170   Xavier C, de la Puente M, Mosquera-Miguel A, Freire-Aradas A, Kalamara V, Ralf A,
et al. Development and inter-laboratory evaluation of the VISAGE Enhanced Tool for
Appearance and Ancestry inference from DNA. *Forensic Sci Int Genet*
2022;61:102779. https://doi.org/10.1016/j.fsigen.2022.102779.

171   Frégeau CJ. A multiple predictive tool approach for phenotypic and biogeographical
ancestry inferences. *Can Soc Forensic Sci J* **2022**;55:71–99.
https://doi.org/10.1080/00085030.2021.2016206.

172   Resutik P, Aeschbacher S, Krützen M, Kratzer A, Haas C, Phillips C, et al.
Comparative evaluation of the MAPlex, Precision ID Ancestry Panel, and VISAGE
Basic Tool for biogeographical ancestry inference. *Forensic Sci Int Genet*
2023;64:1872–4973. https://doi.org/10.1016/j.fsigen.2023.102850.

173   Xavier C, de la Puente M, Phillips C, Eduardoff M, Heidegger A, Mosquera-Miguel A,
et al. Forensic evaluation of the Asia Pacific ancestry-informative MAPlex assay.
Forensic Sci Int Genet **2020**;48:102344. https://doi.org/10.1016/j.fsigen.2020.102344.

174   Pritchard JK, Stephens M, Donnelly P. Inference of population structure using
multilocus genotype data. *Genetics* **2000**;155:945–59.

175   Porras-Hurtado L, Ruiz Y, Santos C, Phillips C, Carracedo Á, Lareu M V. An overview of STRUCTURE: applications, parameter settings, and supporting software. *Front Genet* **2013**;4. https://doi.org/10.3389/fgene.2013.00098.

176   Byrska-Bishop M, Evani US, Zhao X, Basile AO, Abel HJ, Regier AA, et al. High-coverage whole-genome sequencing of the expanded 1000 Genomes Project cohort including 602 trios. *Cell* **2022**;185:3426-3440.e19. https://doi.org/10.1016/j.cell.2022.08.004.

177   Bergström A, McCarthy SA, Hui R, Almarri MA, Ayub Q, Danecek P, et al. Insights into human genetic variation and population history from 929 diverse genomes. *Science (80-)* **2020**;367. https://doi.org/10.1126/science.aay5012.

178   Ralf A, van Oven M, Montiel González D, de Knijff P, van der Beek K, Wootton S, et al. Forensic Y-SNP analysis beyond SNaPshot: High-resolution Y-chromosomal haplogrouping from low quality and quantity DNA using Ion AmpliSeq and targeted massively parallel sequencing. *Forensic Sci Int Genet* **2019**;41:93–106. https://doi.org/10.1016/j.fsigen.2019.04.001.

179   Chaitanya L, Ralf A, Oven M, Kupiec T, Chang J, Lagacé R, et al. Simultaneous Whole Mitochondrial Genome Sequencing with Short Overlapping Amplicons Suitable for Degraded DNA Using the Ion Torrent Personal Genome Machine. *Hum Mutat* **2015**;36:1236–47. https://doi.org/10.1002/humu.22905.

180   Junker K, Staadig A, Sidstedt M, Tillmar A, Hedman J. Phenotype prediction accuracy – A Swedish perspective. *Forensic Sci Int Genet Suppl Ser* **2019**;7:384–6. https://doi.org/10.1016/J.FSIGSS.2019.10.022.

181   Itou T, Ito S, Wakamatsu K. Effects of Aging on Hair Color, Melanosomes, and Melanin Composition in Japanese Males and Their Sex Differences. *Int J Mol Sci* **2022**;23:14459. https://doi.org/10.3390/ijms232214459.

182   Itou T, Ito S, Wakamatsu K. Effects of Aging on Hair Color, Melanosome Morphology, and Melanin Composition in Japanese Females. *Int J Mol Sci* **2019**;20:3739. https://doi.org/10.3390/ijms20153739.

183   Itou T. Morphological changes in hair melanosomes by aging. *Pigment Cell Melanoma Res* **2018**;31:630–5. https://doi.org/10.1111/pcmr.12697.

184   Pośpiech E, Wojas-Pelc A, Walsh S, Liu F, Maeda H, Ishikawa T, et al. The common occurrence of epistasis in the determination of human pigmentation and its impact on DNA-based pigmentation phenotype prediction. *Forensic Sci Int Genet* **2014**;11:64–72. https://doi.org/10.1016/j.fsigen.2014.01.012.

185   Meyer OS, Børsting C, Andersen JD. Perception of blue and brown eye colours for forensic DNA phenotyping. *Forensic Sci Int Genet Suppl Ser* **2019**;7:476–7. https://doi.org/10.1016/J.FSIGSS.2019.10.057.

186   Wollstein A, Walsh S, Liu F, Chakravarthy U, Rahu M, Seland JH, et al. Novel quantitative pigmentation phenotyping enhances genetic association, epistasis, and prediction of human eye colour. *Sci Rep* **2017**;7:43359. https://doi.org/10.1038/srep43359.

187   Liu F, Wollstein A, Hysi PG, Ankra-Badu GA, Spector TD, Park D, et al. Digital Quantification of Human Eye Color Highlights Genetic Association of Three New Loci. *PLoS Genet* **2010**;6:e1000934. https://doi.org/10.1371/journal.pgen.1000934.

188   Atwood L, Raymond J, Sears A, Bell M, Daniel R. From Identification to Intelligence: An Assessment of the Suitability of Forensic DNA Phenotyping Service Providers for Use in Australian Law Enforcement Casework. *Front Genet* **2021**;11. https://doi.org/10.3389/fgene.2020.568701.

189   Martinez-Cadenas C, Penãa-Chilet M, Ibarrola-Villava M, Ribas G. Gender is a major factor explaining discrepancies in eye colour prediction based on HERC2/OCA2 genotype and the IrisPlex model. *Forensic Sci Int Genet* **2013**;7:453–60. https://doi.org/10.1016/J.FSIGEN.2013.03.007.

190   Yun L, Gu Y, Rajeevan H, Kidd KK. Application of six IrisPlex SNPs and comparison of two eye color prediction systems in diverse Eurasia populations. *Int J Legal Med* **2014**;128:447–53. https://doi.org/10.1007/s00414-013-0953-1.

191   Le L, Escobar IE, Ho T, Lefkovith AJ, Latteri E, Haltaufderhyde KD, et al. SLC45A2 protein stability and regulation of melanosome pH determine melanocyte pigmentation. *Mol Biol Cell* **2020**;31:2687–702. https://doi.org/10.1091/mbc.E20-03-0200.

192   Meyer OS, Lunn MMB, Garcia SL, Kjærbye AB, Morling N, Børsting C, et al. Association between brown eye colour in rs12913832:GG individuals and SNPs in TYR, TYRP1, and SLC24A4. *PLoS One* **2020**;15:e0239131. https://doi.org/10.1371/journal.pone.0239131.

193   Millar DS, Horan M, Chuzhanova NA, Cooper DN. Characterisation of a functional intronic polymorphism in the human growth hormone (GHI) gene. *Hum Genomics* **2010**;4:289. https://doi.org/10.1186/1479-7364-4-5-289.

194   Krawczak M, Thomas NST, Hundrieser B, Mort M, Wittig M, Hampe J, et al. Single base-pair substitutions in exon-intron junctions of human genes: nature, distribution, and consequences for mRNA splicing. *Hum Mutat* **2007**;28:150–8.

https://doi.org/10.1002/humu.20400.

195   ENCODE Project Consortium, Moore JE, Purcaro MJ, Pratt HE, Epstein CB, Shoresh
       N, et al. Expanded encyclopaedias of DNA elements in the human and mouse
       genomes. *Nature* **2020**;583:699–710. https://doi.org/10.1038/s41586-020-2493-4.

196   Fitzgerald T, Birney E. CNest: A novel copy number association discovery method
       uncovers 862 new associations from 200,629 whole-exome sequence datasets in the
       UK Biobank. *Cell Genomics* **2022**;2:100167.
       https://doi.org/10.1016/J.XGEN.2022.100167.

197   Moreno-Cabrera JM, del Valle J, Castellanos E, Feliubadaló L, Pineda M, Brunet J, et
       al. Evaluation of CNV detection tools for NGS panel data in genetic diagnostics. *Eur J
       Hum Genet* **2020**;28:1645–55. https://doi.org/10.1038/s41431-020-0675-z.

198   Zhang F, Gu W, Hurles ME, Lupski JR. Copy Number Variation in Human Health,
       Disease, and Evolution. *Annu Rev Genomics Hum Genet* **2009**;10:451–81.
       https://doi.org/10.1146/annurev.genom.9.081307.164217.

199   Simcoe M, Valdes A, Liu F, Furlotte NA, Evans DM, Hemani G, et al. Genome-wide
       association study in almost 195,000 individuals identifies 50 previously unidentified
       genetic loci for eye color. *Sci Adv* **2021**;7:1–12.
       https://doi.org/10.1126/sciadv.abd1239.

Paper 1

Research paper

Predicting eye and hair colour in a Norwegian population using Verogen's ForenSeq™ DNA signature prep kit

Nina Mjølsnes Salvo [a],[*], Kirstin Janssen [a], Maria Kristine Kirsebom [a], Olivia Strunge Meyer [b], Thomas Berg [a], Gunn-Hege Olsen [a]

[a] Centre for Forensic Genetics, Department of Medical Biology, Faculty of Health Sciences, UiT - The Arctic University of Norway, Norway
[b] Section of Forensic Genetics, Department of Forensic Medicine, Faculty of Health and Medical Sciences, University of Copenhagen, Denmark

ABSTRACT

Prediction of eye and hair colour from DNA can be an important investigative tool in forensic cases if conventional DNA profiling fails to match DNA from any known suspects or cannot obtain a hit in a DNA database. The HIrisPlex model for simultaneous eye and hair colour predictions was developed for forensic usage. To genotype a DNA sample, massively parallel sequencing (MPS) has brought new possibilities to the analysis of forensic DNA samples. As part of an in-house validation, this study presents the genotyping and predictive performance of the HIrisPlex SNPs in a Norwegian study population, using Verogen's ForenSeq™ DNA Signature Prep Kit on the MiSeq FGx system and the HIrisPlex webtool. DNA-profiles were successfully typed with DNA input down to 125 pg. In samples with DNA input < 125 pg, false homozygotes were observed with as many as 92 reads. Prediction accuracies in terms of AUC were high for red (0.97) and black (0.93) hair colours, as well as blue (0.85) and brown (0.94) eye colours. The AUCs for blond (0.72) and brown (0.70) hair colour were considerably lower. None of the individuals was predicted to have intermediate eye colour. Therefore, the error rates of the overall eye colour predictions were 37% with no predictive probability threshold (pmax) and 26% with a probability threshold of 0.7. We also observed that more than half of the incorrect predictions were for individuals carrying the rs12913832 GG genotype. For hair colour, 65% of the individuals were correctly predicted when using the highest probability category approach. The main error was observed for individuals with brown hair colour that were predicted to have blond hair. Utilising the prediction guide approach increased the correct predictions to 75%. Assessment of phenotype-genotype associations of eye colours using a quantitative eye colour score (PIE-score), revealed that rs12913832 AA individuals of Norwegian descent had statistically significantly higher PIE-score (less brown eye colour) than individuals of non-northern European descent. To our knowledge, this has not been reported in other studies. Our study suggests that careful assessment of the target population prior to the implementation of forensic DNA phenotyping to case work is beneficial.

1. Introduction

Forensic DNA phenotyping (FDP) is an emerging DNA intelligence area for use in forensic genetics [1]. When conventional DNA profiling fails to match DNA from any known suspects or cannot obtain a hit in a DNA database, FDP can aid police investigations by predicting a person's externally visible characteristics from DNA alone [2,3]. Eye and hair colour are prominent visible traits that are often used to describe an individual. These traits are also highly heritable and are associated with relatively few genes, which makes them suitable for FDP [2].

DNA variants found in the regions of pigmentation genes are widely used to predict eye and hair colour [4–8], including FDP tests in forensic casework [9,10]. One of the most popular models for these tests, namely HIrisPlex, is a simultaneous eye and hair colour prediction system [11–13]. The HIrisPlex DNA marker panel consists of 23 SNPs and one insertion/deletion (INDEL), of which six (referred to as IrisPlex SNPs) are used for eye colour prediction and 22 are used for hair colour prediction [8]. The model predicts colour into categories and reports prediction probability values (p-values) of blue, intermediate and brown eye colour, as well as blond, brown, black and red hair colour. For hair colour, light and dark shade is also reported. IrisPlex is reported to have very good accuracies for blue and brown eye colours, whereas the

accuracy for intermediate eye colour is considerably lower [13]. This is because the model is mainly dependent on the SNP rs12913832 in *HERC2*, which is known as the most important SNP for prediction of blue and brown coloured eyes [4,5,14–17]. The SNP rs12913832 is located upstream of the pigmentation gene *OCA2* and functions as an enhancer. The ancestral rs12913832 A-allele enhances transcription of *OCA2*, and thereby increases melanin production. In contrast, the derived rs12913832 G-allele has the opposite effect on melanin production [18]. Individuals with rs12913832 AA and AG are expected to have brown eyes, and individuals with rs12913832 GG are expected to have blue eyes [19,20]. The remaining five IrisPlex SNPs have only minor additive effects on the eye colour predictions [17]. The genetic basis of hair colour is more complex than iris colour. Although rs12913832 is also associated with hair colour, this association has been shown to be much weaker than for eye colour [8]. Red hair has been extensively studied and is strongly associated with mutations in *MC1R*, often in a homozygous or a compound-heterozygous state [7,21,22]. For the other hair colours ranging from blond via brown to black, predictions are made based on combinations of the 22 DNA variants with various degrees of association [8]. Hence, the hair colour prediction model is reported to have highest accuracy for red hair colour, followed by slightly lower accuracies for black, blond and brown hair [8].

In addition to an accurate prediction model, FDP also depends on a reliable typing method. Because forensic trace samples often contain small amounts of DNA and/or degraded DNA, the typing method needs to be suitable for short DNA fragments and low DNA input amounts. In this study, the HIrisPlex SNPs are typed by massively parallel sequencing (MPS, also known as next generation sequencing, NGS), using the commercially available ForenSeq™ DNA Signature Prep Kit on the MiSeq FGx system (Verogen, San Diego, CA). Primer mix B supplied with the kit contains primers to multiplex 231 forensically relevant genetic markers, including the 24 HIrisPlex SNPs. This kit has been demonstrated to be robust and to produce reliable results with 250 pg DNA [23,24]. Compared to traditional PCR-CE methods, the application of MPS has brought new possibilities to the analysis of forensic DNA samples by enabling simultaneous typing of hundreds of markers in one analysis [25]. Thus, markers for FDP can be genotyped together with ancestry informative marker (AIM) SNPs, human identification (HID) SNPs and short tandem repeats (STR) used for standard DNA profiling. Thereby, several major issues in relation to a forensic DNA sample can be addressed in a single analysis.

As part of an in-house validation of the FDP analysis of eye and hair colour with the ForenSeq™ DNA Signature Prep Kit and the HIrisPlex webtool, we provide data on both technical- and predictive performance of the HIrisPlex SNPs in a Norwegian study population. In this population, individuals with intermediate or blue eyes as well as blond or brown hair are common. Although HIrisPlex is regarded to be an informative and robust model for predicting eye and hair colour, the precise genotype-phenotype associations for these traits are yet to be identified [8,26–29]. Supplementing information on inaccurate predictions of genotype-phenotype combinations might be educational for the interpretation of prediction results in a specific population, as well as helpful when searching for new candidate markers. Other forensic laboratories who are considering implementing FDP in their analysis repertoire might also benefit from the evaluation presented here.

2. Materials and methods

2.1. Samples

Blood samples were collected from 540 unrelated volunteers residing in Tromsø and Bodø, northern Norway from 2015 to 2017. All samples were collected with fully informed consent and subsequently anonymised. The project is approved by the Faculty of Health Sciences, UiT – The Arctic University of Norway (reference number 2021/2034). Digital photographs of the participants' eyes were taken (see below).

Photographs from 519 individuals had sufficient quality to be used for further evaluation of eye colour predictions. The participants also self-reported their natural hair colour at the age around 20, birthplace and grandparents' ancestry. All 540 individuals were used for evaluation of hair colour predictions. Of the 519 individuals included for eye colour predictions, 480 self-reported to be of European descent (all four grandparents were Europeans), of which 441 were Scandinavian (424 Norwegian). The remaining 39 individuals were of non-European, admixed or unknown ancestry. Of the 21 individuals that were only included for hair colour predictions, 20 were European, of which 18 were Scandinavian (17 Norwegian) and one individual was non-European.

2.2. Eye and hair colour phenotyping

High resolution photographs of eyes were taken with a Canon EOS 5D Mark III camera using a Canon EF 100 mm f/2.8 L Macro IS USM lens and a MT-24EX Macro Twin Lite Flash. The photographs were taken at approximately 5–10 cm in "Raw" format with ISO 100, shutter 1/100, AV 22, exposure compensation $+$ 1 and manual focus. According to Andersen et al. [30], the white balance of "Raw" format photographs was changed to "Flash" using Digital Photo Professional 4 version 4.10.40.0 (Canon INC).

For qualitative determination of eye colour, nine untrained individuals were asked to intuitively assign each photograph to one of four categories (blue, intermediate-blue, intermediate-brown and brown eyes), similar to Meyer et al. [31]. To decide the final eye colour for each photograph, a majority-vote was employed. The IrisPlex model reports eye colour according to three categories (blue, intermediate and brown). Therefore, intermediate-blue and intermediate-brown, which includes all eye colours neither perceived as blue nor brown, were afterwards grouped into one category (intermediate). A total of 52% (n = 269) of individuals were categorised as blue-eyed, 34% (n = 179) as intermediate eye coloured (25% intermediate blue and 9% intermediate brown) and 14% (n = 71) as brown-eyed (see Fig. 2 in Section 3.2). This eye colour categorisation was further used as reference for assessment of eye colour predictions. For 31% (n = 163) of the photographs, all the observers agreed completely on the eye colour. For the remaining 69% (n = 356), on average two observers disagreed with the concluded category, demonstrating that perception of eye colours varies. The vast majority of the disagreements were between the categories blue and intermediate-blue, as well as brown and intermediate-brown.

For an objective evaluation of eye colour, a quantitative eye colour score (Pixel Index of the Eye (PIE)- score) was calculated for each individual eye photograph using the custom-made Digital Analysis of Iris Tool software (DIAT) v1\3 [30]. The software labels the pixels in the photograph as either blue or brown and calculates a score on a continuous scale from $-$ 1–1. The value 1 equals to blue pixels only and $-$ 1 equals to brown pixels only. Each photograph was manually corrected for eye-lid boundaries to ensure reliable scores.

Hair colour was self-reported as the participant's natural hair colour at the age around 20 and categorised as either blond, brown, red or black, together with shade (light or dark). In some cases, photographs of the hair were used as a control of the self-reported hair colour. Based on the self-reported hair colour, a vast majority of individuals in the Norwegian study population had blond (53.0%, n = 287), or brown (40.6%, n = 219) hair. Only 3.5% (n = 19) of the individuals had red hair and 2.8% (n = 15) had black hair (see Fig. 5 in Section 3.4).

2.3. Library preparation and sequencing

DNA was purified using either the QIAsymphony DNA Midi Kit (Qiagen) or the PrepFiler™ Express DNA Extraction kit (Thermo Fisher Scientific). The human male reference DNA 2800 M (Verogen) and 007 (Thermo Fisher Scientific) were used for performance testing of the ForenSeq™ DNA Signature Prep kit (Verogen). DNA was quantified

using the Quantifiler™ Trio DNA Quantification kit on the 7500 Real-time PCR system (Thermo Fisher Scientific).

One ng DNA was used to construct sequencing libraries with two different lots of the ForenSeq™ DNA Signature Prep kit (Verogen), following the manufacturer's instructions (VD 2018005 Rev. A). For the technical sensitivity study, serial dilutions of human male reference DNA 2800 M and 007 were prepared for DNA inputs of 500, 250, 125, 62.5 and 31.3 pg. 2800 M was also analysed at 1000 pg and 007 at 15.6 pg. All dilutions were analysed in triplicates.

Briefly, libraries were amplified with Primer mix B. Amplification, tagging and enrichment was carried out on a Veriti Thermal Cycler (Thermo Fisher Scientific). The libraries were purified and normalised using magnetic beads. Batches of 32 libraries, including a positive and negative control, were pooled and denatured. Twelve μl of this pool were loaded on the MiSeq® FGx Reagent Cartridge. Sequencing was otherwise performed on the MiSeq® FGx instrument according to the manufacturer's instructions.

2.4. Data analysis

2.4.1. Analysis of sequence data

Run metrics and sequence data were processed using the ForenSeq™ Universal Analysis Software v1.2 (UAS, Verogen). For interpretation, the default analytical threshold of 1.5% (minimum 10 reads) and interpretation threshold of 4.5% (minimum 30 reads) were applied. If both alleles had between 10 and 30 reads, the genotype was considered heterozygous. Genotypes for which only one allele was detected, and the read count was between 10 and 30 reads were considered inconclusive due to potential allele dropout. Furthermore, a noise limit of 10% was applied for calling homozygous genotypes.

Six representative sequencing runs with cluster densities of $1200 - 1600$ K/mm^2 were chosen to study the typing performance of the DNA ForenSeq™ DNA Signature Prep kit. Of 180 samples (30 samples per run), 177 samples fulfilled the recommended total read count requirement of 85,000 and were included for further analyses. Libraries were prepared with two different reagent lots, but no lot-specific effect was observed (data not shown). For performance evaluation of the multiplex, profile completeness, depth of coverage (DoC) and allele balance were calculated. DoC per locus was defined by all reads per locus. Allele balances, also referred to as allele coverage ratios, were calculated for all heterozygous genotypes by dividing the number of reads of the allele with the lowest read depth, with number of reads of the allele with the highest read depth.

2.4.2. HIrisPlex model-based prediction of eye and hair colour

Predictions of eye and hair colours were obtained by the HIrisPlex multinominal logistic regression model using the current version of the webtool (https://hirisplex.erasmusmc.nl/). The model is based on 9466 individuals for eye colour [4,12,17] and 1878 individuals for hair colour [8,12]. Notably, the UAS (Verogen) also generates eye and hair colour predictions based on the first HIrisPlex model [13]. However, this software was not used because the HIrisPlex webtool generates additional predictions of hair colour shades (light/dark). Prediction results were reported as predictive probability values (p-values) for each category. For eye colour, the colour with the highest p-value (pmax) was considered as the predicted eye colour. Following the recommendation by Walsh et al., probability thresholds of 0.5 and 0.7 were also evaluated [17,32]. For hair colour prediction, both the highest probability category approach (HPCA) and the recommended prediction guide approach (PGA), which also takes shade into account, were evaluated [13].

The accuracy of prediction performance by the HIrisPlex webtool was evaluated by calculating AUC (area under the receiver operating characteristic curve), sensitivity, specificity, positive predictive value (PPV) and negative predictive value (NPV) for each colour category. ROC curves and their corresponding AUC values were computed in R software v3.6.1 [33] using the R packages ROCR [34] and klaR [35].

All other statistical calculations and plot generations were performed using the Real Statistics Resource Pack software (release 6.3), copyright (2013 – 2020) Charles Zaiontz, www.real-statistics.com. Mann-Whitney tests were employed for between group comparisons, and multiple Bonferroni correction was applied. The Spearman's correlation test was employed to test if PIE-scores and eye colour categories obtained by subjective categorisation were correlated.

3. Results

3.1. Genotyping performance of the HIrisPlex SNPs using the ForenSeq™ DNA Signature prep kit

In total, 177 samples with 1 ng DNA input from six representative runs were evaluated for genotyping performance of the 24 HIrisPlex SNPs. These samples had a median read count of 371,573, ranging from 100,008 to 715,552 reads. Complete HIrisPlex profiles were obtained for all samples. The median DoC was 939 reads across the 24 SNPs, ranging from 61 reads in rs12896399 to 9780 reads in rs201326893_Y152OCH (Table S1, Fig. S1). In addition to rs12896399, five other loci, rs2378249, rs12821256, rs12203592, rs28777 and rs1393350, had minimum read numbers below 100 (Table S1). All loci except rs201326893_Y152OCH were heterozygous in one or more samples (see allele frequencies of all SNPs in Table S2). The average allele balance for these loci was 0.82 ± 0.12 (mean $\pm$ SD). SNP rs1800407 had the lowest average allele balance with 0.73 ± 0.17 (mean $\pm$ SD) (Fig. S1). There were very few observations of allele balances below 0.4, and these occurred in rs28777, rs683, rs2402130 and rs1800407 (Fig. S1).

The concordance of the six eye colour SNPs (IrisPlex) was assessed by comparing ForenSeq genotyping data with data obtained using a PCR-SBE assay [36]. SNP profiles for these markers were 100% concordant between methods.

3.1.1. Technical sensitivity

Dilution series of control DNA were sequenced to assess the kit's ability to produce reliable HIrisPlex profiles at low DNA input amounts. DoC decreased nearly linearly with decreasing amount of input DNA, and allele balances became more variable with decreasing amounts of input DNA (ranging from 0.71 to 0.99 and 0.24–1 with 1000 pg and 31.3 pg DNA input, respectively. Fig. S2). However, complete HIrisplex profiles were obtained in all samples with 125 pg DNA input or higher (Fig. 1). With 62.5 pg DNA input, allele dropout was observed in the most important SNP for eye colour prediction, rs12913832. Furthermore, locus dropout was observed in rs12821256, rs16891982, rs12203592 and rs12821256. One of the SNPs with low DoC, rs12203592 (Fig. S1), had the highest number of locus dropout (19% of the samples with 62.5 pg DNA). Applying the default analytical and interpretation thresholds, false homozygotes (drop out of one allele) and thus incorrect genotypes were observed in 56% of the samples with DNA
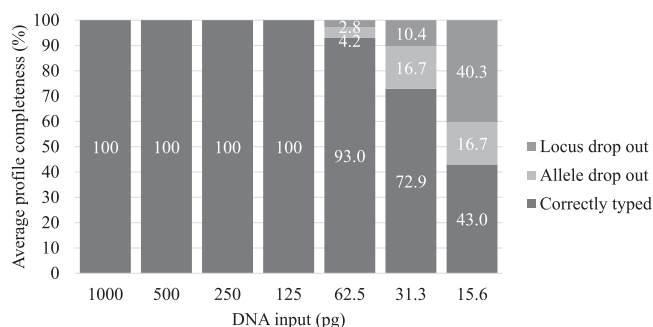

Fig. 1. Sensitivity study of the HIrisPlex SNPs genotyped with the ForenSeq™ DNA Signature Prep Kit, showing profile average completeness in relation to DNA input.

Table 1
: Parameters describing the prediction accuracy of the HIrisPlex webtool using the highest probability category approach for (A) eye colour, categorised by observation from photographs, and (B) hair colour, self-reported by the participants.

A) Eye colour					
Threshold		Blue	Intermediate	Brown	
pmax	Sensitivity	0.96	0.00	1.00	
	Specificity	0.56	1.00	0.82	
	PPV	0.70	0.00	0.47	
	NPV	0.93	0.66	1.00	
	AUC	0.85	0.69	0.94	
0.7 *	Sensitivity	0.98	0.00	1.00	
	Specificity	0.44	1.00	0.90	
	PPV	0.72	0.00	0.55	
	NPV	0.94	0.70	1.00	
B) Hair colour					
Threshold		Blond	Brown	Red	Black
pmax	Sensitivity	0.76	0.50	0.68	0.73
	Specificity	0.60	0.79	0.98	0.99
	PPV	0.68	0.62	0.50	0.61
	NPV	0.69	0.70	0.99	0.99
	AUC	0.72	0.70	0.97	0.93

* Inconclusive samples (samples below the threshold) were excluded from accuracy calculations

input lower than 62.5 pg. This was observed in rs12913832, rs1042602, rs12821256, rs1800407 and rs12896399. Although the number of reads was above the interpretation threshold of 30 reads (ranging from 32 to 92 reads), the other allele had dropped out. The SNP rs1042602 had the overall highest number of allele dropout (in four of 15 samples with DNA input < 125 pg).

3.2. Eye colour prediction performance of IrisPlex

Using the IrisPlex webtool without threshold (pmax), 71% of the individuals (n = 367) were predicted as blue-eyed, 29% as brown-eyed (n = 152) and none as having eyes with intermediate colour. Thus, all individuals with intermediate eyes were either classified as blue (61%) or brown (39%) (Fig. 2).

The AUC reached acceptable values for blue (0.85) and brown (0.94) eye colours but was rather low for intermediate-coloured eyes (0.69) (Table 1A). With pmax, 96% of the blue-eyed individuals and 100% of the brown-eyed individuals were classified correctly (Table 1A). A slight increase of correctly predicted blue eyes was observed when applying a probability threshold of 0.7, e.g. the sensitivity increased from 0.96 to 0.98 (Fig. 2 and Table 1A). In contrast to high sensitivities, the specificities for blue and brown eye colours were comparably low, with pmax of 0.56 and 0.82, respectively (Table 1A). This was mainly due to incorrect predictions of intermediate eye colour that resulted in high numbers of falsely positive predicted blue and brown eyes. With the probability threshold of 0.7, the proportion of false positive prediction of blue eyes increased, reducing the specificity to 0.44, whereas the proportion of false positive predictions of brown eyes decreased, increasing the specificity to 0.90 (Table 1A). With pmax, the number of false positive prediction of brown eyes was slightly higher than the true positives, resulting in a positive predictive value (PPV) of 0.47, whereas the PPV for blue eye colour was 0.70 (Table 1A). The high proportion of correctly classified blue and brown eye colours resulted in high negative predictive values (NPVs) of 0.93 and 1, respectively. The PPVs for blue and brown eye colours, as well as the NPV for blue eye colour increased slightly when applying the probability threshold of 0.7.

The overall correct predictions with pmax were 63% (Fig. 3). When applying thresholds, the incorrect predictions across the eye colour categories decreased from 37% to 34% with p-values > 0.5% and 26% with p-values > 0.7 (Fig. 3). Additionally, the proportion of inconclusive predictions were 3% and 15% with thresholds of 0.5 and 0.7, respectively. Most of the inconclusive predictions with a threshold of 0.7 (52/76) were incorrect predictions with pmax (Fig. 2). Thus, application of thresholds affected the overall error rate. However, with pmax, 94% of individuals with incorrect predictions had intermediate eyes, of which 74% were also incorrect with a threshold of 0.7. Additionally, 34% of the individuals correctly predicted to have brown eye colour with pmax were inconclusive with a threshold of 0.7 (n = 24) (Fig. 2). It is noteworthy to mention that assignment of intermediate eye colour when p-vales for blue and brown are similar (as proposed in [13,17]) did not improve the prediction accuracy in the Norwegian study population considerably (data not shown).

Because eye colour predictions are mainly dependent on HERC2

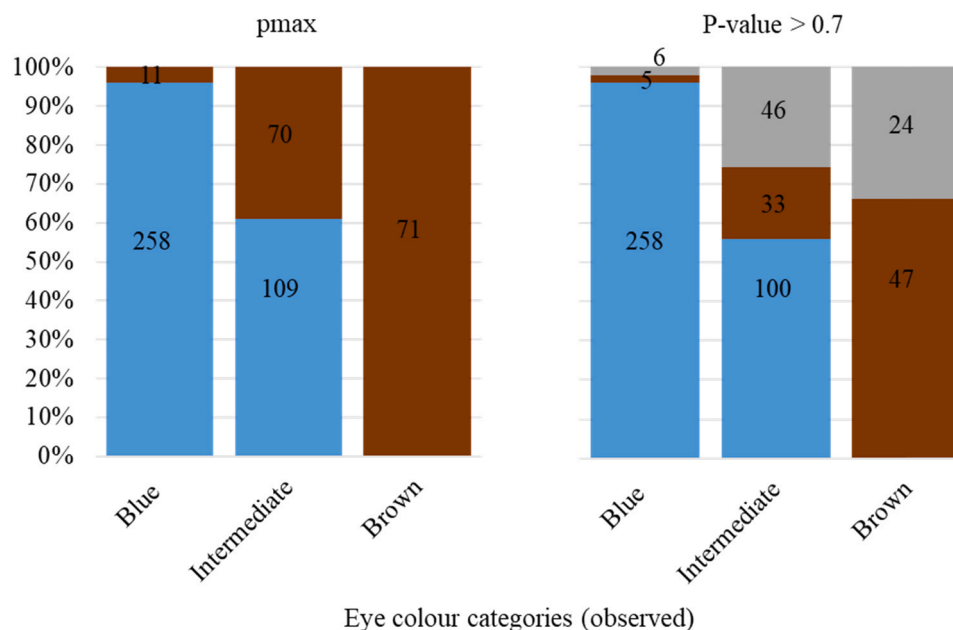**Fig. 2.** IrisPlex eye colour predictions obtained from 519 individuals from Norway with no threshold (pmax) and a probability threshold of 0.7. Colours within bars represent percentage of blue (blue), brown (brown) and inconclusive (grey) eye colour predicted within the respected observed eye colour category. Numbers in the bars represent numbers of individuals predicted within the category.
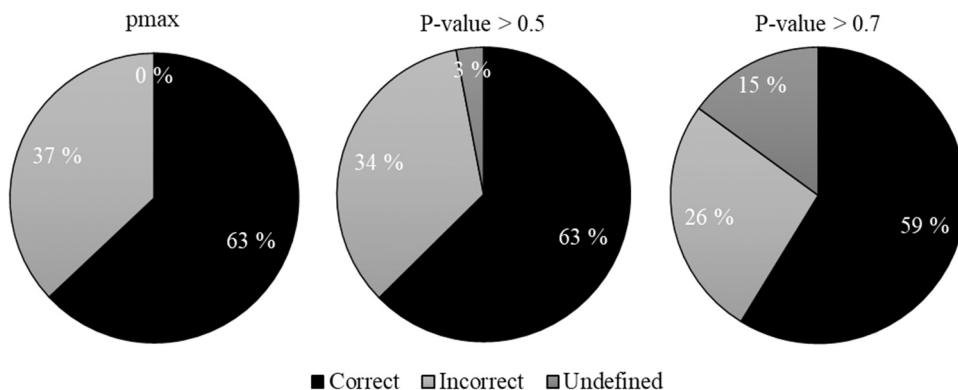
Fig. 3. The overall frequency of correct, incorrect and inconclusive (undefined) eye colour predictions using the IrisPlex webtool, with and without thresholds (n = 519).

rs12913832, eye colours of the Norwegian study group were also analysed based on this SNP (Table S3). Only 70.9% of rs12913832 GG individuals had the expected blue eye colour, whereas 79% and 39% of rs12913832 AA and AG individuals, respectively, had the expected brown eye colour. Intermediate eye colour was observed with all genotypes, but the majority was observed in rs12913832 GG individuals.

3.3. Eye colour phenotype-genotype associations using quantitative PIE-score

For the evaluation of phenotype-genotype associations, the eye colour phenotype was assessed using the quantitative PIE-score [30], an objective method that was found to be highly correlated with the qualitative categorisation by observation from photographs (Spearman's correlation coefficient -0.88; $p < 0.001$) (Fig. S3). Among the six IrisPlex SNPs, rs12913832 showed the strongest association with PIE-score. The PIE-scores were significantly different for all pairwise comparisons between the three genotypes GG, AG and AA (Fig. 4A, $p < 0.001$). The remaining five IrisPlex SNPs were also significantly associated with PIE-score, but not as strongly as rs12913832 (Fig. S4).

The PIE-score in individuals with the genotype rs12913832 AG varied considerably, ranging from 1 (blue eyes) to -1 (brown eyes) (PIE median -0.82) (Fig. 4A). Although there was generally little spread in the PIE-score among individuals with genotype GG (PIE median 0.98)

and genotype AA (PIE median -0.99), we observed some individuals with genotype GG having negative PIE values (perceived as intermediate to brown) and individuals with genotype AA having positive PIE-values (perceived as intermediate). Notably, 94% of individuals carrying the AG genotype were reported to have Norwegian ancestry (n = 123). Norwegian ancestry was also reported in 91% individuals with genotypes GG and low PIE-score (PIE-score < 0, n = 11), as well as the four outliers with genotype AA and high PIE-score (Fig. 4A).

Although all individuals with genotype rs12913832 AA were predicted as brown-eyed by the IrisPlex model with high p-values (> 0.96), we observe that individuals of Norwegian ancestry had statistically significantly higher PIE-scores (perceived as intermediate towards blue eyes) than non-northern Europeans ($p < 0.01$; Fig. 4B). rs12913832 AA individuals in our study population were either of Norwegian or non-northern European ancestry. Additionally, we observed a statistically significant effect of rs16891982 on the PIE-score of rs12913832 AA individuals ($p < 10^{-6}$; Fig. S5). All the individuals with Norwegian ancestry and genotype rs12913832 AA also carried the genotype rs16891982 GG, whereas all except two of the non-northern Europeans carried the ancestral C allele (13 individuals with rs16891982 CC and two individuals with rs16891982 CG). A small but statistically significant effect on the PIE-score was also observed when combining rs12913832 AA with rs1393350 or rs1800407, regardless of ancestry ($p < 0.05$; Fig. S5). It is noteworthy to mention that only few
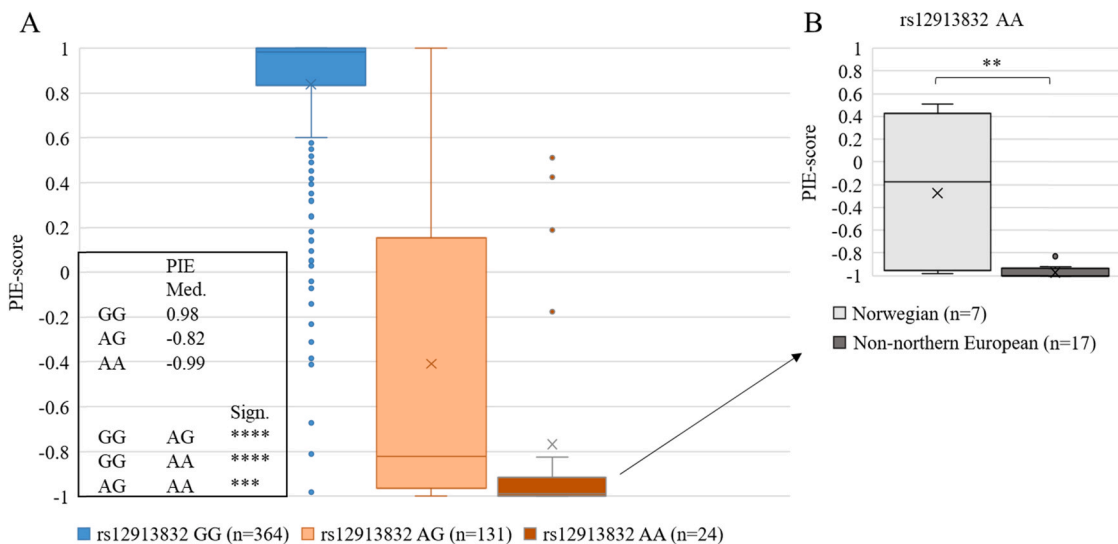

Fig. 4. : A) Boxplot showing PIE-scores of the rs12913832 genotypes (n = 519) and B) subgroups of rs12913832 AA individuals based on ancestry (n = 24), with pairwise comparisons between the genotypes (Mann-Whitney tests). Statistical significance (Sign.) after multiple Bonferroni correction: $p < 0.02$, * *$p < 10^{-2}$, * **$p < 10^{-3}$, * ** *$p < 10^{-6}$. Med.:Median.

rs12913832 AA individuals were observed with rs1393350 AG (n = 4) and rs1800407 AG (n = 2) in our data set.

Among individuals with the genotype rs12913832 GG, we observed a small but statistically significant effect on the PIE-score with the genotypes of rs12203592, rs1393350, rs12896399 and rs168991982 (p < 0.02; Fig. S6). Notably, one individual of Asian ancestry with brown eyes had the rare combination of rs12913832 GG and rs16891982 CC (PIE-score: −0.98). The phenotype was correctly predicted as brown by IrisPlex (p-value: 0.55). However, the prediction was inconclusive when applying the probability threshold of 0.7.

Among individuals with the genotype rs12913832 AG, a statistically significant effect on the PIE-score was only observed for rs16891982 (p < 0.01; Fig. S7).

3.4. Hair colour prediction performance of the HIrisPlex webtool

Using the HIrisPlex webtool with the HPCA, the hair colour of 59% of the individuals (n = 321) were predicted as blond-haired, 32% as brown-haired (n = 175), 5% as red-haired (n = 26) and 3% as black-haired (n = 18) (Fig. 5).

We observed high AUC values for both red and black hair (0.97 and 0.93, respectively) (Table 1B). The AUC values for blond and brown hair were lower (0.72 and 0.70, respectively). The high AUC values for red and black hair reflected the high proportion of true negatives relative to false positives, resulting in high specificity values of 0.98 for red and 0.99 for black hair. For blond and brown hair, false positives were more frequent. Thus, specificities were rather low, with 0.60 for blond and 0.79 for brown hair. In terms of sensitivity, individuals with blond hair had the highest proportion of correct predictions, followed by black and red hair (0.76, 0.73 and 0.68, respectively), whereas only 50% of individuals with brown hair were correctly predicted. PPVs were relatively low for all hair colours (0.50–0.68), whereas the NPVs were higher (0.99 for red and black hair, 0.70 for brown and 0.69 for blond hair).

With the HPCA, the hair colour was predicted correctly in 65% of the individuals (Table 2). The most common prediction error was found in individuals with brown hair who were predicted to have blond hair (44%), or vice versa (21%). Furthermore, neither blond nor red-haired individuals were predicted to have black hair, and none of the black-

haired individuals were predicted to have red hair (Fig. 5, Table 2). Notably, half of the red predictions were false positives (n = 13), and most of them were for individuals with either blond or brown hair (Fig. 5). Two of the false positive predictions were also heterozygous in rs312262906_N29insA. Individuals with this genotype are expected to have red hair and were predicted so with a p-value of 0.93 and 0.61, respectively. When inspecting the photographs that were taken during sample collection, hints of red could be observed in almost half of the individuals with false positive red hair prediction, including one of the individuals with the N29insA variant.

The overall correct predictions increased to 75% when utilising the PGA (Table 2). The PGA combines light/dark hair colour shade probabilities with the categorical hair colour probabilities. Because the shades of hair colour from blond via brown to black are overlapping, adding a p-value for light/dark shade to the categorical predictions provides an additional level of information. Thus, it is possible to differentiate light blond from dark blond and light brown from dark brown/black. Predictions made using HPCA are still considered as correct (e.g., predicted Blond, Blond/D-blond and D-blond/Brown is considered as correct for an individual with self-reported light blond or dark blond hair colour, Table 2). In combination with the HPCA, PGA allows for additional predictions to be considered as correct as there are overlaps between initial categories (e.g., predicted brown and self-reported as dark blond, and predicted D-brown/black and self-reported as black, Table 2). Additionally, dark blond and light brown hair colour were set into one category. The most pronounced increase in correct predictions when applying this approach was for dark blond/light brown (61–76%) and black (73–93%) hair colour categories (Table 2). When applying the rule that p-values above 0.25 for red hair are predictors for red, two additional individuals with red hair were predicted correctly, thereby increasing the correct prediction for red hair from 68% to 79% (Table 2).

4. Discussion

In this study, we assessed both the typing performance of the 24 HIrisPlex SNPs using the ForenSeq™ DNA Signature prep kit (Verogen) and the eye and hair colour prediction by the HIrisPlex webtool in a Norwegian study population. We have shown the performance metrics for each of the HIrisPlex SNPs (typing success, read depth and allele balance) together with parameters describing prediction performance (AUC, sensitivity, specificity, PPV and NPV). Additionally, we assessed genotype-phenotype associations of eye colours using the quantitative PIE-score. Thereby, we show that population specific testing on the intendent target population disclose rare and possibly population specific variation in association patterns, which might be useful for future improvements of prediction models.

4.1. MPS genotyping performance

We evaluated only the performance of the HIrisPlex SNPs within the kit and found the typing performance of the multiplex to be satisfactory as complete profiles were obtained for all samples with optimal DNA input. Although the profiles were complete, in agreement with other studies we observed a locus-to-locus variation in terms of DoC and allele balances [24,29,37]. Despite these variations, the sensitivity study demonstrated that the system was also able to type complete and correct HIrisPlex profiles with DNA input as low as 125 pg. This is slightly better than the developmental validation data showing complete and correct profiles with DNA input ≥ 250 pg [23]. However, locus dropout has been reported for samples with optimal DNA input in other studies [24, 29,37,38]. Notably, Sharma et al. [29] demonstrate that sequencing runs with cluster densities within the recommended range by Illumina (1200–1400 K/mm^2) perform better in terms of dropouts than runs with lower cluster densities. Our runs were within this recommended cluster density range or slightly above.

As expected, read counts and allele balances decreased with
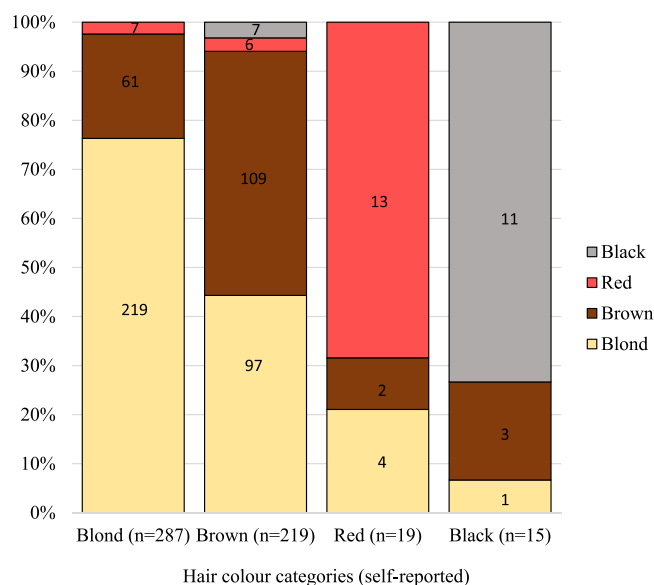

Fig. 5. HIrisPlex hair colour predictions obtained from 540 individuals from Norway. Bars represent percentage of eye colour predicted within the respected self-reported hair colour category. Numbers in the bars represent numbers of individuals predicted within the category.

Table 2

HIrisPlex hair colour predictions obtained from 540 individuals from a Norwegian study population using the highest probability category approach (HPCA) and the prediction guide approach (PGA). Predictions that were considered as correct using the HPCA are highlighted in dark grey, and additional predictions that were considered as correct using the PGA are highlighted in light grey. For the HPCA, the highest p-value for one of the four hair colours (blond, brown, black or red) was considered the predicted phenotype. The PGA combines the highest p-value approach with a p-value for shade (light or dark) in a step-wise model (for the prediction guide see [13]). According to the PGA, hint of red will be seen if a p-value for the red category is more than 0.25.

| | | Self-reported hair colour | | | | | | |
| | | | Dark blond/light brown (n=331) | | | | | |
		Light blond (n=68)	Dark blond (n=219)	Light brown (n=112)	Dark brown (n=107)	Black (n=15)	Red (n=19)	Total (n=540)
Blond	Blond	20	52	15	7	1	0	
	Blond/D-blond	37	99	41	21	0	4(-2)*	
	D-blond/Brown	4	7	6	7	0	0	
Brown	Brown	0	1	0	1	0	0	
	Brown/D-brown	1	22	26	23	0	1	
	D-brown/Black	5	32	19	40	3	1	
Black	D-brown/Black	0	0	0	0	0	0	
	Black	0	0	1	6	11	0	
Red	Red	1	6	4	2	0	13(+2)*	
HPCA		90 %	61 %		60 %	73 %	68 %	**65 %**
PGA		90 %	76 %		60 %	93 %	79 %	**75 %**

(*Predicted* column label runs vertically at left.)

*Two individuals with highest p-value for blond hair but also a p-value > 0.25 for red hair.

*Two individuals with highest p-value for blond hair but also a p-value > 0.25 for red hair.

decreasing amounts of DNA. This caused the poorer performing SNPs to drop out. One of the affected SNPs was rs12913832, which is the most important SNP for eye colour prediction. This SNP also performed poorly in other studies [29,37]. Without this marker, it is not possible to predict eye colour with the IrisPlex webtool [32]. In addition, three other highly ranked SNPs in the HirisPlex model, namely rs16891982, rs12203592 (for eye and hair colour predictions), and rs28777 (for hair colour prediction), were among the lower performing SNPs (also observed by Churchill et al. [37]). These four loci accounted for 36% of all dropouts with 62.5 and 31.3 pg DNA input in the sensitivity study. The consequence of failing to type rs12913832, rs16891982 and rs12203592 combined, is that eye and hair colour cannot be predicted [13]. Importantly, undiscovered allele dropout (false homozygotes) in highly ranked SNPs, especially rs12913832, may lead to false predictions in samples with little DNA input. We observed false homozygotes in these loci with as many as 92 reads, which is far above the default interpretation threshold of 30 reads. This supports the need for more stringent thresholds for genotype interpretation as previously discussed by others [39]. Therefore, to avoid misleading results, we

suggest increasing the interpretation threshold to 100 reads for low input samples or not analysing such samples at all. We emphasise that we did not observe false homozygotes with DNA input of 125 pg or more despite low read counts.

4.2. Eye colour predictions in a Norwegian study population

When testing the IrisPlex model on the Norwegian study population, we obtained high AUCs for blue and brown eye colours, as well as high sensitivities. However, the AUC value for blue eye colour (0.85) was lower than the reported value of 0.94–0.97 in the HirisPlex-S DNA Phenotyping Webtool User Manual Version 2.0 (2018) and other studies [26–28]. This may be because our study resulted in a higher false positive rate for blue eye colour.

In concordance with other studies, no individuals in our study were predicted to have intermediate eyes [26–28]. This immensely affected the error rate, that was found to be 37%. Although the overall prediction error decreased when applying thresholds, most of the intermediate-eyed individuals were still incorrect with a threshold of

0.7. Consequently, the application of probability thresholds only slightly increased the prediction accuracy in the Norwegian population. The overall error rate of 26% with a threshold of 0.7 was still considerably higher than the reported 6% by Walsh et al., [17] who included seven populations across Europe in their dataset. The reason for this substantial difference may be that our Norwegian study population had a higher frequency of intermediate eyes than the other European populations. In addition, the discrepancies might also be partly due to the challenge in categorising eye colours. Both the IrisPlex model and our study were mainly based on subjective categorisation of eye colour by observation. It has been shown that general perception of eye colour varies between observers [31], suggesting that comparisons between studies may be difficult. This challenge of subjective perception was also demonstrated in the Norwegian population by the overlap in PIE-score especially between perceived blue and perceived intermediate eyes. Perception of eye colour might also be influenced by an observer's reference background. For example, a person residing in Norway, where the frequency of light blue eyes is high, might more easily categorise slightly darker eyes as intermediate or brown than a person who is more exposed to darker and brown coloured eyes. Furthermore, categorisation of a continuous trait such as eye colour, will inevitably contribute to some errors.

To be accustomed for forensic applications, a method must be highly reliable. Although the lack of intermediate eye colour predictions leads to a high error rate, none of the brown eyes were classified as blue and only 4% of the blue eyes were classified as brown. Therefore, a blue eye colour prediction indicates that the individual has most likely either blue or intermediate eyes, and a brown eye colour prediction indicates that the individual has most likely brown or intermediate eyes. This observation was also supported when the intermediate-coloured eyes were sub-categorised into intermediate-blue and intermediate-brown (Fig. S8). Most intermediate-blue eyes were predicted as blue (77%), and most intermediate-brown eyes were predicted as brown (83%), a trend also reported by Salvoro et al. [28]. Thus, the obstacles of the IrisPlex model with a three-category system might at least in part be improved by using a two-category system of eye colour (blue and brown), as already suggested by others [15,31,40].

We also observed that more than half of the individuals with incorrect predictions had the *HERC2* genotype rs12913832 GG. This was in contrast to other studies of populations with high frequencies of intermediate eye colours who report highest numbers of incorrect predictions in individuals with rs12913832 AG [26,28,40]. The derived G allele in rs12913832 is known to reduce the production of eumelanin by negatively affecting *OCA2* expression. Hence, homozygous individuals of the derived G allele are expected to have blue eyes [18,19,41]. As only 71% of our individuals with rs12912823 GG genotype had blue eyes, some of the incorrect predictions might be due to the overlap between perceived blue and intermediate-blue, as discussed above. However, when analysing the eye colour based on the objective PIE-score, we also observed rs12913832 GG individuals with intermediate-brown and brown eye colour (low PIE-scores). Brown eye colour in rs12913832 GG individuals has also been observed in other Scandinavian populations (Swedes and Danes), suggesting that other variants might upregulate the expression of OCA2 and overrule the G-allele down regulation of OCA2 in some individuals [30]. A recent study showed that other SNPs than the IrisPlex SNPs, such as rs1126809 in *TYR,* rs62538956 and rs35866166 in *TYRP1* and rs1289469 in *SLC24A4*, were associated with brown eye colour in rs12913832 GG individuals [42]. Inclusion of these SNPs in the model for eye colour prediction, might improve the accuracy in the Norwegian population.

In addition to the rs12913832 GG individuals with non-blue eye colour, we observed some individuals with the AA and AG genotype having the unexpected intermediate and intermediate towards blue eye colours (based on PIE-score). Although the sample size was limited (n = 24), rs12913832 AA individuals of Norwegian ancestry had less brown eye colours (based on PIE-score) than individuals of non-northern

European ancestry. The rs12913832 A allele is positively affecting transcription of *OCA2* and has been shown to be strongly associated with dark iris colour [18,43]. However, a nonsynonymous mutation (A-allele) in rs1800407 is suggested to be a penetrance modifier of rs12913832, associated with lighter eye colour [19,30,44]. Only two of the Norwegians carried the A-allele in rs1800407 with rs12913832 AA, suggesting that other SNPs might explain the lighter eye colour. All the individuals with Norwegian ancestry had the rs16891982 GG genotype, in contrast to non-northern Europeans who nearly all carried the ancestral C-allele. SNP rs16891982 in *SLC45A2* is extensively used as a predictor for European ancestry as the G-allele has a high frequency in Europeans (frequency 97%) and is nearly absent in Africans, South-East Asians and South Americans (frequency of $\sim$ 1–2%) [45,46]. A recent study in mouse models showed that SLC45A2 was involved in melanosome maturation, similar to OCA2 [47]. They also demonstrated that the G variant in rs16891982 lead to an instable protein that negatively affected the melanin synthesis. This might explain the lighter eye colour that we observed in rs12913832 AA individuals. However, some of these individuals were not correctly predicted by IrisPlex. Other nonsynonymous mutations in *OCA2,* such as the T-alleles in s7465330 and rs121918166, have previously been shown to be associated with blue eye colour in heterozygous rs12913832 individuals [44]. These variants might also be associated with lighter eye colour in the Norwegian population. It is also important to note that other factors such as gender, age and iris patterns can affect eye colour [40,48,49]. Reported gender effects on eye colour seems to be population specific [40,49,50], and was not observed in the two Scandinavian populations analysed so far [40]. The number of rs12913832 AA individuals in our sample population was too small to fully explore this effect. However, the individuals that were observed to have lighter eye colour were both males and females of age 30–55 with perceived intermediate-brown and intermediate-blue eye colour.

4.3. Hair colour predictions in a Norwegian study population

When testing the HIrisPlex model on a Norwegian study population, we obtained similar AUC values for hair colour as reported in the HIrisPlex-S DNA Phenotyping Webtool User Manual Version 2.0 (2018). However, the AUC value for blond hair (0.72) was considerably lower than reported by HIrisPlex (0.81). This may be because the most common incorrect prediction across all hair colours were for individuals with brown hair who were predicted to have blond hair, which is also in line with data from a Swedish population [51]. Kukla-Bartoszek et al. suggested that incorrect predictions may be the result of age-dependent hair colour darkening [52]. They regularly observed children with blond hair developing brown hair with increasing age. Most of these individuals were predicted to have blond hair. Although we did not have information about our participants' hair colour as children, we suggest that age-dependent hair colour darkening increased the incorrect predictions of individuals with brown hair. We reduced some of these errors when applying the PGA (prediction guide approach) for interpretation, as recommended by Walsh et al. [8,13]. This approach increased the correct predictions in the dark blond/light brown category considerably, and the overall correct predictions across the hair colours from 65% to 75%. Our findings are in agreement with the reported 77% accuracy by HIrisPlex and another study [8,53]. Therefore, the PGA should always be utilised for interpretation of a prediction, especially in populations in which blond and brown hair is common. However, blond-haired individuals (light and dark shades) were also predicted to have dark brown hair. This cannot be explained by age onset hair darkening. Even though some inaccuracies might arise due to people's subjective perception of hair colour, these findings suggest the need for further investigation of the genetics of hair colour. Moreover, in half of the individuals with false positive red hair prediction, hints of red were observed in photographs. This demonstrates the difficulties of self-categorisation. Additionally, "strawberry blond" and "auburn" might be difficult to distinguish from

blond and light brown. Thus, in a population with a high frequency of blond and brown-haired individuals, an individual that is predicted to have red hair might not have distinct red hair.

5. Conclusions

In this study, we demonstrated that genotyping the HIrisPlex SNPs using the ForenSeq™ DNA Signature Prep kit was highly reliable with DNA input of 125 pg or higher. Using the HIrisPlex webtool, eye and hair colour were predicted with high accuracies in terms of AUC for blue (0.85) and brown-eyed (0.94) individuals, as well as red (0.97) and black-haired (0.93) individuals. The Norwegian study population displayed high frequencies of blue (52%) and intermediate (34%) eyes, as well as blond (59%) and brown hair (32%). Because of the well-known limitation in predicting intermediate eye colours and the challenge with age-dependent hair colour darkening, a relatively high prediction error was observed (26% for eye colour with $p > 0.7\%$ and 35% for hair colour using the HPCA). However, 75% of the hair colour predictions were correct when using the PGA as opposed to the HPCA approach. This study also disclosed rare phenotype-genotype associations, pointing to the importance of population specific testing before implementing FDP in casework.

CRediT authorship contribution statement

Nina Mjølsnes Salvo: Conceptualisation, Formal analysis, Visualisation, Writing – original draft. **Kirstin Janssen**: Conceptualisation, Supervision, Investigation, Writing – review & editing. **Maria Kristine Kirsebom**: Investigation. **Olivia Strunge Meyer**: Writing – review & editing. **Thomas Berg**: Conceptualisation, Supervision. **Gunn-Hege Olsen**: Conceptualisation, Supervision, Project administration, Writing – review & editing.

Declaration of Competing Interest

The authors declare that they have no known competing financial interests or personal relationshipsthat could have appeared to influence the work reported in this paper.

Appendix A. Supporting information

Supplementary data associated with this article can be found in the online version at doi:10.1016/j.fsigen.2021.102620.

References

[1] P.M. Schneider, B. Prainsack, M. Kayser, The use of forensic DNA phenotyping in predicting appearance and biogeographic ancestry, Dtsch. Arztebl. Int 116 (2019) 873–880, https://doi.org/10.3238/arztebl.2019.0873.

[2] M. Kayser, Forensic DNA phenotyping: predicting human appearance from crime scene material for investigative purposes, Forensic Sci. Int. Genet. 18 (2015) 33–48, https://doi.org/10.1016/j.fsigen.2015.02.003.

[3] M. Kayser, P. de Knijff, Improving human forensics through advances in genetics, genomics and molecular biology, Nat. Rev. Genet. 12 (2011) 179–192, https://doi.org/10.1038/nrg2952.

[4] F. Liu, K. van Duijn, J.R. Vingerling, A. Hofman, A.G. Uitterlinden, A.C.J. W. Janssens, M. Kayser, Eye color and the prediction of complex phenotypes from genotypes, Curr. Biol. 19 (2009) R192–R193, https://doi.org/10.1016/J.CUB.2009.01.027.

[5] Y. Ruiz, C. Phillips, A. Gomez-Tato, J. Alvarez-Dios, M. Casares de Cal, R. Cruz, O. Maroñas, J. Söchtig, M. Fondevila, M.J. Rodriguez-Cid, Á. Carracedo, M. V. Lareu, Further development of forensic eye color predictive tests, Forensic Sci. Int. Genet. 7 (2013) 28–40, https://doi.org/10.1016/J.FSIGEN.2012.05.009.

[6] J. Söchtig, C. Phillips, O. Maroñas, A. Gómez-Tato, R. Cruz, J. Alvarez-Dios, M.-Á. C. de Cal, Y. Ruiz, K. Reich, M. Fondevila, Á. Carracedo, M.V. Lareu, Exploration of SNP variants affecting hair colour prediction in Europeans, Int. J. Leg. Med. 129 (2015) 963–975, https://doi.org/10.1007/s00414-015-1226-y.

[7] W. Branicki, F. Liu, K. van Duijn, J. Draus-Barini, E. Pośpiech, S. Walsh, T. Kupiec, A. Wojas-Pelc, M. Kayser, Model-based prediction of human hair color using DNA variants, Hum. Genet. 129 (2011) 443–454, https://doi.org/10.1007/s00439-010-0939-8.

[8] S. Walsh, F. Liu, A. Wollstein, L. Kovatsi, A. Ralf, A. Kosiniak-Kamysz, W. Branicki, M. Kayser, The HIrisPlex system for simultaneous prediction of hair and eye colour from DNA, Forensic Sci. Int. Genet. 7 (2013) 98–115, https://doi.org/10.1016/J.FSIGEN.2012.07.005.

[9] G. Samuel, B. Prainsack, The regulatory landscape of forensic DNA phenotyping in, Europe (2018). http://www.visage-h2020.eu/Report_regulatory_landscape_FDP_in_Europe2.pdf.

[10] G. Samuel, B. Prainsack, Soc., Ethic-.-., Regul. Dimens. Forensic DNA phenotyping (2019). http://www.visage-h2020.eu/#reports.

[11] L. Chaitanya, K. Breslin, S. Zuñiga, L. Wirken, E. Pośpiech, M. Kukla-Bartoszek, T. Sijen, P. de Knijff, F. Liu, W. Branicki, M. Kayser, S. Walsh, The HIrisPlex-S system for eye, hair and skin colour prediction from DNA: Introduction and forensic developmental validation, Forensic Sci. Int. Genet. 35 (2018) 123–135, https://doi.org/10.1016/j.fsigen.2018.04.004.

[12] S. Walsh, L. Chaitanya, K. Breslin, C. Muralidharan, A. Bronikowska, E. Pospiech, J. Koller, L. Kovatsi, A. Wollstein, W. Branicki, F. Liu, M. Kayser, Global skin colour prediction from DNA, Hum. Genet. 136 (2017) 847–863, https://doi.org/10.1007/s00439-017-1808-5.

[13] S. Walsh, L. Chaitanya, L. Clarisse, L. Wirken, J. Draus-Barini, L. Kovatsi, H. Maeda, T. Ishikawa, T. Sijen, P. de Knijff, W. Branicki, F. Liu, M. Kayser, Developmental validation of the HIrisPlex system: DNA-based eye and hair colour prediction for forensic and anthropological usage, Forensic Sci. Int. Genet. 9 (2014) 150–161, https://doi.org/10.1016/J.FSIGEN.2013.12.006.

[14] J.S. Allwood, S. Harbison, SNP model development for the prediction of eye colour in New Zealand, Forensic Sci. Int. Genet. 7 (2013) 444–452, https://doi.org/10.1016/J.FSIGEN.2013.03.005.

[15] K.L. Hart, S.L. Kimura, V. Mushailov, Z.M. Budimlija, M. Prinz, E. Wurmbach, Improved eye- and skin-color prediction based on 8 SNPs, Croat. Med. J. 54 (2013) 248–256, https://doi.org/10.3325/cmj.2013.54.248.

[16] J. Mengel-From, C. Børsting, J.J. Sanchez, H. Eiberg, N. Morling, Human eye colour and HERC2, OCA2 and MATP, Forensic Sci. Int. Genet. 4 (2010) 323–328, https://doi.org/10.1016/J.FSIGEN.2009.12.004.

[17] S. Walsh, A. Wollstein, F. Liu, U. Chakravarthy, M. Rahu, J.H. Seland, G. Soubrane, L. Tomazzoli, F. Topouzis, J.R. Vingerling, J. Vioque, A.E. Fletcher, K. N. Ballantyne, M. Kayser, DNA-based eye colour prediction across Europe with the IrisPlex system, Forensic Sci. Int. Genet. 6 (2012) 330–340, https://doi.org/10.1016/J.FSIGEN.2011.07.009.

[18] M. Visser, M. Kayser, R.-J. Palstra, HERC2 rs12913832 modulates human pigmentation by attenuating chromatin-loop formation between a long-range enhancer and the OCA2 promoter, Genome Res 22 (2012) 446–455, https://doi.org/10.1101/gr.128652.111.

[19] R.A. Sturm, D.L. Duffy, Z.Z. Zhao, F.P.N. Leite, M.S. Stark, N.K. Hayward, N. G. Martin, G.W. Montgomery, A Single SNP in an evolutionary conserved region within intron 86 of the herc2 gene determines human blue-brown eye color, Am. J. Hum. Genet. 82 (2008) 424, https://doi.org/10.1016/J.AJHG.2007.11.005.

[20] S. Walsh, A. Lindenbergh, S.B. Zuniga, T. Sijen, P. de Knijff, M. Kayser, K. N. Ballantyne, Developmental validation of the IrisPlex system: determination of blue and brown iris colour for forensic intelligence, Forensic Sci. Int. Genet. 5 (2011) 464–471, https://doi.org/10.1016/J.FSIGEN.2010.09.008.

[21] P. Valverde, E. Healy, I. Jackson, J.L. Rees, A.J. Thody, Variants of the melanocyte–stimulating hormone receptor gene are associated with red hair and fair skin in humans, Nat. Genet. 11 (1995) 328–330, https://doi.org/10.1038/ng1195-328.

[22] N. Flanagan, E. Healy, A. Ray, S. Philips, C. Todd, I.J. Jackson, M.A. Birch-Machin, J.L. Rees, Pleiotropic effects of the melanocortin 1 receptor (MC1R) gene on human pigmentation, Hum. Mol. Genet 9 (2000) 2531–2537, https://doi.org/10.1093/hmg/9.17.2531.

[23] A.C. Jäger, M.L. Alvarez, C.P. Davis, E. Guzmán, Y. Han, L. Way, P. Walichiewicz, D. Silva, N. Pham, G. Caves, J. Bruand, F. Schlesinger, S.J.K. Pond, J. Varlaro, K. M. Stephens, C.L. Holt, Developmental validation of the MiSeq FGx forensic genomics system for targeted next generation sequencing in forensic DNA casework and database laboratories, Forensic Sci. Int. Genet. 28 (2017) 52–70, https://doi.org/10.1016/J.FSIGEN.2017.01.011.

[24] F. Guo, J. Yu, L. Zhang, J. Li, Massively parallel sequencing of forensic STRs and SNPs using the Illumina® ForenSeqTM DNA Signature Prep Kit on the MiSeq FGxTM Forensic Genomics System, Forensic Sci. Int. Genet. 31 (2017) 135–148, https://doi.org/10.1016/J.FSIGEN.2017.09.003.

[25] C. Børsting, N. Morling, Next generation sequencing and its applications in forensic genetics, Forensic Sci. Int. Genet. 18 (2015) 78–89, https://doi.org/10.1016/J.FSIGEN.2015.02.002.

[26] G.M. Dembinski, C.J. Picard, Evaluation of the IrisPlex DNA-based eye color prediction assay in a United States population, Forensic Sci. Int. Genet. 9 (2014) 111–117, https://doi.org/10.1016/J.FSIGEN.2013.12.003.

[27] V. Kastelic, E. Pośpiech, J. Draus-Barini, W. Branicki, K. Drobnič, Prediction of eye color in the Slovenian population using the IrisPlex SNPs. Croat. Med. J. 54 (2013) 381–386, https://doi.org/10.3325/cmj.2013.54.381.

[28] C. Salvoro, C. Faccinetto, L. Zucchelli, M. Porto, A. Marino, G. Occhi, G. de los Campos, G. Vazza, Performance of four models for eye color prediction in an Italian population sample, Forensic Sci. Int. Genet. 40 (2019) 192–200, https://doi.org/10.1016/J.FSIGEN.2019.03.008.

[29] V. Sharma, K. Jani, P. Khosla, E. Butler, D. Siegel, E. Wurmbach, Evaluation of ForenSeqTM signature prep Kit B on predicting eye and hair coloration as well as biogeographical ancestry by using universal analysis software (UAS) and available web-tools, Electrophoresis 40 (2019) 1353–1364, https://doi.org/10.1002/elps.201800344.

[30] J.D. Andersen, P. Johansen, S. Harder, S.R. Christoffersen, M.C. Delgado, S. T. Henriksen, M.M. Nielsen, E. Sørensen, H. Ullum, T. Hansen, A.L. Dahl, R. R. Paulsen, C. Børsting, N. Morling, Genetic analyses of the human eye colours using a novel objective method for eye colour classification, Forensic Sci. Int. Genet. 7 (2013) 508–515, https://doi.org/10.1016/j.fsigen.2013.05.003.

[31] O.S. Meyer, C. Børsting, J.D. Andersen, Perception of blue and brown eye colours for forensic DNA phenotyping, Forensic Sci. Int. Genet. Suppl. Ser. 7 (2019) 476–477, https://doi.org/10.1016/J.FSIGSS.2019.10.057.

[32] S. Walsh, F. Liu, K.N. Ballantyne, M. van Oven, O. Lao, M. Kayser, IrisPlex: A sensitive DNA tool for accurate prediction of blue and brown eye colour in the absence of ancestry information, Forensic Sci. Int. Genet. 5 (2011) 170–180, https://doi.org/10.1016/J.FSIGEN.2010.02.004.

[33] R Core Team, R: A Lang. Environ. Stat. Comput. (2019). https://www.r-project.org/.

[34] T. Sing, O. Sander, N. Beerenwinkel, T. Lengauer, ROCR: visualizing classifier performance in R, Bioinformatics 21 (2005) 3940–3941, https://doi.org/10.1093/bioinformatics/bti623.

[35] C. Weihs, U. Ligges, K. Luebke, N. Raabe, klaR Analyzing German Business Cycles, in: D. Baier, R. Decker, L. Schmidt-Thieme (Eds.), Data Anal. Decis. Support, Springer-Verlag, 2005, pp. 335–343, https://doi.org/10.1007/3-540-28397-8_36.

[36] O.S. Meyer, N.M. Salvo, A. Kjærbye, M. Kjersem, M.M. Andersen, E. Sørensen, H. Ullum, K. Janssen, N. Morling, C. Børsting, G.-H. Olsen, J.D. Andersen, Prediction of eye colour in scandinavians using the eyecolour 11 (EC11) SNP set, in: Genes, 12, Basel,, 2021, p. 821, https://doi.org/10.3390/GENES12060821.

[37] J.D. Churchill, N.M.M. Novroski, J.L. King, L.H. Seah, B. Budowle, Population and performance analyses of four major populations with illumina's fgx forensic genomics system, Forensic Sci. Int. Genet. 30 (2017) 81–92, https://doi.org/10.1016/j.fsigen.2017.06.004.

[38] A.L. Silvia, N. Shugarts, J. Smith, A preliminary assessment of the ForenSeqTM FGx System: next generation sequencing of an STR and SNP multiplex, Int. J. Leg. Med. 131 (2017) 73–86, https://doi.org/10.1007/s00414-016-1457-6.

[39] C. Hussing, R. Bytyci, C. Huber, N. Morling, C. Børsting, The Danish STR sequence database: duplicate typing of 363 Danes with the ForenSeqTM DNA Signature Prep Kit, Int. J. Leg. Med. 133 (2019) 325–334, https://doi.org/10.1007/s00414-018-1854-0.

[40] C. Pietroni, J.D. Andersen, P. Johansen, M.M. Andersen, S. Harder, R. Paulsen, C. Børsting, N. Morling, The effect of gender on eye colour variation in European populations and an evaluation of the IrisPlex prediction model, Forensic Sci. Int. Genet. 11 (2014) 1–6, https://doi.org/10.1016/J.FSIGEN.2014.02.002.

[41] H. Eiberg, J. Troelsen, M. Nielsen, A. Mikkelsen, J. Mengel-From, K.W. Kjaer, L. Hansen, Blue eye color in humans may be caused by a perfectly associated founder mutation in a regulatory element located within the HERC2 gene inhibiting OCA2 expression, Hum. Genet. 123 (2008) 177–187, https://doi.org/10.1007/s00439-007-0460-x.

[42] O.S. Meyer, M.M.B. Lunn, S.L. Garcia, A.B. Kjærbye, N. Morling, C. Børsting, J. D. Andersen, Association between brown eye colour in rs12913832:GG individuals and SNPs in TYR, TYRP1, and SLC24A4, PLoS One 15 (2020), e0239131, https://doi.org/10.1371/journal.pone.0239131.

[43] M.N. Shapturenko, S.I. Vakula, A.V. Kandratsiuk, I.G. Gudievskaya, M. V. Shinkevich, A.U. Luhauniou, S.R. Borovko, L.N. Marchenko, A.V. Kilchevsky, HERC2 (rs12913832) and OCA2 (rs1800407) genes polymorphisms in relation to iris color variation in Belarusian population, Forensic Sci. Int. Genet. Suppl. Ser. 7 (2019) 331–332, https://doi.org/10.1016/J.FSIGSS.2019.09.127.

[44] J.D. Andersen, C. Pietroni, P. Johansen, M.M. Andersen, V. Pereira, C. Børsting, N. Morling, Importance of nonsynonymous OCA2 variants in human eye color prediction, Mol. Genet. Genom. Med. 4 (2016) 420–430, https://doi.org/10.1002/mgg3.213.

[45] C. Phillips, W. Parson, B. Lundsberg, C. Santos, A. Freire-Aradas, M. Torres, M. Eduardoff, C. Børsting, P. Johansen, M. Fondevila, N. Morling, P. Schneider, Á. Carracedo, M.V. Lareu, Building a forensic ancestry panel from the ground up: The EUROFORGEN global AIM-SNP set, Forensic Sci. Int. Genet. 11 (2014) 13–25, https://doi.org/10.1016/J.FSIGEN.2014.02.012.

[46] K.K. Kidd, W.C. Speed, A.J. Pakstis, M.R. Furtado, R. Fang, A. Madbouly, M. Maiers, M. Middha, F.R. Friedlaender, J.R. Kidd, Progress toward an efficient panel of SNPs for ancestry inference, Forensic Sci. Int. Genet. 10 (2014) 23–32, https://doi.org/10.1016/J.FSIGEN.2014.01.002.

[47] L. Le, I.E. Escobar, T. Ho, A.J. Lefkovith, E. Latteri, K.D. Haltaufderhyde, M. K. Dennis, L. Plowright, E.V. Sviderskaya, D.C. Bennett, E. Oancea, M.S. Marks, SLC45A2 protein stability and regulation of melanosome pH determine melanocyte pigmentation, Mol. Biol. Cell. 31 (2020) 2687–2702, https://doi.org/10.1091/mbc.E20-03-0200.

[48] R.A. Sturm, M. Larsson, Genetics of human iris colour and patterns, Pigment Cell Melanoma Res 22 (2009) 544–562, https://doi.org/10.1111/j.1755-148X.2009.00606.x.

[49] C. Martinez-Cadenas, M. Penãa-Chilet, M. Ibarrola-Villava, G. Ribas, Gender is a major factor explaining discrepancies in eye colour prediction based on HERC2/OCA2 genotype and the IrisPlex model, Forensic Sci. Int. Genet. 7 (2013) 453–460, https://doi.org/10.1016/J.FSIGEN.2013.03.007.

[50] C. Martinez-Cadenas, M. Peña-Chilet, M.J. Llorca-Cardeñosa, R. Cervera, M. Ibarrola-Villava, G. Ribas, Gender and eye colour prediction discrepancies: a reply to criticisms, Forensic Sci. Int. Genet. 9 (2014) e7–e9, https://doi.org/10.1016/J.FSIGEN.2013.10.002.

[51] K. Junker, A. Staadig, M. Sidstedt, A. Tillmar, J. Hedman, Phenotype prediction accuracy – A Swedish perspective, Forensic Sci. Int. Genet. Suppl. Ser. 7 (2019) 384–386, https://doi.org/10.1016/J.FSIGSS.2019.10.022.

[52] M. Kukla-Bartoszek, E. Pośpiech, M. Spólnicka, J. Karłowska-Pik, D. Strapagiel, E. Żądzińska, I. Rosset, M. Sobalska-Kwapis, M. Słomka, S. Walsh, M. Kayser, A. Sitek, W. Branicki, Investigating the impact of age-depended hair colour darkening during childhood on DNA-based hair colour prediction with the HIrisPlex system, Forensic Sci. Int. Genet. 36 (2018) 26–33, https://doi.org/10.1016/j.fsigen.2018.06.007.

[53] M. Diepenbroek, B. Bayer, K. Schwender, R. Schiller, J. Lim, R. Lagacé, K. Anslinger, Evaluation of the ion AmpliseqTM Phenotrivium Panel: MPS-Based Assay for Ancestry and Phenotype Predictions Challenged by Casework Samples, in: Genes, 11, Basel,, 2020, pp. 1–24, https://doi.org/10.3390/genes11121398.

Paper 2

Biogeographical ancestry analyses using the ForenSeq™ DNA Signature Prep kit and multiple prediction tools

Authors: Nina Mjølsnes Salvo*, Gunn-Hege Olsen, Thomas Berg and Kirstin Janssen

Centre for Forensic Genetics, Department of Medical Biology, Faculty of Health Sciences, UiT The Arctic University of Norway, Norway

*Corresponding author. Email: nina.mjolsnes@uit.no. Address: UiT – The Arctic University of Norway, Post Box 6050, 9037 Tromsø, Norway

Abstract

The inference of biogeographical ancestry (BGA) can assist in police investigations of serious crime cases and help to identify missing persons and victims of mass disasters. In this study we evaluated the typing performance of 56 ancestry-informative SNPs using The ForenSeq™ DNA Signature Prep Kit on the MiSeq FGx system. Furthermore, we compared the prediction accuracy of the tools Universal Analysis Software (UAS), the FROG-kb and GenoGeographer when inferring the ancestry of 503 Europeans, 22 non-Europeans and 5 individuals with co-ancestry. The kit was highly sensitive with complete aiSNP profiles in samples with as low as 250pg input DNA. However, in line with others we observed low read depth and occasional drop out in some SNPs. Therefore, we suggest using not less than the recommended 1ng input DNA. FROG-kb and GenoGeographer accurately predicted both Europeans (99.6% and 91.8% correct, respectively) and non-Europeans (95.4% and 90.9% correct, respectively). The UAS was highly accurate when predicting Europeans (96.0% correct) but performed poorer when predicting non-Europeans (40.9% correct). None of the tools were able to correctly predict individuals with co-ancestry. Our study demonstrates that the use of multiple prediction tools will increase the prediction accuracy of BGA inference in forensic casework.

Keywords

Introduction

Biogeographical ancestry (BGA) is a person´s ancestral geographical origin based on population genetic structures [1]. BGA inference is a valuable intelligence tool in forensic genetics. Inferring a person's BGA from crime scene DNA alone can aid police investigations by providing investigative leads and narrowing down a pool of potential suspects in cases where conventional DNA profiling fails to match a suspect or a DNA database record [2,3]. The intelligence tool can also aid identification of missing persons and victims of mass disasters.

BGA inference is possible by using ancestry informative markers (AIMs) that are differently distributed among various populations. In the forensic genetics context, AIMs are often short autosomal sequences such as single nucleotide polymorphisms (SNPs), insertion/deletions (indels), and/or microhaplotypes [4–6]. Short markers are preferred because forensic samples often contain small amounts of DNA and/or degraded DNA. To be able to infer BGA beyond the continental level, many more markers are required than for conventional DNA profiling. High throughput methods such as Massively parallel sequencing (MPS) have enabled typing of a larger number of markers on very small amounts of DNA [7]. Over the last decade various commercial and community developed MPS assays that include AIM panels for BGA prediction have been made available, such as MAPlex [4], Precision ID Ancestry Panel by Thermo Fisher Scientific and VISAGE Basic Tool [8,9]. Herein, we use the ForenSeq™ DNA Signature Prep Kit on the MiSeq FGx system (Verogen, San Diego, CA). This kit has been available for almost a decade now and has been proven to be a robust assay for obtaining reliable SNP profiles from low amounts of DNA [10,11]. Primer mix B supplied with the kit contains primers to multiplex over 200 forensically relevant genetic markers, including 56 ancestry informative SNPs (aiSNPs). The Verogen 56 aiSNP panel comprises the widely used Kidd lab (Yale University) panel of 55 SNPs [12], plus rs1919550. The 55 Kidd aiSNPs were selected based on their ability to predict ancestry on a continental scale. With relatively few SNPs, this panel is able to differentiate five to nine global biogeographic regions, depending on the number of reference populations used [12–14]. Integrated in the forensic MPS workflow by Verogen, the Universal Analysis Software (UAS) both analyses the

sequencing data and performs BGA predictions. The predictions are made based on the 56 aiSNPs using a two-dimensional (2D) principal components analysis (PCA) plot with reference populations from the 1000 Genomes Phase 1 project.

As part of an in-house implementation of forensic BGA analysis we have evaluated the genotyping performance of the aiSNPs using the ForenSeq™ DNA Signature Prep Kit as well as the predictive performance of the UAS when typed in a Norwegian study population. The BGA prediction accuracy was furthermore compared to two other available prediction tools with overlapping SNP panels, the forensic research/reference on genetics knowledge base (FROG-kb) [15,16] and GenoGeographer [17]. FROG-kb calculates relative likelihoods of ancestry on 160 reference populations, whereas GenoGeographer runs a likelihood ratio test on 36 reference populations. When inferring BGA for forensic case work, a multiple tool approach is recommended [18,19]. In this study, we provide comparison- and error assessments of three prediction tools that might be relevant for forensic laboratories.

Materials and methods

Study population

Blood samples were collected from 730 volunteers (presumably unrelated) residing in northern Norway from 2015-2017. Ancestry of the volunteer's grandparents was self-reported. The samples were divided into a reference set of 200 Norwegians (defined by four Norwegian grandparents) [14] and a test set of 530 individuals. Of the individuals in the test set, 503 had European ancestry (395 Norwegian), 22 had non-European ancestry (North African, Sub-Saharan African, Asian, East Asian, Middle Eastern and Siberian) and five had reported co-ancestry from either Europe and Asia or Europe and Africa. All samples were collected with fully informed consent and subsequently anonymised. The project is approved by the Faculty of Health Sciences, UiT The Arctic University of Norway (reference number 2021/2034).

Library preparation and sequencing

All samples were previously genotyped with the ForenSeq™ DNA Signature Prep kit, Primer mix B (Verogen) on a MiSeq® FGx instrument [20]. To assess the technical sensitivity of the 56 aiSNPs, serial dilutions (500, 250, 125, 62.5 and 31.3pg) of human male reference DNA 2800M and 007 were analysed in triplicates (see Salvo *et al.* [20] for more details). For BGA analysis, only complete aiSNP profiles were analysed. In cases with suspected drop outs, the samples were retyped.

Analysis of sequence data

Run metrics and sequence data were processed using the ForenSeq™ Universal Analysis Software v1.2 (UAS, Verogen), with interpretation criteria as described in Salvo *et al.* [20]. The default analytical threshold of 1.5% (minimum 10 reads) and interpretation threshold of 4.5% (minimum 30 reads) were applied for all loci. Assessment of the technical performance of the aiSNPs was performed using the same six representative sequencing runs as in Salvo *et al.* [20], with cluster densities of 1200-1600 K/mm2. The performance evaluation was based on profile completeness, read depth and heterozygote balance. Heterozygote balances, also referred to as allele balances, were calculated for all heterozygous genotypes by dividing the number of reads for one allele with the number of total reads for the nucleotide position.

Description of allele frequencies and Hardy-Weinberg equilibrium (HWE) analysis were performed using GenAlEx v6.5 [21]. Bonferroni correction for multiple testing was applied.

Population structure of the Norwegian reference population

Ancestral proportions of the Norwegian reference set (n=200) were evaluated using STRUCTURE software version 2.3.4 [22–25] and Principal component analysis (PCA) using the ggbiplot package in R version 4.2.2. The structure of the Norwegian reference set was based on the 55 aiSNPs (Kidd panel) together with 31 reference populations (n=2154) from West Africa (W Africa), South-west Asia (SW Asia), Mediterranean Europe (Med. Europe), North Europe (N Europe) and West Siberia (W Siberia), kindly provided by Kenneth K. Kidd (Table S1). We applied the standard admixture model assuming correlated allele frequencies. At each *K* value from 2 to 10, the program was run 20 times with 10 000 burn-ins and 10 000 Markov Chain Monte Carlo (MCMC) iterations. GenAlEx v6.5 [21,26] was used to prepare the input data file for STRUCTURE, Structure Harvester v.0.6.94 [27] was used to choose the most likely value of *K*, and Clumpak [28] was used to obtain averaged Q-matrix data. The SNP rs1919550 was excluded in the STRUCTURE and PCA analysis as the individuals in the reference populations were not typed for this marker.

Biogeographical ancestry prediction

Biogeographical ancestry (BGA) predictions for each individual in the test set (n=530) were carried out using three different prediction tools: UAS, FROG-kb and GenoGeographer. Prior to ancestry analysis,

the Norwegian reference set (n=200) was included as a reference population in FROG-kb and GenoGeographer. This was not possible for the UAS.

UAS

Initial BGA inference was performed using the UAS with default parameters. The UAS obtains ancestry estimation of an unknown sample by PCA using 1000 Genomes data based on the Verogen 56 aiSNPs. The results from several 1000 Genomes populations are clustered into 3 major ancestry groups (African, East Asian and European). A cluster of Ad Mixed American is also included in the PCA plot for reference. BGA estimation of the unknown sample was possible if it clustered with one of the major ancestry clusters. If the unknown sample was plotted outside any of these clusters or clustered within the Ad Mixed American cluster, we considered the estimation as inconclusive (See example in Figure S2).

FROG-kb

The standalone java application, FrogAncestryCalc [16], was applied to directly access the underlying data of the FROG-kb, http://frog.med.yale.edu/FrogKB/ (accessed 02. February 2024), [15], and to run an ancestry likelihood function to assemble the matrix of likelihoods on the 55 Kidd aiSNPs of 160 potential ancestral populations (underlying reference populations). When compared to the unknown sample, the underlying reference populations were ranked based on likelihood of origin. The higher ranked populations are presented as the more likely population of origin. However, population likelihoods within one order of magnitude are not considered significantly different (Rajeevan et al., 2012). Hence, the population ranked as the highest likely population of origin is not necessarily the correct one, and lower ranked populations cannot be excluded. Considering this, all populations within one order of magnitude were considered for predictions. In case of ambiguous results (e.g., if populations within one order of magnitude originated from different continents), the prediction were considered inconclusive.

GenoGeographer

GenoGeographer Version 0.1.14, http://apps.math.aau.dk/aims/ (accessed 19. August 2021), [17], was applied using the Meta-populations, 95% confidence interval (CI) and Kidd loci (55 Kidd aiSNPs). The reference populations were grouped into nine metapopulations plus the Norwegian reference set. GenoGeographer performed a statistical z-score test, a likelihood ratio test, for each aiSNP profile from the test set to assess whether the profile likely originated from any of the reference populations in the

database [17]. When using a one-sided 95% CI, the critical z-score value was 1.64. Z-scores ≤ 1.64 indicate that the unknown profile is likely to originate from the reference population, and it is "accepted" as the most likely population of origin. The unknown individual can have a z-score ≤ 1.64 for more than one population. If two or more populations are accepted, a likelihood ratio (LR) is computed, which can be used together with the CI to evaluate which population is significantly more plausible than others. If the accepted populations were not significantly different, the prediction were considered inconclusive (similar to Mogensen *et al.* [29]).

Results

Genotyping performance of the aiSNPs using the ForenSeq™ DNA Signature prep kit

The technical performance of the ForenSeq multiplex was evaluated based on all 56 aiSNPs in 177 samples from six different sequencing runs, of which all had a cluster density higher than 1200. In total, 9876/9912 (99.64%) individual locus genotype calls were made. Out of the 177 samples typed, 146 (82.49%) generated complete aiSNP profiles. Drop outs/reads below analytical threshold were observed in three SNPs, rs3814134, rs310644 and rs1572018, which failed to type in 19 out of 177 (10,73%), 16 out of 177 (9,04%) and 1 out of 177 samples (0,56%), respectively (Table S3). Markers rs310644 and rs3814134 had median read depth across samples of less than 100 reads (73 and 94 reads, respectively, Figure 1A and Table S3). In total, 23 of 56 (41%) markers showed low read depth with minimum reads <100 (Figure 1A, Table S3). The heterozygote balance varied from 0.13 to 0.74 in the SNP with the largest range (rs4833103, range=0.67, n=78), and from 0.47 to 0.50 in the SNP with the smallest range (rs1229984, range=0.04, n=4, Figure 1B and Table S4). Three of the aiSNPs were homozygous in this data set (rs1871534, rs2814778 and rs3811801), and heterozygote balance calculations were not applicable for these (Table S4). Figure 1 shows that there is no correlation between low read depth and heterozygote balance.
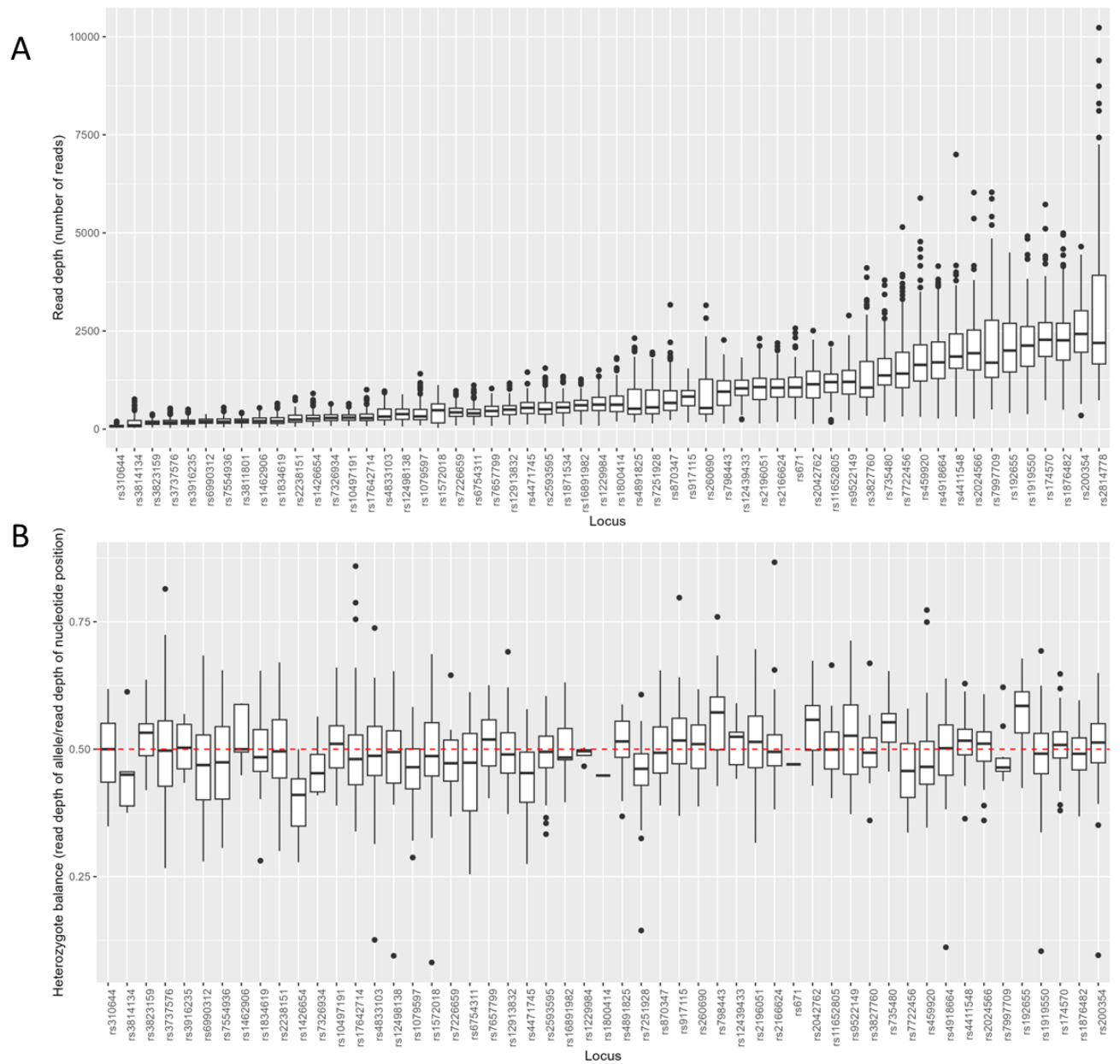
Figure 1: A) Read depth and B) heterozygote balance (read depth of allele/read depth of nucleotide position) of the 56 aiSNPs genotyped with the ForenSeq™ DNA Signature Prep Kit (n=177).

To assess the kit`s ability to produce full profiles from low DNA input amounts, dilution series of control DNA were sequenced. The read depth per locus decreased nearly linearly with decreasing amounts of input DNA, and heterozygote balances became more variable with decreasing amounts of input DNA (Figure S5). For the control DNA, the success rate over all runs was 100% down to 250pg and 99.4% at 125pg (Figure 2). At 125pg, loci rs3737576 and rs310644 dropped out in two samples. At 62.5pg, 15 loci and seven alleles dropped out. The allele drop out was observed in in rs12913832, rs10497191,

rs2238151 and rs1572018. The SNP rs1572018 and rs310644 had the overall highest number of drop outs across all the dilutions, in 13 of 36 (36%) and 12 of 36 (33%) samples, respectively.
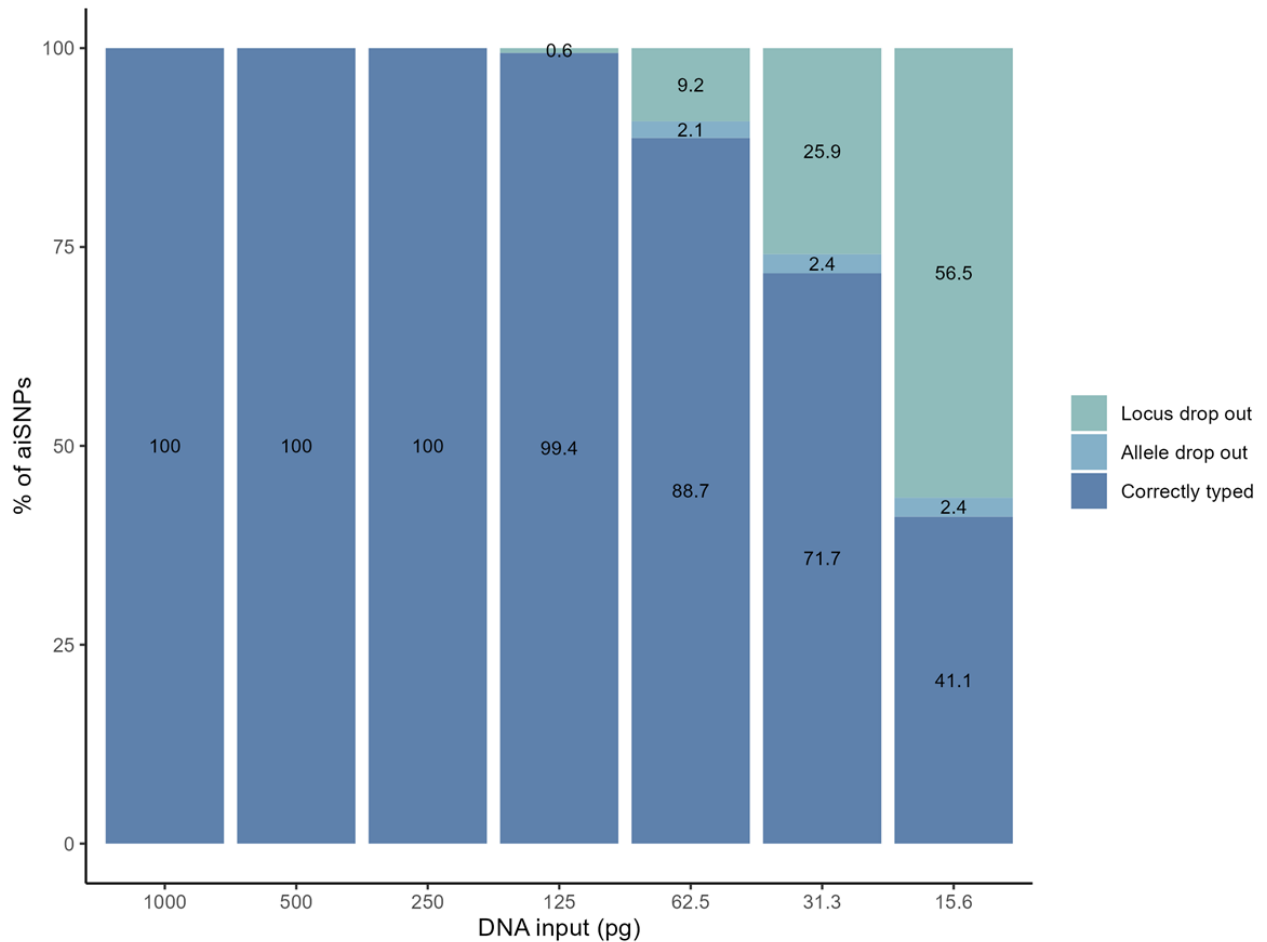
Figure 2: Sensitivity study of the 56 aiSNPs genotyped with the ForenSeq™ DNA Signature Prep Kit, showing profile completeness in relation to DNA input.

False homozygous aiSNP profiles were observed in 19 SNP genotypes in low input samples with less than 250pg DNA. In total 17 alleles were below the default analytical threshold of 10 reads and were therefore not called. The detected alleles in the seemingly homozygous profiles were above interpretation threshold of 30 reads, ranging from 31 to 89 reads (average=50 reads). The remaining two allele drop outs were due to poor balance (<0.1).

Genetic structure of the Norwegian reference population

Prior to prediction analysis using FROG-kb and GenoGeographer, a Norwegian reference population was added to the underlying reference data (see Table S6 for allele frequencies). This population has previously been included in a study on the genetic relationship of European, Mediterranean and South

West Asian populations, analysed with global reference populations using the 55 aiSNP Kidd panel [14]. For a more "zoomed in" perspective, we herein present the genetic structure of the Norwegian reference population when analysed with mainly European populations (Table S1).

There was no significant deviation from Hardy-Weinberg Equilibrium for the aiSNPs in the Norwegian reference set (n=200) after applying the Bonferroni correction (p=0.00089) (Table S7). For five of the 55 aiSNP loci that were monomorphic (rs2814778, rs3811801, rs1871534, rs671, rs1800414), HWE could not be analysed.

To assess the genetic admixture patterns of the Norwegian population, STRUCTURE and PCA analyses were performed using 32 populations (n=2354) from North-Central Europe (including the Norwegian reference population, NOR, and one population from West Siberia, KMZ), Mediterranean and South West Asia, and one outlier population from West Africa (Table S1). Based on delta K calculations [30], K=3 was the optimal number of K for the STRUCTURE analysis (Figure S8). The estimated cluster membership values as average population Q-values for the highest likelihood results are shown in the stacked bar plot in Figure 3. Clustering was observed among West African (green bar), South West Asian (orange bar) and Northern European populations (blue bar). Populations in Central and Mediterranean Europe show both orange and blue clusters. The blue cluster also encompasses the population from West Siberia (the Komi Zyriane, KMZ). The Norwegian population had averages (Q-values) of 95.6% European, 4.1% South West Asian and 0.3% West African origin, and could not be differentiated from other Northern European populations.
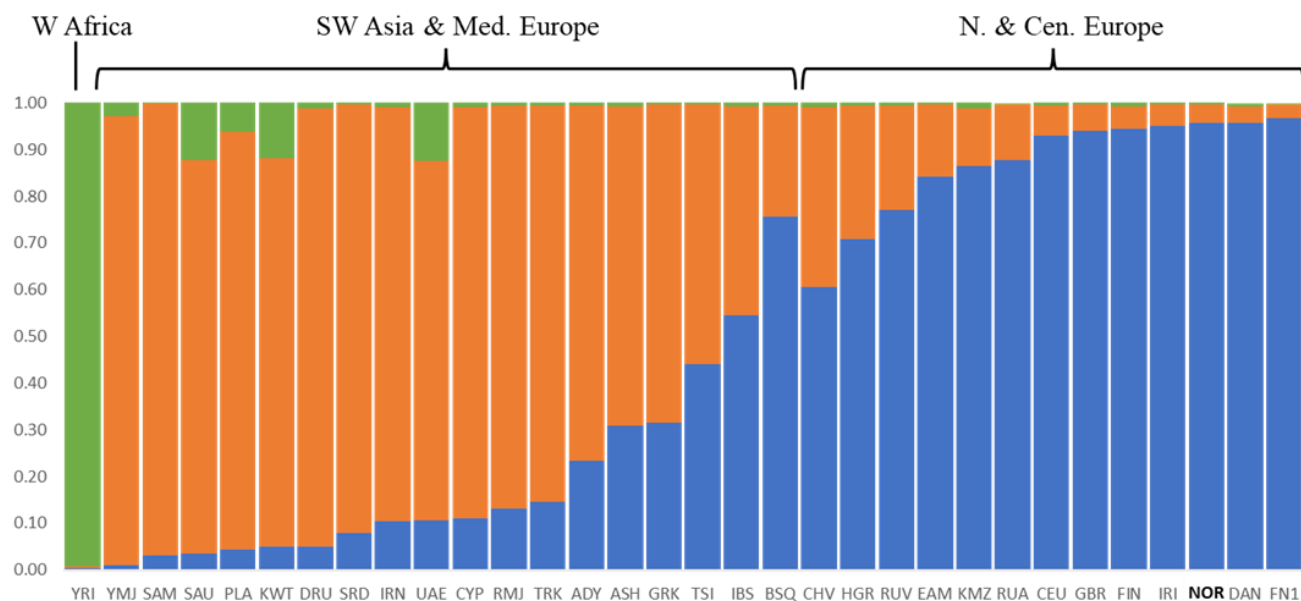
Figure 3: STRUCTURE analysis with *K*=3 using 55 aiSNPs and 32 reference populations (Table S1). "Admixture" and "Correlated allele frequency" models were considered in the analysis.

The PCA plots showed similar results as the STRUCTURE analysis (Figure 4). The first principal component (PC1) separated the West African from the rest. The second PC showed a clinal organisation of the South West Asian to the Mediterranean to the North European populations. The Norwegian population overlap with the North European populations, which infer that the Norwegian population is an admixture of North European populations. Thus, if a Norwegian individual is predicted based on the 55 Kidd aiSNPs to be of Northern European origin, it should be considered as correct.
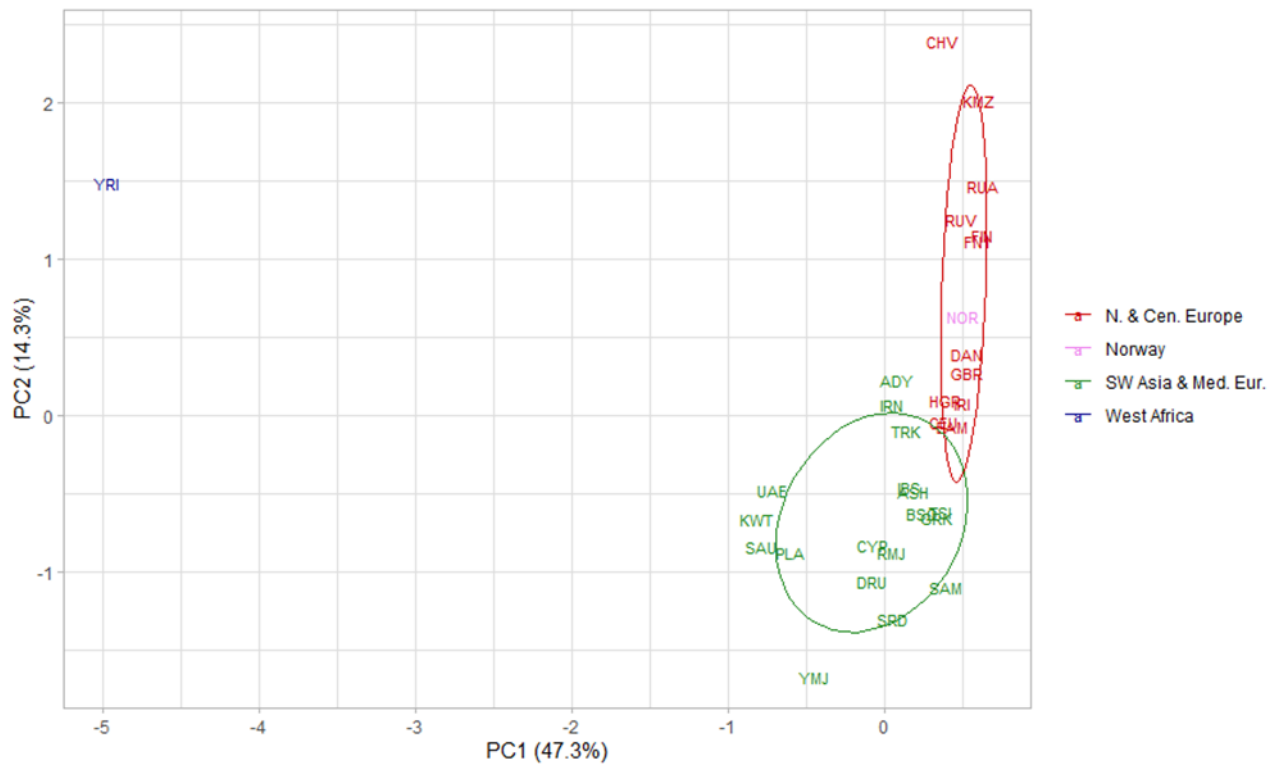
Figure 4: PCA results based on the 55 aiSNP (Kidd panel) allele frequencies for 32 reference populations (including the Norwegian reference population) Table S1.

Biogeographical ancestry prediction

Three different ancestry prediction tools were assessed based on if an individual was assigned to its correct population or not. The test population consisted of 503 Europeans (395 Norwegians), 22 Non-Europeans and 5 individuals with co-ancestry from more than one continent. Figure 5 shows prediction accuracies of the three tools predicting individuals of European and non-European ancestry.
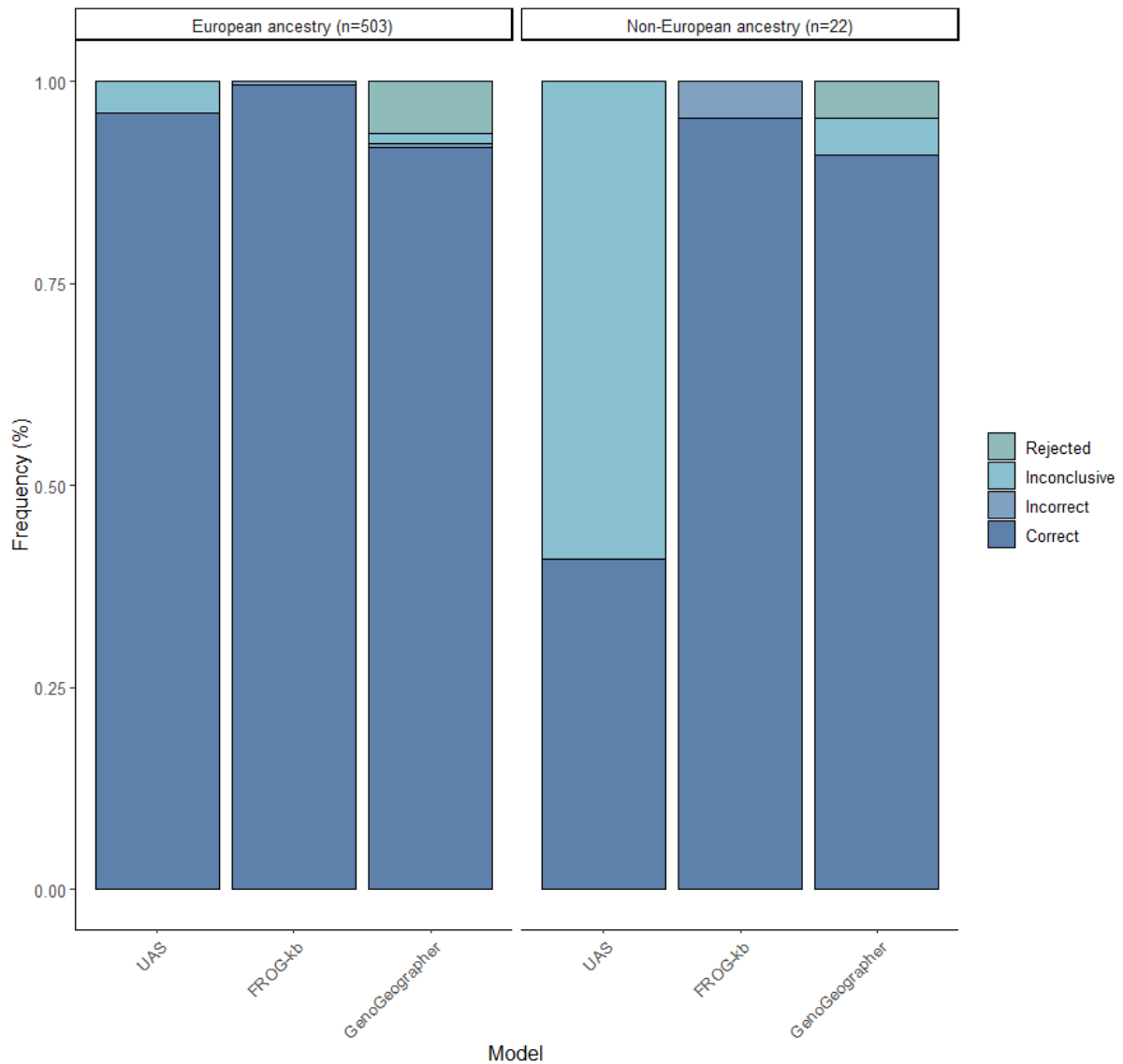
Figure 5: BGA predictions obtained from the three prediction tools, UAS, FROG-kb and Genogeographer using 503 individuals with European ancestry and 22 individuals of non-European ancestry.

The individual aiSNP profiles were initially analysed with the UAS using the default parameters to predict the most likely ancestry. In total 96.0% (483/503) of the European samples were correctly predicted, whereas only 40.9% (9/22) of the non-Europeans were correct (Figure 5). Of the non-Europeans, the model could only predict individuals with sub-Saharan African and East Asian ancestry. The remaining samples (20 European and 13 non-European) were considered as inconclusive as they clustered with the Ad Mixed American cluster or outside any clusters.

FROG-kb had the highest rates of correct predictions, in 99.6% (501/503) of the Europeans and 95.4% (21/22) of the non-Europeans (Figure 5). However, although low, the model also had the highest number of incorrect predictions, in 3 samples. Out of the incorrect predictions, two were of European (one Russian and one Norwegian) and one of North African ancestry, all predicted to be Asians. No sample was considered as inconclusive.

For individual ancestry assignment by GenoGeographer, 91.8% (462/503) of the Europeans and 90.9% (20/22) of the non-Europeans were "accepted" to the correct population (Figure 5). Two European individuals were incorrectly predicted. One of these was a Norwegian predicted to be North African and was not the same Norwegian that was incorrectly predicted with FROG-kb. The other was incorrectly predicted to be East Asian. In total 7 Europeans and one Asian were considered inconclusive because they were accepted to more than one meta-population with overlapping CI. GenoGeographer had the overall lowest correct rate with 32 Europeans and one non-European being "rejected". When only considering the samples that were not rejected by the model, in total 98.1% (462/471) of the Europeans and 95.2% (20/21) of the non-Europeans were correctly predicted.

None of the prediction tools was able to correctly predict the five individuals with reported co-ancestry from two continents. Using the UAS, three individuals were inconclusive and two were incorrectly predicted to be European or African. Using FROG-kb, all five individuals were incorrectly predicted to be Asian, European or African. The GenoGeographer rejected one individual with reported co-ancestry from Europe and Africa, and incorrectly predicted the remaining four individuals to be either Middle Eastern, West Greenlander or admixed European/Middle Eastern/South-Central Asian.

Discussion

In this study we evaluated the technical performance of the 56 aiSNPs in the ForenSeq multiplex and demonstrated that it is highly sensitive. Confirming previous reports, it produced full BGA profiles with input DNA down to 250pg [10,11]. However, when evaluating the technical performance on the 177 samples from six high performing sequencing runs, we observed low read depths and occasional drop out in loci rs3814134, rs310644 and rs1572018 in samples with recommended DNA input (1 ng). Another locus with low read depth, rs3737576, was the first to drop out in low input samples. Low performance (amplification efficiency) of these SNPs is not unique for our study [31–34]. Frégeau *et al.* [33] detected a correlation between amplicon length, AT/GC-content and read depths. Short amplicons with an AT-rich content, such as rs310644, might have lower PCR efficiency, and thereby lower read depth. In a previous study we suggested to increase the interpretation threshold from 30

to 100 reads for phenotype informative SNPs (piSNPs) in this kit when analysing low input samples [20]. As several aiSNPs in our population dataset had low read dept (below 100 reads) even with 1ng input, increasing the interpretation threshold would lead to a high loss of aiSNP genotypes, e.g., rs310644 would drop out in 76% (123/161) of the samples in the present study. Care should be taken when predicting ancestry on partial profiles as drop outs might cause misleading predictions. To avoid drop outs, we therefore suggest striving to use the recommended DNA input (1ng) for BGA analysis. In this study, all samples with suspected drop outs were retyped to obtain complete aiSNP profiles for BGA analysis.

By comparing the different forensic BGA tools' ability to assign an individual to its correct population, we show that the UAS, FROG-kb and GenoGeographer performed similarly well when predicting individuals of European ancestry. When predicting individuals of non-European ancestry, FROG-kb and GenoGeographer performed better than the UAS. A prediction could only be made by the UAS if the unknown sample clustered within one of the three major ancestry groups (African, East Asian and European) in the PCA plot, causing challenge in predicting other non-European samples, e.g. Middle Eastern and Asian samples. Consequently, 59% of the non-Europeans in our study population could not be predicted using the UAS. When utilising the FROG-kb, we were able to predict all individuals except one of the non-Europeans and two of the Europeans that were inconclusive by the UAS. The FROG-kb has more underlying reference populations than the UAS, and instead of using PCA, it calculates relative likelihoods for each reference population and rank them from highest to lowest. This makes the results easier to interpret, and no inconclusive predictions were produced. However, a relative likelihood model will assign the unknown sample to the least unlikely population, regardless of if the correct population is present in the reference data or not, which might lead to misleading predictions. In our study, the FROG-kb produced three incorrect predictions. Despite the high number of global reference populations, the FROG-kb reference data is not exhaustive, which could contribute to some error. To overcome the challenge of non-exhaustive reference data, GenoGeographer employs a likelihood ratio test, similar to an outlier test [35]. Using the likelihood ratio test, the model will "reject" the unknown sample if it is not "similar enough" to any of the reference populations. Herein, the GenoGeographer performed similar to FROG-kb with two incorrect predictions. It is important to note that inaccuracy can also be due to limitations in the SNP panel used, or error in self-reported population affiliation. However, the stringent criteria to be "accepted" led to 34 "rejected" samples (32 Europeans) by GenoGeographer, and thus a lower correct rate than the FROG-kb. As we were only using metapopulations to predict BGA, the high reject rate might be because of non-sufficient homogeneity in the metapopulations causing the underlying populations to be rejected even if they are correct.

Five of the individuals in our sample population had reported co-ancestry from two different continents (Europe and Asia or Europe and Africa). Of these, only two had 1st order of admixture (1:1 admixture ratio of the first generation of admixed parents). As expected, the UAS, FROG-kb and GenoGeographer were not able to predict these samples correctly as the tools are not designed to handle co-ancestry with this SNP panel. Notably, it is possible to choose to analyse 1st order of admixture by GenoGeographer. However, our two individuals with 1st order of co-ancestry were not predicted correctly as they were both predicted to be Middle Eastern. To assess co-ancestry using autosomal markers, STRUCTURE is well recognised in the field as a reliable tool [36]. However, it is advised to use a comprehensive reference dataset when using STRUCTURE for BGA inference in forensic case work [19]. Moreover, substitution of uniparental DNA analysis (Y and mtDNA), would elevate the possibility of accurately detecting ancestral admixture [3]. Due to the few samples with reported co-ancestry in our study population, co-ancestry analysis with STRUCTURE was not performed.

Based on the observations in this study, and in line with other studies, we concur to combine several prediction tools when conducting BGA analyses [18,19]. The UAS is a user-friendly software that integrates analysis of sequence data with immediate BGA predictions. Because the software is integrated in the MPS workflow, it is highly suitable for initial BGA inference in forensic case work, especially for European populations. However, because of its limitations in predicting non-Europeans, additional tools should complement the UAS. Based on our study sample, we demonstrate that the FROG-kb and GenoGeographer accurately predict BGA using the 55 Kidd aiSNPs genotyped by the ForenSeq™ DNA Signature Prep Kit. Additionally, these two tools are user-friendly and freely available. However, the reference data and statistics used by the prediction tool can evidently influence the prediction outcome and should be thoroughly evaluated by any forensic laboratory before implementation.

Conclusions

In this study we demonstrate that the ForenSeq™ DNA Signature Prep Kit produces highly reliable aiSNP profiles using the MiSeq FGx system. However, the user should be aware that some SNPs showed on average lower read depth than others, which can lead to drop out. For forensic BGA analysis, it is advised to analyse complete aiSNP profiles. Therefore, we suggest not using less than 1ng input DNA (the recommended DNA input for the ForenSeq kit) for BGA analysis. Additionally, we demonstrate that the FROG-kb and GenoGeographer are highly reliable BGA tools for prediction of European and

15

non-European individuals using the 55 Kidd aiSNP panel. The UAS was highly reliable when predicting individuals of European ancestry. However, because of the limited underlying reference data, the UAS could not infer over half of the non-Europeans typed in this study. We therefore highly recommend supplementing the initial BGA analysis by UAS with FROG-kb and/or GenoGeographer.

Supplement Materials

The following supporting information can be downloaded at: www.mdpi.com/xxx/s1, Table S1: Summary of Chi-Square Tests for Hardy-Weinberg Equilibrium of the Norwegian reference population; Figure S2: PCA plot obtained from the UAS, demonstrating predictions considered inconclusive; Table S3: Descriptive statistics in number of reads of the 56 aiSNPs genotyped with the ForenSeq™ DNA Signature Prep Kit; Table S4: Descriptive statistics for heterozygite balance calculations of the 56aiSNPs typed using ForenSeq™ DNA Signature Prep Kit; Figure S5: Sensitivity study of the 56 aiSNPs genotyped with the ForenSeq™ DNA Signature Prep Kit. A) Read depth and B) heterozygote balance; Table S6: Allele and genotype frequencies of the 56 aiSNPs in the Norwegian reference set; Table S7: Summary of Chi-Square Tests for Hardy-Weinberg Equilibrium of the Norwegian reference population; Figure S8: Delta K calculations (EVANNO et al., 2005) plotted using Structure Harvester on STRUCTURE results of the Norwegian reference population (n=200) together with 31 other populations (n=2154) (Table S1).

Authors Contributions

Conceptualisation, G.-H.O., T.B., K.J.; formal analysis, N.M.S.; investigation, K.J.; writing-original draft preparation, N.M.S.; visualisation, N.M.S.; writing – review and editing, G.-H.O., T.B., K.J.; supervision, G.-H.O., T.B., K.J.; project administration, K.J. All authors have read and agreed to the published version of the manuscript.

Funding

This research received no external funding.

Institutional Review Board Statement

The study was conducted in accordance with the Declaration of Helsinki, and approved by the Faculty of Health Sciences, UiT - The Arctic University of Norway (2021/2034).

Informed Consent Statement

Informed consent was obtained from all subjects involved in the study.

Data Availability Statement

The data generated in the present study are included within the manuscript and its supplementary files.

Acknowledgements

Conflicts of Interest

The authors declare no conflict of interest.

References

[1]   C. Phillips, Forensic genetic analysis of bio-geographical ancestry, Forensic Sci. Int. Genet. 18 (2015) 49–65. https://doi.org/10.1016/J.FSIGEN.2015.05.012.

[2]   M. Kayser, Forensic DNA Phenotyping: Predicting human appearance from crime scene material for investigative purposes, Forensic Sci. Int. Genet. 18 (2015) 33–48. https://doi.org/10.1016/J.FSIGEN.2015.02.003.

[3]   P.M. Schneider, B. Prainsack, M. Kayser, The use of forensic DNA phenotyping in predicting appearance and biogeographic ancestry, Dtsch. Arztebl. Int. 116 (2019) 873–880. https://doi.org/10.3238/arztebl.2019.0873.

[4]   C. Phillips, D. McNevin, K.K. Kidd, R. Lagacé, S. Wootton, M. de la Puente, A. Freire-Aradas, A. Mosquera-Miguel, M. Eduardoff, T. Gross, L. Dagostino, D. Power, S. Olson, M. Hashiyada, C. Oz, W. Parson, P.M. Schneider, M.V. Lareu, R. Daniel, MAPlex - A massively parallel sequencing ancestry analysis multiplex for Asia-Pacific populations, Forensic Sci. Int. Genet. 42 (2019) 213–226. https://doi.org/10.1016/J.FSIGEN.2019.06.022.

[5]   K.K. Kidd, W.C. Speed, A.J. Pakstis, D.S. Podini, R. Lagacé, J. Chang, S. Wootton, E. Haigh, U. Soundararajan, Evaluating 130 microhaplotypes across a global set of 83 populations, Forensic Sci. Int. Genet. 29 (2017) 29–37. https://doi.org/10.1016/J.FSIGEN.2017.03.014.

[6]   R. Pereira, C. Phillips, N. Pinto, C. Santos, S. Sebd, Straightforward Inference of Ancestry and Admixture Proportions through Ancestry-Informative Insertion Deletion Multiplexing, PLoS One. 7 (2012) 29684. https://doi.org/10.1371/journal.pone.0029684.

[7]   C. Børsting, N. Morling, Next generation sequencing and its applications in forensic genetics, Forensic Sci. Int. Genet. 18 (2015) 78–89. https://doi.org/10.1016/J.FSIGEN.2015.02.002.

[8]   C. Xavier, M. De La Puente, A. Mosquera-Miguel, A. Freire-Aradas, V. Kalamara, A. Vidaki, T.E. Gross, A. Revoir, E. Pośpiech, E. Kartasińska, M. Spólnicka, W. Branicki, C.E. Ames, P.M. Schneider, C. Hohoff, M. Kayser, C. Phillips, W. Parson, Development and validation of the VISAGE AmpliSeq basic tool to predict appearance and ancestry from DNA, Forensic Sci. Int. Genet. 48 (2020). https://doi.org/10.1016/j.fsigen.2020.102336.

[9]   L. Palencia-Madrid, C. Xavier, M. De La Puente, C. Hohoff, C. Phillips, M. Kayser, W. Parson, Evaluation of the VISAGE Basic Tool for Appearance and Ancestry Prediction Using PowerSeq Chemistry on the MiSeq FGx System, Genes (Basel). 11 (2020) 708. https://doi.org/10.3390/genes11060708.

[10]   A.C. Jäger, M.L. Alvarez, C.P. Davis, E. Guzmán, Y. Han, L. Way, P. Walichiewicz, D. Silva, N. Pham, G. Caves, J. Bruand, F. Schlesinger, S.J.K. Pond, J. Varlaro, K.M. Stephens, C.L. Holt, Developmental validation of the MiSeq FGx Forensic Genomics System for Targeted Next Generation Sequencing in Forensic DNA Casework and Database Laboratories, Forensic Sci. Int. Genet. 28 (2017) 52–70. https://doi.org/10.1016/J.FSIGEN.2017.01.011.

[11]   F. Guo, J. Yu, L. Zhang, J. Li, Massively parallel sequencing of forensic STRs and SNPs using the Illumina® ForenSeqTM DNA Signature Prep Kit on the MiSeq FGxTM Forensic Genomics System, Forensic Sci. Int. Genet. 31 (2017) 135–148. https://doi.org/10.1016/J.FSIGEN.2017.09.003.

[12]   K.K. Kidd, W.C. Speed, A.J. Pakstis, M.R. Furtado, R. Fang, A. Madbouly, M. Maiers, M. Middha, F.R. Friedlaender, J.R. Kidd, Progress toward an efficient panel of SNPs for ancestry inference, Forensic Sci. Int. Genet. 10 (2014) 23–32. https://doi.org/10.1016/J.FSIGEN.2014.01.002.

[13]   A.J. Pakstis, L. Kang, L. Liu, Z. Zhang, T. Jin, E.L. Grigorenko, F.R. Wendt, B. Budowle, S. Hadi,

M.S. Al Qahtani, N. Morling, H.S. Mogensen, G.E. Themudo, U. Soundararajan, H. Rajeevan, J.R. Kidd, K.K. Kidd, Increasing the reference populations for the 55 AISNP panel: the need and benefits, Int. J. Legal Med. 131 (2017) 913–917. https://doi.org/10.1007/s00414-016-1524-z.

[14] A.J. Pakstis, C. Gurkan, M. Dogan, H.E. Balkaya, S. Dogan, P.I. Neophytou, L. Cherni, S. Boussetta, H. Khodjet-El-Khil, A. Ben Ammar ElGaaied, N.M. Salvo, K. Janssen, G.-H. Olsen, S. Hadi, E.K. Almohammed, V. Pereira, D.M. Truelsen, O. Bulbul, U. Soundararajan, H. Rajeevan, J.R. Kidd, K.K. Kidd, Genetic relationships of European, Mediterranean, and SW Asian populations using a panel of 55 AISNPs, Eur. J. Hum. Genet. (2019) 1–9. https://doi.org/10.1038/s41431-019-0466-6.

[15] H. Rajeevan, U. Soundararajan, A.J. Pakstis, K.K. Kidd, Introducing the Forensic Research/Reference on Genetics knowledge base, FROG-kb, Investig. Genet. 3 (2012) 18. https://doi.org/10.1186/2041-2223-3-18.

[16] H. Rajeevan, U. Soundararajan, A.J. Pakstis, K.K. Kidd, FrogAncestryCalc: A standalone batch likelihood computation tool for ancestry inference panels catalogued in FROG-kb, Forensic Sci. Int. Genet. 46 (2020) 102237. https://doi.org/10.1016/j.fsigen.2020.102237.

[17] T. Tvedebrink, P.S. Eriksen, H.S. Mogensen, N. Morling, GenoGeographer – A tool for genogeographic inference, Forensic Sci. Int. Genet. Suppl. Ser. 6 (2017) e463–e465. https://doi.org/10.1016/J.FSIGSS.2017.09.196.

[18] C.J. Frégeau, A multiple predictive tool approach for phenotypic and biogeographical ancestry inferences, Can. Soc. Forensic Sci. J. 55 (2022) 71–99. https://doi.org/10.1080/00085030.2021.2016206.

[19] P. Resutik, S. Aeschbacher, M. Krützen, A. Kratzer, C. Haas, C. Phillips, N. Arora, Comparative evaluation of the MAPlex, Precision ID Ancestry Panel, and VISAGE Basic Tool for biogeographical ancestry inference, Forensic Sci. Int. Genet. 64 (2023) 102850. https://doi.org/10.1016/J.FSIGEN.2023.102850.

[20] N.M. Salvo, K. Janssen, M.K. Kirsebom, O.S. Meyer, T. Berg, G.H. Olsen, Predicting eye and hair colour in a Norwegian population using Verogen's ForenSeq™ DNA signature prep kit, Forensic Sci. Int. Genet. 56 (2022) 102620. https://doi.org/10.1016/J.FSIGEN.2021.102620.

[21] R. Peakall, P.E. Smouse, GENALEX 6: genetic analysis in Excel. Population genetic software for teaching and research, Mol. Ecol. Notes. 6 (2006) 288–295. https://doi.org/10.1111/j.1471-8286.2005.01155.x.

[22] D. Falush, M. Stephens, J.K. Pritchard, Inference of population structure using multilocus genotype data: linked loci and correlated allele frequencies., Genetics. 164 (2003) 1567–87. http://www.ncbi.nlm.nih.gov/pubmed/12930761 (accessed October 18, 2019).

[23] D. Falush, M. Stephens, J.K. Pritchard, Inference of population structure using multilocus genotype data: dominant markers and null alleles., Mol. Ecol. Notes. 7 (2007) 574–578. https://doi.org/10.1111/j.1471-8286.2007.01758.x.

[24] M.J. Hubisz, D. Falush, M. Stephens, J.K. Pritchard, Inferring weak population structure with the assistance of sample group information., Mol. Ecol. Resour. 9 (2009) 1322–32. https://doi.org/10.1111/j.1755-0998.2009.02591.x.

[25] J.K. Pritchard, M. Stephens, P. Donnelly, Inference of population structure using multilocus genotype data., Genetics. 155 (2000) 945–59. http://www.ncbi.nlm.nih.gov/pubmed/10835412 (accessed June 7, 2018).

[26] R. Peakall, P.E. Smouse, GenAlEx 6.5: genetic analysis in Excel. Population genetic software for

teaching and research—an update, Bioinformatics. 28 (2012) 2537. https://doi.org/10.1093/BIOINFORMATICS/BTS460.

[27]   D.A. Earl, B.M. Vonholdt, STRUCTURE HARVESTER: a website and program for visualizing STRUCTURE output and implementing the Evanno method, Conserv. Genet. Resour. 4 (2012) 359–361. https://doi.org/10.1007/s12686-011-9548-7.

[28]   N.M. Kopelman, J. Mayzel, M. Jakobsson, N.A. Rosenberg, I. Mayrose, CLUMPAK: a program for identifying clustering modes and packaging population structure inferences across K, Mol. Ecol. Resour. 15 (2015) 1179–1191. https://doi.org/10.1111/1755-0998.12387.

[29]   H.S. Mogensen, T. Tvedebrink, C. Børsting, V. Pereira, N. Morling, Ancestry prediction efficiency of the software GenoGeographer using a z-score method and the ancestry informative markers in the Precision ID Ancestry Panel, Genes (Basel). 44 (2020). https://doi.org/10.1016/j.fsigen.2019.102154.

[30]   G. EVANNO, S. REGNAUT, J. GOUDET, Detecting the number of clusters of individuals using the software structure: a simulation study, Mol. Ecol. 14 (2005) 2611–2620. https://doi.org/10.1111/j.1365-294X.2005.02553.x.

[31]   J.D. Churchill, N.M.M. Novroski, J.L. King, L.H. Seah, B. Budowle, Population and performance analyses of four major populations with Illumina's FGx Forensic Genomics System, Forensic Sci. Int. Genet. 30 (2017) 81–92. https://doi.org/10.1016/j.fsigen.2017.06.004.

[32]   M. Sidstedt, K. Junker, C. Forsberg, L. Boiso, P. Rådström, R. Ansell, J. Hedman, In-house validation of MPS-based methods in a forensic laboratory, Forensic Sci. Int. Genet. Suppl. Ser. 7 (2019) 635–636. https://doi.org/10.1016/J.FSIGSS.2019.10.119.

[33]   C.J. Frégeau, Validation of the Verogen ForenSeqTM DNA Signature Prep kit/Primer Mix B for phenotypic and biogeographical ancestry predictions using the Micro MiSeq® Flow Cells, Forensic Sci. Int. Genet. 53 (2021). https://doi.org/10.1016/J.FSIGEN.2021.102533.

[34]   V. Sharma, K. Jani, P. Khosla, E. Butler, D. Siegel, E. Wurmbach, Evaluation of ForenSeqTM Signature Prep Kit B on predicting eye and hair coloration as well as biogeographical ancestry by using Universal Analysis Software (UAS) and available web-tools, Electrophoresis. 40 (2019) 1353–1364. https://doi.org/10.1002/elps.201800344.

[35]   T. Tvedebrink, P.S. Eriksen, H.S. Mogensen, N. Morling, Weight of the evidence of genetic investigations of ancestry informative markers, Theor. Popul. Biol. 120 (2018) 1–10. https://doi.org/10.1016/j.tpb.2017.12.004.

[36]   E.Y.Y. Cheung, M.E. Gahan, D. McNevin, Prediction of biogeographical ancestry in admixed individuals., Forensic Sci. Int. Genet. 36 (2018) 104–111. https://doi.org/10.1016/j.fsigen.2018.06.013.

Table S1: Reference populations for STRUCTURE and PCA analysis

List of 32 population samples in the dataset

Geographical region	Abbreverat	Description	Source Tag	Pop Order#	Size N
WestAfrica	YRI	Yoruba, Ibadan	1KG[1]	108	108
SW Asia & Med.Eur.	YMJ	Yemenite Jews	Kidd lab	298	42
	SAU	Saudi	Kidd lab	299	91
	UAE	Arabs, AbuDhabi, United Arab Emirates	Dr Hadi[2]	300	38
	KWT	Kuwaiti	Kidd lab	303	14
	PLA	Palestinian Arabs	Kidd lab	304	69
	DRU	Druze, Israel	Kidd lab	305	102
	SAM	Samaritans, Israel	Kidd lab	306	39
	ASH	Ashkenazi Jews	Kidd lab	307	140
	CYP	Turkish Cypriots	Kidd lab	308	59
	TRK	Turkish, Istanbul, Turkey	Kidd lab	309	80
	IRN	Iranians	Kidd lab	310	44
	BSQ	Basque	Oscar Garcia[3]	400	108
	IBS	Iberians	1KG[1]	401	107
	SRD	Sardinians	Kidd lab	402	35
	TSI	Toscani, Italy	1KG[1]	403	107
	RMJ	Roman Jews, Italy	Kidd lab	404	27
	GRK	Greeks,Thesaloniki, Greece	Kidd lab	405	55
	ADY	Adygei	Kidd lab	406	54
N Europe	CHV	Chuvash	Kidd lab	451	42
	HGR	Hungarians	Kidd lab	452	89
	RUA	Russians, Archangelsk	Kidd lab	453	33
	RUV	Russians, Vologda	Kidd lab	454	47
	EAM	European Americans	Kidd lab	455	89
	GBR	British from England and Scotland	1KG[1]	456	91

	CEU	Utah Residents (CEPH), N&W Europe ancestry	1KG[1]	457	99
	IRI	Irish	Kidd lab	458	114
	DAN	Danes	Kidd lab	459	51
	NOR	Norwegians, Tromsø	Tromsø lab	460	200
	FIN	Finns	Kidd lab	461	34
	FN1	Finns, Finland	1KG[1]	462	99
W Siberia	KMZ	Komi Zyriane	Kidd lab	496	47
					2354

[1]Thousand Genomes populations

[2]From Dr Hadi. Published in Andrew J. Pakstis et al., "Increasing the reference populations for the 55 AISNP panel: the need and benefits", 2017 International Journal of Legal Medicine vol 131 pp 913-917

[3]Oscar Garcia et al., "Frequencies of the precision ID ancestry panel markers in Basques using the Ion Torrent PGMTM platform", 2017 Forensic Sci Intl:Genetics vol31 pp e1-e4

Table S3: Descriptive statistics in number of reads of the 56 aiSNPs genotyped with the ForenSeq™ DNA Signature Prep Kit

Locus	Q1	Median	Q3	Maximum reads	Minimum reads	N
rs3814134	60	94	220.5	764	33	158
rs310644	56	73	95	197	32	161
rs1572018	159	481.5	641.75	1126	31	176
rs3811801	159	199	253	422	31	177
rs3737576	126	166	223	529	34	177
rs6990312	150	196	253	387	34	177
rs1462906	149	204	284	542	39	177
rs3823159	123	167	204	381	39	177
rs3916235	130	181	230	504	46	177
rs7554936	147	188	260	552	49	177
rs2238151	177	240	355	807	56	177
rs12498138	249	382	510	886	65	177
rs1426654	201	269	350	908	67	177
rs1871534	417	553	683	1345	69	177
rs1834619	145	203	293	655	71	177
rs17642714	219	282	383	1005	77	177
rs7326934	217	284	365	644	79	177
rs10497191	225	292	361	648	81	177
rs7657799	325	462	581	1035	81	177
rs1229984	473	624	809	1506	84	177
rs7226659	325	426	532	979	89	177
rs4833103	235	319	512	968	91	177
rs1079597	240	324	502	1411	95	177
rs6754311	328	402	503	1118	101	177
rs12913832	369	497	598	1169	109	177
rs16891982	470	608	734	1273	114	177
rs4471745	400	542	679	1450	122	177
rs2042762	794	1143	1474	2509	130	177
rs2593595	380	504	673	1554	139	177
rs798443	604	955	1233	2271	140	177
rs2196051	754	1071	1296	2311	143	177
rs7251928	392	555	994	1958	143	177
rs917115	595	829	983	1545	167	177
rs4891825	380	520	1016	2318	174	177
rs260690	385	538	1270	3155	179	177
rs11652805	938	1198	1401	2177	182	177
rs2166624	816	1056	1274	2193	182	177
rs735480	1126	1368	1797	3795	185	177
rs1800414	447	622	843	1816	194	177
rs870347	477	668	977	3168	226	177
rs9522149	894	1204	1496	2895	228	177
rs12439433	859	1038	1246	1825	246	177
rs671	818	1064	1319	2570	252	177

rs2024566	1508	1934	2525	6028	264	177
rs4918664	1289	1701	2221	4153	270	177
rs459920	1224	1637	2147	5886	311	177
rs4411548	1550	1849	2425	6997	316	177
rs7722456	1056	1415	1957	5149	318	177
rs3827760	817	1058	1724	4107	341	177
rs200354	1959	2425	3017	4651	348	177
rs1919550	1602	2128	2613	4917	381	177
rs192655	1455	2002	2696	4502	411	177
rs1876482	1759	2264	2698	4995	494	177
rs7997709	1317	1693	2773	6035	499	177
rs2814778	1662	2196	3918	10228	734	177
rs174570	1851	2277	2713	5724	735	177

Table S4: Descriptive statistics for heterozygite balance calculations of the 56aiSNPs
 typed using ForenSeq™ DNA Signature Prep Kit

	Median	Range	Maximum	Minimum	Q1	Q3	Count
rs310644	0.5	0.269697	0.618181818	0.348484848	0.435377	0.550712	19
rs3814134	0.45	0.237165	0.6125	0.375335121	0.388646	0.455621	5
rs3823159	0.532258	0.216823	0.636363636	0.41954023	0.487179	0.549801	5
rs3737576	0.497175	0.547705	0.814371257	0.266666667	0.42735	0.555556	41
rs3916235	0.502825	0.135269	0.569230769	0.433962264	0.461501	0.548662	7
rs6990312	0.468834	0.404151	0.683870968	0.27972028	0.400799	0.527973	40
rs7554936	0.474215	0.348807	0.654929577	0.306122449	0.402216	0.544189	72
rs1462906	0.5	0.141198	0.590062112	0.448863636	0.494465	0.587692	5
rs1834619	0.484295	0.372596	0.653846154	0.28125	0.45638	0.538444	30
rs2238151	0.495714	0.370032	0.670212766	0.300180832	0.44356	0.557778	82
rs1426654	0.410323	0.221649	0.5	0.278350515	0.349222	0.441859	6
rs7326934	0.45283	0.154698	0.56402439	0.409326425	0.416309	0.489691	5
rs1049719	0.51049	0.270786	0.660098522	0.389312977	0.463268	0.545906	31
rs1764271	0.480599	0.520329	0.858974359	0.338645418	0.430345	0.527909	80
rs4833103	0.48693	0.611751	0.737704918	0.125954198	0.448386	0.544692	78
rs1249813	0.494382	0.558014	0.652841782	0.094827586	0.433498	0.536082	37
rs1079597	0.464684	0.295322	0.582822086	0.2875	0.422206	0.500687	35
rs1572018	0.486521	0.604935	0.686567164	0.081632653	0.447536	0.55197	51
rs7226659	0.472422	0.277207	0.645107794	0.367901235	0.437387	0.517857	13
rs6754311	0.473423	0.357296	0.611872146	0.254575707	0.379177	0.5307	64
rs7657799	0.518978	0.221737	0.625492773	0.403755869	0.467247	0.557579	8
rs1291383	0.489678	0.318176	0.691056911	0.372881356	0.453095	0.532212	50
rs4471745	0.453205	0.303692	0.578640777	0.274949084	0.395839	0.494136	30
rs2593595	0.494845	0.270806	0.604139715	0.333333333	0.463744	0.525581	49
rs1689198	0.483607	0.235214	0.631090487	0.395876289	0.479252	0.540621	7
rs1229984	0.496112	0.036814	0.503336511	0.466522678	0.487804	0.498829	4
rs1800414	0.448393	0	0.448392555	0.448392555	0.448393	0.448393	1
rs4891825	0.515209	0.219814	0.588068182	0.368253968	0.484044	0.554967	23
rs7251928	0.461512	0.462629	0.607033639	0.144404332	0.429075	0.491043	62
rs870347	0.492958	0.265074	0.654618474	0.389544688	0.453202	0.543575	37
rs917115	0.517063	0.427902	0.797202797	0.369300912	0.471472	0.560664	82
rs260690	0.51	0.230254	0.617834395	0.3875803	0.462277	0.547432	31
rs798443	0.572034	0.331879	0.759493671	0.427615063	0.498718	0.602392	56
rs1243943	0.524297	0.148351	0.590179415	0.441828255	0.46961	0.533337	11
rs2196051	0.514268	0.380044	0.696335079	0.316291161	0.463759	0.564863	69
rs2166624	0.494833	0.484817	0.866666667	0.381849315	0.467529	0.528177	82
rs671	0.47027	0	0.47027027	0.47027027	0.47027	0.47027	1
rs2042762	0.557576	0.245331	0.673584906	0.428253615	0.497897	0.585623	15
rs1165280	0.499296	0.260919	0.664835165	0.403915881	0.461097	0.533842	46
rs9522149	0.526364	0.34066	0.713052859	0.372393247	0.450721	0.586806	63
rs3827760	0.493159	0.308213	0.668449198	0.36023622	0.46474	0.522405	12
rs735480	0.552746	0.197297	0.653325123	0.456028369	0.513836	0.56968	25
rs7722456	0.457262	0.243031	0.579453067	0.336421953	0.405229	0.511226	45
rs459920	0.46536	0.426721	0.772908367	0.346187301	0.431283	0.515221	82

rs4918664	0.501845	0.527217	0.638663053	0.111445783	0.448949	0.54756	43
rs4411548	0.516635	0.264998	0.62863412	0.363636364	0.488884	0.539052	72
rs2024566	0.510794	0.247899	0.608121827	0.360222531	0.476383	0.533977	87
rs7997709	0.464053	0.184171	0.621565578	0.437394451	0.456634	0.482176	10
rs192655	0.584928	0.25414	0.677949228	0.423809524	0.531936	0.612527	35
rs1919550	0.491198	0.588922	0.692734332	0.103812317	0.451975	0.530897	37
rs174570	0.508373	0.267962	0.647664291	0.379701916	0.482808	0.534144	62
rs1876482	0.490993	0.227656	0.595873176	0.368217054	0.459399	0.522122	31
rs200354	0.513046	0.553543	0.649376231	0.095833333	0.4734	0.55009	68
rs1871534	na	na	na	na	na	na	0
rs2814778	na	na	na	na	na	na	0
rs3811801	na	na	na	na	na	na	0

na = Not applicable because the SNP was homozygous

Table S6: Allele and genotype frequencies of the 56 aiSNPs in the Norwegian reference set

Order	SNP	Count A1A1	Count A1A2	Count A2A2	Geno Total	Freq A1	Freq A2	Total	A1A1 hom	A1A2 hets	A2A2 hom
1	rs3737576	0	37	163	200	0.0925	0.9075	1	CC	CT	TT
2	rs7554936	26	75	99	200	0.3175	0.6825	1	CC	CT	TT
3	rs2814778	0	0	200	200	0	1	1	CC	CT	TT
4	rs798443	136	59	5	200	0.8275	0.1725	1	AA	AG	GG
5	rs1876482	4	34	162	200	0.105	0.895	1	AA	AG	GG
6	rs1834619	5	28	167	200	0.095	0.905	1	AA	AG	GG
7	rs3827760	185	15	0	200	0.9625	0.0375	1	AA	AG	GG
8	rs260690	161	39	0	200	0.9025	0.0975	1	AA	AC	CC
9	rs6754311	9	72	119	200	0.225	0.775	1	CC	CT	TT
10	rs1049719:	156	37	7	200	0.8725	0.1275	1	CC	CT	TT
11	rs1249813{	1	34	165	200	0.09	0.91	1	AA	AG	GG
12	rs4833103	54	91	55	200	0.4975	0.5025	1	AA	AC	CC
13	rs1229984	196	4	0	200	0.99	0.01	1	CC	CT	TT
14	rs3811801	0	0	200	200	0	1	1	AA	AG	GG
15	rs7657799	0	5	195	200	0.0125	0.9875	1	GG	GT	TT
16	rs870347	167	33	0	200	0.9175	0.0825	1	AA	AC	CC
17	rs1689198:	0	8	192	200	0.02	0.98	1	CC	CG	GG
18	rs7722456	14	63	123	200	0.2275	0.7725	1	CC	CT	TT
19	rs192655	161	38	1	200	0.9	0.1	1	AA	AG	GG
20	rs3823159	191	9	0	200	0.9775	0.0225	1	AA	AG	GG
21	rs917115	12	87	101	200	0.2775	0.7225	1	CC	CT	TT
22	rs1462906	197	3	0	200	0.9925	0.0075	1	CC	CT	TT
23	rs6990312	144	51	5	200	0.8475	0.1525	1	GG	GT	TT
24	rs2196051	103	77	20	200	0.7075	0.2925	1	AA	AG	GG
25	rs1871534	0	0	200	200	0	1	1	CC	CG	GG
26	rs3814134	198	2	0	200	0.995	0.005	1	AA	AG	GG

27	rs4918664	133	62	5	200	0.82	0.18	1	AA	AG	GG
28	rs174570	136	62	2	200	0.835	0.165	1	CC	CT	TT
29	rs1079597	150	46	4	200	0.865	0.135	1	CC	CT	TT
30	rs2238151	27	93	80	200	0.3675	0.6325	1	CC	CT	TT
31	rs671	0	0	200	200	0	1	1	AA	AG	GG
32	rs7997709	0	17	183	200	0.0425	0.9575	1	CC	CT	TT
33	rs1572018	139	54	7	200	0.83	0.17	1	CC	CT	TT
34	rs2166624	36	83	81	200	0.3875	0.6125	1	AA	AG	GG
35	rs7326934	0	7	193	200	0.0175	0.9825	1	CC	CG	GG
36	rs9522149	108	78	14	200	0.735	0.265	1	CC	CT	TT
37	rs200354	117	72	11	200	0.765	0.235	1	GG	GT	TT
38	rs1800414	0	0	200	200	0	1	1	CC	CT	TT
39	rs1291383:	3	59	138	200	0.1625	0.8375	1	AA	AG	GG
40	rs1243943:	182	18	0	200	0.955	0.045	1	AA	AG	GG
41	rs735480	1	27	172	200	0.0725	0.9275	1	CC	CT	TT
42	rs1426654	196	4	0	200	0.99	0.01	1	AA	AG	GG
43	rs459920	40	86	74	200	0.415	0.585	1	CC	CT	TT
44	rs4411548	92	90	18	200	0.685	0.315	1	CC	CT	TT
45	rs2593595	151	46	3	200	0.87	0.13	1	AA	AG	GG
46	rs176427l₄	89	87	24	200	0.6625	0.3375	1	AA	AT	TT
47	rs4471745	1	27	172	200	0.0725	0.9275	1	AA	AG	GG
48	rs116528O!	6	67	127	200	0.1975	0.8025	1	CC	CT	TT
49	rs2042762	0	22	178	200	0.055	0.945	1	CC	CT	TT
50	rs7226659	182	17	1	200	0.9525	0.0475	1	GG	GT	TT
51	rs3916235	188	12	0	200	0.97	0.03	1	CC	CT	TT
52	rs4891825	166	33	1	200	0.9125	0.0875	1	AA	AG	GG
53	rs7251928	118	73	9	200	0.7725	0.2275	1	AA	AC	CC
54	rs310644	1	20	179	200	0.055	0.945	1	CC	CT	TT
55	rs2024566	84	98	18	200	0.665	0.335	1	AA	AG	GG
56	rs1919550	165	34	1	200	0.91	0.09	1	AA	AT	TT

**Table S7**: Summary of Chi-Square Tests for Hardy-Weinberg Equilibrium of the Norwegian reference population.

No. Loci   55
No. Sample   200
No. Pops.   1

Pop	Locus	DF	ChiSq	Prob	Signif
Pop1	rs3737576	1	2.077879	0.149448	ns
Pop1	rs7554936	1	3.630087	0.056744	ns
Pop1	rs2814778	Monomorphic			
Pop1	rs798443	1	0.222047	0.637485	ns
Pop1	rs1876482	1	1.824208	0.176813	ns
Pop1	rs1834619	1	6.905058	0.008595	**
Pop1	rs3827760	1	0.303593	0.581639	ns
Pop1	rs260690	1	2.334236	0.126557	ns
Pop1	rs6754311	1	0.208117	0.648248	ns
Pop1	rs1049719	1	5.677952	0.017179	*
Pop1	rs1249813	1	0.28654	0.592446	ns
Pop1	rs4833103	1	1.28	0.257899	ns
Pop1	rs1229984	1	0.020406	0.886409	ns
Pop1	rs3811801	Monomorphic			
Pop1	rs7657799	1	0.032046	0.857926	ns
Pop1	rs870347	1	1.617059	0.203502	ns
Pop1	rs1689198	1	0.083299	0.772876	ns
Pop1	rs7722456	1	2.155254	0.142083	ns
Pop1	rs192655	1	0.617284	0.432058	ns
Pop1	rs3823159	1	0.105965	0.744786	ns
Pop1	rs917115	1	1.438949	0.230309	ns
Pop1	rs1462906	1	0.011421	0.914894	ns
Pop1	rs6990312	1	0.036407	0.848678	ns
Pop1	rs2196051	1	0.974283	0.323614	ns
Pop1	rs1871534	Monomorphic			
Pop1	rs3814134	1	0.00505	0.943345	ns
Pop1	rs4918664	1	0.502714	0.47831	ns
Pop1	rs174570	1	3.126134	0.077046	ns
Pop1	rs1079597	1	0.046209	0.829796	ns
Pop1	rs2238151	1	1.17E-05	0.997269	ns
Pop1	rs671	Monomorphic			
Pop1	rs7997709	1	0.394031	0.530188	ns
Pop1	rs1572018	1	0.373797	0.540942	ns
Pop1	rs2166624	1	3.162141	0.075364	ns
Pop1	rs7326934	1	0.063451	0.801122	ns
Pop1	rs9522149	1	0.000267	0.986966	ns
Pop1	rs200354	1	0.000313	0.985878	ns
Pop1	rs1800414	Monomorphic			
Pop1	rs1291383	1	1.404881	0.235908	ns

Pop1	rs1243943?	1	0.444067	0.505166	ns
Pop1	rs735480	1	0.002904	0.957021	ns
Pop1	rs1426654	1	0.020406	0.886409	ns
Pop1	rs459920	1	2.617762	0.105673	ns
Pop1	rs4411548	1	0.365562	0.545434	ns
Pop1	rs2593595	1	0.056443	0.812209	ns
Pop1	rs1764271?	1	0.148552	0.699923	ns
Pop1	rs4471745	1	0.002904	0.957021	ns
Pop1	rs1165280!	1	0.645794	0.421621	ns
Pop1	rs2042762	1	0.677473	0.410458	ns
Pop1	rs7226659	1	0.735533	0.391096	ns
Pop1	rs3916235	1	0.191306	0.661832	ns
Pop1	rs4891825	1	0.221353	0.638011	ns
Pop1	rs7251928	1	0.295584	0.586664	ns
Pop1	rs310644	1	0.288785	0.591	ns
Pop1	rs2024566	1	1.990585	0.15828	ns

Key: ns=not significant, * P<0.05, ** P<0.01, *** P<0.001
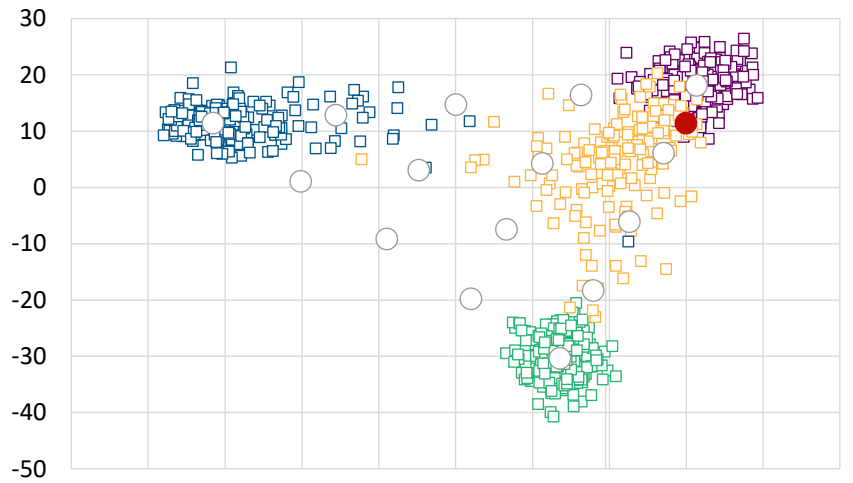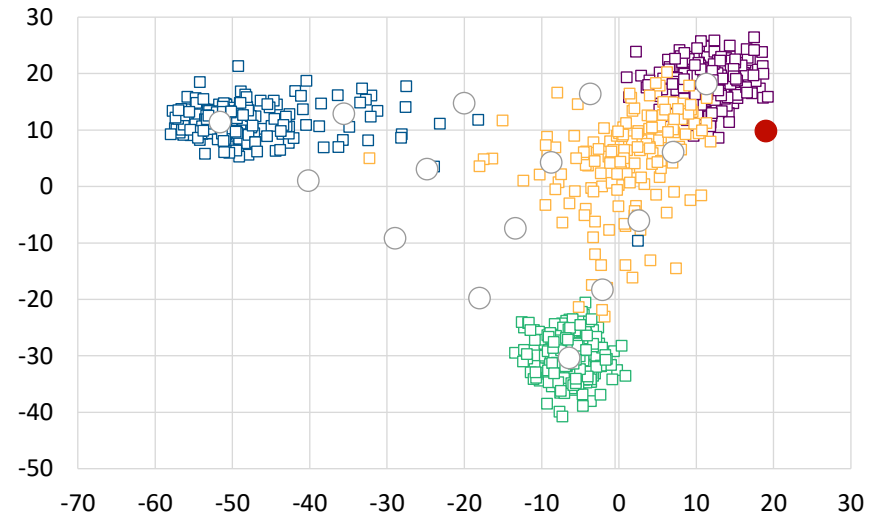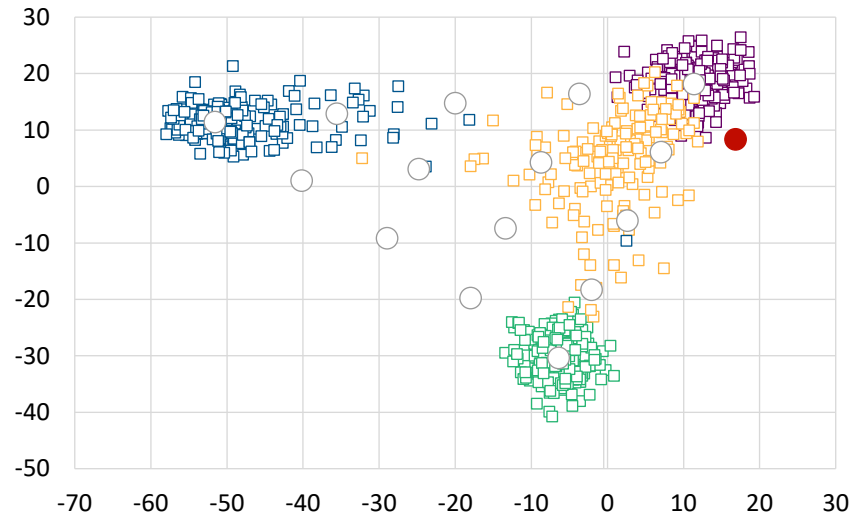
Figure S2: PCA plot obtained from the UAS, demonstrating predictions considered inconclusive
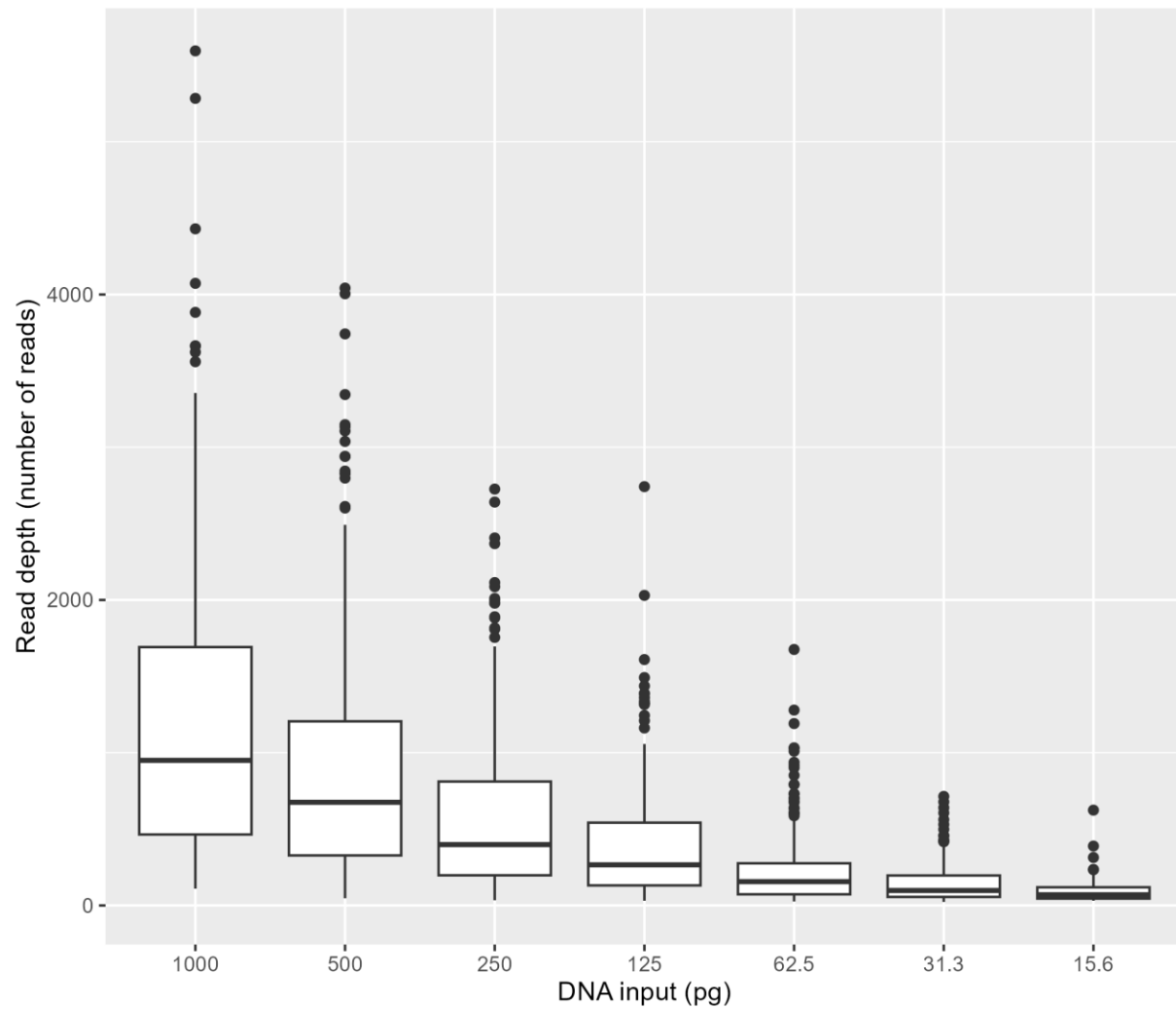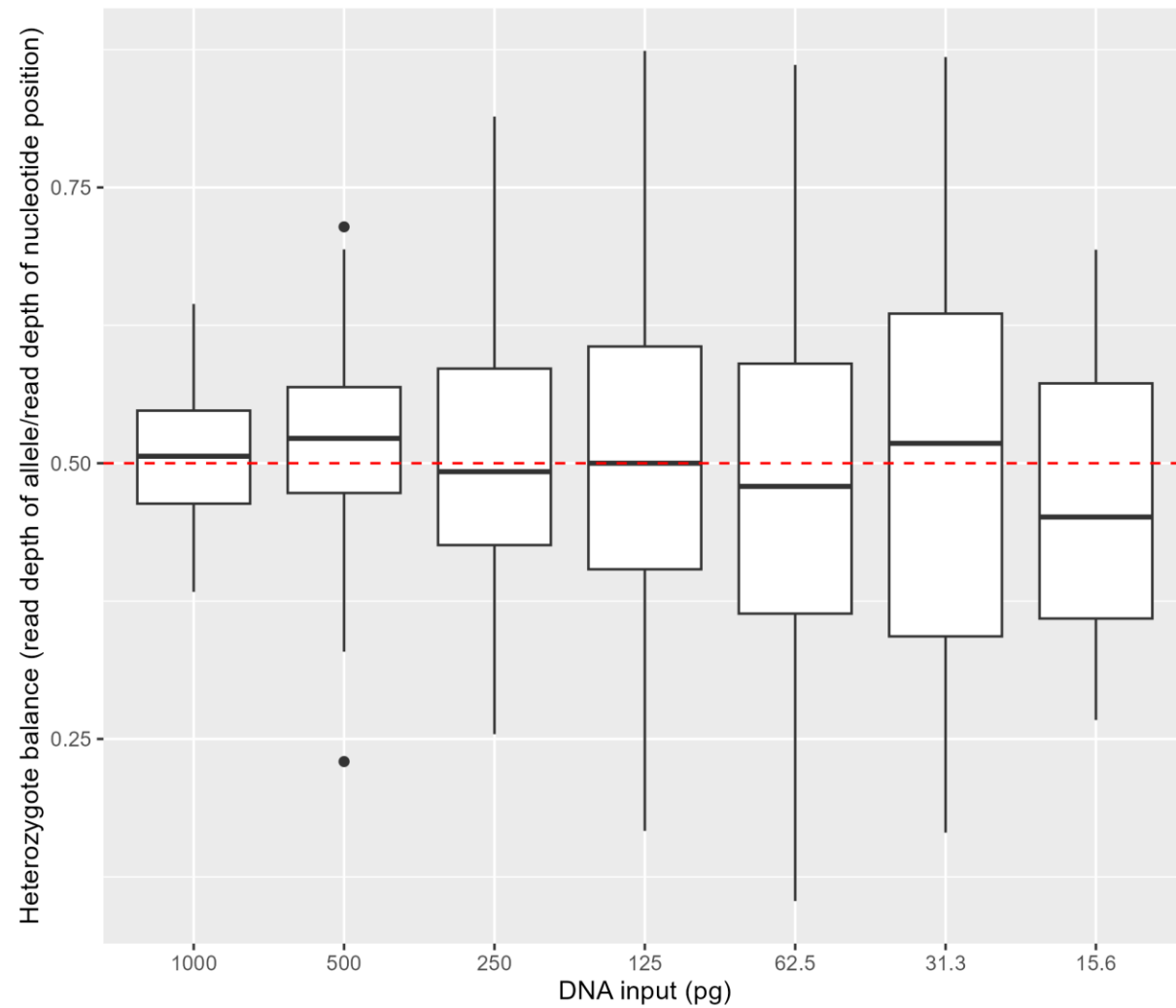
Figure S5: Sensitivity study of the 56 aiSNPs genotyped with the ForenSeq™ DNA Signature Prep Kit.
A) Read depth and B) heterozygote balance.
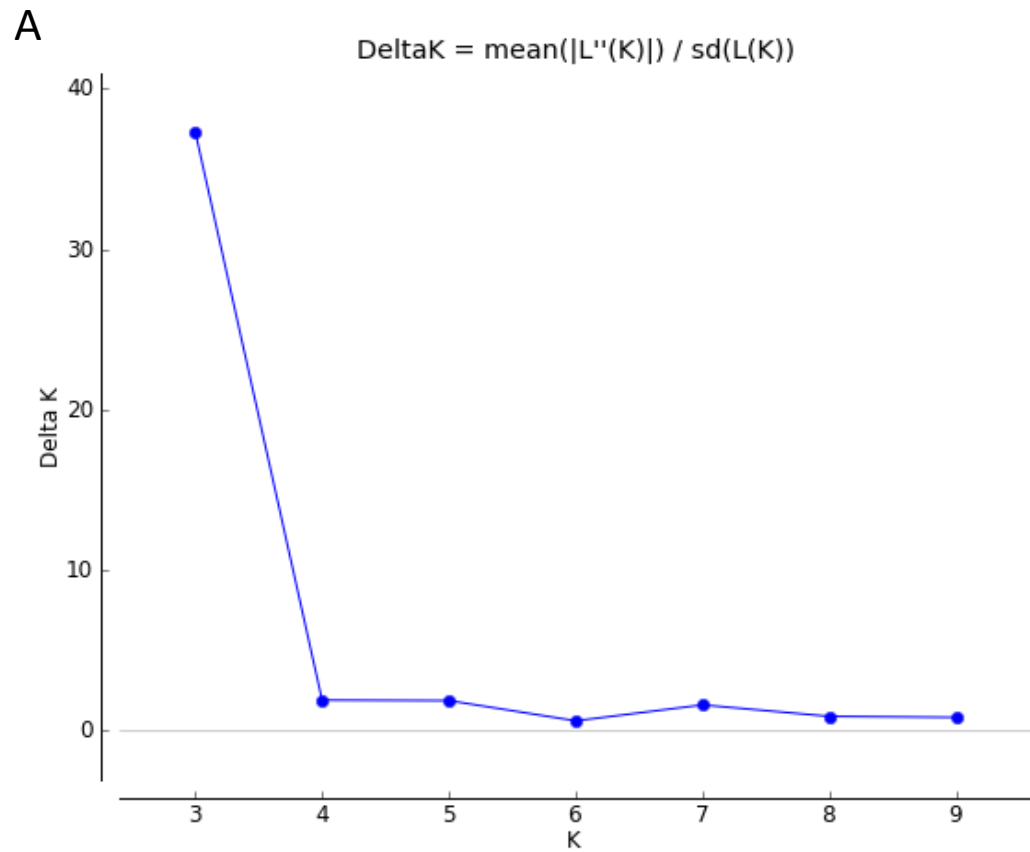
Figure S8: Delta K calculations (EVANNO et al., 2005) plotted using Structure Harvester on STRUCTURE results of the Norwegian reference population (N=200) together with 31 other populations (N=2154) (Table S1)

Paper 3

Prediction of Eye Colour in Scandinavians Using the EyeColour 11 (EC11) SNP Set

Olivia Strunge Meyer [1,*,†] , Nina Mjølsnes Salvo [2,†] , Anne Kjærbye [1] , Marianne Kjersem [2] , Mikkel Meyer Andersen [3] , Erik Sørensen [4] , Henrik Ullum [5] , Kirstin Janssen [2] , Niels Morling [1] , Claus Børsting [1] , Gunn-Hege Olsen [2] and Jeppe Dyrberg Andersen [1]

[1] Section of Forensic Genetics, Department of Forensic Medicine, Faculty of Health and Medical Sciences, University of Copenhagen, 2100 Copenhagen, Denmark; anne.kjaerbye@sund.ku.dk (A.K.); niels.morling@sund.ku.dk (N.M.); claus.boersting@sund.ku.dk (C.B.); jeppe.dyrberg.andersen@sund.ku.dk (J.D.A.)
[2] Centre for Forensic Genetics, Department of Medical Biology, UiT–The Arctic University of Norway, 9037 Tromsø, Norway; nina.mjolsnes@uit.no (N.M.S.); marianne.kjersem@uit.no (M.K.); kirstin.janssen@uit.no (K.J.); gunn-hege.olsen@uit.no (G.-H.O.)
[3] Department of Mathematical Sciences, Aalborg University, 9220 Aalborg, Denmark; mikl@math.aau.dk
[4] Department of Clinical Immunology, Copenhagen University Hospital, Rigshospitalet, 2100 Copenhagen, Denmark; erik.soerensen@regionh.dk
[5] Statens Serum Institut, 2300 Copenhagen, Denmark; heul@ssi.dk
*   Correspondence: olivia.meyer@sund.ku.dk
†   These authors contributed equally.

Abstract: Description of a perpetrator's eye colour can be an important investigative lead in a forensic case with no apparent suspects. Herein, we present 11 SNPs (Eye Colour 11-EC11) that are important for eye colour prediction and eye colour prediction models for a two-category reporting system (blue and brown) and a three-category system (blue, intermediate, and brown). The EC11 SNPs were carefully selected from 44 pigmentary variants in seven genes previously found to be associated with eye colours in 757 Europeans (Danes, Swedes, and Italians). Mathematical models using three different reporting systems: a quantitative system (PIE-score), a two-category system (blue and brown), and a three-category system (blue, intermediate, brown) were used to rank the variants. SNPs with a sufficient mean variable importance (above 0.3%) were selected for EC11. Eye colour prediction models using the EC11 SNPs were developed using leave-one-out cross-validation (LOOCV) in an independent data set of 523 Norwegian individuals. Performance of the EC11 models for the two- and three-category system was compared with models based on the IrisPlex SNPs and the most important eye colour locus, rs12913832. We also compared model performances with the IrisPlex online tool (IrisPlex Web). The EC11 eye colour prediction models performed slightly better than the IrisPlex and rs12913832 models in all reporting systems and better than the IrisPlex Web in the three-category system. Three important points to consider prior to the implementation of eye colour prediction in a forensic genetic setting are discussed: (1) the reference population, (2) the SNP set, and (3) the reporting strategy.

Keywords: forensic genetics; eye colour; rs12913832; pigmentation; DNA phenotyping

1. Introduction

Prediction of physical traits (externally visible characteristics) from DNA can be important in criminal cases with no apparent suspects. Multiple assays for forensic prediction of eye colour, hair colour, skin colour, and biogeographic ancestry have been developed with varying accuracies [1–5]. Prediction of biogeographic ancestry can give an indirect indication of a person's appearance. However, for individuals of European ancestry, there are large variations in eye colour. A direct description of the eye colour of a perpetrator could aid police investigators in focusing on a smaller group of individuals. The most

widely known system for eye colour prediction is the IrisPlex assay [3], which is based on six SNPs in six genes (*HERC2*, *OCA2*, *SLC24A4*, *SLC45A2*, *TYR*, and *IRF4*) that are associated with eye colour variation. The IrisPlex predicts eye colour in three categories: blue, intermediate, and brown [3,6]. It is well known that a single SNP in *HERC2*, rs12913832, is almost perfectly associated with blue and brown eye colour [7,8]. The SNP is located in the promoter region of *OCA2* and strongly associated with *OCA2* expression [9]. In 2012, Visser and co-workers demonstrated that the *OCA2* expression was increased in melanocytes carrying the rs12913832: A allele and decreased in melanocytes carrying the rs12913832: G allele. Hence, individuals carrying a rs12913832: A allele (genotypes rs12913832: AA and rs12913832:AG) are expected to have brown eye colour, and individuals carrying the genotype rs12913832:GG are expected to have blue eye colour. Eye colour prediction using the IrisPlex relies heavily on rs12913832 [10]. Thus, the IrisPlex prediction shows high accuracies for blue and brown eye colour but low accuracy for intermediate eye colour [3]. Some individuals do not follow the expected genotype–phenotype patterns of rs12913832, and for these individuals, the IrisPlex eye colour predictions are incorrect [10,11]. We previously performed in-depth sequencing analyses of individuals with incorrect IrisPlex eye colour predictions and identified variants in *OCA2*, *TYRP1*, *TYR*, and *SLC24A4* that may explain the incorrectly predicted eye colours [11,12]. In this study, we typed those variants and the IrisPlex SNPs in 757 European individuals and selected 11 SNPs for a new eye colour prediction model, named Eye Colour 11 (EC11). We modelled and tested the EC11 in an independent data set of 523 Norwegian individuals and compared the predictions with a model solely based on the rs12913832 SNP and a model based on the six IrisPlex SNPs (called IrisPlex Norway) using different reporting systems. Lastly, we compared the results with those obtained with the IrisPlex online prediction tool (IrisPlex Web) [3].

2. Materials and Methods

2.1. Samples and DNA Extraction

A total of 757 healthy individuals residing in Denmark, Sweden, or Italy comprised the variant discovery data set. The model data set included 523 healthy individuals living in Tromsø and Bodø (Norway). Blood samples were collected from employees and students at universities, residents and employees at health care centres, employees at hospitals, and through the Danish Blood Donor Study as described elsewhere [10,13,14]. DNA was extracted using the QIAamp DNA Blood Mini Kit (Qiagen, Hilden, Germany), the QI-Asymphony DNA Midi Kit (Qiagen, Hilden, Germany), or the PrepFiler™ Express DNA Extraction kit (Thermo Fisher Scientific, Waltham, MA, USA) following instructions from the manufacturers. The use of material was approved by the Danish Ethical Committee (M-20090237, H-4-2009-125, and H-3-2012-023), the Ethical Committee of Azienda Ospedaliera Ospedal Sant'Anna di Como (U.0026484.23-11-2012), the Ethical Committee of the University of Milan-Bicocca (P.U. 0033373/12), and the Faculty of Health Sciences, UiT–The Arctic University of Norway (2021/2034). All participants gave signed and informed consent and all samples were anonymised.

2.2. Quantitative Eye Colour Measurements and Eye Colour Categorisation

A digital photograph of one of the eyes of each participant was taken as described previously [13]. The pixel index of the eye score (PIE-score) was calculated from jpeg images 639 × 426 pixels as: (number of blue pixels–number of brown pixels)/(number of blue pixels + number of brown pixels) using the Digital Iris Analysis Tool (DIAT) [13]. The PIE-scores ranged from −1 to 1; eye colour photos with a PIE-score of 1 had only blue pixels, and eye colour photos with a PIE-score of −1 had only brown pixels. Eye colour was also categorised in a two-category (blue and brown) and a three-category (blue, intermediate, and brown) system. The categorisation was based on the PIE-score and our recent study on the perception of blue and brown eye colours [15]. In the two-category system, eye colours with PIE-score > 0.2 were categorised as blue, and eye colours with

PIE-score ≤ 0.2 were categorised as brown. In the three-category system, eye colours with PIE-score > 0.8 were categorised as blue, eye colours with PIE-score ≤ 0.8 and ≥ -0.5 were categorised as intermediate, and eye colours with PIE-score < -0.5 were categorised as brown. The number of individuals in each eye colour category and the mean PIE-score in the discovery data set and the model data set are shown in Table 1.

Table 1. Eye colour variation in the variant discovery and model data sets.

	Quantitative System [1]	Two-Category System [2]		Three-Category System [3]		
	Mean PIE-Score	Blue	Brown	Blue	Intermediate	Brown
Discovery data set (n = 757)	0.24	447 (59%)	310 (41%)	368 (49%)	148 (20%)	241 (31%)
Model data set (n = 523)	0.44	376 (72%)	147 (28%)	293 (56%)	123 (24%)	107 (20%)

[1] Statistically significant difference in mean PIE-scores between the two data sets ($p < 0.05$). [2] PIE-score > 0.2: blue, and PIE-score ≤ 0.2: brown. [3] PIE-score > 0.8: blue, PIE-score ≤ 0.8 to ≥ -0.5: intermediate, and PIE-score < -0.5: brown.

2.3. Variant Typing (Discovery Data Set)

A total of 44 pigmentary variants were investigated. The variants included all six IrisPlex SNPs [3], five variants in *OCA2* found to be associated with blue eye colour in individuals with the rs12913832:GA genotype [11], as well as 33 variants in *IRF4*, *TYRP1*, *SLC24A4*, and *TYR*, associated with brown eye colour in individuals with the rs12913832:GG genotype [12]. We included three variants in *TYRP1* (rs201447946, rs74606098, and rs79586719, $r^2 \geq 0.91$) to tag one large haploblock associated with eye colour [12]. Two variants in *TYR* were also in strong LD (rs1126809 and rs1393350, $r^2 = 0.92$). rs1393350 was part of the IrisPlex [3], and rs1126809 was found to be of importance in individuals with brown eye colour [12]. The 757 individuals in the variant discovery data set were previously typed for the IrisPlex SNPs and the five *OCA2* variants [10,11]. The 33 variants in *IRF4*, *TYRP1*, *SLC24A4*, and *TYR* were typed using two multiplexes, a 24 plex and an 11 plex, respectively (Table S1). The 24 plex included rs12913832 and 23 variants in *SLC24A4* and *TYRP1* (rs10131374, rs12590749, rs12880508, rs12894551, rs17128288, rs17128324, rs34755843, rs35617057, rs4904887, rs4904891, rs4904897, rs4904927, rs59977926, rs7144273, rs7152962, rs7401792, rs10491745, rs1408799, rs201447946, rs62538950, rs62538956, rs74606098, and rs79586719). The 11 plex comprised rs1393350 from the IrisPlex and 10 variants in *IRF4* and *TYR* (rs1393350, rs1050976, rs10530949, rs12211228, rs9378807, rs11018509, rs1126809, rs2047512, rs34749698, rs7120151, and rs9919559). Samples were typed with the iPLEX™ Assay (Agena Bioscience, Hamburg, Germany) and analysed with matrix-assisted laser desorption-ionization time of flight mass spectrometry (MALDI-TOF MS) using the MassARRAY Analyzer 4 System (Agena Bioscience, Hamburg, Germany). The PCRs contained 0.5 µL 10X PCR buffer, 0.4 µL MgCl2 (25 mM), 0.1 µL dNTP mix (25 mM), 0.2 µL PCR Enzyme, 1 µL primer mix (1 µM of each primer), and 1 µL DNA (≥ 1 ng). Thermal cycling comprised initial denaturation for 2 min at 94 °C followed by 45 cycles of denaturation at 94 °C for 20 s, annealing at 56–58 °C for 30 s (56 °C for the 11 plex and 58 °C for the 24 plex), and extension at 72 °C for 1 min. A final extension step at 72 °C for 3 min was included. Shrimp alkaline phosphate (SAP) treatment, single-base extension (SBE) reactions, and preparation for mass analysis was carried out following the manufacturer's recommendations. In the MassARRAY Nanodispenser RS1000, 5–15 nl sample was robotically spotted onto a SpectroCHIP® II (Agena Bioscience, Hamburg, Germany). Mass analysis was carried out using the MassARRAY Analyzer 4, and the mass spectra were analysed with the Typer 4.0 software (Agena Bioscience, Hamburg, Germany). The Hardy–Weinberg equilibrium (HWE) and pairwise r^2 values for linkage disequilibrium (LD) were calculated with HaploView version 4.2 [16].

2.4. Selection of Variants for Eye Colour Prediction Model (Discovery Data Set)

Eye colour was considered in three different reporting systems, the quantitative system (PIE-score), the two-category system, and the three-category system. For numerical reasons (statistical modelling and stability), the PIE-score (values from −1 to 1) in the quantitative system was transformed to resemble unbounded values. The transformation had an inverse, such that any real number could be transformed into a PIE-score. The PIE-score, r, was transformed by:

$$y = f(r) = \text{logit} (0.5 + r*0.499)$$

Genotypes were coded as 0, 1, or 2 according to the number of minor alleles, where the minor alleles were determined based on the allele frequencies in all samples. Due to low allele frequency, the two variants rs121918166 and rs74653330 were combined [11]. rs12913832 was considered dominant with AA and AG as 0 and GG as 1. For stability, the discovery data set (757 individuals) was randomly divided into a training set (2/3) and a test set (1/3). This was repeated 100 times. If a training set resulted in fixed variants (i.e., only one genotype observed at a base position), a new set was randomly selected. In the quantitative system (transformed PIE-score) and in the two-category system, data were analysed with three different mathematical models: (i) LASSO model with main effects [17,18]; (ii) LASSO model (with the distribution family depending on the system; Gaussian for the quantitative system and binomial for the two-category system) with main effects and all pairwise interactions between rs12913832 and all other variants (still obeying the hierarchical principle such that the main effects must also be included); and (iii) a regression tree [19]. In the three-category system, data were analysed with a classification tree [19]. All seven mathematical models were fitted on the training set, which was also used to compute variable importance of the top 20 variables (variants). The test data were used for testing and estimating the test error. For LASSO regressions, the variables were standardised (such that all had a standard deviation of (1)), and the tuning parameter was chosen by cross-validation with 10 folds to get the most regularised model with an error within one standard error of the minimum error amongst the folds. For LASSO regressions, the absolute value of the estimated effect was used as variable importance. For regression and classification trees, the variable importances provided by the R package *rpart* version 4.1–15 were used [19]. Variable importances were standardised by dividing the importance of each variant with the sum of importances within each model. The mean variable importance (across all models) was used to rank variables (i.e., the variants). The top 12 performing variants were selected for an eye colour prediction model.

2.5. Variant Typing (Model Data Set)

The 12 selected variants and two non-selected SNPs from the IrisPlex [3] were typed with SNaPshot (rs12913832, rs12896399, rs16891982, rs1800407, rs10131374, rs1126809, rs121918166, rs1408799, rs1800401, rs4904927, rs7120151, rs74653330, rs12203592, and rs1393350) in the model data set comprising 523 Norwegian individuals (Table S2). DNA was amplified in one multiplex reaction (14-plex) using the Qiagen Multiplex PCR kit (Qiagen, Hilden, Germany) in a final reaction volume of 10 μL. The PCR comprised denaturation for 15 min at 95 °C followed by 35 cycles of 94 °C for 30 s, 58 °C for 30 s, 72 °C for 30 s, and a final extension step of 72 °C for 10 min. A total of 5 μL amplified DNA/PCR product was treated with 2 μL ExoSAP-IT™ (Thermo Fisher Scientific, Waltham, MA, USA) for 60 min at 37 °C and 15 min at 75 °C. Single-base extension was performed with 1 μL cleaned PCR product, 2 μL SNaPshot™ Multiplex Ready Reaction Mix, 1 μL nuclease-free water (G-Biosciences), and 1 μL SBE primer mix (Table S2). Thermal cycling comprised 30 cycles of 96 °C for 10 s, 55 °C for 5 s, and 60 °C for 30 s. SBE products were treated with 1 μL SAP (Thermo Fisher Scientific, Waltham, MA, USA) for 60 min at 37 °C and 15 min at 75 °C. Separation and detection of SBE products were carried out on an ABI 3500 Genetic Analyser (Thermo Fisher Scientific, Waltham, MA, USA) using the FragmentAnalysis36_POPxl run module (POP-4™ polymer, 36 cm capillary, Dye Set E5).

Capillary electrophoresis was performed with 1 μL SAP-treated SBE products and 20 μL Hi-Di formamide mixed with GeneScan™-120 LIZ® Size Standard (200:1). The results were analysed with GeneMapper® ID-X v.1.5 (Thermo Fisher Scientific, Waltham, MA, USA). One of the selected variants, rs7120151, could not be typed and was excluded. Hence, we used 11 selected variants for the eye colour prediction model (EC11).

2.6. Eye Colour Prediction Modelling (Model Data Set)

Eye colour prediction models were modelled with leave-one-out cross-validation (LOOCV) using the model data set (523 Norwegian individuals) and the selected variants. For observation number *i*, all observations except number *i* were used to train the model. The model was used to predict the eye colour of observation *i*, and the predicted and observed values were compared. Three different reporting systems were used (quantitative system, two-category system, and three-category system), and thereby three different ways of measuring the prediction error were employed. For the quantitative system, a linear regression model was used where the prediction error was the mean squared error. For the two-category system, a logistic regression model was used where blue was chosen as 1 and brown as 0 (without loss of generality). The prediction error for a predicted probability (p) was log(p) if the true eye colour was blue, and log(1-p) if the true eye colour was brown. For the three-category system, a multinomial logistic regression model was used [20]. The prediction error was the Kullback–Leibler divergence between the observed distribution (the observed eye colour has probability 1, and the other two categories probability 0) and the estimated probabilities. All prediction errors were out-of-sample prediction errors. For each reporting system, the modelling was performed with three different variant (SNP) sets: the six IrisPlex SNPs, the 11 SNPs selected in this study (EC11), and rs12913832 alone. This resulted in a total of nine models. Lastly, we used the IrisPlex online tool (model called IrisPlex Web) (https://hirisplex.erasmusmc.nl/, accessed 1 July 2020) to predict eye colour in three categories.

3. Results

3.1. Allele Frequencies of 44 Variants in the Discovery Data Set

We investigated 44 pigmentary variants in our discovery data set of 757 individuals. In this work, we typed 33 variants [12] in two multiplexes using single-base extension. Eleven variants were typed in previous studies [11,13]. The allele frequencies of the 44 variants are shown in Table 2. The allele frequencies were similar in the Danish, Swedish, and Italian populations with small discrepancies between the Scandinavian (Danish and Swedish) and Italian populations, especially in rs12913832 and rs1800407 (Table S3). Moreover, two variants, rs12913832 and rs16891982, deviated significantly from the Hardy–Weinberg equilibrium (HWE) (*p*-value < 0.001) in the discovery data set. This could be explained by positive selection in the European population or a lack of random mating between the Scandinavian (Danish and Swedish) and the Italian populations.

Table 2. Allele frequencies of 44 variants typed in the discovery data set and 13 variants typed in the model data set.

Gene	Variant [1]	Reference Allele	Variant Allele	Variant Allele Frequency	
				Discovery Data Set (n = 757)	Model Data Set (n = 523)
HERC2	**rs12913832 ***	**A**	**G**	**0.74**	**0.83**
IRF4	rs1050976	C	T	0.44	
IRF4	rs10530949	TCT	-	0.43	
IRF4	rs12211228	G	C	0.14	
IRF4	rs9378807	C	T	0.49	
TYR	rs11018509	T	A	0.29	
TYR	**rs1126809**	**G**	**A**	**0.24**	**0.24**
TYR	rs1393350 *	G	A	0.23	0.23
TYR	rs2047512	T	C	0.35	
TYR	rs34749698	T	C	0.23	
TYR	**rs7120151 [2]**	**A**	**G**	**0.74**	**NA**
TYR	rs9919559	T	C	0.33	
SLC24A4	**rs10131374**	**G**	**A**	**0.14**	**0.15**
TYRP1	rs10491745	T	C	0.82	
SLC24A4	rs12590749	C	A	0.37	
SLC24A4	rs12880508	C	T	0.74	
SLC24A4	rs12894551	T	C	0.65	
TYRP1	**rs1408799**	**T**	**C**	**0.68**	**0.69**
SLC24A4	rs17128288	A	G	0.30	
SLC24A4	rs17128324	C	T	0.17	
TYRP1	rs201447946	T	TA	0.06	
SLC24A4	rs34755843	CGACTCT	-	0.16	
SLC24A4	rs35617057	G	T	0.41	
SLC24A4	rs4904887	C	G	0.36	
SLC24A4	rs4904891	G	C	0.35	
SLC24A4	rs4904897	C	T	0.22	
SLC24A4	**rs4904927**	**A**	**G**	**0.87**	**0.89**
SLC24A4	rs59977926	T	C	0.18	
TYRP1	rs62538950	A	T	0.10	
TYRP1	rs62538956	T	C	0.11	
SLC24A4	rs7144273	C	T	0.49	
SLC24A4	rs7152962	G	A	0.23	
SLC24A4	rs7401792	G	A	0.62	
TYRP1	rs74606098	C	T	0.06	
TYRP1	rs79586719	G	A	0.06	
OCA2	**rs1800407 ***	**C**	**T**	**0.07**	**0.03**
IRF4	rs12203592 *	C	T	0.08	0.09
SLC24A4	**rs12896399 ***	**G**	**T**	**0.49**	**0.52**
SLC45A2	**rs16891982 ***	**C**	**G**	**0.93**	**0.95**
OCA2	**rs1800401**	**G**	**A**	**0.04**	**0.05**
OCA2	rs1800414	T	C	<0.01	
OCA2	rs62008729	C	T	0.09	
OCA2	**rs121918166 [2]**	**C**	**T**	**<0.01**	**0.01**
OCA2	**rs74653330 [2]**	**C**	**T**	**<0.01**	**0.02**

[1] Variants in bold were part of the EC11 SNPs and typed in the model data set. rs7120151 was not included in the final prediction modelling. [2] The combined frequency of rs121918166 and rs74653330 was 0.01 in the discovery data set. * Part of the IrisPlex prediction model [3]. NA: not analysed.

3.2. Selection of Variants for Eye Colour Prediction (Discovery Data Set)

The discovery data set with information on eye colour and the 44 pigmentary variants was analysed with seven different mathematical models. Variants were ranked according to the mean variable importance across the mathematical models (Table 3 and Table S4). rs12913832 was the top-performing SNP in all seven mathematical models and ranked number one (Table 3). The mean variable importance for rs12913832 was 74.6% (Table 3). rs121918166 and rs74653330 were combined as one variable and ranked second (Table 3).

We saw a drop in mean variable importance after rank 11 (Table S4). Hence, we selected the top 11 performing variables (comprising 12 variants) for a new eye colour SNP set (Table 3). These variants had mean variable importances of at least 0.3% (Table 3 and Table S4). Four of six variants in the IrisPlex assay [3] were among the selected variants (rs12913832, rs16891982, rs1800407, and rs12896399), whereas the *TYR* variant rs1393350 (ranked 18) and the *IRF4* variant rs12203592 (not in top 20) from the IrisPlex were not selected.

Table 3. Twelve variants selected for the EC11 SNP set.

Rank	Gene	Variant	Mean Variable Importance
1	*HERC2*	rs12913832 *	74.63%
2	*OCA2*	rs121918166 + rs74653330	8.54%
3	*SLC45A2*	rs16891982 *	6.23%
4	*OCA2*	rs1800407 *	5.26%
5	*TYRP1*	rs1408799	1.54%
6	*SLC24A4*	rs4904927	1.19%
7	*SLC24A4*	rs12896399 *	0.68%
8	*TYR*	rs1126809	0.47%
9	*TYR*	rs7120151 [1]	0.46%
10	*SLC24A4*	rs10131374	0.32%
11	*OCA2*	rs1800401	0.32%

[1] Variant not included in the final prediction modelling. * Part of the IrisPlex prediction model [3].

3.3. Typing of Selected Variants and IrisPlex SNPs (Model Data Set)

The 12 selected variants (SNPs) were typed with single-base extension in an independent data set, the model data set of 523 Norwegians (bold in Tables 2 and 3). To enable comparison with the IrisPlex, we included two SNPs from the IrisPlex assay, rs12203592 and rs1393350, in a multiplex comprising 14 SNPs. One SNP, rs7120151, that was ranked as number 9 (Table 3), was excluded due to poor amplification of the A allele. We obtained 523 complete profiles, including the 11 selected SNPs (EC11) (Table 2) and the two additional IrisPlex SNPs.

3.4. Eye Colour Prediction Models with EC11, IrisPlex SNPs, and rs12913832

We constructed nine different eye colour prediction models based on the model data set with 523 Norwegians by using three different reporting systems and three different SNP sets (Tables 2 and 3). We also used the IrisPlex Web for eye colour prediction using the three-category system. Prediction errors for each eye colour prediction model are presented in Table 4. Since we used three different reporting systems, the models within each system have their own measure of prediction error. Therefore, the performance of SNP sets (including prediction errors) can only be directly compared within the same but not across different reporting systems. The EC11 models had the smallest error under all reporting systems, followed by IrisPlex Norway and rs12913832. Under the three-category system, the IrisPlex Web resulted in the highest prediction error (Table 4).

Table 4. Prediction errors for the nine eye colour prediction models (three reporting systems modelled with three SNP sets) and the IrisPlex online tool (IrisPlex Web).

Eye Colour Prediction Model	Quantitative System [1]	Two-Category System [2]	Three-Category System [3]
EC11	5.07	0.26	0.59
IrisPlex Norway	5.90	0.30	0.66
rs12913832	6.96	0.32	0.69
IrisPlex Web *	NA	NA	0.80

[1] Prediction error is the mean squared error. [2] Prediction error for a predicted probability, p, is log(p) if the true eye colour was blue, and log(1-p) if the true eye colour was brown. [3] Prediction error is the Kullback–Leibler divergence. * The IrisPlex Web predicts eye colour according to a three-category system. NA: not analysed.

The sensitivity and specificity of eye colour prediction models in the two-category and the three-category reporting systems were determined without applying a probability threshold (pmax) (Tables 5 and 6). Hence, the predicted eye colour was the eye colour with the highest probability value. The rs12913832 and IrisPlex Norway models showed the same sensitivity and specificity (0.92 and 0.84, respectively) in the two-category system. The EC11 was slightly more sensitive (0.96), and in turn, slightly less specific (0.82) (Table 5 and Table S5).

Table 5. Sensitivity and specificity of eye colour prediction models in the two-category reporting system modelled with three SNP sets. No probability threshold was applied (pmax).

Two-Category System	Sensitivity [1]	Specificity [1]
rs12913832	0.92	0.84
IrisPlex Norway	0.92	0.84
EC11	0.96	0.82

[1] Reference is blue eye colour.

Table 6. Sensitivity and specificity of eye colour prediction models in the three-category reporting system modelled with three SNP sets and the IrisPlex Web model. No probability threshold was applied (pmax).

Three-Category System		Sensitivity [1]	Specificity [1]
rs12913832	Blue	0.95	0.61
	Intermediate	0.00	1.00
	Brown	0.95	0.87
IrisPlex Norway	Blue	0.94	0.61
	Intermediate	0.10	0.97
	Brown	0.86	0.90
EC11	Blue	0.95	0.59
	Intermediate	0.15	0.95
	Brown	0.88	0.96
IrisPlex Web	Blue	0.95	0.60
	Intermediate	0.00	1.00
	Brown	0.95	0.88

[1] Reference is blue eye colour.

In the three-category system, the sensitivity was highest for blue and brown eye colours and lowest for intermediate eye colour with all three SNP sets and the IrisPlex Web (Table 6). The rs12913832 and IrisPlex Web predictions resulted in the highest sensitivity for brown eye colour: 0.95, whereas the IrisPlex Norway and EC11 models had slightly lower sensitivities (Table 6). For blue eye colour, the sensitivities were similar for all models. No individuals were predicted to have intermediate eye colour with either rs12913832 or the IrisPlex Web. Hence, the sensitivity was 0, and the specificity was 1 (Table 6). Of the individuals with intermediate eye colours, 69% and 72% were incorrectly predicted to have blue eye colours with the two models, respectively (Table S6). In contrast, intermediate eye colour predictions were obtained with IrisPlex Norway and EC11. However, only 48% and 46% of the predictions were correct (Table S6). Thus, the sensitivity was low (0.10 and 0.15, respectively), and the specificity was high (0.97 and 0.95, respectively) (Table 6).

Figure 1 shows the percentages of correct, incorrect, and inconclusive predictions for prediction models in the two-category reporting system. Using pmax, 89% of the predictions with both rs12913832 and IrisPlex Norway were correct (Figure 1, Table S5). The EC11 model resulted in 92% correct predictions (Figure 1). Here, 93% of the blue eye colour predictions and 90% of the brown eye colour predictions were correct (Table S5). We also evaluated the prediction with a probability threshold of 0.7 in the two-category

reporting system (Figure 1). If the highest prediction value was below 0.7, the prediction was defined as inconclusive. No eye colours were inconclusive with rs12913832 (Figure 1). The IrisPlex Norway and EC11 resulted in 9% and 5% inconclusive predictions, respectively (Figure 1). With the IrisPlex Norway, 62% of the inconclusive eye colours were brown according to the PIE score. With EC11, it was only 46% (Table S5).
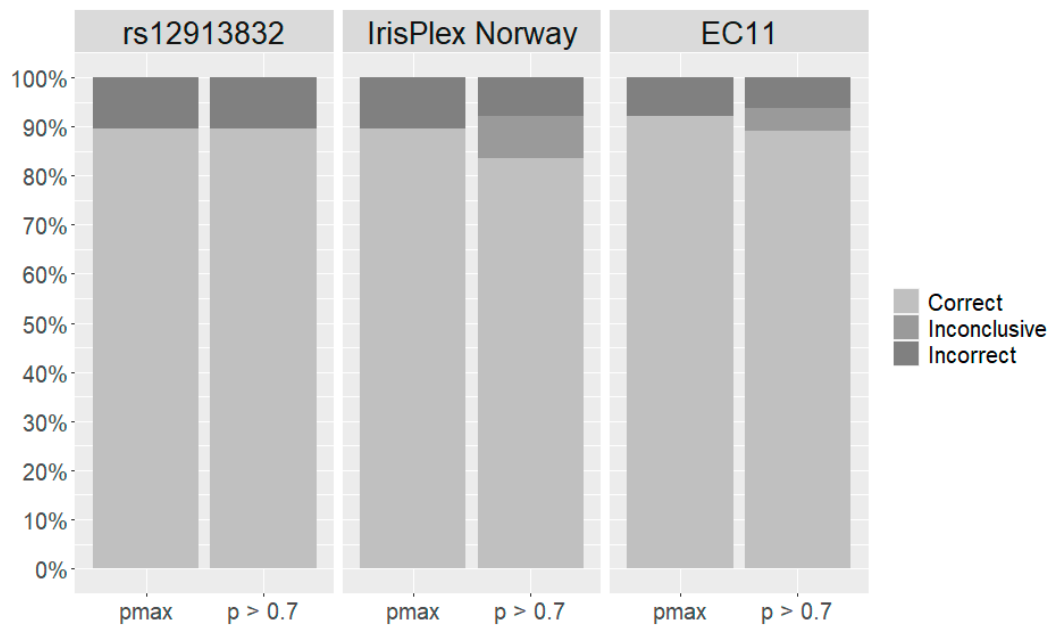

Figure 1. Performance of eye colour prediction models in the two-category reporting system modelled with three SNP sets: rs12913832, IrisPlex Norway, and EC11. Bars represent the percentage of correct, incorrect, and inconclusive predictions with no probability threshold (pmax) and a probability threshold of 0.7 (p > 0.7).

In the three-category reporting system, we tested the prediction with pmax, a probability threshold of 0.5, and a probability threshold of 0.7 (Figure 2). With no probability threshold, the rs12913832, IrisPlex Norway, and IrisPlex Web models all resulted in 72% correct predictions (Figure 2, Table S6). The EC11 model resulted in a slightly higher number of correct predictions (75%) (Figure 2, Table S6). When applying a probability threshold of 0.5, predictions with rs12913832 were unchanged compared with predictions without probability threshold (Figure 2). Predictions with the IrisPlex Web tool were also similar though 3% of the total predictions were inconclusive. There was a slight decrease in the number of correct and incorrect predictions with EC11 and IrisPlex Norway as both models resulted in 2% inconclusive predictions (Figure 2). When applying a probability threshold of 0.7, blue eye colour was correctly predicted in 95% of the blue-eyed individuals with rs12913832, but no individuals were predicted to have brown eye colours (Table S6). Thus, the total number of correct predictions with rs12913832 was only 53%. The number of correct predictions using the 0.7 probability threshold was highest with IrisPlex Web (Figure 2). However, the IrisPlex Web also resulted in the highest percentage of incorrect predictions (20%) and resulted in 15% inconclusive predictions (Figure 2). The IrisPlex Norway model resulted in only 8% incorrect predictions but a high number of inconclusive predictions (51%) (Figure 2). Prediction with EC11 resulted in 12% incorrect predictions, 32% inconclusive predictions, and only 54% correct predictions (Figure 2). Of the 32% inconclusive eye colour predictions, 49% had blue eye colour, 39% had intermediate eye colour, and only 12% had brown eye colour based on the PIE-score (Table S6). Especially the percentage of brown-eyed individuals with inconclusive predictions was much lower than compared with rs12913832, IrisPlex Norway, and IrisPlex Web. For these models, the percentages were 32–65% (Table S6).
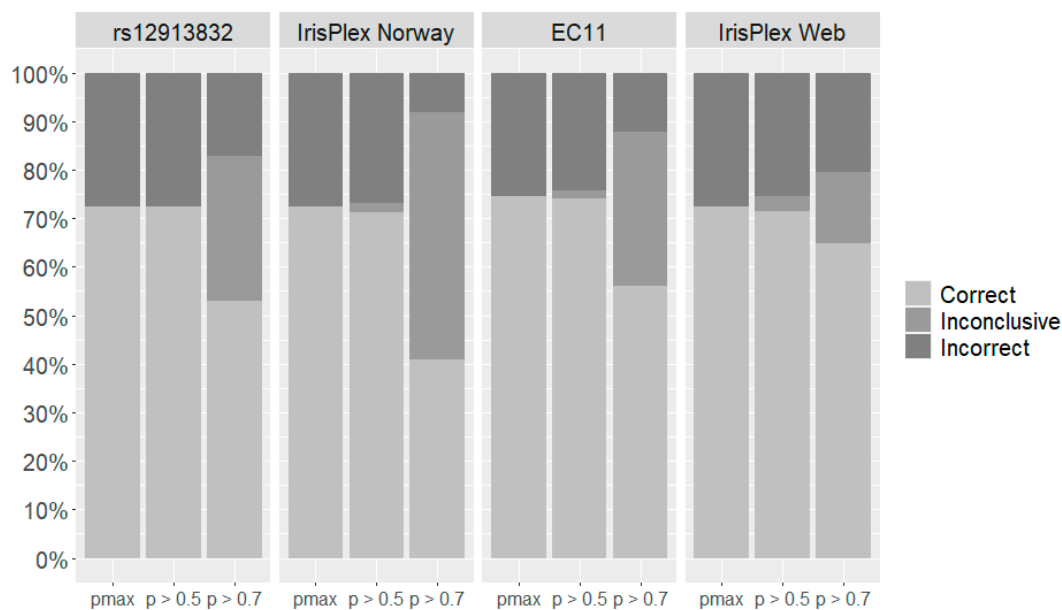
Figure 2. Performance of eye colour prediction models in the three-category reporting system modelled with three SNP sets: rs12913832, IrisPlex Norway and EC11, as well as performance of the IrisPlex Web prediction model. Bars represent the percentage of correct, incorrect, and inconclusive predictions with no probability threshold (pmax), probability threshold of 0.5 (p > 0.5), and probability threshold of 0.7 (p > 0.7).

4. Discussion

In this study, we selected 11 SNPs (EC11) for eye colour prediction and developed new eye colour prediction models for a two-category and a three-category system that performed better than the corresponding IrisPlex and rs12913832 prediction models. The 11 SNPs in EC11 were selected from a group of 44 pigmentary variants that were originally identified in eye colour association studies [3,6] and from detailed sequence analyses of individuals with eye colours that deviated from the expected eye colour based on the genotype of rs12913832 [11,12]. The 44 variants were typed in 757 Europeans whose eye colours were quantitatively determined. Seven different mathematical models were used to rank the variants according to informativeness, and all variants with more than 0.3% mean variable importance were selected. Four of the six SNPs in the IrisPlex assay [3] were included in EC11. However, the *TYR* SNP, rs1393350 (ranked 18), was replaced by another *TYR* SNP, rs1126809 (ranked 8), and the *IRF4* gene represented by the SNP rs12203592 (not in top 20) from the IrisPlex, was not included in EC11. For the selection of SNPs, we combined individuals of Scandinavian (Danish and Swedish) and Italian descent and treated these as one population. We are aware that we may had selected different SNPs if the selection was performed solely on either the Scandinavian or the South European population. We typed the EC11 SNPs and the two additional IrisPlex SNPs in an independent data set of 523 Norwegians whose eye colours were determined with the same quantitative method as the 757 individuals in the discovery data set. We modelled nine different eye colour prediction models on the Norwegian population using the LOOCV method. Each eye colour prediction model consisted of a combination of one of three reporting systems: the quantitative system (prediction of PIE score), the two-category system (blue and brown), and the three-category system (blue, intermediate, brown), and one of three SNP sets: EC11, IrisPlex SNPs, and rs12913832. We also evaluated the IrisPlex Web model for prediction of eye colour in three categories. Based on the analysis of error rates, sensitivity, and specificity of the different eye colour prediction models, there are three main points to consider prior to implementation of eye colour prediction in a forensic genetic setting: (1) the reference population, (2) the SNP set, and (3) the reporting strategy.

4.1. The Reference Population

The rs12913832, IrisPlex Norway, and IrisPlex Web models showed almost identical results in the three-category system (Figure 2, Table 6). Nevertheless, a detailed comparison between the three-category IrisPlex Norway and the IrisPlex Web models highlights the importance of the reference population. The two models were based on the exact same SNPs. However, the IrisPlex Norway model was developed on the Norwegian population, which was the intended target population, whereas the IrisPlex Web model was developed on 9466 individuals of primarily European descent [6,21,22]. The two models resulted in the same number of correct predictions (72%) when no probability threshold was applied. With probability thresholds, inconclusive results were possible, and the IrisPlex Web model resulted in a higher number of correct predictions than the IrisPlex Norway model (Figure 2). However, when applying the recommended threshold for the IrisPlex Web model (p > 0.7) [21], the number of incorrect predictions was also higher (Figure 2). The two models showed similar sensitivities and specificities for blue and brown eye colour but differed for the intermediate eye colour category (Table 6). A total of 123 Norwegian individuals had intermediate eye colours according to the PIE-score (Table 1). Intermediate eye colour predictions were obtained with the IrisPlex Norway model using both pmax and p > 0.5 (Table S6), whereas no individuals were predicted to have intermediate eye colours with the IrisPlex Web model (Table S6). Hence, the IrisPlex Norway model showed an overall lower prediction error than the IrisPlex Web model (Table 4), and this emphasises the importance of modelling a prediction model on the appropriate reference population. This is in agreement with previous evaluations of the IrisPlex model which showed that prediction models based on the intended target population (the reference population) performed better than the IrisPlex Web tool [23,24]. However, it is important to note that the differences between the IrisPlex Web and the IrisPlex Norway models may not only be due to the different reference populations. Different strategies on phenotyping and categorisation of eye colour may also have contributed here. In our study, we determined the eye colour quantitatively, and the eye colour prediction models were modelled accordingly. For the IrisPlex Web model, the eye colour was evaluated by a medical researcher who categorised eye colours in blue, brown, and non-blue/non-brown (called intermediate) categories [3,6,21,22].

4.2. The SNP Set

The eye colour prediction models based on EC11 had the lowest prediction error rates in all three reporting systems and consistently performed better than the rs12913832, IrisPlex Norway, and IrisPlex Web models in the Norwegian population (Table 4). In the three-category reporting system, only EC11 and IrisPlex Norway were able to predict intermediate eye colours (Table 6, Table S6). For the EC11 model, intermediate eye colour predictions were even obtained with a probability threshold of 0.7 (Table S6). We did expect the prediction errors to decrease when the number of loci increased. However, the prediction errors obtained with EC11 (11 SNPs) were only slightly smaller than with IrisPlex Norway (six SNPs), closely followed by rs12913832 (one SNP) and IrisPlex Web (six SNPs) (Table 4). This shows that a single SNP, rs12913238, may be sufficient for prediction of eye colour. This SNP was ranked as number one across all mathematical models with a mean variable importance of 74.6% (Table 3). We modelled rs12913832 in a dominant matter and acknowledge that it is unreasonable to predict eye colour in three categories with a predictor variable containing only two levels (AA/AG and GG). However, even in the three-category reporting system, prediction with rs12913832 showed a lower prediction error than prediction with the IrisPlex Web (Table 4). In both the three-category reporting system and the two-category reporting system, prediction with rs12913832 and IrisPlex Norway performed almost identically (Figure 1, Figure 2). This stresses the importance of rs12913832 for prediction of eye colour and shows that the remaining five SNPs in the IrisPlex SNP set have very small effects on the outcome of the eye colour prediction in the studied population.

4.3. The Reporting Strategy

In this work, we tested three different eye colour categorisation systems: the quantitative system (prediction of PIE score), the two-category system (blue and brown), and the three-category system (blue, intermediate, and brown). Although it is possible to report the predicted eye colour in the form of a PIE-score, this likely requires that the end-user or the reporting laboratory translate the PIE-score into an eye colour category. Therefore, the use of a quantitative system for reporting is not relevant in a forensic genetic setting. The difference between the two- and three-category system is the definition of the intermediate eye colour, which is very difficult to perceive. When multiple individuals were asked to evaluate eye colours categorised as intermediate, they often disagreed, whereas they agreed much more frequently when eye colours were blue or brown [15]. Intermediate eye colour is predicted as the most likely eye colour (without any probability threshold) for only 8% (60 out of 729) and 14% (7.508 out of 52,488) of the possible genotype combinations in the IrisPlex Web and EC11 models, respectively [10] (Table S7). For the IrisPlex Web, the maximum probability value for prediction of intermediate eye colour is 0.62 [10]. With EC11, it is 0.94 (Table S7). In this study, we did observe intermediate eye colour predictions with EC11 with high probability values (maximum: 0.82). However, the intermediate eye colour predictions were incorrect more than half of the time (Table S6). Overall, eye colour prediction in two categories resulted in more correct predictions than eye colour prediction in three categories (92% vs. 75% for EC11; 89% vs. 72% for IrisPlex Norway and 89% vs. 72% for rs12913832) (Figures 1 and 2). Hence, the definition of an intermediate eye colour category is counterintuitive, as it is both difficult to identify and predict. A recent study discusses the need for standardised methods for reporting forensic DNA phenotyping predictions to the police [25]. Reducing the complexity of eye colour predictions to only two categories results in only two hypotheses (H_1: The person has brown eyes and H_2: The person has blue eyes). Hence, it is possible to report the weight of the evidence with a single likelihood ratio, which resembles standard STR-profiling reports. The likelihood ratio could be supplemented with picture examples of eye colours represented by each category. This may overcome any misunderstandings or subjective opinions of eye colour interpretation, especially for eye colours that may appear non-blue and non-brown.

4.4. DNA Phenotyping in Forensic Genetics

The Section of Forensic Genetics in Denmark recently began offering eye colour prediction to the police using the two-category system based on the genotype of rs12913832. Prediction of EVCs can cause ethical concerns as discussed in [26]. This is especially apparent if the genetic markers used for prediction a certain trait are also linked to diseases [26]. That is not the case for rs12913832. The SNP is included in the Precision ID Ancestry Panel (Thermo Fisher Scientific, Waltham, MA, USA), which has already been validated for case work [5,27,28]. The weight of the evidence for both ancestry and eye colour predictions are reported as likelihood ratios. For eye colour predictions in the Danish population, LR = (rs12913832:GG|H_1/rs12913832:GG|H_2) = 0.1, LR = (rs12913832:AG|H_1/rs12913832:AG|H_2) = 19, and LR = (rs12913832:AA|H_1/rs12913832:AA|H_2) = 54 [15], where H_1: The person has brown eyes and H_2: The person has blue eyes. The EC11 model may be implemented at the Section of Forensic Genetics in Denmark in the future once the EC11 markers are included in a validated massively parallel sequencing (MPS) assay. The most important shortcoming of the rs12913832 two-category prediction model is the lack of information gained when including the two *OCA2* variants, rs121918166 and rs74653330. These variants were previously shown to be of importance for blue eye colour in Scandinavians with the rs12913832:AG genotype [11]. The variants had low frequencies in Danes and Swedes and were completely absent in Italians [11] (Table S3). These variants combined were ranked as second most important, with a mean variable importance of 8.5% (Table 3). In the Norwegian data set, 30 individuals with the rs12913832:AG genotype had blue eye colours according to the PIE-score. Seventeen of the 30 individuals had at least one of the *OCA2* variants and were correctly predicted to have

blue eyes using the EC11 two-category model. By contrast, only one of the 30 individuals was correctly predicted with the IrisPlex Norway model, and none were correctly predicted with rs12913832. Moreover, two Norwegians with the rs12913832:AA genotype had blue eye colours according to the PIE-score. One of the two individuals was correctly predicted to have blue eye colour with the EC11 two-category model. This individual was homozygous for the rs74653330 variant. We hypothesise that the second individual has other variants in or around the *OCA2* gene that could explain the formation of blue eye colour in the rs12913832:AA genotype background. Both individuals were incorrectly predicted to have brown eye colours with the IrisPlex Norway and rs12913832 models. Lastly, 10 Norwegians with the rs12913832:GG genotype had brown eyes according to the PIE-score. Only one of them was correctly predicted to have brown eyes with the two-category EC11 and IrisPlex Norway models. This shows that we do not fully understand the formation of brown eye colour in rs12913832:GG individuals and that the EC11 model may have to be expanded further.

Supplementary Materials: The following are available online at https://www.mdpi.com/article/10.3390/genes12060821/s1; Table S1: Primer sequences and primer concentrations for 24 plex and 11 plex typed in the variant discovery data set; Table S2: Primer sequences and primer concentrations for 14 plex typed with SNaPshot in the model data set; Table S3: Allele frequencies of 44 variants typed in the discovery data set comprising Danish, Swedish, and Italian individuals (DK/SWE/ITA) and 13 variants typed in the model data set comprising Norwegian individuals (NO); Table S4: Mean variable importance of top 20 variants; Table S5: Confusion matrices for two-category system prediction models; one for each SNP set and each threshold (pmax and p > 0.7); Table S6: Confusion matrices for three-category system prediction models; one for each SNP set and each threshold (pmax, p > 0.5, and p > 0.7); Table S7: Eye colour prediction outcomes for 52,488 possible genotype combinations using the EC11 three-category model.

Author Contributions: Conceptualization, O.S.M., N.M., C.B. and J.D.A.; formal analysis, O.S.M. N.M.S, A.K., M.K. and M.M.A.; data curation, E.S. and H.U .; writing—original draft prep-aration, O.S.M. and N.M.S.; writing—review and editing, A.K., M.K., M.M.A., E.S., H.U., K.J., N.M., C.B., G.-H.O. and J.D.A. All authors have read and agreed to the published version of the manuscript.

Institutional Review Board Statement: The study was conducted according to the guidelines of the Declaration of Helsinki, and approved by the Danish Ethical Committee (M-20090237, H-4-2009-125, and H-3-2012-023), the Ethical Committee of Azienda Ospedaliera Ospedal Sant'Anna di Como (U.0026484.23-11-2012), the Ethical Committee of the University of Milan-Bicocca (P.U. 0033373/12), and the Faculty of Health Sciences, UiT–The Arctic University of Norway (2021/2034).

Informed Consent Statement: Informed consent was obtained from all subjects involved in the study.

Data Availability Statement: The data generated in the present study are included within the manuscript and its supplementary files.

Conflicts of Interest: The authors declare no conflict of interest.

References

1.   Walsh, S.; Liu, F.; Wollstein, A.; Kovatsi, L.; Ralf, A.; Kosiniak-Kamysz, A.; Branicki, W.; Kayser, M. The HIrisPlex system for simultaneous prediction of hair and eye colour from DNA. *Forensic Sci. Int. Genet.* **2013**, *7*, 98–115. [CrossRef] [PubMed]
2.   Chaitanya, L.; Breslin, K.; Zuñiga, S.; Wirken, L.; Pośpiech, E.; Kukla-Bartoszek, M.; Sijen, T.; de Knijff, P.; Liu, F.; Branicki, W.; et al. The HIrisPlex-S system for eye, hair and skin colour prediction from DNA: Introduction and forensic developmental validation. *Forensic Sci. Int. Genet.* **2018**, *35*, 123–135. [CrossRef] [PubMed]
3.   Walsh, S.; Liu, F.; Ballantyne, K.N.; van Oven, M.; Lao, O.; Kayser, M. IrisPlex: A sensitive DNA tool for accurate prediction of blue and brown eye colour in the absence of ancestry information. *Forensic Sci. Int. Genet.* **2011**, *5*, 170–180. [CrossRef] [PubMed]

4. Ruiz, Y.; Phillips, C.; Gomez-Tato, A.; Alvarez-Dios, J.; Casares de Cal, M.; Cruz, R.; Maroñas, O.; Söchtig, J.; Fondevila, M.; Rodriguez-Cid, M.; et al. Further development of forensic eye color predictive tests. *Forensic Sci. Int. Genet.* **2013**, *7*, 28–40. [CrossRef] [PubMed]

5. Mogensen, H.S.; Tvedebrink, T.; Børsting, C.; Pereira, V.; Morling, N. Ancestry prediction efficiency of the software GenoGeographer using a z-score method and the ancestry informative markers in the Precision ID Ancestry Panel. *Forensic Sci. Int. Genet.* **2020**, *44*, 102154. [CrossRef]

6. Liu, F.; van Duijn, K.; Vingerling, J.R.; Hofman, A.; Uitterlinden, A.G.; Janssens, A.C.J.; Kayser, M. Eye color and the prediction of complex phenotypes from genotypes. *Curr. Biol.* **2009**, *19*, R192–R193. [CrossRef] [PubMed]

7. Sturm, R.A.; Duffy, D.L.; Zhao, Z.Z.; Leite, F.P.; Stark, M.; Hayward, N.K.; Martin, N.; Montgomery, G.W. A single SNP in an evolutionary conserved region within Intron 86 of the HERC2 gene determines human blue-brown eye color. *Am. J. Hum. Genet.* **2008**, *82*, 424–431. [CrossRef]

8. Eiberg, H.; Troelsen, J.T.; Nielsen, M.; Mikkelsen, A.; Mengel-From, J.; Kjaer, K.W.; Hansen, L. Blue eye color in humans may be caused by a perfectly associated founder mutation in a regulatory element located within the HERC2 gene inhibiting OCA2 expression. *Hum. Genet.* **2008**, *123*, 177–187. [CrossRef]

9. Visser, M.; Kayser, M.; Palstra, R.-J. HERC2 rs12913832 modulates human pigmentation by attenuating chromatin-loop formation between a long-range enhancer and the OCA2 promoter. *Genome Res.* **2012**, *22*, 446–455. [CrossRef]

10. Pietroni, C.; Andersen, J.D.; Johansen, P.; Andersen, M.M.; Harder, S.; Paulsen, R.R.; Børsting, C.; Morling, N. The effect of gender on eye colour variation in European populations and an evaluation of the IrisPlex prediction model. *Forensic Sci. Int. Genet.* **2014**, *11*, 1–6. [CrossRef]

11. Andersen, J.D.; Pietroni, C.; Johansen, P.; Andersen, M.M.; Pereira, V.; Børsting, C.; Morling, N. Importance of nonsynonymous OCA 2 variants in human eye color prediction. *Mol. Genet. Genom. Med.* **2016**, *4*, 420–430. [CrossRef]

12. Meyer, O.S.; Lunn, M.M.B.; Garcia, S.L.; Kjærbye, A.B.; Morling, N.; Børsting, C.; Andersen, J.D. Association between brown eye colour in rs12913832:GG individuals and SNPs in TYR, TYRP1, and SLC24A4. *PLoS ONE* **2020**, *15*, e0239131. [CrossRef] [PubMed]

13. Andersen, J.D.; Johansen, P.; Harder, S.; Christoffersen, S.R.; Delgado, M.C.; Henriksen, S.T.; Nielsen, M.M.; Sørensen, E.; Ullum, H.; Hansen, T.; et al. Genetic analyses of the human eye colours using a novel objective method for eye colour classification. *Forensic Sci. Int. Genet.* **2013**, *7*, 508–515. [CrossRef]

14. Salvo, N.M.; Janssen, K.; Kirsebom, M.K.; Meyer, O.S.; Berg, T.; Olsen, G.-H. Forensic DNA phenotyping—Predicting eye and hair colour in a Norwegian population using Verogen's ForenSeqTM DNA Signature Prep Kit. *Forensic Sci. Int. Genet.* **2021**. submitted.

15. Meyer, O.S.; Børsting, C.; Andersen, J.D. Perception of blue and brown eye colours for forensic DNA phenotyping. *Forensic Sci. Int. Genet. Suppl. Ser.* **2019**, *7*, 476–477. [CrossRef]

16. Barrett, J.C.; Fry, B.; Maller, J.; Daly, M.J. Haploview: Analysis and visualization of LD and haplotype maps. *Bioinformatics* **2005**, *21*, 263–265. [CrossRef] [PubMed]

17. Santosa, F.; Symes, W.W. Linear inversion of band-limited reflection seismograms. *SIAM J. Sci. Stat. Comput.* **1986**, *7*, 1307–1330. [CrossRef]

18. Tibshirani, R. Regression shrinkage and selection via the Lasso. *J. R. Stat. Soc. Ser. B* **1996**, *58*, 267–288. [CrossRef]

19. Breiman, L.; Friedman, J.H.; Olshen, R.A.; Stone, C.J. *Classification and Regression Trees*; Taylor & Francis: Abingdon, UK, 1984; ISBN 9781351460491.

20. Venables, W.N.; Ripley, B.D. *Modern Applied Statistics with S*, 4th ed.; Springer: New York, NY, USA, 2002; pp. 435–446.

21. Walsh, S.; Wollstein, A.; Liu, F.; Chakravarthy, U.; Rahu, M.; Seland, J.H.; Soubrane, G.; Tomazzoli, L.; Topouzis, F.; Vingerling, J.R.; et al. DNA-based eye colour prediction across Europe with the IrisPlex system. *Forensic Sci. Int. Genet.* **2012**, *6*, 330–340. [CrossRef] [PubMed]

22. Walsh, S.; Chaitanya, L.; Breslin, K.; Muralidharan, C.; Bronikowska, A.; Pospiech, E.; Koller, J.; Kovatsi, L.; Wollstein, A.; Branicki, W.; et al. Global skin colour prediction from DNA. *Qual. Life Res.* **2017**, *136*, 847–863. [CrossRef]

23. Dembinski, G.M.; Picard, C.J. Evaluation of the IrisPlex DNA-based eye color prediction assay in a United States population. *Forensic Sci. Int. Genet.* **2014**, *9*, 111–117. [CrossRef]

24. Salvoro, C.; Faccinetto, C.; Zucchelli, L.; Porto, M.; Marino, A.; Occhi, G.; de los Campos, G.; Vazza, G. Performance of four models for eye color prediction in an Italian population sample. *Forensic Sci. Int. Genet.* **2019**, *40*, 192–200. [CrossRef]

25. Atwood, L.; Raymond, J.; Sears, A.; Bell, M.; Daniel, R. From identification to intelligence: An assessment of the suitability of forensic DNA phenotyping service providers for use in Australian law enforcement casework. *Front. Genet.* **2021**, *11*, 11. [CrossRef]

26. Kayser, M. Forensic DNA phenotyping: Predicting human appearance from crime scene material for investigative purposes. *Forensic Sci. Int. Genet.* **2015**, *18*, 33–48. [CrossRef] [PubMed]

27. Pereira, V.; Mogensen, H.S.; Børsting, C.; Morling, N. Evaluation of the precision ID Ancestry Panel for crime case work: A SNP typing assay developed for typing of 165 ancestral informative markers. *Forensic Sci. Int. Genet.* **2017**, *28*, 138–145. [CrossRef] [PubMed]

28. Tvedebrink, T.; Eriksen, P.S.; Mogensen, H.S.; Morling, N. Weight of the evidence of genetic investigations of ancestry informative markers. *Theor. Popul. Biol.* **2018**, *120*, 1–10. [CrossRef] [PubMed]

Paper 4

Experimental long-distance haplotyping of *OCA2-HERC2* variants

Nina Mjølsnes Salvo, Marie Gule Mathisen, Kirstin Janssen, Thomas Berg, Gunn-Hege Olsen[*]

Centre for Forensic Genetics, Department of Medical Biology, Faculty of Health Sciences, UiT - The Arctic University of Norway, Norway

ARTICLE INFO

ABSTRACT

The regulatory *HERC2* SNP, rs12913832, is strongly associated with blue and brown eye colour. However, eye colour in heterozygous rs12913832 individuals is observed to vary greatly. Missense mutations in *OCA2,* such as rs1800407 and rs74653330, are associated with lighter eye colour in some but not all heterozygous rs12913832 individuals. Determining the physical linkage of these variants might help to further explain eye colour variation. So far, experimental haplotyping of these variants has been challenging because the genomic distance between them (∼ 135 kb) exceeds the fragment lengths produced by commonly used DNA isolation kits. The aim for this study was to explore novel methods for long distance haplotyping to assess associations between *OCA2-HERC2* haplotypes and eye colour. DNA was isolated from frozen blood samples collected from Norwegians that are known to be heterozygous for both *HERC2* rs12913832 and *OCA2* SNPs, either rs1800407 (n = 23) or rs74653330 (n = 17), using the newly commercially available Monarch® HMW (heigh molecular weight) DNA Extraction Kit (New England BioLabs$_{inc}$). We successfully isolated DNA fragments up to 210 kb, which were long enough to haplotype *OCA2-HERC2* loci by droplet digital PCR (ddPCR). Three haplotypes were observed in the study population: rs12913832:A-rs1800407:T in 22/23 individuals, rs12913832:A-rs1800407:C in 1/23 individuals and rs12913832:A-rs74653330:T in 16/16 individuals. As expected, all individuals with the rs12913832:A-rs74653330:T haplotype had intermediate to blue eye colour. However, the rs12913832:A-rs1800407:T haplotype was observed in both blue and brown-eyed individuals, suggesting more research is needed.

1. Introduction

The *HERC2* SNP rs12913832 (enhancer region of *OCA2*) is the main predictor of blue and brown eye colour [1], especially in the homozygous state (AA and GG). However, eye colour in heterozygous rs12913832 individuals is observed to vary greatly [2]. Missense mutations in *OCA2* (e.g. rs1800407:T and rs74653330:T) are associated with lighter eye colour in some but not all rs12913832:AG Scandinavians [2–4]. Thus, the physical linkage of *HERC2* rs12913832 and *OCA2* variants may further explain eye colour variation. So far, experimental long distance haplotyping has been technically challenging, because the genomic distance between these loci (∼135 kb) is much greater than the DNA fragments size produced by commonly used DNA isolation kits. In this study, we aim to demonstrate the feasibility of isolating long DNA fragments for long distance haplotyping by ddPCR and use this methodology to assess associations between *OCA2-HERC2* haplotypes and eye colour.

2. Material and methods

Frozen blood samples from 40 rs12913832:AG Norwegians with either rs1800407:CT (n = 23) or rs74653330:CT (n = 17) were selected for experimental haplotyping from a database of 545 Norwegians, described in previous studies [2,3]. Eye colour varied from blue to brown (PIE-score [5]: from −1 to 1). The project is approved by the Faculty of Health Sciences, UiT - The Arctic University of Norway (reference number 2021/2034).

DNA was isolated using the newly commercially available Monarch® HMW DNA Extraction Kit (New England BioLabs$_{inc}$). DNA fragment length was tested with ddPCR using the "mile marker" assays, targeting the *RPP30* locus, as described in Regan et al., 2015 [6]. Assays are FAM-labelled and target sequences at distances from 1 to 210 kb from an HEX-labelled anchor assay. As a negative control the "mile marker" assays were also haplotyped with another anchor, on the *EIF2C1* locus, residing on a different chromosome.

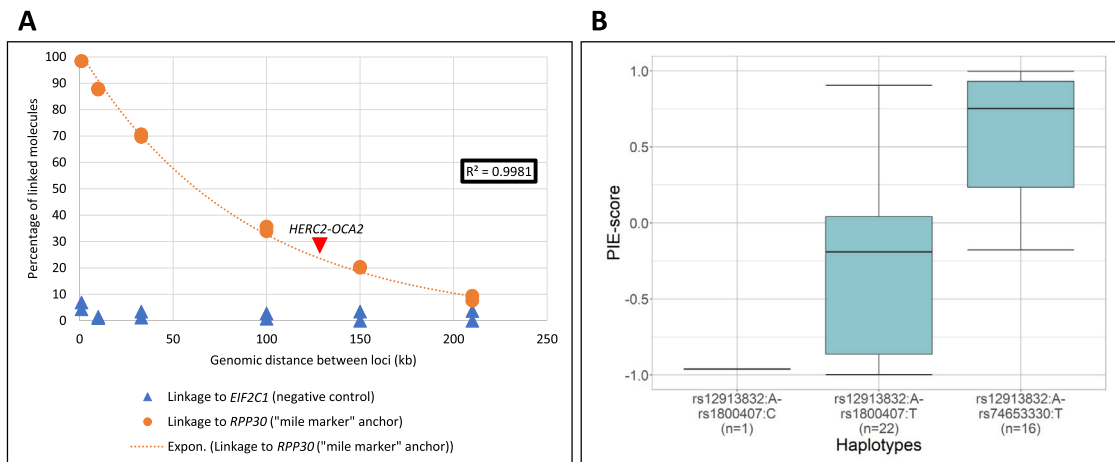Individuals were haplotyped by ddPCR using Bio-Rad's QX200

Fig. 1. **A)** DNA fragment lengths in Monarch® extracted HMW DNA visualised by plotting percentage of linked loci after ddPCR against genomic distance of "mile marker" assays. ▼ genomic distance between OCA2-HERC2 targets. **B)** Haplotypes and Pixel Index of the Eye (PIE)-scores from − 1 (brown) to 1 (blue), in a Norwegian study population (n = 39).

ddPCR system and the phasing protocol by Regan and Karlin-Neumann, 2018 [7]. Only two targets can be haplotyped in one analysis. Thus, to cover all possible allele combinations, four unique HEX-FAM duplexes per marker pair were designed by Bio-Rad (assay ID dHsaMDM2285425001/dHsaMDW2285425003 for rs12913832, assay ID dHsaMDW8577445873/dHsaMDM8577445871 for rs1800407 and assay ID dMDM1502681141/dMDW1502681143 for rs74653330). Primers and Iowa Black quenched probes were designed with an optimal annealing temperature of 55ºC, and standard cycling conditions for ddPCR. To minimise cross-reaction, dark competitor probes for each assay were added. Data was analysed for linkage of markers with QX Manager v.1.2.

3. Results and discussion

We successfully isolated DNA fragments up to 210 kb, which was long enough for experimental haplotyping of *OCA2-HERC2* (Fig. 1A). Additionally, by using the "mile marker" assays, we observe that over 20% of the fragments were longer than 135 kb (▼ in Fig. 1A), clearly distinguishable from the background (▲ in Fig. 1A). Thus, variants of interest could successfully be phased by ddPCR. Notably, care should be taken when working with HMW DNA due to susceptibility to fragmentation and sample viscosity. Long DNA fragments are more difficult to mix to homogeneity due to entangling and might therefore compromise droplet generation. Hence, we used 20 ng input DNA per reaction instead of the recommended 40 ng [7]. When experimentally haplotyping *OCA2-HERC2* in the study population, linkage down to 5% was observed. This was possibly due to low DNA concentration and fragmentation in the respective samples as the blood had been stored for up to seven years. However, by utilising all four duplexes, all but one sample could be haplotyped with confidence.

Successful haplotyping in 39 Norwegians revealed three haplotypes (Fig. 1B): rs12913832:A-rs1800407:T in 22/23 individuals, rs12913832:A-rs1800407:C in 1/23 individuals and rs12913832:A-rs74653330:T in 16/16 individuals. This means that all but one individual carried the derived G-allele in rs12913832 in *trans*-phase with either the *OCA2* missense mutations rs1800407:T or rs74653330:T. *OCA2* expression is reduced in the presence of rs12913832:G [8]. Hence, it was expected to find these haplotypes in intermediate and blue-eyed individuals as they have one protein at reduced production and one variant protein. This agrees with the observation that all rs12913832:A-rs74653330:T individuals had intermediate and blue eyes. Surprisingly, eye colour in rs12913832:A-rs1800407:T individuals varied from blue to brown, questioning the effect of rs1800407 on eye colour in the

Norwegian population. Only one brown eyed individual had the expected rs12913832:A-rs1800407:C haplotype. rs1800407 is included in the forensically validated prediction tool, IrisPlex, and has been reported to have low, but measurable effect on eye colour in several populations [5,9]. Association of the rs1800407 and eye colour has also been observed in the Norwegian population, but not on a rs12913832: AG and AA background [2]. We suggest to haplotype these SNPs in other populations as well to get a deeper understanding of their impact on eye colour.

4. Conclusion

Phasing by ddPCR was rapid and enabled screening of particular *OCA2-HERC2* haplotypes in a Norwegian study population. The newly available Monarch® HMW DNA Extraction Kit was an excellent choice for isolating long DNA fragments, even from frozen blood samples, making long-distance haplotyping possible. As expected, all rs74653330:T individuals had intermediate and blue eyes and had the derived T-allele in trans-phase with the derived G-allele in rs12913832. However, the rs12913832:A-rs1800407:T haplotype was observed in individuals with varying eye colour (from blue to brown), suggesting more research is needed to better understand normal eye colour variation.

Declaration of Competing Interest

None.

Acknowledgements

References

[1] R.A. Sturm, D.L. Duffy, Z.Z. Zhao, F.P.N. Leite, M.S. Stark, N.K. Hayward, N. G. Martin, G.W. Montgomery, A single SNP in an evolutionary conserved region within Intron 86 of the HERC2 gene determines human blue-brown eye color, Am. J. Hum. Genet 82 (2008) 424, https://doi.org/10.1016/J.AJHG.2007.11.005.

[2] N.M. Salvo, K. Janssen, M.K. Kirsebom, O.S. Meyer, T. Berg, G.H. Olsen, Predicting eye and hair colour in a Norwegian population using Verogen's ForenSeq™ DNA signature prep kit, Forensic Sci. Int. Genet. 56 (2022) 102620, https://doi.org/10.1016/J.FSIGEN.2021.102620.

[3] O.S. Meyer, N.M. Salvo, A. Kjærbye, M. Kjersem, M.M. Andersen, E. Sørensen, H. Ullum, K. Janssen, N. Morling, C. Børsting, G.-H. Olsen, J.D. Andersen, Prediction of eye colour in scandinavians using the EyeColour 11 (EC11) SNP set, Genes 12 (2021) 821, https://doi.org/10.3390/GENES12060821.

[4] J.D. Andersen, C. Pietroni, P. Johansen, M.M. Andersen, V. Pereira, C. Børsting, N. Morling, Importance of nonsynonymous OCA2 variants in human eye color prediction, Mol. Genet. Genom. Med. 4 (2016) 420–430, https://doi.org/10.1002/mgg3.213.

[5] J.D. Andersen, P. Johansen, S. Harder, S.R. Christoffersen, M.C. Delgado, S. T. Henriksen, M.M. Nielsen, E. Sørensen, H. Ullum, T. Hansen, A.L. Dahl, R. R. Paulsen, C. Børsting, N. Morling, Genetic analyses of the human eye colours using a novel objective method for eye colour classification, Forensic Sci. Int. Genet. 7 (2013) 508–515, https://doi.org/10.1016/j.fsigen.2013.05.003.

[6] J.F. Regan, N. Kamitaki, T. Legler, S. Cooper, N. Klitgord, G. Karlin-Neumann, C. Wong, S. Hodges, R. Koehler, S. Tzonev, S.A. McCarroll, A rapid molecular approach for chromosomal phasing, PLoS One 10 (2015), e0118270, https://doi.org/10.1371/JOURNAL.PONE.0118270.

[7] J. Regan, G. Karlin-Neumann, Phasing DNA markers using digital PCR, Methods Mol. Biol. 1768 (2018) 489–512, https://doi.org/10.1007/978-1-4939-7778-9_28/FIGURES/10.

[8] M. Visser, M. Kayser, R.-J. Palstra, HERC2 rs12913832 modulates human pigmentation by attenuating chromatin-loop formation between a long-range enhancer and the OCA2 promoter, Genome Res. 22 (2012) 446–455, https://doi.org/10.1101/gr.128652.111.

[9] S. Walsh, A. Wollstein, F. Liu, U. Chakravarthy, M. Rahu, J.H. Seland, G. Soubrane, L. Tomazzoli, F. Topouzis, J.R. Vingerling, J. Vioque, A.E. Fletcher, K.N. Ballantyne, M. Kayser, DNA-based eye colour prediction across Europe with the IrisPlex system, Forensic Sci. Int. Genet. 6 (2012) 330–340, https://doi.org/10.1016/J.FSIGEN.2011.07.009.

Paper 5

Article

Association between Variants in the *OCA2-HERC2* Region and Blue Eye Colour in *HERC2* rs12913832 AA and AG Individuals

Nina Mjølsnes Salvo [1],[*] , Jeppe Dyrberg Andersen [2] , Kirstin Janssen [1] , Olivia Luxford Meyer [2] , Thomas Berg [1] , Claus Børsting [2] and Gunn-Hege Olsen [1]

1   Centre for Forensic Genetics, Department of Medical Biology, Faculty of Health Sciences, UiT The Arctic University of Norway, 9037 Tromsø, Norway
2   Section of Forensic Genetics, Department of Forensic Medicine, Faculty of Health and Medical Sciences, University of Copenhagen, 2100 Copenhagen, Denmark
*   Correspondence: nina.mjolsnes@uit.no

Abstract: The *OCA2-HERC2* region is strongly associated with human pigmentation, especially eye colour. The *HERC2* SNP rs12913832 is currently the best-known predictor for blue and brown eye colour. However, in a previous study we found that 43 of 166 Norwegians with the brown eye colour genotype rs12913832:AA or AG, did not have the expected brown eye colour. In this study, we carried out massively parallel sequencing of a ~500 kbp *HERC2-OCA2* region in 94 rs12913832:AA and AG Norwegians (43 blue-eyed and 51 brown-eyed) to search for novel blue eye colour variants. The new candidate variants were subsequently typed in a Norwegian biobank population (total *n* = 519) for population specific association analysis. We identified five new variants, rs74409036:A, rs78544415:T, rs72714116:T, rs191109490:C and rs551217952:C, to be the most promising candidates for explaining blue eye colour in individuals with the rs12913832:AA and AG genotype. Additionally, we confirmed the association of the missense variants rs74653330:T and rs121918166:T with blue eye colour, and observed lighter skin colour in rs74653330:T individuals. In total, 37 (86%) of the 43 blue-eyed rs12913832:AA and AG Norwegians could potentially be explained by these seven variants, and we suggest including them in future prediction models.

Keywords: forensic genetics; DNA phenotyping; massively parallel sequencing; *OCA2-HERC2*; eye colour; pigmentation

1. Introduction

Many pigmentation genes have been extensively studied to explain human eye colour variation [1]. Oculocutaneous albinism type 2 (*OCA2*) and its neighbouring gene the HECT domain and RCC1-like domain 2 (*HERC2*) are of special interest because of their strong genetic influence on human pigmentation, especially eye colour variation [1,2]. *OCA2* expression is regulated by the intronic SNP rs12913832, which is situated in a conserved enhancer region in *HERC2* [3,4]. The ancestral A-allele in rs12913832 allows transcription factors to modulate long-range chromatin looping that leads to contact between the *OCA2* promotor and the enhancer. This enhances *OCA2* expression and thereby, melanin production. In contrast, the derived G-allele reduces chromatin looping and thereby, *OCA2* expression and melanin production [3]. European populations have the largest variation in eye colour, and recent selection for the G-allele in Europeans has been documented [5]. The strong association between genotypes of rs12913832 and blue and brown eye colour allows accurate eye colour prediction, which has an important application in forensic genetics [4,6,7]. According to the dominant hypothesis, the genotypes rs12913832:AA or AG lead to brown eye colour, whereas the genotype rs12913832:GG is found in individuals with blue eye colour. This is correct for most individuals, but discrepancies in European populations are documented, where individuals with the genotype rs12913832:AA or AG have blue eye colour, and individuals with the genotype rs12913832:GG have brown eye

colour [8–10]. Other polymorphisms in *OCA2*, both in regulatory and coding regions, have shown associations with eye colour, albeit with minor additive effects [11,12]. The missense *OCA2* SNP rs1800407 was included in the IrisPlex prediction tool and improved the prediction accuracy of eye colour in a European population [6,13,14], whereas the missense variants rs74653330 and rs121918166 have been suggested to explain blue eye colour in Scandinavians [8]. Additionally, rs74653330 and rs121918166 are found to be associated with human skin colour variation [8,15]. In a previous study, we showed that the eye colour prediction accuracy in a Norwegian study population increased when rs74653330 and rs121918166 were included in the prediction model [16]. However, the eye colour of some blue-eyed Norwegians were still not accurately predicted, suggesting that other variants in or around *OCA2* could affect eye colour formation in individuals with the rs12913832:AA and AG genotypes. Therefore, in this study, we sequenced the *OCA2-HERC2* region in a Norwegian biobank population in order to find new candidate variants that may explain blue eye colour in individuals with the rs12913832:AA and AG genotype.

2. Materials and Methods

2.1. Study Population and Selection of Individuals for Genotyping

A Norwegian biobank population of 540 volunteers (presumably unrelated) residing in northern Norway from 2015 to 2017, was used to search for candidate variants that may explain blue eye colour [10]. The *OCA2-HERC2* region was sequenced in a selected study cohort of 94 individuals, previously genotyped as *HERC2* rs12913832 AA or AG [10]. For the sequenced study cohort, 43 individuals were selected because they did not follow the dominant hypothesis and had blue eye colour (study group, Table 1). Additionally, 41 of the 43 individuals were previously predicted incorrectly to have brown eye colour using the IrisPlex model [10,13] (Table S1). The remaining 51 individuals had the expected brown eye colour phenotype and were used as controls (control group, Table 1). The new candidate variants were subsequently typed in the remaining Norwegian samples (*n* = 446). All samples were collected with informed consent and subsequently anonymised. The project was approved by the Faculty of Health Sciences, UiT-The Arctic University of Norway (reference number 2021/2034).

Table 1. Number of rs12913832 AA and AG individuals with blue or brown eye colour selected for sequencing of the *OCA2-HERC2* region.

rs12913832	Brown (Control Group)	Blue (Study Group)
AA	21	3
AG	30	40
Total	51	43

2.2. Eye Colour Categorisation and Quantitative Eye Colour Measurements

High resolution photographs were taken of the participants' eyes, and categorisation of eye colours was performed in the recent study from Salvo et al. [10]. In short, nine untrained individuals were asked to intuitively assign each photograph to one of four categories: blue, intermediate-blue, intermediate-brown, or brown eyes. Herein, a two-category system (blue and brown) was used. Therefore, blue and intermediate-blue were grouped into the blue category (*n* = 43), and brown and intermediate-brown were grouped into the brown category (*n* = 51). A quantitative eye colour score (Pixel Index of the Eye (PIE)—score) was calculated for each individual's eye photograph using the custom-made Digital Analysis of Iris Tool software (DIAT) v.1 [9]. All the photographs from individuals categorised with blue eye colour had PIE-scores ranging from −0.3 to 1, and all the photographs from individuals categorised with brown eye colour had PIE-scores from −1 to −0.07 (Table S1). Only two individuals with blue eyes and six individuals with brown eyes had PIE-scores in the overlapping region (−0.3 to −0.07). The categorised eye colour highly correlated with

the PIE-scores (Spearman's correlation coefficient: −0.85, *p* < 0.001). For further details, see Salvo et al. [10].

2.3. Quantitative Skin Colour Measurements

Quantitative measurements of skin colour were performed using a NCS (Natural Colour System) Colour Scan 2.0 on the inside of the upper arm on 507 individuals in the Norwegian biobank population. The output metrics consisted of L^* a^* b^* (L^* = lightness, a^* = red, b^* = yellow). The L^* value measures skin lightness, ranging from 0 to 100, where 0 is the darkest and 100 is the lightest. For a consensus measurement, at least three measurements were made, avoiding pigmentation spots and hair.

2.4. Probe Design and Sequencing the OCA2-HERC2 Region

The software SureDesign (Agilent Technologies, Santa Clara, CA, USA) was used to design capture-probes for a ~500 kbp region on chromosome 15 (GRCh38, chr15: 27,754,870–28,254,863) for SureSelectXT HS2 Target Enrichment System (Agilent Technologies, Santa Clara, CA, USA). The design included 15,627 probes targeting 427,954 bp. The library preparation was carried out according to the SureSelextXT HS2 DNA System protocol, version D0. All samples were sequenced on an Illumina MiSeq (Illumina, San Diego, CA, USA) according to the manufacturer's instructions with paired-end sequencing (2 × 150 bp) using the MiSeq Reagent Kit V2 (300 cycles).

2.5. Analysis of Sequencing Data

The sequencing output was automatically converted to FASTQ files with the MiSeq Reporter Software. Agilent's molecular barcode (MBC) sequences were extracted using the Agilent Genomics NextGen Toolkit (AGeNT), and the FASTQ files were trimmed using AdapterRemoval version 2.1.3 [17,18] with a minimum read length of 30 bp and Phred quality score of Q = 30. The files were subsequently aligned to the human reference sequence assembly GRCh38/hg38 with the Burrows–Wheeler Aligner, BWA-MEM algorithm [19,20]. Sequence alignment map (SAM) files were converted into binary alignment map (BAM) files using SAMtools [21]. The Genome Analysis Toolkit (GATK) with HaplotypeCaller version 4.0.0.0 [22] was used to create Variant Call Format (VCF) files. Variants located in the regions of interest were extracted using BEDTools version 2.22.1 [23]. Genotypes were accepted if the read depth was ≥10 and the heterozygote balance (Hb = read depth of allele/read depth of nucleotide position) was 0.20 < Hb < 0.80.

The *fisher.test* and *Kruskal.test* commands in R: A Language and Environment for Statistical Computing version 4.2.1 (R Foundation for Statistical Computing, Vienna, Austria) [24] were used to perform Fisher's exact test and Kruskal–Wallis test of the statistical association between genotype data, and eye colour categories and PIE-scores, respectively. Mann–Whitney tests for two independent samples and linear regression analysis were performed using the Real Statistics Resource Pack software (release 6.3; copyright (2013–2021) Charles Zaiontz, www.real-statistics.com, accessed on 16 January 2022). Hardy–Weinberg equilibrium (HWE) and pairwise r^2 values for linkage disequilibrium (LD) testing were calculated using Haploview 4.2 [25]. For predictions of regulatory elements, the positions of the candidate variants were overlapped with datasets from the SCREEN: Search Candidate cis-Regulatory Elements by ENCODE platform, Registry of cCREs V3 [26]. Haplotypes were estimated using PHASE version 2.1 (University of Washington, Seattle, WA, USA) [27,28], using default settings.

2.6. Variant Typing

Eight candidate variants for blue eye colour, rs551217952, rs543971307, rs191109490, rs78544415, rs74409036, rs62008729, rs72714116 and rs12913832, were typed in the remaining 446 individuals in the Norwegian biobank population (total *n* = 540) using the SNaPshot™ multiplex system (Thermo Fisher Scientific, Waltham, MA, USA). The SNPs rs543971307 and rs191109490 were in complete LD. Qiagen Multiplex PCR kit (Qiagen,

Hilden, Germany) was used to amplify DNA in one multiplex reaction in a final volume of 10 μL. The following PCR conditions were used: 95 °C for 15 min, 35 cycles of 94 °C for 30 s, 58 °C for 30 s and 72 °C for 30 s, and final extension at 72 °C for 10 min. A total of 5 μL amplified DNA was treated with 2 μL ExoSAP-ITTM PCR product clean-up reagent (Thermo Fisher Scientific, Waltham, MA, USA) at 37 °C for 60 min and 75 °C for 15 min. Single base extension (SBE) was performed with 1 μL purified PCR product, 1 μL MilliQ-water, 2 μL SNaPshot™ Multiplex Ready Reaction Mix (Thermo Fisher Scientific, Waltham, MA, USA) and 1 μL SBE primer mix (Table S2). The following cycle conditions were used: 30 cycles of 96 °C for 10 s, 55 °C for 5 s and 60 °C for 30 s. The SBE PCR products were then treated with 1 μL SAP (Thermo Fisher Scientific, Waltham, MA, USA) at 37 °C for 30 min and 75 °C for 15 min. Separation and detection of treated SBE products were carried out on a 3500xL Genetic Analyzer (Thermo Fisher Scientific, Waltham, MA, USA) using FragmentAnalysis with POP-4™ polymer, a 36 cm capillary and Dye Set E5. The analysis was performed with 1 μL SAP-treated SBE products, 20 μL Hi-Di formamide and GeneScan™-120 LIZ® Size Standard (200:1). The results were analysed with GeneMapper® ID-X v.1.5 (Thermo Fisher Scientific, Waltham, MA, USA), with a minimum peak height threshold of 50 RFU. In total, 425 individuals were successfully typed for all variants and were, together with the 94 sequenced individuals, used for population-specific analysis (total $n = 519$).

3. Results

3.1. Sequencing of the HERC2-OCA2 Region and Discovery of Candidate Blue Eye Colour Variants

Approximately 500 kbp of the *HERC2-OCA2* region was sequenced in a study cohort of 94 individuals (43 in study group and 51 in control group). Across the target region, the median read depth ranged from 116 to 498 reads. In the captured 427,954 bp, a total of 2571 variants were identified after excluding 16 variant positions with less than 10 reads in more than 5% of the samples. Of the 2571 variants, 146 showed significant deviations from HWE (*p*-value < 0.05), and many variants were in strong or complete LD (pairwise $r^2 \geq 0.8$). A total of 419 independent variants were identified using the Tagger function in Haploview. Among the rs12913832 AA individuals, 24 variants were statistically significantly associated with both the PIE-score and eye colour categories (Kruskal–Wallis test and Fisher's exact test, raw *p*-values < 0.05; Table S3). Among the rs12913832 AG individuals, 47 variants were statistically significantly associated with eye colour using both tests (Table S3). None of the variants were statistically associated with eye colour after Bonferroni correction for multiple testing (*p*-value < 0.00012 with m = 419 independent loci).

Six missense *OCA2* variants were observed in the study cohort (rs1800414, rs74653330, rs121918166, rs1800407, rs1800401 and rs33929465). The SNPs rs74653330:T and rs121918166:T were observed in 24 individuals (56%) from the study group, whereas they were only observed in five individuals (9.8%) from the control group. These variants were statistically significantly associated with both quantitative and categorical eye colour (Kruskal–Wallis/Mann–Whitney test and Fisher's exact test, raw *p*-values < 0.05). Thus, rs74653330:T and rs121918166:T could potentially explain blue eye colour (Figure S1). These two variants were previously typed in the same biobank population [16]. The other four missense variants (rs1800414, rs1800407, rs1800401 and rs33929465) were not associated with blue eye colour.

When searching among the individuals who did not carry the two missense variants, rs74653330:T and rs121918166:T (*n* = 65), we selected the six *OCA2-HERC2* candidate variants rs74409036, rs78544415, rs72714116, rs191109490, rs551217952 and rs62008729 as the most promising candidates to explain blue eye colour (Table 2). These variants had a significant association with the PIE-score (Mann–Whitney test, raw *p*-value < 0.05), and the variant (minor) alleles were primarily observed in the study group and not in the control group (Figure 1 and Table 2). For population-specific association analysis, these candidate variants were typed in the remaining samples of the Norwegian biobank population.

Table 2. The six *OCA2-HERC2* candidate blue eye colour variants.

Candidate Variant	Chromosomal Position (GRCh38)	Frequency Brown (*n* = 46) [1]	Frequency Blue (*n* = 19) [1]	Variants in Strong LD [2] ($r^2 \geq 0.8$)
rs74409036	27,818,606	0.03	0.11	rs78114576
rs78544415	27,842,634	0.00	0.05	rs79071800, rs28565430, rs28423991, rs74474678 and rs80177321
rs72714116	28,083,061	0.00	0.08	rs72714116
rs191109490	28,120,403	0.00	0.05	rs543971307 and rs145048438
rs551217952	28,139,387	0.01	0.05	rs182498200 and rs184120129
rs62008729	28,173,140	0.01	0.08	rs62008729

[1] Frequency of variant allele in 65 rs12913832 AA and AG individuals that did not have the missense variants rs74653330:T and rs121918166:T; [2] LD = Linkage disequilibrium.
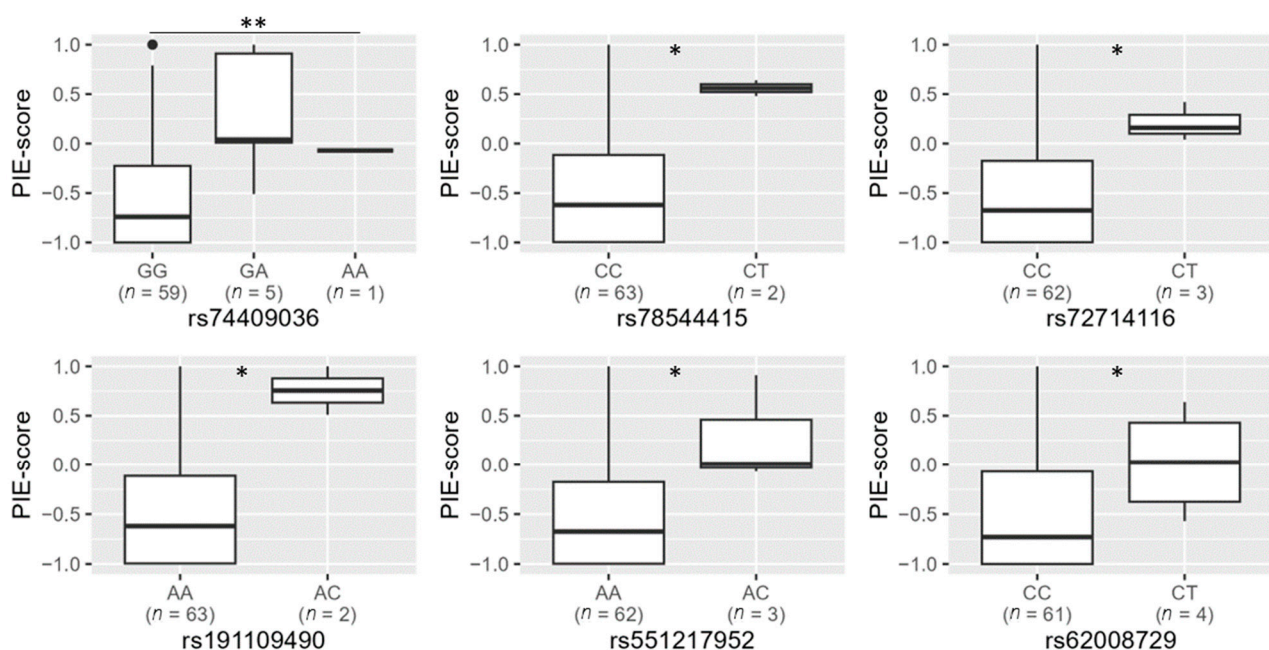
Figure 1. Genotypes and PIE-scores for the candidate blue eye colour variants rs74409036, rs78544415, rs72714116, rs191109490, rs551217952 and rs62008729 in 65 rs12913832 AA and AG individuals that did not have the missense variants rs74653330:T and rs121918166:T. Statistical significance (Mann–Whitney test): * $p < 0.05$, ** $p < 0.01$.

3.2. Candidate Blue Eye Colour Variants and Their Association with Eye Colour in the Norwegian Population

The six candidate variants were all intronic, either in *OCA2* or *HERC2* (Figure S2). Only one variant, rs191109490, was predicted by SCREEN [26] to be in a candidate cis-regulatory element (cCRE) in foreskin melanocytes (EH38E1749549). Interestingly, the locus is located in *HERC2*, only 69bp from rs12913832 ($r^2 = 0$). Notably, rs191109490 was in complete LD with rs543971307 ($r^2 = 1$), which was also found to be in the cCRE in *HERC2*, close to rs12913832.

When typed in the Norwegian biobank population (*n* = 519), the six candidate variants had low frequencies (0.002–0.082) and were mainly observed in blue eyed individuals (Table 3 and Figure S3). Of the six variants, the SNP rs62008729:T showed the highest frequency of 0.082 (Table 1). However, five of eleven (45%) rs12913832 AG individuals carrying this variant had brown eyes (Figure S3). Therefore, this SNP was excluded from further analysis.

Table 3. The frequencies of the six candidate variant alleles in the Norwegian biobank population.

rs ID	Reference Allele	Variant Allele	Variant Allele Frequency	
			Frequency Norway (*n* = 519)	Frequency Europe (GnomAD)
rs74409036	G	A	0.031	0.052
rs78544415	C	T	0.026	0.035
rs72714116	C	T	0.004	0.020
rs191109490	A	C	0.002	0.002
rs551217952	A	C	0.003	0.003
rs62008729	C	T	0.082	0.024

For statistical association analysis with eye colour variation in the Norwegian biobank population, haplotypes were estimated based on the genotypes of the five candidate variants, rs74409036:A, rs78544415:T, rs72714116:T, rs191109490:C and rs551217952:C, and with the missense variants, rs74653330:T and rs121918166:T. In total, 11 haplotypes were estimated (Table 4). The best estimated haplotype pairs (by PHASE) and PIE-scores for all 519 individuals are shown in Figure 2. Despite some of the haplotypes being observed in only a few individuals, the total correlation of the haplotypes to the PIE-score was 0.8 (linear regression, adjusted R^2 = 0.80). All haplotype pairs, except AA, AG, AA3 and AG1, had a median PIE-score higher than −0.3, indicating blue eye colour (Figure 2A). The median PIE-scores of the haplotype pair AA and AG were −1 (Q1 = −1 and Q3 = −0.95) and −0.92 (Q1 = −0.97 and Q3 = −0.74), respectively. This indicates that most rs12913832 AA and AG individuals with blue eye colour did not carry one of these two haplotype pairs. The haplotype AG1 had the largest variation, with PIE-score ranging from −0.94 (brown) to 1 (blue), but this haplotype was only observed in five individuals. The haplotype A5G had a smaller variation (PIE-score ranging from −1 to 0.42), but the median PIE-score was 0.10. All, except one brown-eyed individual carrying this haplotype, had blue eyes with a pupillary ring of brown, resulting in perception of green elements. Interestingly, AA6 and A6G, with the rs191109490:C variant that was predicted to be in a cCRE, both showed high PIE-scores of 0.51 (blue) and 1 (blue), respectively. All rs12913832 GG haplotype pairs had median PIE-scores of 0.98 to 1 (blue) (Figure 2B).

Table 4. *HERC2-OCA2* haplotypes estimated by PHASE.

Haplotypes [a,c]	rs74409036:A	rs78544415:T	rs74653330:T	rs121918166:T	rs72714116:T	rs191109490:C	rs551217952:C	Frequency NOR [b] (*n* = 519)
A	-	-	-	-	-	-	-	0.135
G	-	-	-	-	-	-	-	0.772
G1	A	-	-	-	-	-	-	0.028
G2	-	T	-	-	-	-	-	0.025
G3	-	T	T	-	-	-	-	0.001
G4	-	-	-	T	-	-	-	0.001
A1	A	-	-	-	-	-	C	0.003
A3	-	-	T	-	-	-	-	0.024
A4	-	-	-	T	-	-	-	0.006
A5	-	-	-	-	T	-	-	0.004
A6	-	-	-	-	-	C	-	0.002

[a] Haplotype A and G indicates the A-allele and G-allele in rs12913832, respectively; [b] NOR = Norwegian biobank population; [c] Reference allele.
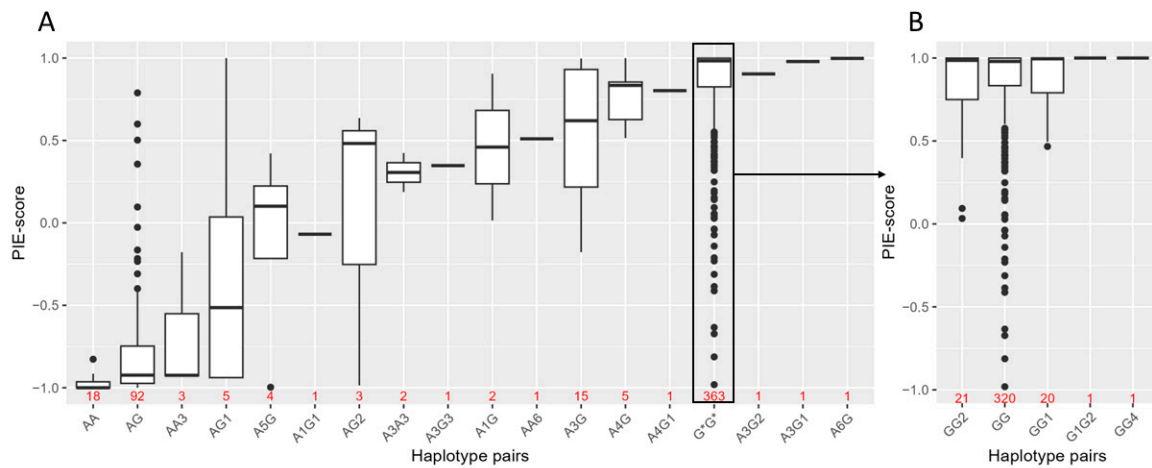
Figure 2. Estimated haplotype pairs by PHASE and PIE-scores in the Norwegian biobank population (*n* = 519) comprised of the haplotypes in Table 4. (**A**) Shows rs12913832 AA and AG haplotype pairs. All rs12913832 GG haplotype pairs are grouped together as G*G* and are shown in more detail in (**B**) (*n* = 363). G* = rs12913832:G genotype regardless of haplotype. The number of individuals carrying the haplotype pair is indicated in red.

3.3. HERC2-OCA2 Haplotypes and Their Association with Skin Colour in the Norwegian Population

Because SNPs in *HERC2-OCA2* are also associated with skin pigmentation, the haplotypes in Table 4 were assessed for association with skin shade, from dark to light, in the Norwegian biobank population (Figure 3). The lightness values (*L**) of 507 individuals were measured and used as a metric for skin colour. The *L** value in the population varied from 46.92 to 77.58, with a median of 68.51. No overall significant associations were observed between the haplotypes and *L** values. However, a trend of lighter skin colour was observed in individuals with rs74653330:T on a background of rs12913832:AA and AG genotypes. In total, 21 (91%) of 23 individuals with rs74653330:T (Haplotypes A3 and G3) had *L** values higher or equal to the median skin colour in the population (*L** = 68.51), indicating light skin colour. Furthermore, individuals with A3G had significantly lighter skin colour than the rest of the population (raw *p*-value < 0.02).
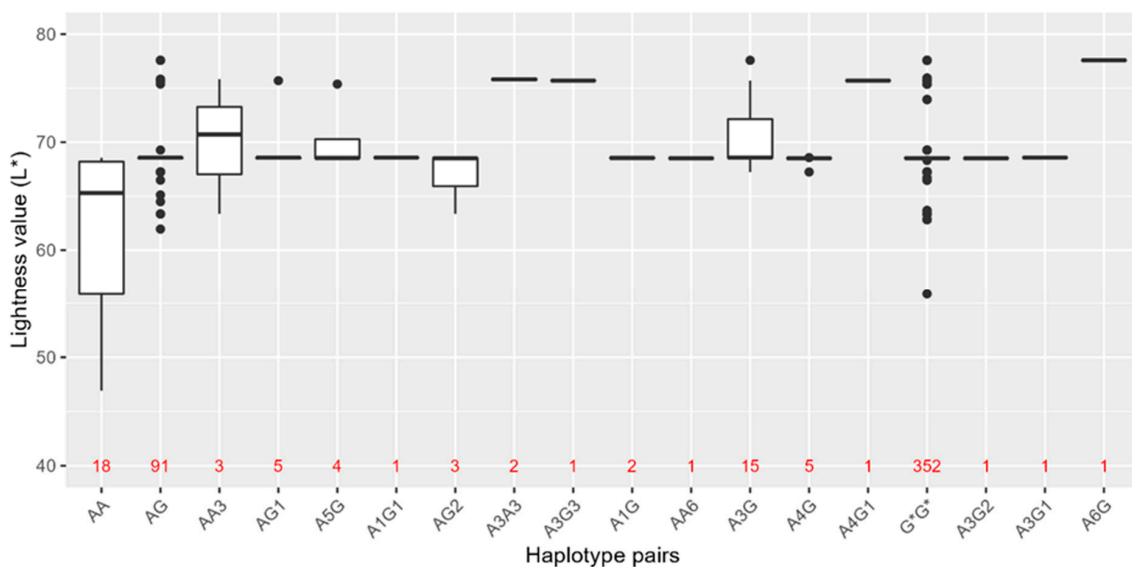
Figure 3. Estimated haplotype pairs by PHASE and lightness value (*L**) of skin colour in the Norwegian biobank population (*n* = 507), comprised of the rs12913832 AA and AG haplotype pairs (Table 4). All rs12913832 GG haplotype pairs are grouped together as G*G*. G* = rs12913832:G genotype regardless of haplotype. The number of individuals carrying each haplotype pair is indicated in red.

4. Discussion

In the present study, we sequenced a ~500 kbp region of *OCA2-HERC2* to search for candidate blue eye colour variants in individuals carrying the rs12913832:AA or AG genotype. In the Norwegian biobank population, 43 individuals (study group) did not have the expected brown eye colour based on rs12913832 [10]. Because of the strong selection pressure on *OCA2-HERC2* in blue-eyed Europeans [5], it was hypothesised that other variants in this region may have an effect on OCA2 function, either by regulating the protein expression or by altering the protein.

Assessment of the sequencing quality showed that the captured region was successfully sequenced with good quality (median read depth between samples ranged from 116 to 498 reads across the target regions). Only 16 variant positions had less than 10 reads in more than 5% of the samples and were excluded. Four of these variants were in *OCA2*, and one of them overlapped with a deletion that was previously identified in 35% (15/43) of the study samples, which could potentially explain the low read depth [29].

In addition, to confirm the association of the missense variants rs74653330 and rs121918166 with eye colour, we identified five new candidate variants (rs74409036:A, rs78544415:T, rs72714116:T, rs191109490:C and rs551217952:C) that may potentially explain blue eye colour in individuals with the rs12913832:AA and AG genotype. Independently, they were all associated with quantitative eye colour (PIE-score) in the Norwegian biobank population, and 37 (86%) of the 43 blue-eyed individuals in the study group had at least one of the seven variants (including rs74653330:T and rs121918166:T). To our knowledge, this is the first time that the variants rs74409036, rs78544415, rs72714116, rs191109490 and rs551217952 are reported to be associated with human eye colour variation. These variants have very low frequencies and are mainly observed in Europeans, and some of them also in Americans (https://gnomad.broadinstitute.org/, accessed on 8 December 2022). The SNP rs74653330:T is also moderately frequent in East Asia, where it is associated with lighter skin colour [15].

The candidate variants rs74409036, rs78544415, rs72714116, rs551217952 and rs191109490 are all intronic. With the currently available data, rs191109490 was the only variant found by SCREEN to be in a cCRE in melanocytes [26]. Interestingly, rs191109490 is contained in a distal enhancer-like signature in *HERC2* in foreskin melanocytes, indicating a regulatory effect on *OCA2* expression and thereby, pigmentation. However, the specific role of rs191109490 in the cCRE is yet to be identified. Despite rs191109490:C only being observed in two individuals (haplotype pairs: AA6 and A6G), these had higher PIE-scores (perceived as blue) than individuals with the AA and AG haplotype pairs. Notably, one individual carried the rs12913832:AA genotype and was incorrectly predicted to have brown eyes with a high probability (*p*-value = 0.96) by the IrisPlex tool (Table S1). Additionally, the individual with A6G showed lighter skin colour than most GG haplotypes, supporting the hypothesis that rs191109490:C influences *OCA2* expression.

Individuals with rs72714116:T had the same haplotype pair, A5G, and four of the five rs72714116:T individuals had PIE-scores close to the mid-scale (0.05–0.4). These individuals had intermediate-blue eye colour that might be perceived as green or hazel. As discussed in many studies, eye colour is on a continuous scale from dark brown to light blue, and perception of colour varies from person to person (e.g., [10,30,31]). The most popular prediction tool for eye colour in forensic genetics, the IrisPlex, uses three eye colour categories, blue, intermediate and brown [6,13,14]. However, prediction of intermediate eye colour has proved to be difficult because of the lack of markers associated with the intermediate eye colour and because of the individual perception of eye colour [6,10,30,31]. Thus, several authors have suggested using a two-category system (blue and brown) [16,32,33] and others a quantitative system [9,34]. Our results indicate that the variant rs72714116:T may be an example of a marker for non-blue/non-brown eye colours in the Norwegian biobank population. However, this was observed in only four individuals, and the findings needs to be replicated in more samples.

Individuals estimated with the rs74409036:A rs12913832:G haplotype (AG1) had large variations in PIE-scores, and therefore it may not be easy to predict the eye colour of AG1 individuals. However, when rs74409036:A was observed together with other variants in the haplotype pairs A1G, A3G1 and A4G1, the individuals' PIE-scores were significantly higher (perceived as blue) than AG1 individuals. Individuals with A3G1 and A4G1 haplotypes also carried the missense mutations rs74653330:T and rs121918166:T. These two variants are associated with blue eye colour in Scandinavians [8]. We have previously demonstrated that inclusion of these variants in the EC11 prediction model led to more correct predictions in the Norwegian biobank population than with the IrisPlex model [16], which supports their importance for prediction of eye colour. Interestingly, three blue-eyed individuals in the study group had the genotype rs12913832:AA, but were predicted to have brown eye colour by the IrisPlex model with high *p*-values (0.96, 0.97 and 0.98). In addition to the one individual with rs191109490:C (already mentioned), two had the rs74653330:T variant, potentially explaining blue eye colour in all these rs12913832:AA individuals.

In the present study, we also observed lighter skin colour in individuals with the rs74653330:T rs12913832:A haplotype (haplotype pairs: AA3, A3A3, A3G3 and A3G). This is in line with previous findings that this variant is associated with skin pigmentation variation in East Asians and Scandinavians [8,15]. Andersen et al. [8] observed lighter skin colour in individuals with the rs121918166:T rs12913832:A haplotype compared to rs12913832:GG individuals. However, we did not observe this trend in the Norwegian biobank population.

Here, we demonstrate high correlation between variants in the *HERC2-OCA2* region and eye colour in the Norwegian biobank population. Their independent effect on human eye colour variation may be smaller than the *HERC2* SNP rs12913832. However, including them in prediction models improves the precision for prediction of blue-eyed individuals with rs12913832:AA and AG genotypes. It would be interesting to assess the associations in similar populations, e.g., other Scandinavian or Northern European populations. While the *HERC2-OCA2* region explains most of the blue and brown eye colour variability in Europeans, SNPs in other pigmentation genes, such as *TYR, TYRP1, SLC24A4, SLC45A2, ASIP* and *IRF4*, are also found to be associated with eye colour [35–39], albeit with varying population-specific effects [32,40]. We previously assessed the association between the IrisPlex SNPs (rs12913832 in *HERC2*, rs1800407 in *OCA2*, rs12896399 in *SLC24A4*, rs16891982 in *SLC45A2*, rs1393350 in *TYR* and rs12203592 in *IRF4*) and PIE-score in the Norwegian biobank population, and only observed rs16891982 in *SLC45A2* to be significantly associated with blue eye colour in rs12913832:AA and AG individuals [10]. The protein SLC45A2 might have a similar role in melanosome maturation as OCA2 [41]. Thus, *SLC45A2* may also be a target of interest to search for new blue eye colour variants. A recent GWAS identified 50 novel loci associated with eye colour, including pigmentation genes and genes involved in iris morphology and structure [42]. This demonstrates that human eye colour is a genetically highly complex trait, and the molecular mechanisms behind eye colour formation are yet to be fully understood. In the current study, we identify intronic variants to be associated with blue eye colour. Although the functional role of these variants in eye colour formation is still unknown, we suggest including them in future prediction models.

Supplementary Materials: The following supporting information can be downloaded at: https://www.mdpi.com/article/10.3390/genes14030698/s1, Figure S1: PIE-scores and genotypes of rs121918166 and rs74653330 in the study cohort (*n* = 94); Figure S2: Chromosomal position of the six blue eye colour candidate variants (red), the two missense variants rs74653330 and rs121918166, and the main eye colour predictor SNP rs12913832. Pos = chromosomal position (GRCh38); Figure S3: Genotypes and PIE-scores for the candidate blue eye colour variants typed in rs12913832 AA and AG individuals (*n* = 165) from the Norwegian biobank population; Table S1: Genotype and eye colour information of the study population; Table S2: Information on primers used for SBE typing of candidate variants; Table S3: Variants that were statistically significantly associated with both PIE-score and eye colour categories (Kruskal–Wallis test and Fisher's exact test, raw *p*-values ≤0.05) in rs12913832 AA and AG individuals.

References

1. Sturm, R.A.; Larsson, M. Genetics of human iris colour and patterns. *Pigment. Cell Melanoma Res.* **2009**, *22*, 544–562. [CrossRef] [PubMed]
2. Liu, F.; Wen, B.; Kayser, M. Colorful DNA polymorphisms in humans. *Semin. Cell Dev. Biol.* **2013**, *24*, 562–575. [CrossRef] [PubMed]
3. Visser, M.; Kayser, M.; Palstra, R.-J. HERC2 rs12913832 modulates human pigmentation by attenuating chromatin-loop formation between a long-range enhancer and the OCA2 promoter. *Genome Res.* **2012**, *22*, 446–455. [CrossRef]
4. Sturm, R.A.; Duffy, D.L.; Zhao, Z.Z.; Leite, F.P.; Stark, M.S.; Hayward, N.K.; Martin, N.G.; Montgomery, G.W. A Single SNP in an Evolutionary Conserved Region within Intron 86 of the HERC2 Gene Determines Human Blue-Brown Eye Color. *Am. J. Hum. Genet.* **2008**, *82*, 424–431. [CrossRef] [PubMed]
5. Donnelly, M.P.; Paschou, P.; Grigorenko, E.; Gurwitz, D.; Barta, C.; Lu, R.-B.; Zhukova, O.V.; Kim, J.-J.; Siniscalco, M.; New, M.; et al. A global view of the OCA2-HERC2 region and pigmentation. *Hum. Genet.* **2011**, *131*, 683–696. [CrossRef] [PubMed]
6. Walsh, S.; Wollstein, A.; Liu, F.; Chakravarthy, U.; Rahu, M.; Seland, J.H.; Soubrane, G.; Tomazzoli, L.; Topouzis, F.; Vingerling, J.R.; et al. DNA-based eye colour prediction across Europe with the IrisPlex system. *Forensic Sci. Int. Genet.* **2012**, *6*, 330–340. [CrossRef]
7. Eiberg, H.; Troelsen, J.; Nielsen, M.; Mikkelsen, A.; Mengel-From, J.; Kjaer, K.W.; Hansen, L. Blue eye color in humans may be caused by a perfectly associated founder mutation in a regulatory element located within the HERC2 gene inhibiting OCA2 expression. *Hum. Genet.* **2008**, *123*, 177–187. [CrossRef] [PubMed]
8. Andersen, J.D.; Pietroni, C.; Johansen, P.; Andersen, M.M.; Pereira, V.; Børsting, C.; Morling, N. Importance of nonsynonymous *OCA 2* variants in human eye color prediction. *Mol. Genet. Genom. Med.* **2016**, *4*, 420–430. [CrossRef]
9. Andersen, J.D.; Johansen, P.; Harder, S.; Christoffersen, S.R.; Delgado, M.C.; Henriksen, S.T.; Nielsen, M.M.; Sørensen, E.; Ullum, H.; Hansen, T.; et al. Genetic analyses of the human eye colours using a novel objective method for eye colour classification. *Forensic Sci. Int. Genet.* **2013**, *7*, 508–515. [CrossRef]
10. Salvo, N.M.; Janssen, K.; Kirsebom, M.K.; Meyer, O.S.; Berg, T.; Olsen, G.-H. Predicting eye and hair colour in a Norwegian population using Verogen's ForenSeq™ DNA signature prep kit. *Forensic Sci. Int. Genet.* **2021**, *56*, 102620. [CrossRef]
11. Liu, F.; van Duijn, K.; Vingerling, J.R.; Hofman, A.; Uitterlinden, A.G.; Janssens, A.C.J.; Kayser, M. Eye color and the prediction of complex phenotypes from genotypes. *Curr. Biol.* **2009**, *19*, R192–R193. [CrossRef] [PubMed]
12. Duffy, D.; Montgomery, G.; Chen, W.; Zhao, Z.Z.; Le, L.; James, M.R.; Hayward, N.K.; Martin, N.; Sturm, R.A. A Three–Single-Nucleotide Polymorphism Haplotype in Intron 1 of OCA2 Explains Most Human Eye-Color Variation. *Am. J. Hum. Genet.* **2007**, *80*, 241–252. [CrossRef] [PubMed]
13. Walsh, S.; Liu, F.; Ballantyne, K.N.; van Oven, M.; Lao, O.; Kayser, M. IrisPlex: A sensitive DNA tool for accurate prediction of blue and brown eye colour in the absence of ancestry information. *Forensic Sci. Int. Genet.* **2011**, *5*, 170–180. [CrossRef] [PubMed]
14. Walsh, S.; Liu, F.; Wollstein, A.; Kovatsi, L.; Ralf, A.; Kosiniak-Kamysz, A.; Branicki, W.; Kayser, M. The HIrisPlex system for simultaneous prediction of hair and eye colour from DNA. *Forensic Sci. Int. Genet.* **2012**, *7*, 98–115. [CrossRef]
15. Eaton, K.; Edwards, M.; Krithika, S.; Cook, G.; Norton, H.; Parra, E.J. Association study confirms the role of two *OCA2* polymorphisms in normal skin pigmentation variation in East Asian populations. *Am. J. Hum. Biol.* **2015**, *27*, 520–525. [CrossRef]
16. Meyer, O.; Salvo, N.; Kjærbye, A.; Kjersem, M.; Andersen, M.; Sørensen, E.; Ullum, H.; Janssen, K.; Morling, N.; Børsting, C.; et al. Prediction of Eye Colour in Scandinavians Using the EyeColour 11 (EC11) SNP Set. *Genes* **2021**, *12*, 821. [CrossRef]

17. Schubert, M.; Lindgreen, S.; Orlando, L. AdapterRemoval v2: Rapid adapter trimming, identification, and read merging. *BMC Res. Notes* **2016**, *9*, 88. [CrossRef]
18. Lindgreen, S. AdapterRemoval: Easy cleaning of next-generation sequencing reads. *BMC Res. Notes* **2012**, *5*, 337. [CrossRef]
19. Li, H.; Durbin, R. Fast and accurate long-read alignment with Burrows–Wheeler transform. *Bioinformatics* **2010**, *26*, 589–595. [CrossRef] [PubMed]
20. Li, H. Aligning Sequence Reads, Clone Sequences and Assembly Contigs with BWA-MEM. 2013. Available online: http://github.com/lh3/bwa (accessed on 31 January 2022).
21. Li, H.; Durbin, R. Fast and accurate short read alignment with Burrows–Wheeler transform. *Bioinformatics* **2009**, *25*, 1754–1760. [CrossRef]
22. McKenna, A.; Hanna, M.; Banks, E.; Sivachenko, A.; Cibulskis, K.; Kernytsky, A.; Garimella, K.; Altshuler, D.; Gabriel, S.; Daly, M.; et al. The Genome Analysis Toolkit: A MapReduce framework for analyzing next-generation DNA sequencing data. *Genome Res.* **2010**, *20*, 1297–1303. [CrossRef] [PubMed]
23. Quinlan, A.R.; Hall, I.M. BEDTools: A flexible suite of utilities for comparing genomic features. *Bioinformatics* **2010**, *26*, 841–842. [CrossRef] [PubMed]
24. R Core Team. R: A Language and Environment for Statistical Computing. 2019. Available online: https://www.r-project.org/ (accessed on 10 March 2023).
25. Barrett, J.C.; Fry, B.; Maller, J.; Daly, M.J. Haploview: Analysis and visualization of LD and haplotype maps. *Bioinformatics* **2005**, *21*, 263–265. [CrossRef] [PubMed]
26. The ENCODE Project Consortium; Moore, J.E.; Purcaro, M.J.; Pratt, H.E.; Epstein, C.B.; Shoresh, N.; Adrian, J.; Kawli, T.; Davis, C.A.; Dobin, A.; et al. Expanded encyclopaedias of DNA elements in the human and mouse genomes. *Nature* **2020**, *583*, 699–710. [CrossRef] [PubMed]
27. Stephens, M.; Smith, N.J.; Donnelly, P. A New Statistical Method for Haplotype Reconstruction from Population Data. *Am. J. Hum. Genet.* **2001**, *68*, 978–989. [CrossRef]
28. Stephens, M.; Scheet, P. Accounting for Decay of Linkage Disequilibrium in Haplotype Inference and Missing-Data Imputation. *Am. J. Hum. Genet.* **2005**, *76*, 449–462. [CrossRef] [PubMed]
29. Salvo, N.M.; Janssen, K.; Olsen, G.-H.; Berg, T.; Andersen, J.D. Association between copy number variations in the OCA2-HERC2 locus and human eye colour. *Forensic Sci. Int. Genet. Suppl. Ser.* **2022**, *8*, 82–84. [CrossRef]
30. Meyer, O.S.; Børsting, C.; Andersen, J.D. Perception of blue and brown eye colours for forensic DNA phenotyping. *Forensic Sci. Int. Genet. Suppl. Ser.* **2019**, *7*, 476–477. [CrossRef]
31. Ruiz, Y.; Phillips, C.; Gomez-Tato, A.; Alvarez-Dios, J.; de Cal, M.C.; Cruz, R.; Maroñas, O.; Söchtig, J.; Fondevila, M.; Rodriguez-Cid, M.; et al. Further development of forensic eye color predictive tests. *Forensic Sci. Int. Genet.* **2012**, *7*, 28–40. [CrossRef]
32. Pietroni, C.; Andersen, J.D.; Johansen, P.; Andersen, M.M.; Harder, S.; Paulsen, R.R.; Børsting, C.; Morling, N. The effect of gender on eye colour variation in European populations and an evaluation of the IrisPlex prediction model. *Forensic Sci. Int. Genet.* **2014**, *11*, 1–6. [CrossRef]
33. Hart, K.L.; Kimura, S.L.; Mushailov, V.; Budimlija, Z.M.; Prinz, M.; Wurmbach, E. Improved eye- and skin-color prediction based on 8 SNPs. *Croat. Med. J.* **2013**, *54*, 248–256. [CrossRef] [PubMed]
34. Paparazzo, E.; Gozalishvili, A.; Lagani, V.; Geracitano, S.; Bauleo, A.; Falcone, E.; Passarino, G.; Montesanto, A. A new approach to broaden the range of eye colour identifiable by IrisPlex in DNA phenotyping. *Sci. Rep.* **2022**, *12*, 12803. [CrossRef] [PubMed]
35. Sulem, P.; Gudbjartsson, D.; Stacey, S.N.; Helgason, A.; Rafnar, T.; Magnusson, K.P.; Manolescu, A.; Karason, A.; Palsson, A.; Thorleifsson, G.; et al. Genetic determinants of hair, eye and skin pigmentation in Europeans. *Nat. Genet.* **2007**, *39*, 1443–1452. [CrossRef] [PubMed]
36. Han, J.; Kraft, P.; Nan, H.; Guo, Q.; Chen, C.; Qureshi, A.; Hankinson, S.E.; Hu, F.B.; Duffy, D.; Zhao, Z.Z.; et al. A Genome-Wide Association Study Identifies Novel Alleles Associated with Hair Color and Skin Pigmentation. *PLoS Genet.* **2008**, *4*, e1000074. [CrossRef]
37. Sulem, P.; Gudbjartsson, D.F.; Stacey, S.N.; Helgason, A.; Rafnar, T.; Jakobsdottir, M.; Steinberg, S.; Gudjonsson, S.A.; Palsson, A.; Thorleifsson, G.; et al. Two newly identified genetic determinants of pigmentation in Europeans. *Nat. Genet.* **2008**, *40*, 835–837. [CrossRef] [PubMed]
38. Kanetsky, P.A.; Swoyer, J.; Panossian, S.; Holmes, R.; Guerry, D.; Rebbeck, T.R. A Polymorphism in the Agouti Signaling Protein Gene Is Associated with Human Pigmentation. *Am. J. Hum. Genet.* **2002**, *70*, 770–775. [CrossRef]
39. Frudakis, T.; Thomas, M.; Gaskin, Z.; Venkateswarlu, K.; Chandra, K.S.; Ginjupalli, S.; Gunturi, S.; Natrajan, S.; Ponnuswamy, V.K.; Ponnuswamy, K.N. Sequences Associated with Human Iris Pigmentation. *Genetics* **2003**, *165*, 2071–2083. [CrossRef]
40. Pośpiech, E.; Karłowska-Pik, J.; Ziemkiewicz, B.; Kukla, M.; Skowron, M.; Wojas-Pelc, A.; Branicki, W. Further evidence for population specific differences in the effect of DNA markers and gender on eye colour prediction in forensics. *Int. J. Leg. Med.* **2016**, *130*, 923–934. [CrossRef]

41. Le, L.; Escobar, I.E.; Ho, T.; Lefkovith, A.J.; Latteri, E.; Haltaufderhyde, K.D.; Dennis, M.K.; Plowright, L.; Sviderskaya, E.V.; Bennett, D.C.; et al. SLC45A2 protein stability and regulation of melanosome pH determine melanocyte pigmentation. *Mol. Biol. Cell* **2020**, *31*, 2687–2702. [CrossRef]

42. Simcoe, M.; Valdes, A.; Liu, F.; Furlotte, N.A.; Evans, D.M.; Hemani, G.; Ring, S.M.; Smith, G.D.; Duffy, D.L.; Zhu, G.; et al. Genome-wide association study in almost 195,000 individuals identifies 50 previously unidentified genetic loci for eye color. *Sci. Adv.* **2021**, *7*, eabd1239. [CrossRef]

Paper 6

Association between copy number variations in the *OCA2-HERC2* locus and human eye colour

Nina Mjølsnes Salvo [a,*], Kirstin Janssen [a], Gunn-Hege Olsen [a], Thomas Berg [a], Jeppe Dyrberg Andersen [b]

[a] *Centre for Forensic Genetics, Department of Medical Biology, Faculty of Health Sciences, UiT – The Arctic University of Norway, Norway*
[b] *Section of Forensic Genetics, Department of Forensic Medicine, Faculty of Health and Medical Sciences, University of Copenhagen, Denmark*

ARTICLE INFO

ABSTRACT

Human eye colour variation is strongly associated with single nucleotide polymorphisms (SNPs) in the *OCA2-HERC2* locus, especially rs12913832 that is found in an enhancer element of *OCA2*. In a previous study we found that 43 out of 166 individuals in a Norwegian population with the brown eye colour genotype *HERC2* rs12913832:AA or AG, did not have the expected brown eye colour. To investigate if duplications or deletions in the *OCA2-HERC2* locus could explain the blue eye colour in these individuals, we analysed massively parallel sequencing (MPS) data for copy number variations (CNVs) in the *OCA2-HERC2* region. The ~500 kb long *OCA2-HERC2* locus was sequenced in 94 individuals with the rs12913832:AG and AA genotypes. Of these, 43 were observed to have blue eye colour and 51 were observed to have brown eye colour. CNVs were analysed using R and the R-package *panelcn.MOPS* - CNV detection tool for targeted NGS panel data. In rs12913832:AG individuals, CNVs in 32 regions were significantly associated with blue eye colour (Benjamini-Hochberg adjusted p-value ≤ 0.05). In rs12913832:AA individuals, CNVs in 14 regions were associated with blue eye colour using raw p-values ($p \leq 0.05$). The functional effects of these CNVs on *OCA2* expression are yet to be investigated. However, this study suggests that CNVs in the *OCA2-HERC2* locus might explain why some of the rs12913832:AG and AA individuals have unexpectedly blue eyes.

1. Introduction

Single nucleotide polymorphisms (SNPs) in the *OCA2-HERC2* locus have been extensively studied to explain human eye colour variations. The main predictor for eye colour is the SNP rs12913832 in *HERC2* [1]. This SNP is located ~21kb upstream to the promoter of the pigmentation gene *OCA2*, and acts as a distal *OCA2* enhancer [2]. Individuals with the genotypes rs12913832:AA and AG are predicted to have brown eye colour, whereas individuals with rs12913832:GG are predicted to have blue eye colour [3]. However, we found that 43/166 individuals in a Norwegian study population with the genotype rs12913832:AA or AG did not have brown eye colour [4].

The aim for this study was to analyse massively parallel sequencing (MPS) data for copy number variations (CNV) to investigate if duplications or deletions in the *OCA2-HERC2* locus could explain the unexpected blue eye colour in rs12913832:AA and AG individuals.

2. Materials and methods

The *OCA2-HERC2* locus (~500kb) was sequenced in 94 *HERC2* rs12913832:AG and AA individuals with SureSelectXT HS2 Target Enrichment System (Agilent Technologies) on an Illumina MiSeq with paired-end sequencing (2×150bp) using the MiSeq Reagent Kit V2 (300 cycles). Individuals were grouped into a control group with observed brown eye colour (21 AA and 30 AG individuals) and a case group with observed blue eye colour (three AA and 40 AG individuals). All samples were collected with fully informed consent and subsequently anonymised. The project was approved by the Faculty of Health Sciences, UiT - The Arctic University of Norway (reference number 2021/2034).

All samples were aligned to the GRCh38 human genome assembly using Burrows-Wheeler Aligner, BWA-MEM algorithm [5,6]. SAM files were converted into BAM files using SAMtools [7]. CNVs were detected in bins of 100 bp with 50 bp overlap, using R and the R-package *panelcn. MOPS* – CNV detection tool for targeted NGS panel data, with default

---

Table 1

CNVs detected in each CN class for selected regions that were significantly associated (adjusted p-value ≤ 0.05) with eye colour in rs12913832:AG individuals. The estimated CN classes are based on expected fold changes in RC: 0.025 (CN0), 0.57 (CN1), 1 (CN2), 1.46 (CN3) and 2 (CN4). All control samples (brown) were set to CN2.

Gene Intron[a]	Start	End	#Homozygous deletions (CN0)		#Heterozygous deletions (CN1)		#CN2		#Duplications (CN3)		#Amplifications (CN4)		Adjusted p-value value[b]	LowQual[c]
			Blue	Brown	Blue	Brown	Blue	Brown	Blue	Brown	Blue	Brown		
OCA2 23	27760520	27760619	0	0	13	0	25	30	2	0	0	0	5.0E-02	27/40
	27787649	27787748	0	0	13	0	26	30	1	0	0	0	5.0E-02	23/40
	27787699	27787798	0	0	13	0	25	30	2	0	0	0	4.8E-02	23/40
	27787799	27787898	1	0	11	0	25	30	3	0	0	0	4.9E-02	26/40
	27798376	27798475	0	0	18	0	22	30	0	0	0	0	4.9E-03	12/40
	27798426	27798525	0	0	14	0	24	30	2	0	0	0	2.8E-02	11/40
	27839862	27839961	0	0	18	0	20	30	2	0	0	0	2.1E-03	24/40
	27839912	27840011	0	0	18	0	18	30	4	0	0	0	9.2E-04	33/40
	27839962	27840061	0	0	16	0	23	30	1	0	0	0	1.2E-02	29/40
	27840012	27840111	0	0	17	0	21	30	2	0	0	0	4.4E-03	36/40
	27840062	27840161	0	0	15	0	23	30	2	0	0	0	1.5E-02	30/40
	27840162	27840261	0	0	14	0	26	30	0	0	0	0	4.6E-02	11/40
	27840212	27840311	0	0	15	0	25	30	0	0	0	0	2.9E-02	15/40
	27840312	27840411	0	0	15	0	25	30	0	0	0	0	2.7E-02	1/40
OCA2 21	27858553	27858652	0	0	16	0	24	30	0	0	0	0	1.9E-02	31/40
	27858653	27858752	0	0	15	0	24	30	1	0	0	0	2.1E-02	39/40
	27858703	27858802	0	0	14	0	25	30	1	0	0	0	3.3E-02	40/40
	27858753	27858852	0	0	14	0	26	30	0	0	0	0	4.5E-02	40/40
	27873420	27873519	0	0	14	0	26	30	0	0	0	0	4.3E-02	0/40
OCA2 19	27892556	27892655	0	0	13	0	26	30	1	0	0	0	4.8E-02	8/40
	27892606	27892705	0	0	13	0	26	30	1	0	0	0	4.7E-02	5/40
OCA2 14	27976556	27976655	0	0	11	0	25	30	4	0	0	0	4.7E-02	21/40
OCA2 2	28042549	28042670	0	0	3	0	23	30	12	0	2	0	2.6E-02	32/40
	28067438	28067559	0	0	18	0	21	30	1	0	0	0	4.6E-03	7/40
HERC2 82	28125690	28125789	0	0	14	0	26	30	0	0	0	0	4.1E-02	0/40

[a] Intron annotation from GRCh38, chr.15, NM_000275.3 (*OCA2*) and NP_000266.2 (*HERC2*), NCBI.

[b] Benjamini-Hochberg adjusted *p*-value.

[c] Number of test samples flagged for low quality by *panelcn.MOPS*.

settings [8]. The *panelcn.MOPS* assign all case samples to a CN class per region of interest based on fold changes in read counts (RC) relative to control samples: CN0 (homozygous deletion), CN1 (heterozygous deletion), CN2 (no change), CN3 (heterozygous duplication) and CN4 (homozygous duplication). All control samples were set to have two copies throughout the investigated region (CN2). Association with eye colour was tested using Fisher's exact test.

3. Results

When comparing CNV frequencies between the blue and brown eye colour category, CNVs in 32 regions were statistically significantly associated with blue eye colour in rs12913832:AG individuals (Benjamini-Hochberg adjusted *p*-value ≤ 0.05). A total of 25 of these regions were considered as candidate regions to explain eye colour variation as they were located in *OCA2* or close to the *OCA2* enhancer SNP, rs12913832 in *HERC2* (Table 1). Seven CNVs were in *HERC2,* ~100 kb upstream rs12913832. Notably, some regions in rs12913832:AG individuals, especially in *OCA2* intron 21 and 23, were flagged for low quality (possibly low read counts) in a substantial proportion of the samples (Table 1). Thus, results should be interpreted with care.

In rs12913832:AA individuals, CNVs in 14 regions were associated with blue eye colour using raw *p*-values (*p* ≤ 0.05). Deletions were observed in two of these regions in *OCA2* (intron 23), whereas both deletions and duplications were observed in 12 regions in *HERC2,* ~100 kb upstream rs12913832.

4. Discussion

With current prediction models, blue and brown eye colours are predicted with high accuracies [3]. However, blue eye colour has frequently been observed in individuals with the non-blue rs12913832:

AG and AA genotypes in Scandinavian populations [9]. *OCA2* SNPs such as rs1800407, rs75643330 and rs121918166 can potentially explain this lighter eye colour in some, but not all of these individuals [9,10]. In this study we observed intronic duplications and deletions in the *OCA2--HERC2* locus in blue-eyed individuals, including regions in *OCA2* intron 2 (upstream the missense mutations rs1800407, rs121918166 and rs75643330), and regions in *HERC2* intron 82 (upstream rs12913832). It is well known that CNVs can have significant impact on human traits, but copy-number-based genome-wide association studies (GWASs) from MPS data is scarce. One large-scale association study found CNV to be associated with hair colour at *HERC2* in a British biobank [11]. To the best of our knowledge, we suggest for the first time CNVs in these regions to be candidates to explain eye colour variation in rs12913832:AG or AA individuals with unexpected blue eye colour. However, other studies must confirm the results and it is yet to be functionally investigated if these structural variants have regulatory effects on *OCA2*.

5. Conclusion

Preliminary results from MPS data revealed CNVs in the *OCA2-HERC2* region in blue-eyed rs12913832:AG and rs12913832:AA individuals. Despite the small sample size, we identified candidate regions with significantly more deletions or duplications in blue-eyed compared to brown-eyed individuals. These could potentially explain the unexpected blue eyes in these individuals. However, the functional effects of these CNVs on *OCA2* expression are yet to be investigated.

Declaration of Competing Interest

None.

Acknowledgements

References

[1] R.A. Sturm, D.L. Duffy, Z.Z. Zhao, F.P.N. Leite, M.S. Stark, N.K. Hayward, N. G. Martin, G.W. Montgomery, A single SNP in an evolutionary conserved region within intron 86 of the HERC2 gene determines human blue-brown eye color, Am. J. Hum. Genet. 82 (2008) 424, https://doi.org/10.1016/J.AJHG.2007.11.005.

[2] M. Visser, M. Kayser, R.-J. Palstra, HERC2 rs12913832 modulates human pigmentation by attenuating chromatin-loop formation between a long-range enhancer and the OCA2 promoter, Genome Res. 22 (2012) 446–455, https://doi.org/10.1101/gr.128652.111.

[3] S. Walsh, A. Wollstein, F. Liu, U. Chakravarthy, M. Rahu, J.H. Seland, G. Soubrane, L. Tomazzoli, F. Topouzis, J.R. Vingerling, J. Vioque, A.E. Fletcher, K. N. Ballantyne, M. Kayser, DNA-based eye colour prediction across Europe with the IrisPlex system, Forensic Sci. Int. Genet. 6 (2012) 330–340, https://doi.org/10.1016/J.FSIGEN.2011.07.009.

[4] N.M. Salvo, K. Janssen, M.K. Kirsebom, O.S. Meyer, T. Berg, G.H. Olsen, Predicting eye and hair colour in a Norwegian population using Verogen's ForenSeq™ DNA signature prep kit, Forensic Sci. Int. Genet. 56 (2022), 102620, https://doi.org/10.1016/J.FSIGEN.2021.102620.

[5] H. Li, R. Durbin, Fast and accurate long-read alignment with Burrows–Wheeler transform, Bioinformatics 26 (2010) 589–595, https://doi.org/10.1093/BIOINFORMATICS/BTP698.

[6] H. Li, Aligning sequence reads, clone sequences and assembly contigs with BWA-MEM, 2013. ⟨http://github.com/lh3/bwa⟩ (Accessed 31 January 2022).

[7] H. Li, R. Durbin, Fast and accurate short read alignment with Burrows–Wheeler transform, Bioinformatics 25 (2009) 1754, https://doi.org/10.1093/BIOINFORMATICS/BTP324.

[8] G. Povysil, A. Tzika, J. Vogt, V. Haunschmid, L. Messiaen, J. Zschocke, G. Klambauer, S. Hochreiter, K. Wimmer, panelcn.MOPS: copy-number detection in targeted NGS panel data for clinical diagnostics, Hum. Mutat. 38 (2017) 889, https://doi.org/10.1002/HUMU.23237.

[9] O.S. Meyer, N.M. Salvo, A. Kjærbye, M. Kjersem, M.M. Andersen, E. Sørensen, H. Ullum, K. Janssen, N. Morling, C. Børsting, G.-H. Olsen, J.D. Andersen, Prediction of eye colour in scandinavians using the eyecolour 11 (EC11) SNP set, Genes 12 (2021) 821, https://doi.org/10.3390/GENES12060821.

[10] J.D. Andersen, C. Pietroni, P. Johansen, M.M. Andersen, V. Pereira, C. Børsting, N. Morling, Importance of nonsynonymous OCA2 variants in human eye color prediction, Mol. Genet. Genom. Med. 4 (2016) 420–430, https://doi.org/10.1002/mgg3.213.

[11] T. Fitzgerald, E. Birney, CNest: A novel copy number association discovery method uncovers 862 new associations from 200,629 whole-exome sequence datasets in the UK Biobank, Cell Genom. 2 (2022), 100167, https://doi.org/10.1016/J.XGEN.2022.100167.